



**UFBA**

**UNIVERSIDADE FEDERAL DA BAHIA  
FACULDADE DE MEDICINA  
FUNDAÇÃO OSWALDO CRUZ  
INSTITUTO GONÇALO MONIZ**



**FIOCRUZ**

**Curso de Pós-Graduação em Patologia**

**TESE DE DOUTORADO**

**TERAPIA COM CÉLULAS-TRONCO MESENQUIMAIS GENETICAMENTE  
MODIFICADAS PARA SUPEREXPRESSION DE G-CSF E IGF-1 NA DOENÇA DE  
CHAGAS CRÔNICA EXPERIMENTAL**

**DANIELA NASCIMENTO SILVA**

**Salvador – Bahia**

**2018**

**UNIVERSIDADE FEDERAL DA BAHIA  
FACULDADE DE MEDICINA  
FUNDAÇÃO OSWALDO CRUZ  
INSTITUTO GONÇALO MONIZ**

**Curso de Pós-Graduação em Patologia**

**TERAPIA COM CÉLULAS-TRONCO MESENQUIMAIS GENETICAMENTE  
MODIFICADAS PARA SUPEREXPRESSION DE G-CSF E IGF-1 NA DOENÇA DE  
CHAGAS CRÔNICA EXPERIMENTAL**

**DANIELA NASCIMENTO SILVA**

Orientadora: Dra. Milena Botelho Pereira Soares

Tese apresentada ao Curso de Pós-  
Graduação em Patologia Experimental  
para obtenção do grau de Doutor.

**Salvador - Bahia**

**2018**

Ficha Catalográfica elaborada pela Biblioteca do  
Instituto Pesquisas Gonçalo Moniz / FIOCRUZ - Salvador - Bahia.

S586t Silva, Daniela Nascimento  
Terapia com células-tronco mesenquimais geneticamente modificadas para  
superexpressão de G-CSF e IGF-1 na Doença de Chagas crônica experimental. /  
Daniela Nascimento Silva. - 2018.  
85 f. : il. ; 30 cm.

Orientador: Prof<sup>ª</sup>. Dra. Milena Botelho Pereira Soares, Laboratório de  
Engenharia Tecidual e Imunofarmacologia.

Tese (Doutorado em Patologia) – Universidade Federal da Bahia, Faculdade  
de Medicina. Fundação Oswaldo Cruz, Instituto Gonçalo Moniz, 2018.

1. Cardiomiopatia chagásica. 2. Terapia celular. 3. Células-Tronco  
Mesenquimais. I. Título.

CDU 616.937:57.086.83

Título da Tese: " TERAPIA COM CÉLULAS-TRONCO MESENQUIMAIS GENETICAMENTE MODIFICADAS PARA SUPEREXPRESSION DE G-CSF E IGF-1 NA DOENÇA DE CHAGAS CRÔNICA EXPERIMENTAL."

DANIELA NASCIMENTO SILVA

FOLHA DE APROVAÇÃO

Salvador, 09 de novembro de 2018

COMISSÃO EXAMINADORA



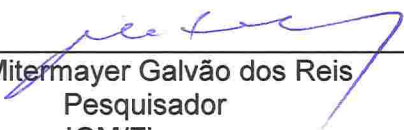
---

Dr. Antônio Carlos Campos de Carvalho  
Professor  
UFRJ



---

Dr. Vitor Antonio Fortuna  
Professor Associado  
UFBA



---

Dr. Mitermayer Galvão dos Reis  
Pesquisador  
IGM/Fiocruz



---

Dra. Dalila Luciola Zanette  
Pesquisadora  
IGM/Fiocruz



---

Dra. Milena Botelho Pereira Soares  
Pesquisadora  
IGM/Fiocruz

**FONTE DE FINANCIAMENTO**

CNPq

## **AGRADECIMENTOS**

A Deus por mais uma graça alcançada.

À minha família pelo apoio, incentivo e admiração em todos os momentos da minha vida.

Ao Marcio Saeger por todo amor e companheirismo durante esta jornada.

À Dra. Milena Soares, minha orientadora, agradeço por todo apoio, ensinamentos e paciência durante estes anos no laboratório, os quais foram essenciais para meu crescimento científico e pessoal.

Ao Dr. Bruno Solano pela co-orientação, incentivo, amizade e aprendizado durante a minha formação científica.

Ao Dr. Ricardo Ribeiro dos Santos por todo apoio, conhecimento e confiança ao longo de todos esses anos.

Aos colegas do CBTC e LETI: técnicos, estudantes de pós-graduação e aos ICs, pelo apoio e colaboração, tornando os anos de trabalho muito mais divertidos.

Ao Hospital São Rafael e CPqGM / FIOCRUZ pela excelente infra-estrutura disponibilizada para o desenvolvimento deste trabalho.

“É impossível crer e não fazer,  
e é lógico fazer no modo e na  
medida em que se crê”.

*Dom Luigi M. Verzé*

SILVA, Daniela Nascimento. Terapia com células-tronco mesenquimais geneticamente modificadas para superexpressão de G-CSF e IGF-1 na Doença de Chagas crônica experimental. 85 f. il. Tese (Doutorado em Patologia) – Universidade Federal da Bahia. Fundação Oswaldo Cruz, Instituto Gonçalo Moniz, Salvador, 2018.

## RESUMO

**INTRODUÇÃO:** A doença de Chagas é uma doença parasitária causada pelo *Trypanosoma cruzi*, a qual representa uma das principais causas de morbimortalidade na América Latina. As intervenções terapêuticas existentes não são totalmente eficazes, sendo o transplante cardíaco a única alternativa para os pacientes com cardiopatia chagásica crônica (CCC) grave. Neste sentido, a ausência de terapias capazes de atuar diretamente sobre os determinantes fisiopatológicos da doença torna necessária a identificação de novas abordagens terapêuticas. Estudos previamente realizados pelo nosso grupo mostraram que a utilização de células-tronco obtidas da medula óssea e de outras fontes teve efeitos benéficos no tratamento da CCC experimental. A possibilidade de potencializar os efeitos parácrinos das células-tronco através de modificação genética tem sido alvo de investigações científicas. **OBJETIVO:** Avaliar os efeitos da terapia com células-tronco mesenquimais (CTMs) da medula óssea, modificadas geneticamente para superexpressar o fator estimulador de colônias de granulócitos (hG-CSF) ou o fator de crescimento semelhante à insulina 1 (hIGF-1) em um modelo experimental de CCC. **MATERIAL E MÉTODOS:** Camundongos C57BL/6 foram infectados com 1000 tripomastigotas da cepa Colombiana de *T. cruzi* e, após seis meses de infecção, foram tratados com CTM, CTM-G-CSF, ou CTM-IGF-1. Grupos de animais não infectados ou infectados tratados com salina (veículo) foram utilizados como controles. Todos os animais foram eutanasiados sob anestesia após dois meses de tratamento para análises histopatológicas e morfométricas do coração ou músculo esquelético, bem como para avaliação da expressão de citocinas inflamatórias. **RESULTADOS:** As secções de corações de camundongos dos grupos tratados com CTM, CTM-GCSF ou CTM-IGF-1 apresentaram redução significativa do número de células inflamatórias e do percentual de fibrose em comparação aos animais chagásicos tratados com salina, sendo esta diferença mais evidente no grupo que foi tratado com células-tronco que superexpressam o G-CSF. Além disto, a terapia com CTM-G-CSF induziu a mobilização de células imunomoduladoras para o coração, tais como células supressoras de origem mielóide (MDSC) e células T regulatórias Foxp3<sup>+</sup> que expressam IL-10. A avaliação da expressão gênica das citocinas inflamatórias no tecido cardíaco mostrou um aumento das citocinas inflamatórias em animais chagásicos crônicos quando comparados aos controles não infectados, sendo a maioria delas moduladas de forma significativa nos grupos que foram tratados com CTM ou CTM-G-CSF. Apesar da terapia utilizando CTM-IGF-1 não ter apresentado benefício adicional ao tecido cardíaco comparado ao grupo que foi tratado com CTM não modificadas, foi observado um efeito regenerativo desta terapia no músculo esquelético dos animais, resultando em um aumento de fibras musculares esqueléticas 60 dias após o tratamento. **CONCLUSÃO:** Nossos resultados demonstram que o tratamento com CTM da medula óssea que superexpressam hG-CSF ou hIGF-1 potencializou o efeito terapêutico das CTMs através de ações imunomoduladoras e pró-regenerativas no coração e músculo esquelético de camundongos cronicamente infectados por *T. cruzi*. Desse modo, a modificação genética de CTMs para superexpressão de fatores com potencial terapêutico representa uma estratégia promissora para o desenvolvimento de novas terapias para a cardiomiopatia chagásica crônica.

**PALAVRAS-CHAVE:** Cardiomiopatia chagásica, Terapia celular, Células-Tronco Mesenquimais, G-CSF, IGF-1.



SILVA, Daniela Nascimento. Therapy with genetically modified mesenchymal stem cells overexpressing G-CSF and IGF-1 in experimental chronic Chagas' disease. 85 f. il. Tese (Doutorado em Patologia) – Universidade Federal da Bahia. Fundação Oswaldo Cruz, Instituto Gonçalo Moniz, Salvador, 2018.

## ABSTRACT

**INTRODUCTION:** Chagas' disease is a parasitic disease caused by *Trypanosoma cruzi*, which is one of the main causes of cardiovascular morbidity and mortality in Latin America. Existing therapeutic interventions are not fully effective, and heart transplantation is the only alternative for patients with severe chronic Chagas' heart disease. In this sense, the absence of therapies capable of acting directly on the pathophysiological determinants of the disease demonstrates the necessity of identifying new therapeutic approaches. Studies previously conducted by our group demonstrated that the use of stem cells obtained from bone marrow and other sources had beneficial effects in the treatment of experimental chagas disease. Additionally, the possibility of enhancing stem cell paracrine effects through genetic modification has been the subject of scientific investigations. **OBJECTIVE:** To evaluate the effects of genetically modified mesenchymal stem cell therapy to overexpress granulocyte colony stimulating factor (hG-CSF) or insulin-like growth factor 1 (hIGF-1) in an experimental model of Chagas disease. **MATERIAL AND METHODS:** C57BL/6 mice were infected with 1000 trypomastigotes from the Colombian strain of *T. cruzi* and, after six months of infection, were treated with CTM, CTM-G-CSF, or CTM-IGF-1. Groups of uninfected or infected animals treated with saline (vehicle) were used as controls. All animals were euthanized under anesthesia after two months of treatment for histopathological and morphometric analysis of the heart or skeletal muscle, as well as for evaluation of inflammatory cytokine expression. **RESULTS:** Mouse heart sections from groups treated with CTM, CTM-G-CSF or CTM-IGF-1 showed a significant reduction in the number of inflammatory cells and the percentage of fibrosis when compared to chagasic animals treated with saline. This difference was more evident in the group that was treated with stem cells overexpressing G-CSF. In addition, CTM-G-CSF therapy induced mobilization of immunomodulatory cells to the heart, including myeloid suppressor cells (MDSC) and Foxp3 + regulatory T cells expressing IL-10. Expression of inflammatory cytokine genes in cardiac tissue revealed an increase in inflammatory cytokines in chronic chagasic animals when compared to uninfected controls, where most cytokines were significantly modulated in groups treated with CTM or CTM-G-CSF. Although CTM-IGF-1 therapy demonstrated no additional benefit to cardiac tissue when compared to the group treated with unmodified CTM, a regenerative effect of this therapy was observed in chagasic mice skeletal muscle, resulting in an increase in skeletal muscle fibers 60 days after treatment. **CONCLUSION:** Our results demonstrate that bone marrow derived CTM treatment overexpressing hG-CSF or hIGF-1 enhanced the therapeutic effects of MSCs through immunomodulation and pro-regenerative actions in the heart and skeletal muscle of mice chronically infected with *T. cruzi*. Thus, the genetic modification of CTMs for overexpression of factors with therapeutic potential represents a promising strategy for the development of new therapies for chronic chagasic cardiomyopathy.

**KEY WORDS:** Chagas cardiomyopathy, Cell therapy, Mesenchymal stem cells, G-CSF, IGF-1.

## LISTA DE FIGURAS

<b>Figura 1</b>	Representação da distribuição de número de casos e transmissão vetorial da doença de Chagas no mundo	17
<b>Figura 2</b>	Efeitos das CTM geneticamente modificadas aplicadas em cardiologia	30
<b>Figura 3</b>	Efeitos da interação do IGF-1 e seu receptor na ativação da via PI3k/Akt no músculo esquelético	34
<b>Figura 4</b>	Representação esquemática dos efeitos terapêuticos das células-tronco mesenquimais modificadas geneticamente na CCC experimental	70

## LISTA DE ABREVIATURAS

<b>ANG1</b>	Angiopietina 1
<b>ARG1</b>	Arginase 1
<b>CCC</b>	Cardiopatia chagásica crônica
<b>CFU</b>	Unidade formadora de colônia de fibroblatos
<b>CREG</b>	<i>Cellular repressor of E1 stimulated genes</i>
<b>CRISPR</b>	<i>Clustered regularly interspaced short palindromic repeats</i>
<b>CT</b>	Células-tronco
<b>CTM</b>	Células-tronco mesenquimais
<b>CXCR4</b>	Receptor CXCR4 de quimiocinas 4
<b>G-CSF</b>	Fator estimulador de colônias de granulócitos
<b>GH</b>	Hormônio do crescimento
<b>GSK-3</b>	Glicogênio sintase quinase 3
<b>HGF</b>	Fator de crescimento de hepatócitos
<b>HO-1</b>	Heme oxigenase 1
<b>HSP20</b>	<i>Heat shock protein 20</i>
<b>IDO</b>	Indolamina
<b>IFN<math>\gamma</math></b>	Interferon gama
<b>IGF-1</b>	Fator de crescimento semelhante à insulina 1
<b>IL-10</b>	Interleucina 10
<b>IL12</b>	Interleucina 12
<b>IL1<math>\beta</math></b>	Interleucina 1 beta
<b>IL6</b>	Interleucina 6
<b>IL8</b>	Interleucina 8
<b>ILK</b>	Quinase ligada à integrina
<b>iNOS</b>	Óxido nítrico sintase induzida
<b>LTR</b>	<i>Long terminal repeat</i>
<b>M-CSF</b>	Fator estimulador de colônias de monócitos
<b>MYOD1</b>	<i>Myogenic differentiation 1</i>
<b>NK</b>	<i>Natural killer</i>
<b>PAMPs</b>	Padrões moleculares associados a patógenos
<b>PAX7</b>	<i>Paired box 7</i>

<b>PCR</b>	Reação da polimerase em cadeia
<b>Pi3K</b>	Fosfatidil inositol quinase
<b>RNA</b>	Ácido ribonucléico
<b>SCF</b>	Fator de células-tronco
<b>SDF-1</b>	Fator derivado de célula estromal 1
<b>TALENS</b>	<i>Transcription activator-like effector nuclease</i>
<b>TGF <math>\beta</math></b>	Fator transformador de crescimento beta
<b>TLR</b>	Receptores do tipo <i>toll</i>
<b>TNFR</b>	Receptor de fator de necrose tumoral
<b>TNF<math>\alpha</math></b>	Fator de necrose tumoral alfa
<b>VEGF</b>	Fator de crescimento do endotélio vascular
<b>ZFN</b>	<i>Zinc finger nuclease</i>

## SUMÁRIO

1	<b>INTRODUÇÃO</b>	12
2	<b>JUSTIFICATIVA E HIPÓTESE</b>	15
3	<b>REVISÃO DA LITERATURA</b>	16
3.1	A DOENÇA DE CHAGAS	16
3.1.1	<b>Imunopatologia da cardiomiopatia chagásica crônica</b>	17
3.2	CÉLULAS-TRONCO	19
3.2.1	<b>Células-tronco mesenquimais</b>	21
3.2.2	<b>Modificação genética de células-tronco mesenquimais</b>	23
3.2.2.1	<i>Vetores virais para modificação genética de CTMs</i>	25
3.2.2.2	<i>Adenovírus e vírus adeno-associado</i>	25
3.2.2.3	<i>Retrovírus e lentivírus</i>	26
3.3	TERAPIA CELULAR EM CARDIOLOGIA	27
3.4	G-CSF	31
3.5	IGF-1	33
4	<b>OBJETIVOS</b>	36
4.1	OBJETIVO GERAL	36
4.2	OBJETIVOS ESPECÍFICOS	36
5	<b>RESULTADOS</b>	37
	CAPÍTULO I	37
	CAPÍTULO II	50
6	<b>DISCUSSÃO</b>	62
7	<b>CONCLUSÃO</b>	71

**REFERÊNCIAS**

72

**ANEXOS**

86

## 1 INTRODUÇÃO

A doença de Chagas é uma zoonose causada pelo protozoário *Trypanosoma cruzi*, que afeta entre 6 e 7 milhões de pessoas no mundo. Inicialmente endêmica na América Latina, tem sido observado que nos últimos anos, os casos de infecção têm aumentado de forma significativa em outros continentes (WORLD HEALTH ORGANIZATION, 2017). Apesar das iniciativas de controle da transmissão natural da doença terem sido efetivas em vários países com relação ao controle do vetor, à triagem em bancos de sangue e ao controle de casos de transmissão congênita, a doença de Chagas ainda representa um problema de saúde pública grave, principalmente na América Latina (MATSUO, 2010; WHO, 2017). O tratamento da doença de Chagas ainda é desafiador. A intervenção terapêutica que utiliza fármacos antiparasitários é limitada ao uso do benzonidazol e do nifurtimox, os quais possuem eficácia no tratamento da fase aguda da doença e baixa efetividade na fase crônica. Além disso, a ocorrência de efeitos colaterais graves associadas a estas terapias e a indução de cepas resistentes limitam o espectro de utilização desses fármacos (SALES-JUNIOR, 2017).

Durante a fase crônica da doença de Chagas, o tratamento medicamentoso para insuficiência cardíaca é paliativo e o transplante cardíaco é a única alternativa terapêutica para os pacientes com CCC grave (RASSI et al., 2010). Neste sentido, a ausência de tratamentos eficazes para as formas graves da doença de Chagas torna necessária a identificação de novas abordagens terapêuticas.

A utilização de células-tronco na área da cardiologia tem ganhado atenção nos últimos anos devido ao crescente número de estudos que tem comprovado a eficácia desta terapia com potencial imunomodulador e regenerativo do tecido cardíaco (JADCZIK et al., 2017). Estudos previamente realizados pelo nosso grupo mostraram que a utilização de células-tronco obtidas da medula óssea e de outras fontes contribuiu de forma benéfica para o tratamento da CCC experimental principalmente através de um efeito imunomodulador (ANEXO I; SOARES et al., 2004; SOARES et al., 2011; LAROCCA et al., 2013; SILVA et al., 2014; SOUZA et al., 2014). No entanto, os estudos clínicos que utilizaram células mononucleares derivadas da medula-óssea para tratar pacientes com insuficiência cardíaca grave de etiologia chagásica mostram-se limitados quanto ao seu efeito terapêutico (VILAS-BOAS et al., 2006; DOS-SANTOS et al., 2012), sendo necessário o aprimoramento deste tipo de terapia.

Recentemente, a possibilidade de potencializar os efeitos parácrinos das células-tronco através de modificação genética tem sido alvo de investigações científicas (NOLTA, 2016). A

utilização de células-tronco como ferramentas terapêuticas oriundas de manipulações genéticas tem gerado grande interesse na comunidade científica, pois a introdução de genes que codificam fatores de crescimento indutores de regeneração tecidual pode contribuir de forma sinérgica ao potencial terapêutico exercido pelos fatores que já são secretados pelas células-tronco (MAROFI et al., 2017).

O G-CSF é um fator amplamente utilizado na prática clínica para mobilização de progenitores hematopoiéticos (ANDERLINI; CHAMPLIN, 2007). A mobilização e recrutamento de populações celulares com potencial imunomodulador, tais como células supressoras de origem mielóide (MDSC) e células T regulatórias (Treg) Foxp3<sup>+</sup> pelo efeito do G-CSF já foi descrita (WAIGTH et al., 2011). Os resultados dos estudos que utilizaram G-CSF para tratar infarto do miocárdio ou outras doenças de etiologia cardíaca demonstram que este fator possui efeito direto sobre o coração, promovendo angiogênese, remodelamento cardíaco e melhora da função cardíaca (IWANAGA et al., 2004; HARADA et al., 2005; FUJITA et al., 2007).

Recentemente, nosso grupo de pesquisa demonstrou o efeito benéfico do G-CSF no modelo experimental de cardiomiopatia chagásica crônica. Os principais efeitos desta terapia foram causados pela atividade imunomoduladora do G-CSF, que promoveu a redução da inflamação e fibrose no coração, bem como modulação de citocinas pró-inflamatórias e mobilização de células T regulatórias Foxp3<sup>+</sup>. Além disso, a terapia com G-CSF contribuiu para redução do parasitismo e melhora da função cardíaca dos animais (MACAMBIRA et al., 2009; VASCONCELOS et al., 2013).

Assim como o G-CSF, nosso grupo identificou o IGF-1 como outro fator envolvido na regeneração tecidual durante a infecção pelo *T. cruzi*. Durante a fase aguda da infecção, foi observado um aumento significativo do IGF-1 no músculo esquelético dos animais que apresentaram regeneração do músculo esquelético e aumento de células-tronco residentes do músculo esquelético Pax7<sup>+</sup> após a terapia com células-tronco derivadas da medula óssea (SOUZA et al., 2014). Estes achados reforçam a utilização de fatores com potenciais regenerativos e imunomoduladores como uma estratégia promissora para o tratamento da CCC.

Nesse contexto, geramos e caracterizamos células-tronco mesenquimais para a superexpressão ectópica do hG-CSF e hIGF-1 e demonstramos que a modificação genética não alterou suas características fenotípicas e o seu potencial imunomodulador *in vitro* (ANEXO II). No presente trabalho, investigamos se os efeitos parácrinos exercidos pelas células-tronco



mesenquimais, associados aos efeitos terapêuticos do G-CSF e IGF-1, poderiam constituir uma estratégia terapêutica mais eficaz para o tratamento da cardiopatia chagásica crônica. Sendo assim, esse trabalho se propõe a investigar os efeitos da terapia utilizando células-tronco mesenquimais geneticamente modificadas para a superexpressão do hG-CSF e hIGF-1 no modelo experimental de cardiopatia chagásica crônica.

## 2 JUSTIFICATIVA E HIPÓTESE

A doença de Chagas é uma das doenças parasitárias mais graves no mundo. As intervenções terapêuticas existentes não são totalmente eficazes, sendo o transplante cardíaco a única alternativa para os pacientes com CCC grave. A CCC tem frequentemente um curso fatal, já que o tratamento é sintomático e a realização de transplantes cardíacos não é suficiente para a demanda. Neste sentido, a ausência de terapias capazes de atuar diretamente sobre os determinantes fisiopatológicos da doença torna necessária a identificação de novas abordagens terapêuticas. Os estudos que avaliaram o potencial terapêutico das células-tronco mesenquimais obtidas da medula óssea e de outras fontes apresentaram resultados com efeitos benéficos ao coração dos animais chagásicos após a terapia celular. Recentemente, a possibilidade de potencializar os efeitos tróficos das células-tronco mesenquimais e sua utilização como vetores para fatores identificados com potencial terapêutico são alvos de investigações científicas. A utilização dos fatores G-CSF e IGF-1 para o tratamento das doenças cardíacas mostrou-se promissora para tratar doenças cardíacas de diferentes etiologias. Este trabalho se propõe a avançar o conhecimento no âmbito da utilização de células-tronco modificadas geneticamente no contexto da cardiopatia chagásica crônica experimental.

Tendo em vista as atividades terapêuticas do IGF-1 e G-CSF descritas anteriormente e todas as propriedades inerentes às CTMs, a hipótese desse trabalho é avaliar se o potencial terapêutico das células-tronco mesenquimais modificadas geneticamente para a superexpressão de fatores associados a regeneração cardíaca é superior às células-tronco mesenquimais não modificadas no tratamento da CCC experimental.

### 3 REVISÃO DA LITERATURA

#### 3.1 A DOENÇA DE CHAGAS

A doença de Chagas, juntamente com o seu agente causal, foi inicialmente descrita por Carlos Chagas no Brasil, em 1909. Classicamente transmitida por insetos triatomíneos hematófagos, que depositam as fezes contaminadas com formas tripomastigotas do *Trypanosoma cruzi* no local da picada no momento do repasto sanguíneo, a doença de Chagas recebeu atenção devido às outras formas de transmissão, tais como transfusões de sangue, transplantes de órgãos e transmissão congênita (RASSI et al., 2010). O parasito pode ainda penetrar no hospedeiro por outras vias, tais como ingestão acidental de insetos triturados junto com alimentos (contaminação por via oral) ou por acidente em laboratórios. Recentemente, casos agudos resultantes da ingestão acidental do parasito têm sido registrados por surtos em diferentes localidades, com maior incidência na região amazônica, onde o consumo de açaí é uma frequente causa de contaminação (YOSHIDA, 2008; MONCAYO; SILVEIRA, 2009; BASTOS et al., 2010).

Embora as iniciativas de controle do vetor tenham reduzido consideravelmente o número de pessoas infectadas nas áreas endêmicas, estima-se que 20% da população latino-americana esteja sob risco de infecção (RASSI et al., 2010). Segundo a Organização Mundial da Saúde, cerca de 6 a 7 milhões de pessoas estão infectadas pelo *T. cruzi* no mundo (WHO, 2017). No Brasil, esta estimativa encontra-se em torno de 1,9 milhões a 4,6 milhões (MARTINS, 2014). Devido à globalização e ao aumento do fluxo migratório, observou-se um aumento do número de casos em países não endêmicos da América do Norte, Europa, Ásia e Oceania (Figura 1) (BEZINGER; CARMO; RIBEIRO, 2017). Na América Latina, a doença de Chagas representa um grave problema de saúde pública, sendo uma das principais causas de morte por insuficiência cardíaca, com um custo anual de 50 milhões de dólares para cada 100 pacientes infectados, e um impacto sócio-econômico significativo nos países endêmicos (WHO, 2017).

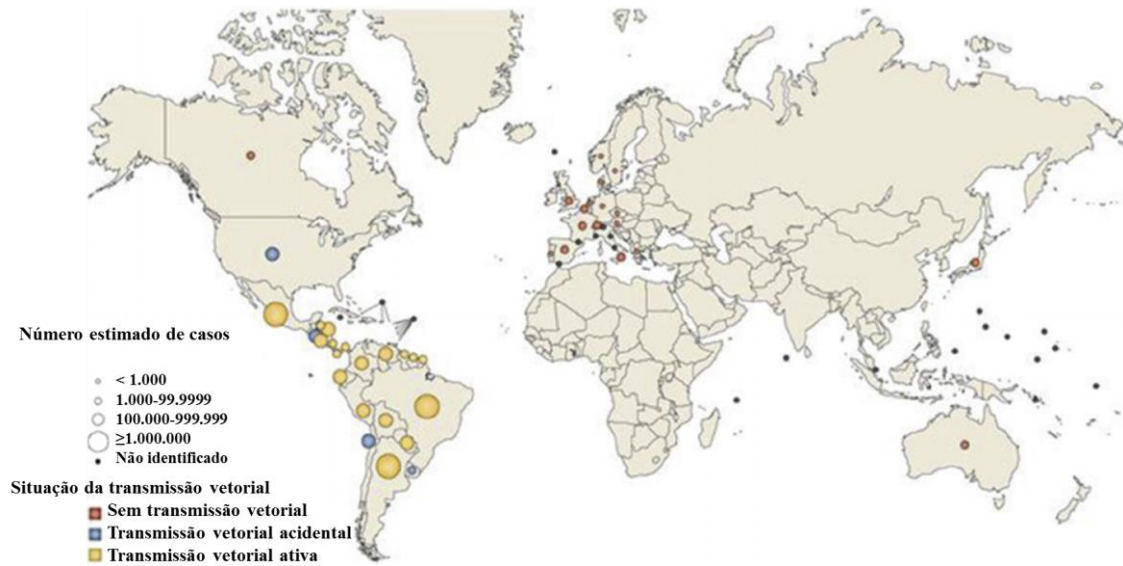


**Figura 1:** Representação da distribuição de número de casos e transmissão vetorial da doença de Chagas no mundo. Adaptado de Bezinger, 2017.

### 3.1.1 Imunopatologia da cardiomiopatia chagásica

A doença de Chagas se apresenta em duas fases consecutivas: a fase aguda e crônica. Após a infecção pelo *T. cruzi*, há o desenvolvimento da fase aguda, que é transitória e geralmente sem manifestações clínicas ou com manifestações clínicas de pequena relevância. A fase aguda se caracteriza pela presença de formas tripomastigotas do parasito no sangue periférico e formas amastigotas que se multiplicam nos compartimentos intracelulares das células do hospedeiro (BRENER et al., 2000). Nesta fase, a participação das células do sistema imune inato, tais como macrófagos e células dendríticas, são cruciais para o controle da infecção pelo *T. cruzi* (TARLETON, 2007; MAYA, 2010). Essas células são ativadas a partir da interação dos seus receptores do tipo *Toll* (*Toll Like Receptors*-TLR) e os padrões moleculares associados a patógenos (PAMPs). A ativação da resposta imune via TLR desencadeia a produção de componentes pró-inflamatórios envolvidos na resposta local e sistêmica contra o parasito. Foi identificado que, na doença de Chagas, as citocinas IL-1 $\beta$ , IL-6, IL-8, IL-12, fator de necrose tumoral alfa (TNF $\alpha$ ) e o interferon gama (IFN $\gamma$ ), como também quimiocinas e a produção de substâncias microbicidas, tais como o óxido nítrico participam ativamente no controle da infecção na fase aguda (RODRIGUES; OLIVEIRA; BELLIO, 2012). Já foi demonstrado, que a persistência de níveis elevados de citocinas pró-inflamatórias, tais como IFN $\gamma$  e TNF $\alpha$  e o aumento de linfócitos T CD4 e CD8 produtores de

IFN $\gamma$  no sangue periférico contribuem diretamente para o desencadeamento de lesão tecidual (NOGUEIRA, 2014).

Após a fase aguda, há o estabelecimento da fase crônica, na qual aproximadamente 70% dos indivíduos infectados apresentam a forma indeterminada da doença sem manifestações clínicas, radiológica ou eletrocardiográfica detectadas. Nestes casos, há a predominância de um ambiente de resposta imune mais regulatório, já que, além das células produtoras de citocinas pró-inflamatórias, há também um aumento no número de células regulatórias e uma alta produção de IL-10, que é uma citocina anti-inflamatória responsável por desativar os macrófagos e conseqüentemente inibir os efeitos das células T e células NK, contribuindo para a redução da lesão tecidual e da não manifestação clínica da doença (GOMES, 2003; CUNHA-NETO, 2009). A resistência à infecção pelo *T. cruzi* e a minimização das lesões teciduais parecem depender de um balanço entre a produção de citocinas pró-inflamatórias, anti-inflamatórias, bem como o de quimiocinas e a expressão de seus receptores na superfície das células, podendo ser este o principal mecanismo de controle da morbidade durante a fase crônica da doença (GOMES et al., 2003; TEIXEIRA et al., 2006; DUTRA et al., 2014).

Estima-se que 30% dos indivíduos infectados pelo *T. cruzi* apresentarão manifestações clínicas cardíacas e/ou digestivas dentro de um período que pode variar de alguns anos até décadas após a infecção aguda, representando a forma crônica sintomática da doença de Chagas (SOARES; LAIN-PONTES; RIBEIRO-DOS-SANTOS, 2001). A forma cardíaca é considerada a mais grave e frequente manifestação clínica da fase crônica. A cardiomiopatia chagásica crônica (CCC) é caracterizada por mionecrose, miocitólise e intensa fibrose intersticial, resultado das lesões no miocárdio que estão associados ao efeito combinado do parasitismo persistente, à inflamação tecidual e microvascular, disfunção neurogênica e às respostas auto-imunes desencadeadas pela infecção (MARIN-NETO et al., 2010).

A lesão inflamatória clássica descrita nos corações de pacientes com cardiomiopatia chagásica é composta por infiltrado inflamatório predominantemente composto por linfócitos T, poucos linfócitos B, e macrófagos. A intensa resposta inflamatória provoca lesões progressivas da microcirculação cardíaca, do miocárdio e do sistema de condução, que resulta no aparecimento de arritmias, comprometimento mecânico e, por fim, a insuficiência cardíaca (SOARES; LAIN-PONTES; RIBEIRO-DOS-SANTOS, 2001; RASSI, 2010).

A morte súbita e a insuficiência cardíaca refratária são as principais causas de óbito nos pacientes com a forma crônica sintomática da doença de Chagas (KRANSDORF et al.,

2016; MARTÍ-CARVAJAL; KWONG, 2016). Em geral, a CCC tem um curso fatal, e os diversos tratamentos com drogas, como o benzonidazol, trazem uma série de complicações para os pacientes e não erradicam o parasito na fase crônica (MARTÍ-CARVAJAL; KWONG, 2016).

O transplante cardíaco é a única opção terapêutica para pacientes com insuficiência cardíaca de etiologia chagásica. Este procedimento tem diversos agravantes, tais como a demanda por órgãos superior à oferta, um custo elevado e o uso de imunossupressores, que após o transplante em pacientes chagásicos pode acarretar em reativação da parasitemia latente (MARIN-NETO et al., 2010). Dessa forma, o desenvolvimento de terapias capazes de interferir em um quadro já instalado da doença, ou de prevenir o desenvolvimento da CCC é de grande importância.

### **3.2 Células-tronco**

As células-tronco (CT) são células indiferenciadas e não especializadas, com potencial prolongado ou ilimitado de auto renovação e capacidade de diferenciação em diversos tipos celulares (WATT; HOGAN, 2000; ZAGO et al., 2006).

Wagers e Weissman (2004) classificam as CT de acordo com o seu potencial de diferenciação e plasticidade. Células totipotentes são aquelas capazes de originar todos os tipos celulares embrionários e extraembrionários. As CT pluripotentes são aquelas com capacidade para gerar todos os tecidos dos três folhetos embrionários do organismo, como é o caso das CT embrionárias. As CT multipotentes são capazes de originar um subconjunto de linhagens celulares e as oligopotentes, células pertencentes a um mesmo folheto embrionário. Por fim, as CT unipotentes são as que apresentam capacidade para originar apenas um tipo de célula madura.

As CT podem ainda ser classificadas em três categorias, de acordo com o seu estágio de desenvolvimento: as CT embrionárias (THOMSON et al., 1998), as CT fetais (PAPPA; ANAGNOU et al., 2009) e as CT adultas (DA SILVA MEIRELLES et al., 2006). Dentre as adultas, destacam-se as células-tronco hematopoiéticas e as células-tronco mesenquimais (CTMs).

Essa classificação está em constante mudança com os avanços das pesquisas na área. Mais recentemente, a publicação do trabalho realizado por Takahashi (2006) introduziu o conceito das células-tronco pluripotentes induzidas (iPSC), que são obtidas a partir de células

do adulto, tais como fibroblastos da pele e eritroblastos, reprogramados à pluripotência a partir da expressão forçada de quatro fatores de transcrição indutores (Oct-4, Sox-2, c-Myc e KLF-4) (TAKAHASHI ; YAMANAKA., 2006).

A demonstração da capacidade das CT embrionárias de se diferenciar em muitos tipos celulares tem gerado um grande interesse na aplicação clínica destas células. Contudo, o seu potencial tumorigênico, como a formação de teratomas, problemas decorrentes da falta de histocompatibilidade (LA FLAME; MURRAY, 2005) e as questões éticas (CHAPMAN et al., 2009) ainda dificultam a utilização terapêutica das células-tronco embrionárias.

As CT adultas são células indiferenciadas, responsáveis pela geração de células especializadas durante os processos de crescimento, diferenciação tecidual, renovação celular e regeneração tecidual. Elas podem ser remanescentes ou derivadas das CT embrionárias e estão presentes no organismo após o nascimento para promover vários processos fisiológicos ao longo da vida (CAPLAN, 2007).

Estas células podem ser encontradas em tecidos, tais como a medula óssea, tecido adiposo, fígado, pele, cérebro, músculo esquelético, pâncreas, pulmão, coração, sangue periférico, e atualmente um número crescente de evidências tem se acumulado, indicando o potencial de diferenciação dessas células em diversos tipos celulares, o que representa uma grande perspectiva terapêutica, e as torna objeto de estudo para o tratamento de diversas doenças ( ZAGO, 2006; PASSIER et al., 2008; GOODELL et al., 2015).

Desta forma, as CT adultas são inseridas no grupo de tipos celulares mais apropriados para a utilização autóloga na terapia celular, pois estas estão presentes em vários tecidos, podendo ser isoladas do próprio indivíduo, o que evitaria eventuais processos de rejeição imunológica.

As CT da medula óssea são as CT adultas mais estudadas. A medula óssea contém CT hematopoiéticas e mesenquimais (JACKSON et al., 2002; KRAUSE et al., 2002; ROWE et al., 2016). As CT hematopoiéticas derivadas da medula óssea constituem as CTs mais estudadas até hoje e são caracterizadas por sua capacidade plástica e por serem facilmente isoladas. Essas células possuem a capacidade de auto renovação e diferenciação em células especializadas do tecido sanguíneo e células do sistema imune, e foram também descritas como tendo um potencial de diferenciação em células epiteliais do fígado, pulmão, trato gastro-intestinal e pele (KRAUSE et al., 2002; ALBELLA et al., 2003). Na medula óssea, as CT hematopoiéticas são cercadas pelas células estromais, conhecidas como CT mesenquimais, que nos últimos anos, tem recebido uma atenção especial devido a facilidade

de obtenção e expansão *in vitro*, e em especial à sua capacidade de secretar moléculas biologicamente ativas. Além disso, estas células podem ser isoladas de praticamente todos os tecidos adultos, e induzidas a diferenciação em múltiplas linhagens celulares (LIU et al., 2009; LI et al., 2016).

### 3.3.1 Células-tronco mesenquimais (CTMs)

As CTMs são células multipotentes, não hematopoiéticas, que foram isoladas da medula óssea nos estudos pioneiros de Friedenstein e colaboradores, como células morfológicamente semelhantes a fibroblastos e com alta capacidade proliferativa e de adesão à superfície plástica (FRIEDENSTEIN et al., 1970). Esse mesmo grupo desenvolveu o método de isolamento de CTMs da medula óssea baseado na sua capacidade de aderência ao plástico, que é utilizado até hoje como o método padrão de isolamento destas células (FRIEDENSTEIN et al., 1970).

As CTMs constituem uma população heterogênea de células em termos de morfologia e expressão de antígenos de superfície. Para a caracterização fenotípica dessas células, deve-se empregar um conjunto de anticorpos que permitem a avaliação quantitativa e qualitativa da expressão dos antígenos de superfície por citometria de fluxo, caracterizando um perfil imunofenotípico das células isoladas (DOMINICI et al., 2006). Diante da diversidade de marcadores utilizados para caracterização das CTMs, o Comitê de Células-Tronco Tecidual e Mesenquimal da Sociedade Internacional para Terapia Celular (ISCT) propôs alguns critérios para a caracterização das CTMs. As células devem expressar CD73, CD90 e CD105 e não devem expressar os marcadores de linhagem hematopoiéticas c-kit, CD14, CD11b, CD34, CD45, CD19 e CD79 (DOMINICI et al., 2006).

Além da capacidade de auto renovação, aderência, e conjunto de marcadores de superfície, outro critério de caracterização das CTMs proposto pelo ISCT, é a avaliação da sua capacidade de diferenciação nas linhagens osteogênica, adipogênica e condrogênica *in vitro*.

Embora esses critérios sejam bem aceitos para a caracterização das CTMs, a expressão desses antígenos e o potencial de diferenciação podem mudar durante o cultivo das células, tornando a associação do perfil de CTM isolado e a eficácia terapêutica, um desafio para a terapia celular (WYSE et al., 2014). Já foi descrito que o perfil fenotípico e o potencial terapêutico das CTM podem variar a depender da fonte de obtenção, do protocolo de



isolamento, das condições de suplementação da cultura celular, bem como do tempo em cultura e o número de passagens após o isolamento. Dessa forma, uma caracterização adicional aos critérios já definidos pelo ISCT, faz-se necessário, já que a influência de muitos fatores podem alterar os parâmetros de caracterização e eficácia terapêutica das CTMs. (DA SILVA MEIRELLES et al., 2006; PSALTIS et al., 2008; HO et al., 2008; BOXAL; JONES, 2012; HAGMANN et al., 2013). Além das propriedades descritas acima, a baixa imunogenicidade, revelada pela pouca expressão de MHC classe II e de moléculas co-estimulatórias (D40, CD80, CD86), como também o potencial de secretar moléculas biotivas que tem efeito imunomodulatório e pró-regenerativo, podem ser consideradas as principais propriedades das CTMs (TSE et al., 2003).

Os mecanismos exatos ligados às propriedades imunomoduladoras das CTMs, ainda permanece sob investigação. No entanto, sua capacidade de modular a resposta imune inata e adaptativa atuando sobre a função e ativação dos linfócitos T, bem como na maturação e função das células dendríticas e na proliferação e diferenciação de linfócitos B, são bem descritas (HOFFSTETER et al., 2002; BARTHOLOMEU et al., 2002; KRAMPERA et al., 2006; LE BLANC et al., 2003; GLENNIE, et al., 2005). Sabe-se que a interação das células do sistema imune com as CTMs estimula estas a secretarem fatores solúveis, que as tornam excelentes agentes imunomoduladores. Entre esses fatores solúveis estão: o fator de células-tronco (SCF), interleucina 6 (IL-6), interleucina 8 (IL-8), interleucina 10 (IL10), interleucina 12 (IL12), indolamina 2.3-dioxigenase (IDO), fator de crescimento do endotélio vascular (VEGF), fator estimulatório de colônia de macrófagos (M-CSF), fator estimulador de colônia de granulócitos (G-CSF), fator de crescimento de hepatócitos (HGF) e fator de transformação do crescimento beta ( $TGF\beta 1$ ) (SAKATA et al., 2010; LE BLANC; MOUGIAKAKOS., 2012; DORRONSORO et al., 2014).

As CTMs são altamente influenciadas pelas condições ambientais, pois a secreção de tantos fatores e moléculas biologicamente ativas pode ser direcionada por citocinas tipicamente presentes do local de lesão (WAGNER et al., 2009). Já foi demonstrado, que a presença de citocinas pró-inflamatórias, como  $IFN\gamma$ , reforça a capacidade imunossupressora das CTMs por meio da produção aumentada de IDO, HGF,  $TGF\beta$  e IL-10 (PROCKOP, 2013). Por isso, existe um interesse crescente em explorar e compreender melhor as propriedades imunomoduladoras das CTMs.

O potencial de migração das CTMs é outra propriedade que tem sido bastante explorada atualmente. A capacidade de migração das CTMs para tecidos lesionados ou sítios

inflamatórios contribuí positivamente para o reparo tecidual (JI et al., 2004; WYSE, et al., 2014). Neste caso, ocorre a participação de moléculas de adesão, liberação de quimiocinas e expressão de receptores que fazem com que as CTMs sejam recrutadas para os tecidos (PONTE et al., 2007). Foi demonstrado que o recrutamento das CTMs para tecidos com processo inflamatório ativo, se deu através da interação do receptor de quimiocina 4 (CXCR4R) e SDF-1 liberado nas áreas de lesão (BAJETTO et al., 1999; HILL et al., 2004). Essa característica, impulsionou o uso terapêutico das CTMs como ferramentas potenciais para regeneração de tecidos após lesão renal aguda, infarto agudo do miocárdio e acidente vascular cerebral (CHENG et al., 2008; YU et al., 2012; LIU et al., 2013). Outra forma de explorar a capacidade de migração das CTMs é através da utilização dessas células como veículo para entrega de agentes químicos ou biológicos que agem diretamente na região onde ocorreu o dano tecidual (XIAN et al., 2006).

Foi demonstrado que, após as CTMs alcançarem as áreas de lesão, há a estimulação de regeneração tecidual através da secreção de diversas moléculas biologicamente ativas, tais como fatores de crescimento, citocinas e quimiocinas (PAREKKADAN et al., 2007). O potencial de liberação de fatores tróficos pelas CTMs com ações parácrinas representa seu maior potencial como agente terapêutico (BARANIAK; MCDEVITT, 2010). As análises de secretoma e proteômica das CTMs revelam que a secreção de fatores, tais como BDNF, NGF, HGF e VEGF, contribuem para os efeitos anti-fibróticos, angiogênicos e neurotróficos exercidos pelas CTMs (CHEN et al., 2002; CRIGLER et al., 2006; CAPLAN; DENNIS, 2006). Dentre os fatores secretados pelas CTMs, o IGF-1 e o G-CSF já foram descritos como fatores cardioprotetores que aumentam a proliferação endotelial e epitelial, inibem apoptose e inflamação excessiva e estimulam angiogênese no coração (BARANIAK; MCDEVITT, 2010; ZHOU et al., 2018).

### **3.2.2 Modificação genética de células-tronco mesenquimais**

Embora as terapias com CTMs tenham se mostrado seguras e com efeitos terapêuticos para tratar um grande espectro de doenças, alguns estudos têm demonstrado baixa eficácia terapêutica dessas células quando utilizadas isoladamente (HUANG, 2012). Muitas vezes, a falha terapêutica está associada à incapacidade de sobrevivência, retenção ou enxertia das CTMs no ambiente de lesão (PARK et al., 2015). Já foi descrito que as CTMs transplantadas,

quando expostas a microambientes na presença de processos inflamatórios e estresse oxidativo, entram em apoptose (SHI; LI, 2008).

Para melhorar a sua eficácia terapêutica, as CTMs podem ser modificadas geneticamente utilizando ferramentas da engenharia genética que visam, principalmente, a introdução de genes para codificação de agentes terapêuticos, bem como genes com atuação anti-apoptótica que favorecem a sobrevivência das CTMs após o transplante (WYSE et al., 2014). Além disso, tem sido bastante explorada a introdução de modificações da superfície celular e adição de genes que codificam para citocinas e quimiocinas que atuam no direcionamento das CTMs para sítios específicos (PARK et al., 2015). Na maioria das vezes, o principal objetivo destas modificações genéticas tem sido suplementar o repertório dos fatores e moléculas bioativas secretadas pelas CTMs.

A fim de aprimorar e direcionar a eficiência terapêutica, vários métodos já foram descritos para modificar geneticamente as CTMs. De maneira geral, essas técnicas podem ser classificadas como as que utilizam vetores virais ou as que usam métodos não-virais (SAGE; THAKRAR; JANES, 2016).

Dentre todos os sistemas de transferência gênica já descritos, os virais são os mais utilizados, devido principalmente à alta eficiência de transdução celular alcançada. Além disso, a maioria dos sistemas virais utilizam vírus deficientes em replicação, através da deleção de genes responsáveis pela replicação viral. Esta característica garante a segurança do processo, já que o vírus é capaz de transferir seu material genético para células-alvo, mas não tem a habilidade de se replicar e dar continuidade ao seu ciclo infeccioso (NARDI et al., 2002).

Apesar dos métodos que utilizam vetores virais terem demonstrado alta eficiência de transdução, a utilização na prática clínica tem sido limitada pelo alto custo na produção das linhagens celulares e a possibilidade de reações imunológicas adversas, ou mesmo a ocorrência de mutagênese insercional podendo levar à ativação de oncogenes (PARK et al., 2015).

Os métodos não-virais, por outro lado, são mais custo-efetivos, são passíveis de fabricação em larga escala e possuem baixa imunogenicidade. O grupo de vetores não-virais inclui o DNA na forma plasmidial e lipossomas (LI; HUANG, 2000).

Atualmente, os métodos utilizados para modificação genética de CTMs que utilizam vetores não-virais podem ser divididos em físicos ou químicos. Os métodos físicos utilizados em CTMs contemplam as técnicas de eletroporação, nucleofecção e sonoporação (OTANI et

al., 2009; BARANIAK; MCDEVITT, 2010; CANTINIEUUX et al., 2013). Já os métodos químicos utilizam agentes lipídicos, polímeros e nanopartículas inorgânicas (USHIMURA et al., 2007; PARK et al., 2010; SANTOS et al., 2011). Apesar da utilização de vetores não-virais apresentar algumas vantagens para o processo de modificação genética de CTMs comparado aos vetores virais, o comprometimento da viabilidade celular, a baixa eficiência e a expressão transitória dos transgenes tornam esses métodos menos utilizados na prática (MAROFI et al., 2017).

### 3.2.2.1 Vetores virais para modificação genética de CTMs

A utilização de vetores virais nos protocolos de modificação genética de CTM é o mais requerido para este fim, pois foi demonstrado que a alta eficiência da transdução viral nessas células (aproximadamente 90%) não afeta suas características imunofenotípicas, bem como seu potencial de diferenciação celular e secreção de moléculas bioativas, que são preservados após a modificação genética (DELCAIRE et al., 2005; BIANCONE et al., 2012). Além disso, a transdução viral garante a transcrição do gene de interesse de forma estável e à longo prazo, o que garante maior eficiência desses métodos comparado aos outros que não utilizam vetores virais como ferramenta de modificação genética de CTMs (SAGE; THAKRAR; JANES, 2016). Os principais vírus utilizados como vetores de transferência gênica são o adenovírus, o vírus adeno-associado e o retrovírus (SOMIA; VERMA, 2000; GNECCHI et al., 2009). O último grupo abrange os lentivírus, vetor empregado no desenvolvimento das linhagens de CTMs utilizadas neste trabalho.

### 3.2.2.2 Adenovírus e vírus adeno-associado

Os adenovírus são vetores da família *Parvoviridae* que apresentam forte tropismo por células humanas. Os vetores adenovirais não se integram ao genoma do hospedeiro e podem infectar tanto células em divisão como quiescentes, com alta eficiência. A obtenção de altos títulos dos vetores recombinantes é relativamente fácil com pouco efeito citotóxico para as células empacotadoras. No entanto, a alta imunogenicidade e a expressão transiente do transgene limitam sua aplicação na prática clínica (SOMIA; VERMA, 2000; NARDI et al.,

2002). O desfecho morte já foi descrito como consequência de uma forte resposta inflamatória sistêmica após transferência gênica *in vivo* utilizando vetor adenoviral (RAPER et al., 2003).

Já os vírus adeno-associados, são os vetores virais mais promissores e o primeiro aprovado para terapia gênica, pois são de baixa imunogenicidade, patogenicidade e sua integração no genoma do hospedeiro é mais específica (YLA-HERTYUALA, 2012). No entanto, os vírus adeno-associados são dependentes de genes extras para replicação, os quais são fornecidos por adenovírus. Seus genes estruturais são citotóxicos para as células empacotadoras, o que dificulta a obtenção de altos títulos dos vetores recombinantes. Além disso, existe uma limitação no tamanho do transgene carregado e a possível perda de integração sítio-dirigida tem reduzido a utilização desses vetores (SOMIA; VERMA, 2000; NARDI et al., 2002; SAGE; THAKRAR; JANES, 2016). Outro fator limitante, é a ação de anticorpos neutralizantes presentes em grande parte da população, o que reduz drasticamente sua eficácia *in vivo* (NAYAK; HERZOG, 2010).

### 3.2.2.3 Retrovírus e lentivírus

Os sistemas de transdução celular baseados na utilização de retrovírus são altamente eficientes, pois eles são capazes de se integrar ao genoma do hospedeiro e dessa forma garantem a expressão estável e a longo prazo do gene de interesse (KARSHIEVA; KRASIKOV; BELIAVSKII, 2013).

Os retrovírus são vírus de RNA constituído por três genes essenciais: *gag*, *pol* e *env*, que codificam a proteína estrutural, a transcriptase reversa/intergrase e a glicoproteína do envelope viral, respectivamente. Esses genes são dispostos em plasmídeos distintos e separadamente para as células empacotadoras a fim de evitar a recombinação ou geração de retrovírus competentes para replicação viral.

A obtenção de altos títulos virais é relativamente fácil utilizando esses vetores, no entanto, a maior limitação dos vetores retrovirais consiste em sua inabilidade de infectar células quiescentes (SOMIA; VERMA, 2000). Por outro lado, os lentivírus, que assim como os retrovírus, fazem parte da família *retroviridae*, os quais adquiriram a propriedade de transduzir células em divisão e quiescentes (LEWIS; HENSEL; EMERMAN, 1992). A maioria dos vetores lentivirais se baseiam no genoma do HIV, sendo, portanto, mais complexos. Além dos genes estruturais flanqueados por duas sequências terminais repetidas

(LTR - *long terminal repeats*), estão presentes também, pelo menos, dois genes acessórios *tat* e *rev*, fundamentais para replicação *in vitro* (SOMIA; VERMA, 2000).

Atualmente, os vetores lentivirais são os mais utilizados na terapia gênica, pois garantem alta eficiência do processo (LIECHTENSTEIN; JANICES; ESCORS, 2013). No entanto, o número de estudos clínicos de fase I que avaliam a segurança de terapias gênicas que utilizam lentivírus têm crescido nos últimos anos (SAGE; THAKRAR; JANES, 2016). O fato dos lentivírus se integrarem no genoma do hospedeiro de forma randômica e aleatória, pode levar a ocorrência de mutagênese insercional, resultando em ativação de oncogenes . Evento como esse, foi observado em quatro de um número total de quinze pacientes de terapia gênica que utilizaram retrovírus como vetor viral para corrigir mutações genéticas (HACEIN-BEY-ABINA et al., 2008).

Recentemente, as ferramentas de modificação genética foram aprimoradas a fim de direcionar a inserção, deleção ou correção de genes em sítios específicos do genoma. A integração de genes sítio-específica pode ser obtida utilizando ferramentas como ZNF (*Zinc finger nuclease*), TALENS (*transcription activator-like effector nuclease*) ou CRISPR/Cas9 (*clustered regularly interspaced short palindromic repeats*), que atuam através de nucleases capazes de reconhecer e direcionar a integração de genes de forma sítio-específica, tornando o processo de transdução celular altamente eficiente e mais seguro (PARK et al., 2015).

### **3.3 Terapia celular em cardiologia**

A utilização de células-tronco na terapia celular contempla uma ampla gama de produtos que são mais comumente classificados de acordo com o tipo de célula que se pretende utilizar. Atualmente, os tipos celulares mais estudados são as células-tronco hematopoiéticas, células-tronco mesenquimais, células-tronco embrionárias, células-tronco pluripotente induzidas, e células T modificadas (SAGE; THAKRAR; JANES, 2016).

O capítulo da terapia celular em cardiologia se iniciou com os primeiros estudos a partir da década de 90, nos quais foram utilizados diversos tipos celulares, incluindo os cardiomiócitos fetais (PFEFFER e BRAUNWALD, 1990), mioblastos esqueléticos (EGLITIS et al., 1997; FERRARI et al., 1998; JACKSON et al., 1999), fibroblastos (VOGEL et al., 2000), e CT embrionárias (ORLIC et al., 1993). No início dos anos 2000, os pesquisadores começaram a utilizar CT derivadas da medula óssea para regenerar lesões no miocárdio (FERRARI et al., 1998; JACKSON, et al., 1999). A partir desse momento, a pesquisa com CT

creceu exponencialmente e outros tipos celulares foram testados, dentre esses estão as células-tronco progenitoras endoteliais (DAI et al., 2005), células-tronco mesenquimais (NAGAYA *et al*, 2005; HUANG et al., 2010; MARTIRE et al., 2016), células-tronco pluripotentes induzidas (NELSON *et al*, 2009), e células-tronco cardíacas (BELTRAMI et al., 2003; OH et al., 2003; MARTIN et al, 2004; SILVA et al., 2014; MALLIARAS et al., 2016).

No Brasil, a eficácia da terapia com células derivadas da medula óssea foi testada em quatro diferentes cardiopatias: doença isquêmica do coração aguda e crônica, cardiomiopatia chagásica e cardiomiopatia dilatada, em um estudo financiado pelo Ministério da Saúde, através do Estudo Multicêntrico Randomizado de Terapias Celulares em Cardiopatias (*Multicenter Randomized Trial of Cell Therapy in Cardiopathies – MiHeart Study*). Parte deste estudo foi realizado pelo nosso grupo, que desenvolve pesquisas em terapia celular e realizou o estudo pioneiro, no Hospital Santa Izabel da Santa Casa de Misericórdia da Bahia, em cooperação com a FIOCRUZ/ BA, incluindo pacientes com insuficiência cardíaca grave de etiologia chagásica (DOS-SANTOS et al., 2012).

Esses primeiros estudos, desencadearam a busca por novos tipos celulares e novas estratégias terapêuticas, como tentativa de obtenção de resultados melhores no processo de regeneração do miocárdio lesado, já que os resultados descritos nestes estudos demonstraram um benefício discreto na melhora da função cardíaca. Desde então, os pesquisadores têm dirigido o foco para populações celulares mais homogêneas e bem definidas, bem como também populações celulares capazes de serem modificadas geneticamente para potencializar os efeitos da terapia celular.

Diversos estudos têm demonstrado o potencial terapêutico das CTMs em doenças de diferentes etiologias, tais como câncer (LAZENNEC; JORGENSEN, 2008), GVHD (LE BLANC et al., 2008), acidente vascular cerebral (GERVOIS et al., 2016), e infarto do miocárdio (HARE et al., 2012). As CTMs também estão sendo utilizadas para o reparo e regeneração tecidual nos casos em que a diferenciação celular é direcionada para tipos celulares específicos, como células do tecido ósseo e cartilaginoso (DORAN, 2015). Atualmente, existem mais de 500 ensaios clínicos registrados no banco de estudos clínicos do NIH que utilizam CTM, sendo 17 deles realizados no Brasil (<http://www.clinicaltrials.gov>; acessado em agosto de 2018).

Alguns estudos têm demonstrado o efeito benéfico da terapia celular utilizando CTMs para o tratamento de diferentes cardiopatias (JADCZIK et al., 2017). Inicialmente, Orlic e colaboradores (2001) relataram sucesso na regeneração do miocárdio de camundongos

infartados após o tratamento com CTM. Em seguida, outro grupo de pesquisadores demonstrou a regeneração do miocárdio em cinco pacientes com histórico de infarto que foram tratados com CTMs autólogas (STAMM et al., 2003). Outro estudo clínico envolvendo um grupo de 69 pacientes que foram submetidos à intervenção coronária percutânea, com até 12 horas após o infarto do miocárdio, foi randomizado para receber infusão de CTM autólogas ou placebo. Os dados evidenciam que o tratamento com CTM resultou em significativa melhora na função ventricular esquerda (CHEN et al., 2004). O estudo do potencial terapêutico das CTMs em cardiologia permanece bastante explorado. Atualmente, aproximadamente 15 estudos de fase II/III estão sendo realizados com CTMs derivadas da medula óssea, tecido adiposo e geleia de Wharton para tratar doenças cardíacas, tais como infarto agudo do miocárdio, cardiopatia isquêmica crônica e angina refratária (MAJKA et al., 2017; JADCZYK et al., 2017). Porém, atualmente, o potencial terapêutico das CTMs em cardiologia tem sido questionado, uma vez que foram demonstrados benefícios muito discretos relacionados à regeneração tecidual e melhora da função cardíaca.

Na doença de Chagas, o potencial terapêutico das CTMs ainda não foi explorado em estudos clínicos. No entanto, em modelos experimentais, as CTMs isoladas de diferentes fontes, tais como coração, tecido adiposo, e medula óssea já foram testadas com resultados bastante promissores quanto ao potencial imunomodulatório, porém limitados quanto ao potencial regenerativo do miocárdio (LAROCCA et al., 2013; SILVA et al., 2014; JASMIN et al., 2014; MELLO et al., 2015). Foi demonstrado pelo nosso grupo que as CTMs adotam um fenótipo cardíaco, expressando marcadores cardioespecíficos, porém falham na diferenciação em cardiomiócitos funcionais (SILVA et al., 2014).

Com base nos dados obtidos nestes estudos, é possível que algumas das melhoras cardíacas que são descritas após a infusão das CTMs em doenças do coração não estejam relacionadas com a geração de novos cardiomiócitos, mas sejam fruto dos efeitos tróficos que elas exercem sobre o tecido cardíaco ou sistemicamente. Tais resultados reforçam a necessidade de mais estudos que esclareçam os mecanismos de ação das CTMs no reparo tecidual. É possível que as CTMs atuem de maneira benéfica no coração por pelo menos três mecanismos: (1) Aumento da vascularização por meio do estímulo a angiogênese e diferenciação em células endoteliais; (2) reparo miogênico pela liberação de fatores que previnem a apoptose dos cardiomiócitos; (3) produção de citocinas e outros fatores que promovem a imunomodulação e redução de fibrose (ORLIC et al., 2001; MAJKA et al., 2017).



O desenvolvimento de ferramentas capazes de modificar geneticamente CTM ampliou o entendimento e a possibilidade de utilização dessas células em medicina regenerativa, principalmente na área da engenharia tecidual. Utilizando estas ferramentas, as CTMs foram modificadas geneticamente para expressão de genes e fatores que resultaram em melhorias expressivas da recuperação cardíaca. Atualmente, são descritos aproximadamente 20 tipos de CTMs geneticamente modificadas, que foram utilizadas para aumentar a eficácia da terapia com CTM no tratamento de doenças cardíacas (Figura 2). Os principais benefícios obtidos com a utilização dessas células se resumem ao aumento da sobrevivência, migração e enxertia celular nas áreas de lesão, bem como aumento da secreção de fatores pró-regenerativos, angiogênicos e anti-fibróticos. Juntos, esses efeitos potencializaram a capacidade regenerativa que a terapia com CTM oferece, promovendo um benefício adicional a regeneração do miocárdio e melhora da função cardíaca (JADCZYK et al., 2017).

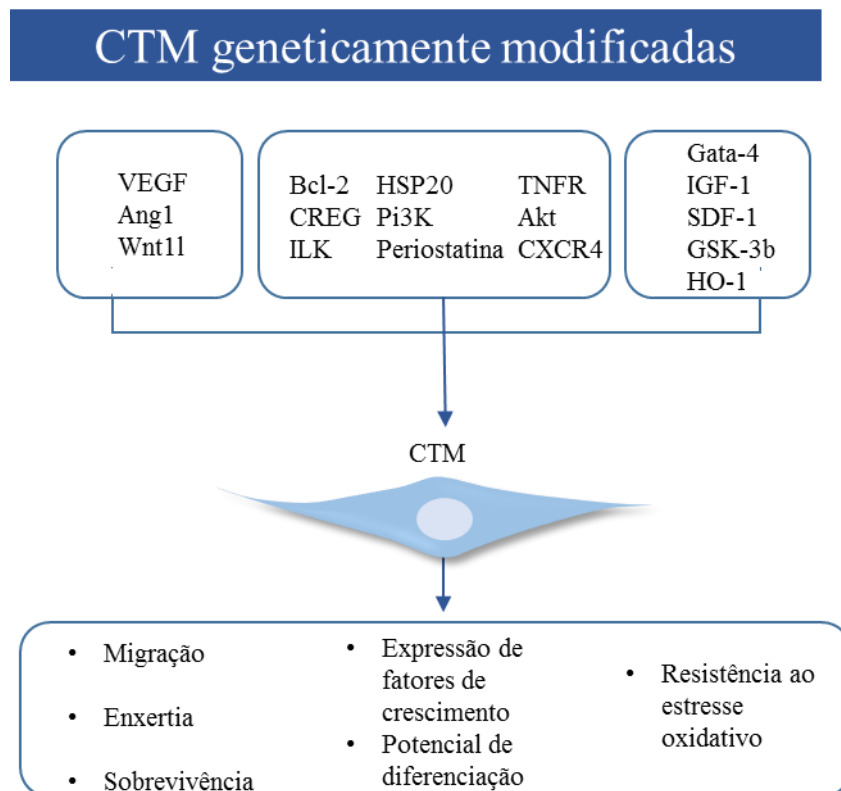


**Figura 2: Efeitos da terapia celular utilizando células-tronco mesenquimais modificadas geneticamente para o tratamento de doenças cardíacas.** VEGF (fator de crescimento endotelial vascular), Ang1 (Angiopietina-1), CREG (*cellular repressor of E1 stimulated genes*), Hsp20 (*heat shock protein 20*), Pi3K (fosfotidil 3 quinase), ILK (quinase ligada à integrina), TNFR (receptor de TNF $\alpha$ ), CXCR4 (receptor de quimiocina 4), HO-1 (heme oxigenase 1), GSK-3b (glicogêniosintase quinase), IGF-1 (fator semelhante à insulina 1), SDF-1 (fator derivado de célula estromal 1). Adaptado de JADCZYK et al., 2017.

Neste trabalho, enfocaremos nas atividades parácrinas e autócrinas dos fatores G-CSF e IGF-1, secretados por CTMs modificadas geneticamente, descritos como potenciais fatores para regeneração tecidual no tratamento da cardiopatia chagásica crônica experimental.

### 3.4 FATOR ESTIMULADOR DE COLÔNIAS DE GRANULÓCITOS (G-CSF)

O G-CSF é uma glicoproteína, comumente utilizado na prática clínica para mobilizar células-tronco da medula óssea para a circulação periférica com o objetivo de aumentar o número de células-tronco hematopoiéticas para coleta e uso no transplante de medula óssea autólogo (ANDERLINI; CHAMPLIN, 2007). Foi evidenciado que o G-CSF induz a quimiotaxia mediada pelo fator derivado de células estromais, o SDF-1, através do aumento da expressão do receptor de superfície, CXCR4, em células-tronco hematopoiéticas. Este estudo esclarece um dos principais mecanismos envolvidos na regulação biológica da mobilização de células progenitoras da medula óssea para circulação (PETIT et al., 2002).

No coração, foi demonstrado inicialmente que as CT da medula óssea que são mobilizadas para a área de infarto agudo do miocárdio são capazes de se diferenciarem em cardiomiócitos, por efeito do G-CSF (KAWADA et al., 2004). Em seguida, foram realizados estudos que avaliaram o efeito do G-CSF em lesões isquêmicas cardíacas, com redução da mortalidade e remodelamento cardíaco, inclusive quando administrado concomitantemente com células-tronco derivadas da medula óssea (ORLIC et al., 2001). Ainda no modelo de infarto, o G-CSF foi descrito como um fator que regula a síntese de colágeno, ação que contribui para prevenção do remodelamento cardíaco e estímulo da angiogênese em áreas infartadas (IWANAGA et al., 2004; HARADA et al., 2005; SUGANO et al., 2005). Já foi demonstrado que o uso do G-CSF juntamente com o transplante de CT da medula óssea, em pacientes com falência cardíaca refratária não-isquêmica, mostrou-se eficaz em melhorar a fração de ejeção, aumentar a classe funcional dos pacientes submetidos ao tratamento, como também promoveu a melhora da qualidade de vida dos pacientes (BOCCHI et al., 2010). Alguns estudos atribuíram aos efeitos benéficos do G-CSF na cardiopatia isquêmica e no infarto agudo experimentais à indução da neovascularização e aumento de conexina 43 no coração, uma proteína responsável pela comunicação intercelular de cardiomiócitos e células vizinhas (IWANAGA et al., 2004; HARADA et al., 2005; FUJITA et al., 2007).

Na doença de Chagas, nossos estudos demonstraram que a administração repetida de G-CSF induziu efeitos benéficos na estrutura cardíaca, tais como redução da inflamação e

fibrose no coração dos animais infectados cronicamente pelo *T. cruzi* (MACAMBIRA et al., 2009; VASCONCELOS et al., 2013). Nestes trabalhos, foram descritos benefícios na função cardíaca por análise eletrocardiográfica e ergométrica e redução da inflamação com aumento do número de células inflamatórias apoptóticas e mobilização de células T regulatórias para o coração de camundongos chagásicos após o uso do G-CSF (VASCONCELOS et al., 2013). No entanto, os mecanismos de ação envolvidos na ação benéfica do G-CSF sobre a recuperação da função cardíaca na cardiomiopatia chagásica experimental ainda não foram elucidados.

O G-CSF possui um amplo efeito na resposta imune inata, especialmente sobre monócitos / macrófagos, promovendo expansão e reforço da fagocitose e regulação da produção de citocinas inflamatórias. G-CSF foi caracterizado como um dos principais reguladores extracelulares da hematopoese e da resposta imune inata. Alguns estudos têm demonstrado que este fator possui função importante também sobre a resposta imune adaptativa. Estudos em modelos experimentais *in vivo*, *in vitro*, além de estudos clínicos, indicam que o G-CSF altera a função de células T e modula a ação de outras células, tais como células NK e dendríticas (FRANZKE et al., 2006; MARTINS; HAN; KIM, 2010; MELVE et al., 2016).

Recentemente, foi demonstrado que o G-CSF pode atuar sobre outras células do sistema imune através do recrutamento e ativação de células supressoras de origem mielóide (MDSC) (WAIGHT et al., 2011). Os estudos em câncer demonstraram que o G-CSF secretado pelas células do estroma tumoral atua sobre a mobilização e ativação de MDSCs, as quais modulam fortemente a resposta imune a favor do tumor, permitindo o crescimento tumoral (WAIGHT et al., 2011; TALMADGE; GABRILOVICH, et al., 2013). Na doença de Chagas, as MDSCs têm um papel importante no controle da inflamação durante a infecção pelo *T. cruzi*. Um dos mecanismos de imunomodulação dessas células está relacionado à sua capacidade de suprimir a proliferação de linfócitos dos infiltrados inflamatórios na miocardite causada pelo *T. cruzi* (CUERVO et al., 2011). Além disso, Arocena e colaboradores mostraram que a depleção farmacológica de MDSCs, seguida da infecção pelo *T. cruzi*, aumenta a susceptibilidade ao parasito (AROCENA et al., 2014).

Já foi descrito que o G-CSF atua na resposta imune adaptativa através da polarização das células T para uma resposta Th2, o que sugere ser um dos principais mecanismos envolvidos com sua propriedade imunomoduladora (FRANZKE et al., 2006). Foi demonstrado que as ações do G-CSF na mobilização de células da medula para o sangue

periférico regulam a ativação e diferenciação de linfócitos T via IL-10, favorecendo um ambiente de resposta inflamatória mais tolerante com a participação de células T regulatórias CD4<sup>+</sup>/CD25<sup>+</sup> (MACDONALD et al., 2014; PROBELLI, et al 2016). Outro mecanismo de imunomodulação do G-CSF é descrito através do aumento da regulação da expressão do GATA-3, direcionando e estabilizando o perfil de resposta Th2 mais regulatória, enquanto se opõe à diferenciação para uma resposta Th1 mais inflamatória e lesiva para o organismo (FRANZKE et al., 2006). Sendo assim, o G-CSF representa um fator com potencial terapêutico que pode ser mais explorado no contexto do tratamento da cardiomiopatia chagásica crônica da doença de Chagas.

### 3.5 FATOR DE CRESCIMENTO SEMELHANTE À INSULINA-1 (IGF-1)

Os IGFs compreendem uma família de peptídeos importantes para o crescimento e desenvolvimento dos mamíferos, com propriedades mitogênicas e regeneradoras conhecidas. Foi demonstrado, inicialmente, que a principal função dos IGFs era mediar os efeitos de crescimento do hormônio do crescimento, o GH (FLORINI; EWTON; COOLICAN, 1996). Posteriormente, outras ações biológicas foram descritas, e as principais delas contemplam o estímulo a proliferação e diferenciação celular, bem como ações com efeito regenerativo em tecidos expostos a situações de estresse oxidativo, isquemia e hipóxia. (NAKAE; KIDO; ACCILI, 2001; CONTI et al., 2011).

Como a maioria dos fatores de crescimento, o IGF-1 e IGF-2 são produzidos amplamente pelo organismo, sendo o fígado a principal fonte do peptídeo circulante (MURPHY; BEL; FRISSEN et al., 1987). Os efeitos biológicos dos IGFs são mediados por receptores específicos, que são identificados por receptores do tipo I e II. No caso de IGF-1, seus receptores são encontrados em adipócitos, mioblastos, cardiomiócitos, condrócitos, fibroblastos, células endoteliais e hepatócitos (JONES; CLEMMONS, 1995).

A ligação de IGF-1 ao seu receptor IGF1R induz a ativação de tirosinas quinases que promovem a sinalização celular pela ativação da cascata de proteínas da via PI3K/Akt/mTOR (LAVIOLA; NATALICCHIO; GIORGINO, 2007). A ativação dessa via é iniciada pela ação da proteína quinase de membrana PI3k (fosfoinositol 3 quinase) que ativa a Akt. A ativação da PI3k por meio de um ligante específico e seu receptor (IGF-1-IGF-1R) irá fosforilar o fosfolípido de membrana PI2p e converte-o em PI3p que criará um sítio de ligação para a Akt, que por sua vez será fosforilado (Figura 3). A ativação da via de sinalização PI3K/Akt

tem como função principal a inibição de moléculas pró-apoptóticas além disso, estimulam a proliferação, hipertrofia e diferenciação de células musculares esqueléticas (HUANG et al., 2011).

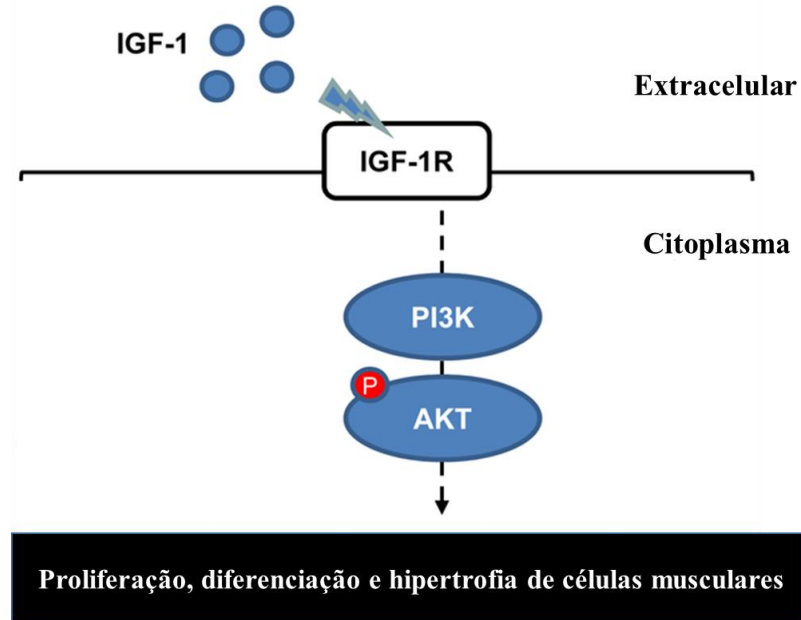


**Figura 3:** Efeitos da interação do IGF-1 e seu receptor na ativação da via PI3k/Akt no músculo esquelético.

A ativação da via PI3K/Akt pelo IGF-1 tem resultado em efeitos promissores para a terapia celular. Enoki e colaboradores, descreveram a potencialização dos efeitos terapêuticos de células-tronco mesenquimais pelo IGF-1, através da inibição de apoptose das CTM e dos cardiomiócitos submetidas à hipóxia. Foi observado também, aumento da enxertia celular na área de lesão do miocárdio, angiogênese e melhora da função cardíaca (ENOKI et al., 2010). Outro estudo também demonstrou que o IGF-1 aumentou os benefícios provenientes do transplante de mioblastos em modelos de infarto, através da prevenção de apoptose, indução de angiogênese e proliferação de mioblastos (KANEMITSU et al., 2006).

Assim como o G-CSF, o IGF-1 aumenta a resposta migratória de CTMs através do aumento da expressão do receptor de SDF-1 e CXCR4 (LI et al., 2007). No modelo de infarto, GUO e colaboradores, atribuiu a eficiência terapêutica do transplante de CTMs à potencialização do efeito migratório do IGF-1 sobre as CTMs, resultando numa mobilização maior de células para a área infartada do coração (GUO et al., 2008).

No músculo esquelético, o IGF-1 atua nos processos de hiperplasia e hipertrofia muscular. Utilizando um modelo animal transgênico para a superexpressão de IGF-1, foi

demonstrado que a capacidade regenerativa do músculo esquelético é estimulada pelo IGF-1 principalmente por ele atuar, tanto na ativação de células satélites, como na mobilização periférica de células-tronco (MUSARO et al, 2001; MUSARO et al., 2004). As células satélites representam uma população celular multipotente residente do músculo esquelético, que se encontram no estado quiescente em condições fisiológicas (SERRANO et al., 2008). Os processos relacionados à ativação, diferenciação e proliferação das células satélites são regulados pela ação de hormônios como a testosterona, insulina e por fatores de crescimento como GH, VEGF, HGF, IGF-1, ou por citocinas e mediadores inflamatórios, tais como IL-6 e prostaglandina E2 (KADI et al., 2004; HO et al.,2017).

## 4 OBJETIVOS

### 4.1 OBJETIVO GERAL

Investigar o potencial terapêutico de células-tronco mesenquimais da medula óssea geneticamente modificadas em camundongos cronicamente infectados pelo *T. cruzi*.

### 4.2 OBJETIVOS ESPECÍFICOS

- 1) Investigar os efeitos da terapia celular utilizando CTMs que superexpressam hG-CSF ou hIGF-1 na inflamação e fibrose nos corações de camundongos chagásicos crônicos;
- 2) Comparar o perfil de citocinas e fatores de transcrição expressos no coração dos animais chagásicos tratados e não tratados com CTMs que superexpressam hG-CSF e hIGF-1;
- 3) Avaliar a capacidade migratória das CTMs que superexpressam hG-CSF ou hIGF-1 para o coração e músculo esquelético de camundongos chagásicos crônicos;
- 4) Investigar os efeitos da terapia celular utilizando CTMs que superexpressam hG-CSF na função cardíaca;
- 5) Avaliar o potencial terapêutico das CTM que superexpressam hG-CSF na mobilização de populações celulares imunossupressoras no coração de camundongos chagásicos crônicos;
- 6) Avaliar o potencial pró-regenerativo das CTMs que superexpressam hIGF-1 no músculo esquelético de camundongos chagásicos crônicos.

## 5 RESULTADOS

### CAPÍTULO I

Neste capítulo, descrevemos os efeitos imunomoduladores da terapia com células-tronco mesenquimais que superexpressam hG-CSF por meio do recrutamento de células imunossupressoras no modelo experimental de cardiopatia chagásica crônica.

Artigo publicado na revista *Frontiers in Immunology*, vol.9, article 1449, 25 de junho de 2018.  
doi: 10.3389/fimmu.2018.01449

**Granulocyte Colony Stimulating Factor-overexpressing mesenchymal stem cells exhibit enhanced immunomodulatory actions through the recruitment of suppressor cells in experimental Chagas disease cardiomyopathy**

Daniela N. Silva, Bruno S. F. Souza, Juliana F. Vasconcelos, Carine A. Azevedo, Clarissa V. X. R. Valim, Bruno D. Paredes, Vinicius P. C. Rocha, Gisele B. Carvalho, Pamela S. Daltro, Simone G. Macambira, Carolina K. V. Nonaka, Ricardo Ribeiro-dos-Santos, Milena B. P. Soares.





# Granulocyte-Colony Stimulating Factor-Overexpressing Mesenchymal Stem Cells Exhibit Enhanced Immunomodulatory Actions Through the Recruitment of Suppressor Cells in Experimental Chagas Disease Cardiomyopathy

## OPEN ACCESS

### Edited by:

Celio Geraldo Freire-de-Lima,  
Universidade Federal do Rio de  
Janeiro, Brazil

### Reviewed by:

Marcin Wysoczynski,  
University of Louisville,  
United States  
Fernanda Fortes De Araújo,  
Fiocruz Research Center René  
Rachou, Brazil

### \*Correspondence:

Milena B. P. Soares  
milena@bahia.fiocruz.br

### Specialty section:

This article was submitted to  
Microbial Immunology,  
a section of the journal  
Frontiers in Immunology

Received: 09 March 2018

Accepted: 11 June 2018

Published: 25 June 2018

### Citation:

Silva DN, Souza BSF,  
Vasconcelos JF, Azevedo CM,  
Valim CXR, Paredes BD, Rocha VPC,  
Carvalho GB, Daltro PS,  
Macambira SG, Nonaka CKV,  
Ribeiro-dos-Santos R and  
Soares MBP (2018) Granulocyte-  
Colony Stimulating Factor-  
Overexpressing Mesenchymal  
Stem Cells Exhibit Enhanced  
Immunomodulatory Actions  
Through the Recruitment of  
Suppressor Cells in Experimental  
Chagas Disease Cardiomyopathy.  
Front. Immunol. 9:1449.  
doi: 10.3389/fimmu.2018.01449

Daniela N. Silva<sup>1,2</sup>, Bruno S. F. Souza<sup>1,2,3</sup>, Juliana F. Vasconcelos<sup>1,2</sup>, Carine M. Azevedo<sup>1,2</sup>, Clarissa X. R. Valim<sup>1</sup>, Bruno D. Paredes<sup>1,3</sup>, Vinicius P. C. Rocha<sup>1,2</sup>, Gisele B. Carvalho<sup>1</sup>, Pamela S. Daltro<sup>1</sup>, Simone G. Macambira<sup>1,4</sup>, Carolina K. V. Nonaka<sup>1,2</sup>, Ricardo Ribeiro-dos-Santos<sup>1,3</sup> and Milena B. P. Soares<sup>1,2,3\*</sup>

<sup>1</sup> Center for Biotechnology and Cell Therapy, Hospital São Rafael, Salvador, Brazil, <sup>2</sup> Gonçalo Moniz Institute, FIOCRUZ, Salvador, Brazil, <sup>3</sup> National Institute of Science and Technology for Regenerative Medicine, Rio de Janeiro, Brazil, <sup>4</sup> Federal University of Bahia (UFBA), Salvador, Brazil

Genetic modification of mesenchymal stem cells (MSCs) is a promising strategy to improve their therapeutic effects. Granulocyte-colony stimulating factor (G-CSF) is a growth factor widely used in the clinical practice with known regenerative and immunomodulatory actions, including the mobilization of regulatory T cells (Tregs) and myeloid-derived suppressor cells (MDSCs). Here we evaluated the therapeutic potential of MSCs overexpressing G-CSF (MSC\_G-CSF) in a model of inflammatory cardiomyopathy due to chronic Chagas disease. C57BL/6 mice were treated with wild-type MSCs, MSC\_G-CSF, or vehicle (saline) 6 months after infection with *Trypanosoma cruzi*. Transplantation of MSC\_G-CSF caused an increase in the number of circulating leukocytes compared to wild-type MSCs. Moreover, G-CSF overexpression caused an increase in migration capacity of MSCs to the hearts of infected mice. Transplantation of either MSCs or MSC\_G-CSF improved exercise capacity, when compared to saline-treated chagasic mice. MSC\_G-CSF mice, however, were more potent than MSCs in reducing the number of infiltrating leukocytes and fibrosis in the heart. Similarly, MSC\_G-CSF-treated mice presented significantly lower levels of inflammatory mediators, such as IFN $\gamma$ , TNF $\alpha$ , and Tbet, with increased IL-10 production. A marked increase in the percentage of Tregs and MDSCs in the hearts of infected mice was seen after administration of MSC\_G-CSF, but not MSCs. Moreover, Tregs were positive for IL-10 in the hearts of *T. cruzi*-infected mice. *In vitro* analysis showed that recombinant hG-CSF and conditioned medium of MSC\_G-CSF, but not wild-type MSCs, induce chemoattraction of MDSCs in a transwell assay. Finally, MDSCs purified from hearts of MSC\_G-CSF transplanted mice inhibited the proliferation of activated splenocytes in a co-culture assay. Our results demonstrate

that G-CSF overexpression by MSCs potentiates their immunomodulatory effects in our model of Chagas disease and suggest that mobilization of suppressor cell populations such as Tregs and MDSCs as a promising strategy for the treatment of chronic Chagas disease. Finally, our results reinforce the therapeutic potential of genetic modification of MSCs, aiming at increasing their paracrine actions.

**Keywords:** mesenchymal stem cells, granulocyte-colony stimulating factor, immunomodulation, Chagas disease, cardiomyopathy

## INTRODUCTION

Mesenchymal stem cells (MSCs) are known to participate in tissue homeostasis and repair processes in different physiological and pathological settings (1). MSCs have the ability to migrate to injury sites and promote tissue repair through the secretion of trophic and immunomodulatory factors (2). Currently, there is great interest in investigating the therapeutic potential of MSCs, since they are easily obtainable, expandable, and can act by modulating the microenvironment through the secretion of soluble factors, with systemic repercussions (3). The results of clinical trials with MSC-based therapies, however, have frequently been heterogeneous, possibly due to product and patient heterogeneity, but also to the complexity involved in the administration of living cells that respond differently to different microenvironments, leading to unpredictable outcomes (4). Therefore, the development of strategies that can increase and optimize the paracrine actions of MSCs to enhance the effectiveness of MSC-based therapies is highly desired.

The use of genetically modified MSCs, aiming to deliver bioactive factors systemically or locally to damaged tissues may improve their therapeutic potential (5). Granulocyte-colony stimulating factor (G-CSF) has received significant attention in the regenerative medicine field due to well-known actions, especially regarding the mobilization of bone marrow-derived stem cells to the peripheral blood (6). Moreover, G-CSF exerts direct regenerative actions, including protective effects over cardiomyocytes, which express the G-CSF receptor (7). Recently, G-CSF has also been described as a tumor-derived factor that recruits and expand myeloid-derived suppressor cells (MDSCs), which secrete cytokines involved in the induction of regulatory T cells (Tregs), contributing to the immunosuppressive tumor microenvironment (8). These mechanisms of immune escape are now being applied to potentiate immunomodulatory interventions to treat inflammatory diseases (9).

Chagas disease cardiomyopathy, caused by chronic infection with *Trypanosoma cruzi*, is characterized by chronic myocardial inflammation and fibrosis due to parasite persistence and inflammation, that may ultimately lead to chronic heart failure (10). Treatment with MSCs was previously shown to be effective in promoting immunomodulation in the experimental model of Chagas disease (11, 12). After treatment with MSCs, increased levels of anti-inflammatory cytokines, such as TGF- $\beta$  or IL-10, were induced in mice chronically infected with *T. cruzi* (11–13). Moreover, we have previously described that treatment with G-CSF in the mouse model of Chagas disease cardiomyopathy is associated with mobilization of Tregs and modulation of cardiac inflammation and fibrosis (14).

Due to its beneficial properties and different mechanisms of actions of G-CSF and MSCs, we hypothesized that G-CSF-overexpressing MSCs (MSC\_G-CSF) present increased therapeutic actions in chronic Chagas disease, through the synergistic association of MSCs' paracrine actions with the effects of local release of G-CSF in the myocardium. Therefore, in this study we investigated the therapeutic potential of MSC\_G-CSF in a mouse model of chronic Chagas disease, and evaluated the participation of suppressor cells in the control of this inflammation-driven cardiomyopathy.

## MATERIALS AND METHODS

### Animals

Six- to eight-week-old female C57BL/6 mice were used for *T. cruzi* infection or to evaluate the number of leukocytes in the peripheral blood. Male GFP transgenic C57BL/6 mice were used for harvest of bone marrow cells and splenocytes. All animals were raised and maintained in the animal facility of the Center for Biotechnology and Cell Therapy, Hospital São Rafael (Salvador, Brazil), and provided with rodent diet and water *ad libitum*. Animals were handled according to the NIH guidelines for animal experimentation. All procedures described had prior approval from the local animal ethics committee under number 012/09 (FIOCRUZ, Bahia, Brazil).

### Cultures of MSCs

Wild-type bone marrow-derived MSCs were obtained from male GFP transgenic C57BL/6 mice. A genetically modified MSC line with stable overexpression of hG-CSF (MSC\_G-CSF) was previously generated and characterized by our group (15). MSCs were cultured in Dulbecco's Modified Eagle's Medium (DMEM) supplemented with 10% fetal bovine serum and 1% penicillin/streptomycin (ThermoFisher Scientific, Waltham, MA, USA) in a humidified incubator at 37°C and 5% CO<sub>2</sub>, with complete medium replacement every 3 days. In order to validate dose, route of administration and to assess *in vivo* biological activity of the G-CSF overexpressing MSCs, naïve C57BL/6 mice, were intraperitoneally injected with the cell suspensions, and peripheral blood was collected for 7 days for leukocyte counts. Control group was treated with vehicle (saline), under the same conditions. Mice were anesthetized with inhaled isoflurane (Abbott, Chicago, IL, USA), allowing for peripheral blood to be collected by tail vein puncture. The number of leukocytes was determined by analysis in a hematological counter BC 3000 Plus (Mindray, Shenzhen, China).

## T. cruzi Infection and Cell Therapy

Trypomastigotes of the myotropic Colombian *T. cruzi* strain were obtained from culture supernatants of infected LLC-MK2 cells. C57BL/6 mice were infected by intraperitoneal injection with 1,000 *T. cruzi* trypomastigotes in 100  $\mu$ L PBS. Six months after the infection, mice were randomly assigned into three groups for administrations of MSCs, MSC\_G-CSF, or saline. Age-matched naïve mice were used as normal controls. Cell transplantation was performed by weekly intraperitoneal injections of cell suspensions containing  $10^6$  MSCs or MSC\_G-CSF. An equal volume of vehicle (100  $\mu$ L) was used in the saline group. At different time points, mice were euthanized by cervical dislocation, under anesthesia with ketamine (100 mg/kg) and xylazine (10 mg/kg). Depending on the time point evaluated, *T. cruzi*-infected mice received one (7 days-time point), four (30 days-time point), or seven cell administrations (60 days-time point). In the latter, the fifth administration of MSCs or MSC\_G-CSF was performed by close-chest echography-guided intramyocardial injection, as previously described (11). Four independent experiments were performed.

## Flow Cytometry Analysis and Cell Sorting

Cell suspensions were obtained from digested cardiac tissue samples of infected mice treated with MSCs, MSC\_G-CSF, or saline, as previously described (16). The cell suspensions were allowed to pass through a 70  $\mu$ m cell strainer (BD Biosciences, Franklin Lakes, NJ, USA) and counted with a hemacytometer. Aliquots of  $10^6$  cells were used for each test tube and 1  $\mu$ L of Fc blocking reagent (BD Biosciences) was added. Fluorochrome-conjugated antibodies used were: CD11b-PE-Cy5, CD45-APC and GR-1-FITC, or Ly6C-FITC and Ly6C-PE (BD Biosciences). Samples were incubated with the antibodies for 20 min at RT. Sample acquisition was performed using a BD LSRFortessa SORP cytometer using BD FACS Diva v.6.2. Acquired data were analyzed by FlowJo v7.5 (FlowJo Enterprise, Ashland, OR, USA). CD11b<sup>+</sup>GR-1<sup>+</sup> MDSCs were sorted from digested hearts of MSC\_G-CSF-treated mice or from the bone marrow, as indicated in Section "Results." The cells were stained with GR-1-PE (BD Biosciences), CD11b-APC (ThermoFisher Scientific), and CD45-APC-Cy7 (BD Biosciences), using a FACS Aria cell sorter (BD Biosciences), achieving a purity of approximately 98%.

## Immunofluorescence Analyses

Frozen heart sections of 10  $\mu$ m were fixed with 4% paraformaldehyde and incubated overnight at 4°C with the following primary antibodies: anti-Foxp3 (Santa Cruz Biotechnology, Dallas, TX, USA) and anti-CD3 (BD Biosciences) or anti-IL10 (BD Biosciences) diluted 1:1,500, 1:200, and 1:50, respectively. On the following day, the sections were incubated for 1 h with secondary antibodies anti-goat IgG Alexa fluor 488-conjugated and anti-rat IgG Alexa fluor 594-conjugated diluted 1:200 (Thermo Scientific). Nuclei were stained with 4,6-diamidino-2-phenylindole (VectaShield mounting medium with DAPI H-1200; Vector Laboratories, Burlingame, CA, USA). The presence of fluorescent cells was determined by observation A1<sup>+</sup> confocal microscope (Nikon, Tokyo, Japan). Quantifications of CD3/FoxP3<sup>+</sup> cells were

performed in 10 random fields captured under 400 $\times$  magnification, using the Image Pro Plus v.7.0 software (Media Cybernetics, Rockville, MD, USA).

## MDSCs Migration Assay

Bone marrow cells were obtained from tibiae and femurs of C57BL/6 mice. Mononuclear cells were then isolated by Ficoll-Paque gradient (GE healthcare, Boston, MA, USA) and washed with PBS twice. MDSCs (CD11b/GR-1<sup>+</sup>) were obtained by FACS. Migration was evaluated using a modified 3  $\mu$ m-pore size Boyden chamber (Cell Biolabs, San Diego, CA, USA) with the lower chamber filled with serum-free conditioned media obtained from MSCs or MSC\_G-CSF, and the upper chamber filled with  $10^6$  MDSCs. DMEM (Life technologies) or DMEM supplemented with 50  $\mu$ g/mL Filgrastim (Aché, Guarulhos, Brazil) were used as controls. After 4 h, the cells in the bottom wells were counted using a hemocytometer. The experiments were performed in biological triplicates.

## Lymphocyte Proliferation Assay

Splenocytes ( $10^6$  cells/well) obtained from EGFP mice were plated in 96-well plate and stimulated with concanavalin A (Con A; 2  $\mu$ g/mL, Sigma-Aldrich, St. Louis, MO, USA). Purified MDSCs sorted from the hearts of infected mice treated with MSC\_GCSF were co-cultured in a 1:10 ratio with Con A-stimulated splenocytes. After incubation at 37°C and 5% CO<sub>2</sub> for 72 h, cell proliferation was measured as the number of GFP<sup>+</sup> proliferative blast cells for treated-cells in comparison to untreated cells. Dexamethasone was used as a positive control. Image acquisition and quantification of blasts were performed using the Operetta High Content Imaging System (Perkin Elmer, Waltham, MA, USA). Images were segmented using the Find Cells building block of the Harmony 3.5.2 software (Perkin Elmer), which provides a dedicated algorithm for segmenting digital phase-contrast images. GFP<sup>+</sup> proliferative blast cells were tracked using the Track Objects building block. The experiments were performed three times.

## Functional Analyses

Animals were anesthetized by isoflurane inhaled (0.5%) to obtain the Electrocardiography records performed using the Bio Amp PowerLab System (PowerLab 2/20; ADInstruments, Sydney, NSW, Australia), recording the bipolar lead I. All data were acquired for computer analysis using Chart 5 for Windows (PowerLab). Records were bandpass filtered (1 to 100 Hz) to minimize environmental signal disturbances. The sampling rate was 1 kHz. The ECG analysis included heart rate and arrhythmias. Treadmill test was performed 6 months after *T. cruzi* infection, as a baseline evaluation, and 8 months after infection (60 days after the treatment). A motor-driven treadmill chamber for one animal (LE 8700; Panlab, Barcelona, Spain) was used to exercise the animals. The speed of the treadmill and the intensity of the shock (mA) were controlled by a potentiometer (LE 8700 treadmill control; Panlab). Room air was pumped into the chamber at a controlled flow rate (700 mL/min) by a chamber air supplier (Oxylet LE 400; Panlab). The mean room temperature was maintained at  $21 \pm 1^\circ\text{C}$ . After an adaptation period of 20 min in the treadmill chamber, the mice exercised at five different velocities (7.2, 14.4, 21.6, 28.8,

and 36.0 m/min), with increasing velocity after 10 min of exercise at a given speed. Total running time was recorded. Velocity was increased until the animal could no longer sustain a given speed and remained 10 s on an electrified stainless-steel grid, which provided an electrical stimulus to keep the mice running.

### Morphometric Analyses

Groups of mice were euthanized 60 days after the therapy under anesthesia, 5% ketamine, and 2% xylazine, the hearts were removed and fixed in 10% buffered formalin. Heart sections were analyzed by light microscopy after paraffin embedding, followed by standard hematoxylin and eosin (H&E) staining. Inflammatory cells were counted using the software Image Pro Plus v.7.0 (Media Cybernetics). The number of inflammatory cells was determined by counting 10 fields (400× magnification) per heart section. Sirius red-stained sections were entirely digitalized using a confocal microscope A1+ (Nikon). The percentage of fibrosis was determined by analysis of whole sections stained with Sirius red-stained heart sections and semiautomatic morphometric quantification using Image Pro Plus v.7.0. Two blinded investigators performed the analyses.

### Reverse Transcription Quantitative PCR (RT-qPCR)

Total RNA was isolated from heart samples using TRIzol reagent (Thermo Scientific) and concentration was determined by photometric measurement. High Capacity cDNA Reverse Transcription Kit (Thermo Scientific) was used to synthesize cDNA of 1 µg RNA following manufacturer's recommendations. RT-qPCR assays were performed to detect the expression levels of *Tbet* (Mm00450960\_m1), *Gata3* (Mm00484683\_m1), *Tnf* (Mm00443258\_m1), *Irfng* (Mm00801778\_m1), *Nos2* (Mm01309898m1), *Arg1* (Mm00475988\_m1) *Il6* (Mm0446190\_m1), and *Il10* (Mm00439616\_m1). For the detection of GFP and human G-CSF mRNA, the following primer sequences were used in Real Time PCR assays: GFP: 5'-AGCAGAACACCCCATCG-3' and 3'-TCCAGCAGGACCATGTGATC-5'; G-CSF 5'-CTGGCAGCAGATGGAAGAACT-3' and 3'-CAGGAAGCTCTGCAGATGGGA-5'. The RT-qPCR amplification mixtures contained 20 ng template cDNA, Taqman Master Mix (10 µL), and probes in a final volume of 20 µL (all from Thermo Scientific). All reactions were run in duplicate on an ABI7500 Sequence Detection System (Thermo Scientific) under standard thermal cycling conditions. The mean Ct (Cycle threshold) values from duplicate measurements were used to calculate expression of the target gene, with normalization to an internal control (*Gapdh*) using the  $2^{-\Delta Ct}$  formula. Experiments with coefficients of variation greater than 5% were excluded. A non-template control and non-reverse transcription controls were also included. Quantification of parasites by qPCR was performed as previously described (15).

### Statistical Analyses

Statistical comparisons between groups were performed by Student's *t*-test when comparing two groups and ANOVA followed by Newman-Keuls test for multiple comparisons, using GraphPad Prism program (Software Inc., San Diego, CA, USA) version 5.0. Results were considered significant when  $P < 0.05$ .

## RESULTS

### G-CSF Overexpression Increases Peripheral Blood Leukocyte Counts and Homing of MSCs to the Hearts of *T. cruzi*-Infected Mice

In order to establish the therapeutic scheme to be used in our study, we first evaluated the duration of the biological activity of MSC\_G-CSF by measuring leukocyte mobilization (Figure S1A in Supplementary Material). A single dose ( $10^6$  cells, i.p.) of MSCs or MSC\_G-CSF was administered to naïve mice and serial hemograms were performed in the following days. As shown in **Figure 1A**, administration of either wild-type MSCs or MSC\_G-CSF increased white blood cell counts, compared to saline injected controls. Transplantation of MSC\_G-CSF, however, was associated with even higher numbers of leukocytes, compared to regular MSCs. Leukocyte numbers dropped to the level of controls, in both groups, 7 days after the transplantation (**Figure 1A**).

In order to evaluate if the cells, administered through intraperitoneal injection, could reach the heart, we performed cell transplantation and tracking in mice chronically infected with *T. cruzi* (Figure S1B in Supplementary Material). Transplanted MSCs and MSC\_G-CSF were detected in the hearts of infected mice 3 and 7 days after cell transplantation, as shown by quantification of the reporter gene GFP by RT-qPCR (**Figure 1B**). In mice transplanted with MSC\_G-CSF, however, significantly higher levels of GFP mRNA were detected in the hearts 3 days after transplantation, when compared to mice transplanted with MSCs. We were also able to detect the expression of hG-CSF mRNA in the hearts of MSC\_G-CSF-treated mice, 3 days after transplantation. Gene expression of human G-CSF, however, was not sustained, being reduced 7 days after MSC\_G-CSF transplantation (**Figure 1C**). Therefore, the following experiments were performed with repeated cell administrations (Figure S1C in Supplementary Material).

### Mobilization of MDSCs and Tregs After MSC\_G-CSF Transplantation

Since G-CSF is known to induce the mobilization of immune regulatory cells (17), we evaluated the presence of MDSCs and Tregs in the hearts of *T. cruzi*-infected mice 30 days after the beginning of the cell therapy protocol. In order to evaluate the recruitment of MDSCs, hearts of *T. cruzi*-infected mice were digested for analysis of CD11b<sup>+</sup>GR-1<sup>+</sup>, CD11b<sup>+</sup>Ly6C<sup>+</sup>, and CD11b<sup>+</sup>Ly6G<sup>+</sup> by flow cytometry (**Figure 2A**). The percentage of MDSCs in both saline and MSCs groups was similar, while MSC\_G-CSF significantly increased the percentage of the monocytic subset (M-MDSC) (CD11b<sup>+</sup>Ly6C<sup>+</sup>Ly6G<sup>-</sup>) within the infiltrating CD11b<sup>+</sup> population (**Figure 2B**).

In order to evaluate whether MSC\_G-CSF-derived secreted factors could induce the recruitment of MDSCs, we performed an *in vitro* chemotaxis assay, using CD11b<sup>+</sup>GR-1<sup>+</sup> cells sorted from the bone marrow of naïve mice. Conditioned media from MSCs or MSC\_G-CSF cultures or human recombinant G-CSF were placed in the lower chamber of transwell plates, while MDSCs were

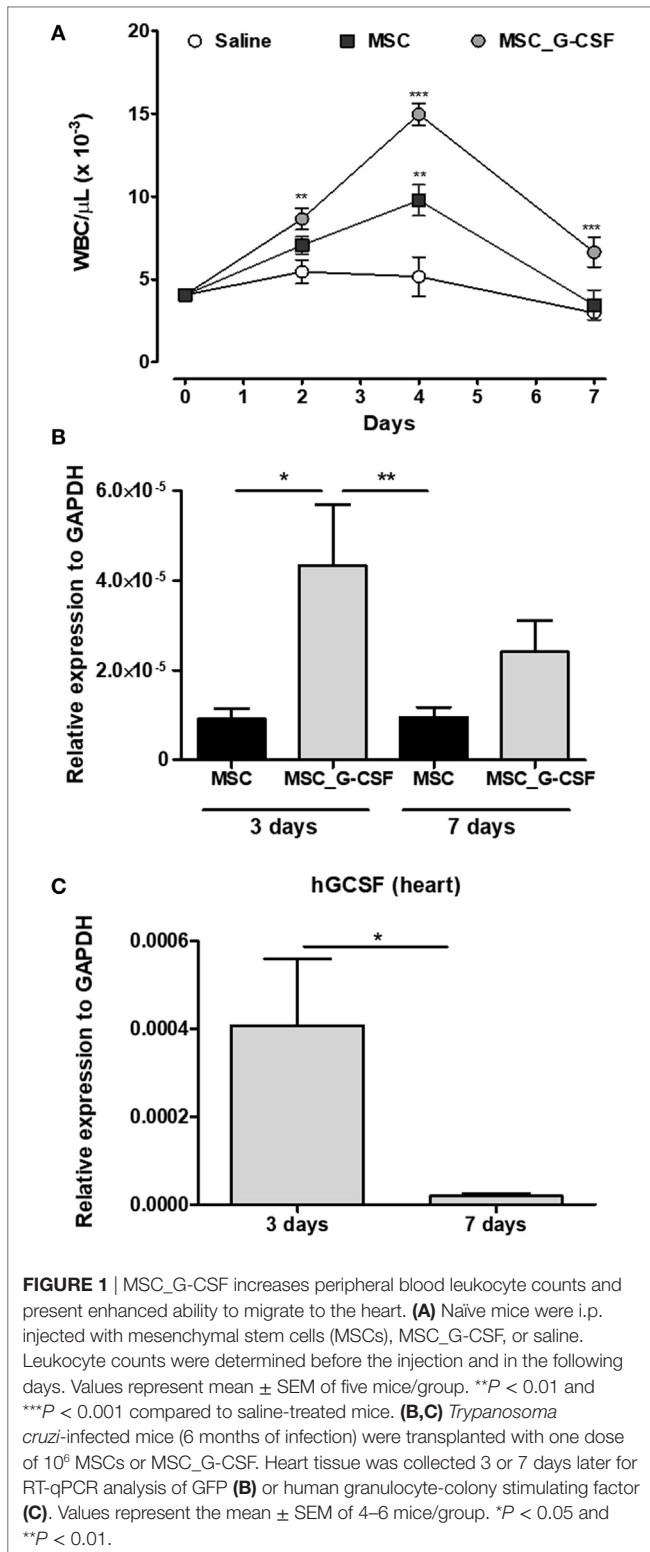


**FIGURE 1** | MSC\_G-CSF increases peripheral blood leukocyte counts and present enhanced ability to migrate to the heart. **(A)** Naïve mice were i.p. injected with mesenchymal stem cells (MSCs), MSC\_G-CSF, or saline. Leukocyte counts were determined before the injection and in the following days. Values represent mean  $\pm$  SEM of five mice/group. \*\* $P < 0.01$  and \*\*\* $P < 0.001$  compared to saline-treated mice. **(B,C)** *Trypanosoma cruzi*-infected mice (6 months of infection) were transplanted with one dose of  $10^6$  MSCs or MSC\_G-CSF. Heart tissue was collected 3 or 7 days later for RT-qPCR analysis of GFP **(B)** or human granulocyte-colony stimulating factor **(C)**. Values represent the mean  $\pm$  SEM of 4–6 mice/group. \* $P < 0.05$  and \*\* $P < 0.01$ .

placed in the upper chamber. We found that both MSC\_G-CSF conditioned media and regular media supplemented with G-CSF, but not MSCs' conditioned media, were able to increase the migration of MDSCs (Figure 2C). Finally, in order to demonstrate the suppressor activity of the recruited MDSCs, CD11b<sup>+</sup>GR-1<sup>+</sup> cells

were sorted from the hearts of *T. cruzi*-infected mice treated with MSC\_G-CSF and co-cultured with mouse splenocytes activated with concanavalin A (Figure 2D). MDSCs caused a marked reduction in blast formation, showing a potent inhibitory effect on lymphocyte proliferation. As expected, dexamethasone, a positive control, completely blocked blast formation.

Next, we evaluated the frequency of Tregs in the hearts, by performing immunostaining for CD3 and FoxP3 in heart sections of mice treated with saline, MSCs, or MSC\_G-CSF (Figure 3A). Quantification showed a significant increase (~threefold) in the percentage of Tregs, compared to saline and MSCs groups (Figure 3B). Confocal analysis showed that FoxP3<sup>+</sup> cells, in addition to other cell populations, were positive for IL-10 (Figure 3C).

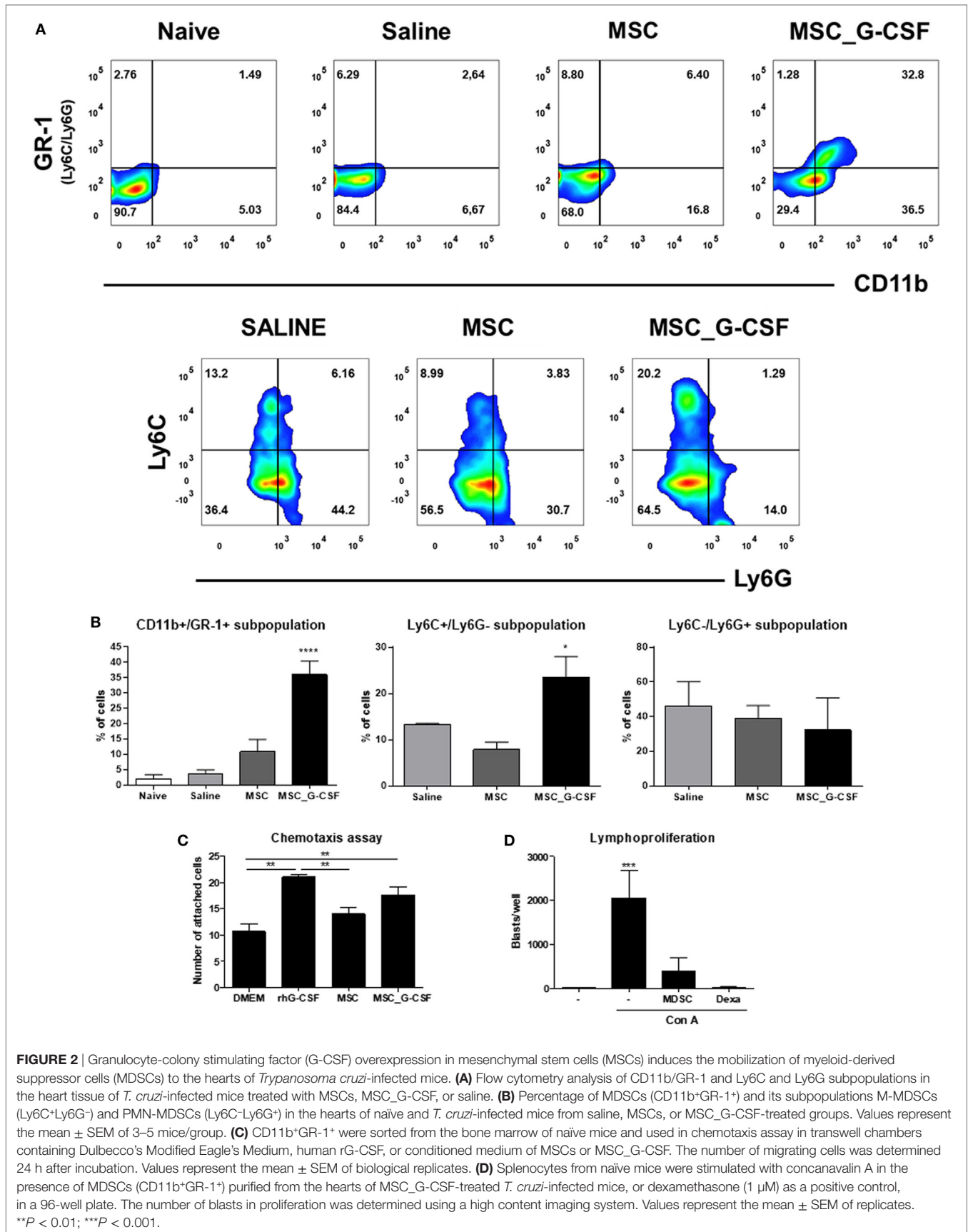
### Improvement of Exercise Capacity and Reduction of Inflammation and Fibrosis in Mice Transplanted With MSC\_G-CSF

In order to evaluate long-term effects of the cell therapy and assess functional recovery, treadmill tests and electrocardiograms were performed before treatment and 60 days after the beginning of the cell therapy protocol. Exercise capacity, evaluated by a treadmill test, showed a significant reduction in distance and time run in saline-treated, *T. cruzi*-infected mice, compared to naïve controls (Figures 4A,B). Both MSCs and MSC\_G-CSF treated mice showed a partial recovery in exercise capacity. ECG analyses were also performed before and after treatment. All *T. cruzi*-infected groups presented similar degrees of conduction disturbances, which included first-degree atrium-ventricular block, intra-atrial conduction disturbance, junctional rhythm, intraventricular conduction disturbance, ventricular bigeminy, polymorphic ventricular tachycardia, and atrioventricular dissociation (Figure 4C). These findings were not reversed by any of the cell therapy protocols evaluated.

In accordance with the results of the 7 days-time point, peripheral blood leukocyte counts were found to be significantly increased in the MSC\_G-CSF group, compared to the other groups, 60 days after the beginning of the treatment (Figure 5A). Moreover, spleen weight, which was increased by infection in saline-treated mice, compared to naïve controls, was reduced in MSCs group, but not in MSC\_G-CSF group (Figure 5B). In order to determine if the cell therapy affected the parasite load, we performed RT-qPCR to quantify *T. cruzi* parasites in the spleen. We found that infected mice treated with either MSCs or MSC\_G-CSF had similar parasite load than saline-treated mice (Figure 5C).

Heart sections were prepared from mice euthanized 60 days after beginning of treatment and stained with H&E and Sirius red to evaluate inflammation and fibrosis, respectively (Figure 6A). A significant reduction of inflammation and fibrosis was observed in the hearts of mice treated with either MSCs or MSC\_G-CSF, compared to saline (Figures 6B,C). In the group treated with MSC\_G-CSF, however, a more pronounced reduction in the number of infiltrating inflammatory cells and in the area of fibrosis was observed (Figure 6C).

Gene expression analysis was performed in heart samples obtained from *T. cruzi* infected, in order to evaluate the expression

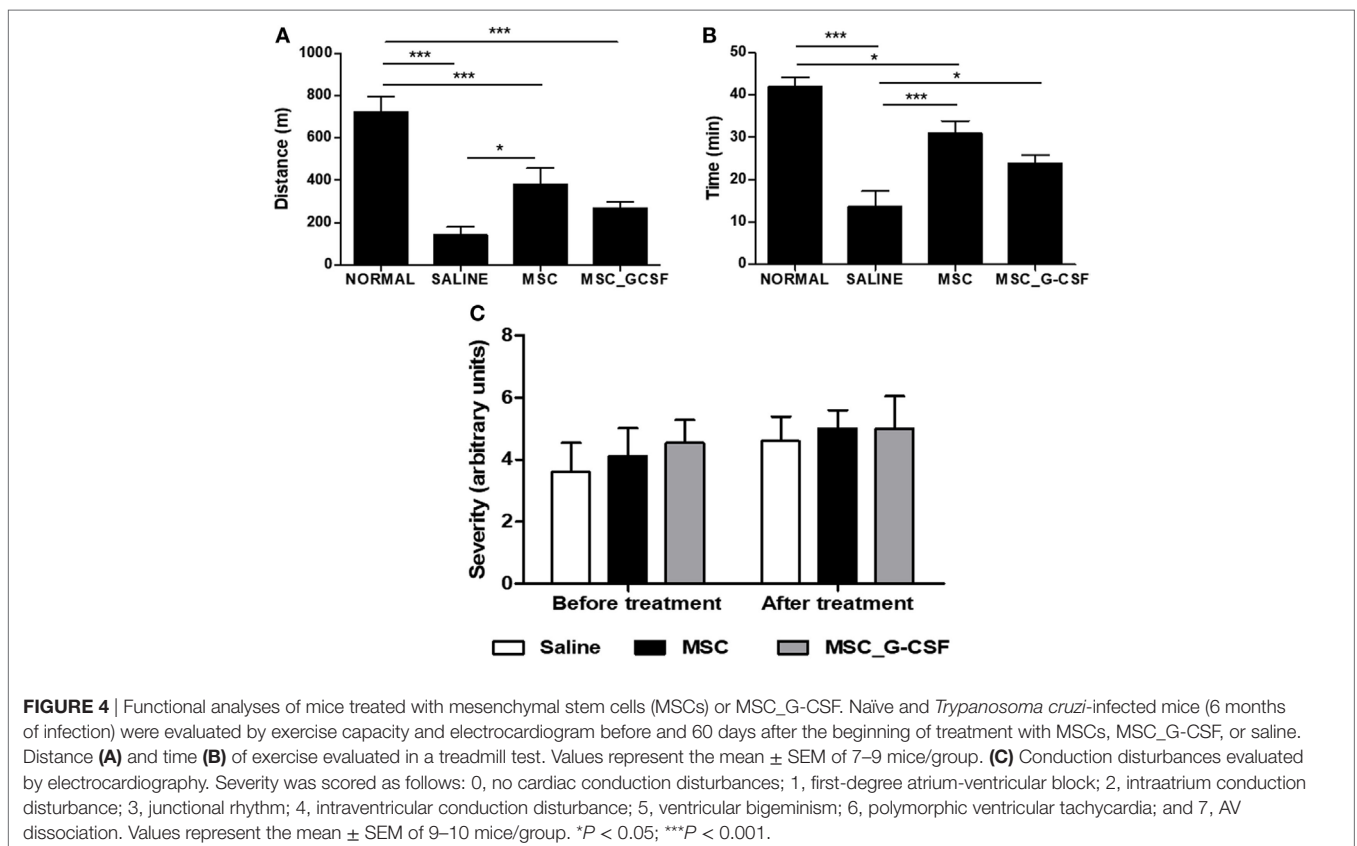
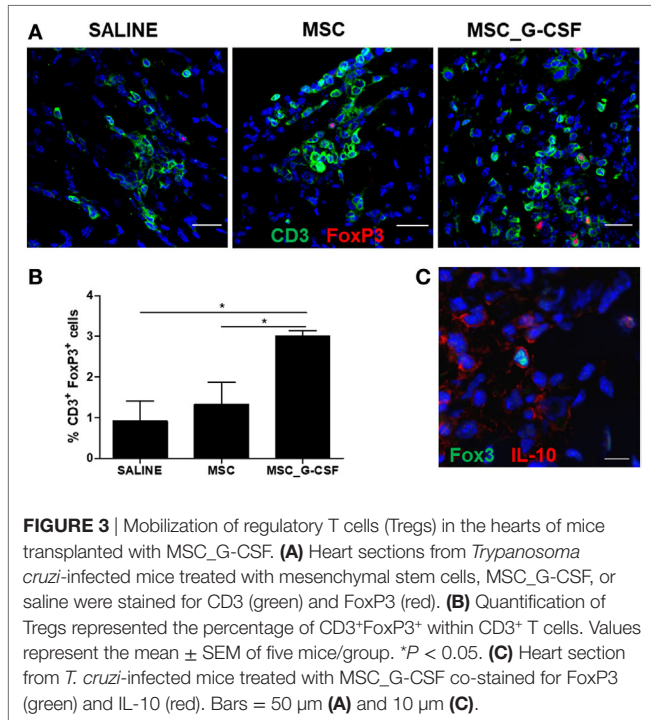


levels of transcription factors and mediators associated with the immune response and inflammation. We found that infected mice presented a significant increase in inflammatory mediators, including

inflammatory cytokines TNF $\alpha$ , IL-6, IFN $\gamma$ , and transcription factors associated with Th1 and Th2, respectively, Tbet (Tbx21) and GATA-3, when compared to naïve controls (Figure 7). A significant reduction in the expression levels of TNF $\alpha$ , IFN $\gamma$ , GATA3, and Tbet was seen in MSC\_G-CSF mice, while the expression of the anti-inflammatory cytokine IL-10 was significantly increased, compared to saline group. In contrast, treatment with MSCs caused a significant reduction in TNF $\alpha$ , while increasing arginase 1 expression (Figure 7).

## DISCUSSION

The use of cell therapies has been investigated in a number of cardiac diseases, including chronic Chagas disease, but currently no efficient treatment has been established for clinical practice (18, 19). Previous studies have shown improvements after MSC-based therapy in the mouse model of Chagas disease (11–14, 20). Genetic modification of MSCs is a promising strategy to deliver therapeutic agents for the treatment of several medical applications, which is already progressing into clinical trials (5). MSCs producing anti-inflammatory cytokines, such as IL-10 and TGF- $\beta$ , have been tested in autoimmune disease models (21, 22). Here we investigated the effectiveness of combined gene and cell therapy in a mouse model of chronic Chagas disease. We found that G-CSF-overexpressing MSCs have increased immunomodulatory properties, promoting a more profound reduction in inflammation, fibrosis, and modulation of inflammatory mediators, when compared to regular MSCs. This effect



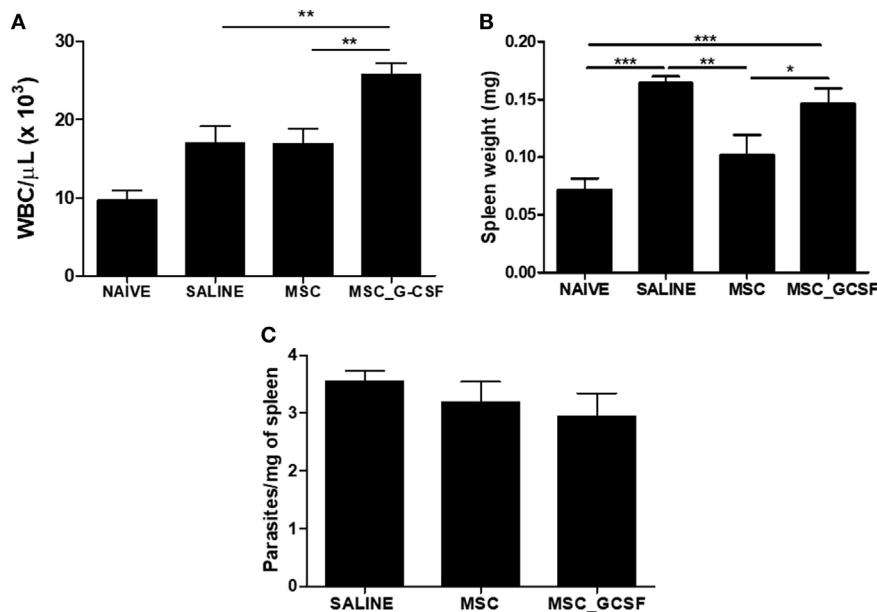


**FIGURE 5** | Effects of cell therapy on leukocyte mobilization, spleen weight, and parasitism. **(A)** Peripheral blood leukocyte counts 60 days after the treatment with mesenchymal stem cells (MSCs), MSC\_G-CSF, or saline. **(B)** Spleen weight was found to be increased in infected mice, and decreased by treatment with MSCs, but not MSC\_G-CSF. **(C)** Parasitism in the spleens, evaluated by qPCR, was not altered by the cell therapy. Values represent the mean  $\pm$  SEM of 7–9 mice/group. \* $P < 0.05$ ; \*\* $P < 0.01$ ; \*\*\* $P < 0.001$ .

was associated with an increased ability to recruit suppressor cell populations, such as Tregs and MDSCs.

The interplay between G-CSF-overexpressing MSCs and suppressor cells explains the increased immunomodulatory potential observed *in vivo*, since MSC\_G-CSF present similar ability to suppress lymphocyte proliferation *in vitro*, when compared to wild-type MSCs (16). G-CSF was previously shown to promote mobilization of Tregs, modulating allogeneic immune responses (23). Moreover, treatment with G-CSF recruits Tregs to the hearts of mice chronically infected with *T. cruzi* (14). In line with this, we found here a higher frequency of Tregs in the hearts of chagasic mice transplanted with MSC\_G-CSF. Treg cells were shown to act ameliorating cardiac damage and suppressing cardiac hypertrophy and fibrosis in a model of angiotensin II-mediated cardiac damage (24).

A marked increase in MDSCs was also found in the hearts of MSC\_G-CSF-treated mice. These cells play important immune regulatory roles in several diseases, including chronic infections, autoimmunity, and cancer (9). G-CSF was found to be a key molecule in the regulation of migration, proliferation, and function maintenance of MDSCs in a mouse model of colitis (25). In fact, by using a chemotaxis assay, we found that culture supernatants from MSC\_G-CSF, but not MSCs, had similar MDSCs recruitment capacity than the recombinant G-CSF. A previous study showed the increase of MDSCs in spleens and hearts during acute *T. cruzi* infection in mice (26). These cells express Arg-1 and iNOS, which suppress T cell proliferation, allowing the host to avoid an excessive immune response that may also cause damage (27). In the present study, accumulation of MDSCs was associated

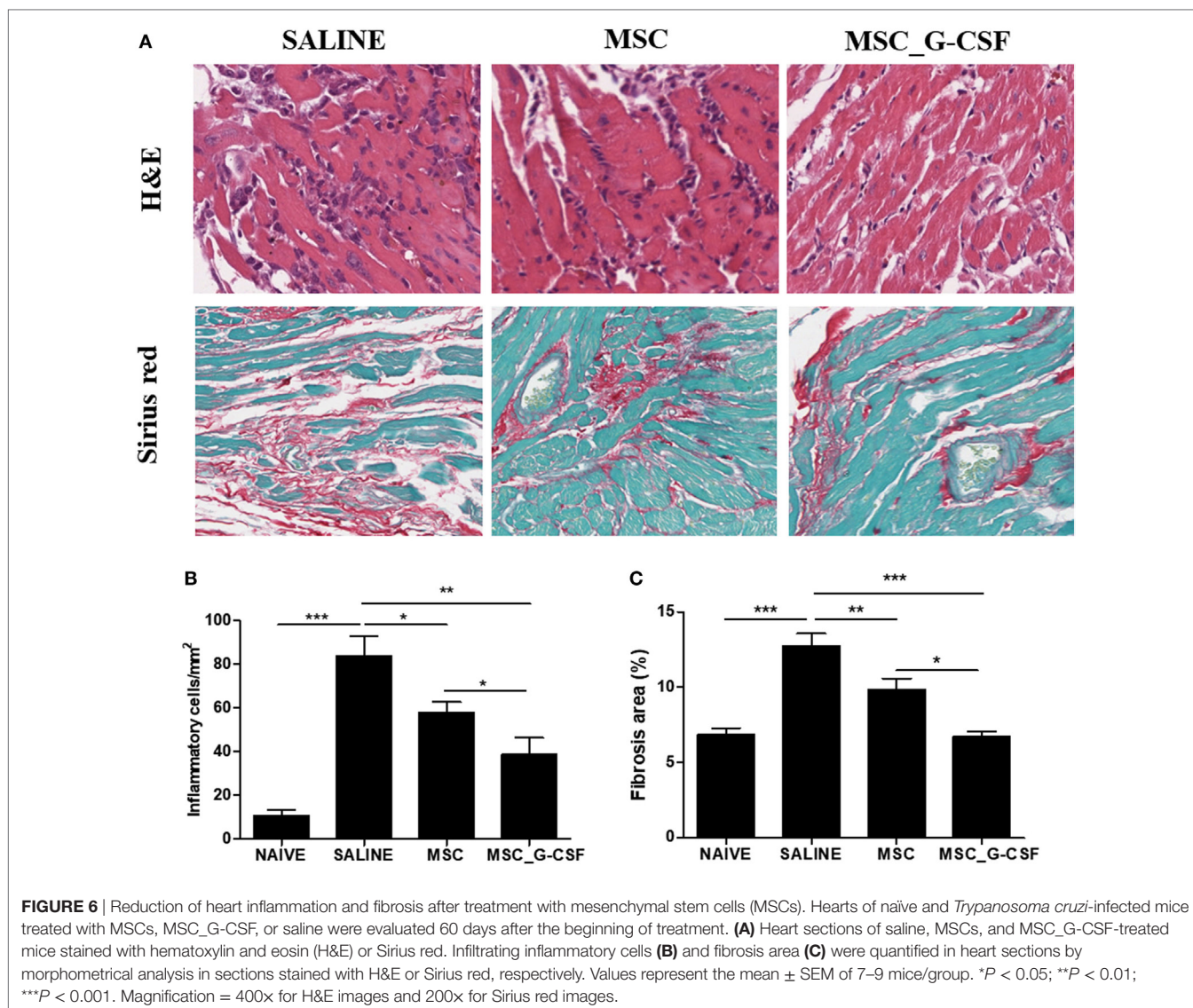
with decreased inflammation, without disrupting the parasitism control by the anti-*T. cruzi* immune response.

Myeloid-derived suppressor cells extracted from the hearts were also shown to be functional and to suppress T cell activation *in vitro*. It is known that MDSCs are potent suppressor cells that act through the secretion of anti-inflammatory cytokines, such as IL-10 and TGF- $\beta$ . Moreover, both M- and PMN-MDSCs have been recently shown to exert antihypertrophic and anti-inflammatory properties, in the context of heart failure, through IL-10 (28). A marked increase in IL-10 expression was observed in the hearts of mice treated with MSC\_G-CSF in our study.

A number of studies have shown that G-CSF can induce T cell tolerance (29). In addition to its indirect effects *via* mobilization of suppressor cell populations, G-CSF may exert a direct effect on T cells. The interaction between G-CSF and its receptor (G-CSFR), which is expressed in various hematopoietic cell types, including T cells, can favor Th2 over Th1 imbalance by the induction of activation of GATA3 (30). The analysis of GATA3 and Tbet expression, the transcription factors associated with Th2 and Th1 differentiation, respectively, in the hearts of MSC\_G-CSF mice failed to show a polarization to Th2 phenotype, since the gene expression of both transcription factors were reduced compared to saline-treated chagasic control mice.

A role for Tregs in the control of pathological T cell responses in chronic Chagas disease cardiomyopathy has been suggested by studies showing that patients with the indeterminate form of the disease (asymptomatic) have increased frequency of Tregs in the peripheral blood, compared to patients with severe





cardiomyopathy (29, 30). In contrast, there are no studies indicating a protective role for MDSCs in chronic Chagas disease patients. Our results demonstrate that MDSCs, with confirmed immunosuppressive actions, accumulate in the hearts of MSC\_G-CSF-treated mice, being associated with reduction of cardiac inflammation. This suggests that strategies to increase MDSC mobilization may be beneficial for the treatment of patients with chronic Chagas disease cardiomyopathy.

The presence of multifocal inflammatory infiltrates, composed mainly of mononuclear cells, is a hallmark of chronic Chagas disease cardiomyopathy. Here we show that G-CSF-overexpressing MSCs reduce not only the number of inflammatory cells but also the production of pro-inflammatory cytokines, such as TNF $\alpha$  and IFN $\gamma$ . These are important mediators of chronic Chagas disease cardiomyopathy, as shown in the mouse model (10, 31) and in the human disease (32–34). This reduction in pro-inflammatory mediators correlated with an increase in IL-10, a potent anti-inflammatory cytokine.

Also, MSC\_G-CSF therapy caused a more pronounced reduction in cardiac fibrosis than wild-type MSCs. The finding of reduced cardiac fibrosis may be the result of decreased cardiac inflammation, since it is known that the exacerbated immune response, frequently seen in Chagas disease, progressively leads to the destruction of cardiac myocytes, increasing fibrosis. Cardiac fibrosis may promote conduction disturbances, leading to arrhythmias and accounting for a high percentage of the mortality due to chronic Chagas disease (35). Despite the reduction in fibrosis, treatment with MSC\_G-CSF did not improve the electrical disturbances. Mice treated with stem cells, however, had a partial recovery in the exercise capacity. This suggests that cell therapy may be more effective if applied earlier to prevent or block the evolution of the disease.

Immunosuppressive drugs can reactivate infection in mice and patients with residual parasitism during the chronic phase of infection (36, 37). To rule out that the immunosuppressive activity of MSC\_G-CSF were reactivating the parasite growth, we

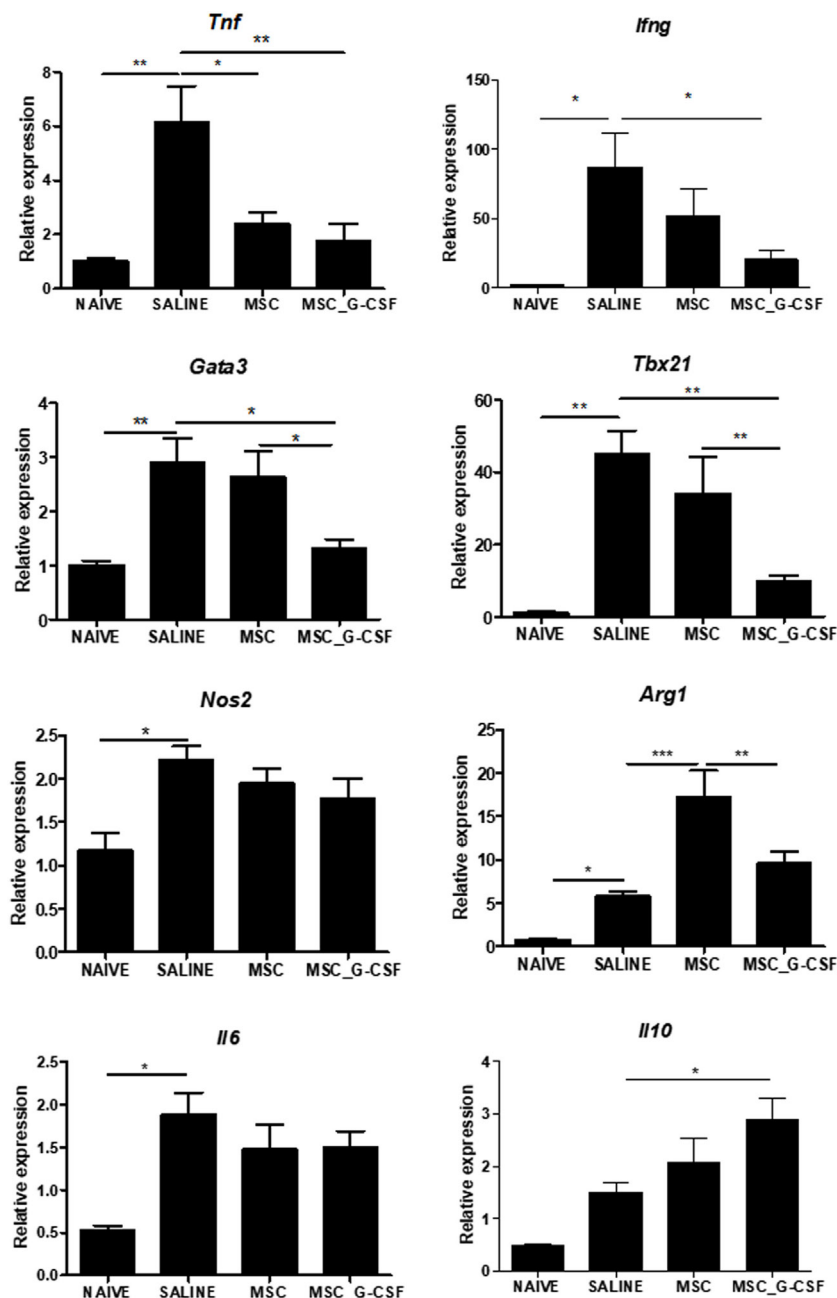


**FIGURE 7** | Modulation of gene expression for inflammatory mediators in the hearts of mice transplanted with MSC\_G-CSF. Hearts from naïve and *Trypanosoma cruzi*-infected mice treated with mesenchymal stem cells, MSC\_G-CSF, or saline were submitted to RT-qPCR analysis for evaluation of the gene expression for TNF $\alpha$ , IFN $\gamma$ , GATA3, Tbet, iNOS, Arg, IL-6, and IL-10. Results are shown as relative expression to GAPDH. Values represent the mean  $\pm$  SEM of 5–7 mice/group. \* $P < 0.05$ ; \*\* $P < 0.01$ ; \*\*\* $P < 0.001$ .

performed RT-qPCR analysis to quantify *T. cruzi* parasite load in spleen samples from infected mice. This analysis demonstrated that, despite the marked immunosuppressive activity of MSC\_G-CSF, the cell transplantation scheme did not interfere with host-parasite equilibrium. Since the elimination of the parasite is desirable, the possibility that combining MSC\_G-CSF therapy with benznidazole administration promotes additional improvements than the cell therapy alone needs to be further investigated.

While the use of many recombinant factors is frequently associated with side effects, the use of recombinant G-CSF is considered safe and well tolerated. Moreover, we have previously shown that recombinant G-CSF promotes beneficial effects in the mouse model of Chagas disease (14). We hypothesized here that MSC\_G-CSF could offer some advantages, such as the ability to migrate to the injury site and promote local release of G-CSF and other growth factors which may act

synergistically to promote tissue repair and immunomodulation. Our previous results with recombinant G-CSF, however, were effective not only in reducing inflammation and fibrosis, as seen with MSC\_G-CSF but also caused reduction of tissue parasitism and amelioration of arrhythmias. Although the effect of MSC\_G-CSF may not bring advantage when compared to repeated courses of G-CSF alone, we have here demonstrated, for the first time, that genetic manipulation may improve the therapeutic effects of MSC in the context of Chagas disease. The fact that transplantation of MSC alone causes some immunomodulatory action suggests that the effect seen in mice treated with MSC\_G-CSF is due to the release of G-CSF and other mediators.

In conclusion, we show that overexpression of G-CSF in MSCs potentiates their *in vivo* immunosuppressive effects in a model of chronic Chagas disease. Moreover, our results indicate a role of MDSCs in the regulation of pathological immune responses, opening new avenues for the development of cell-based therapies in chronic Chagas disease.

## ETHICS STATEMENT

All procedures described had prior approval from the local animal ethics committee under number 012/09 (FIOCRUZ, Bahia, Brazil).

## REFERENCES

- Klimczak A, Kozłowska U. Mesenchymal stromal cells and tissue-specific progenitor cells: their role in tissue homeostasis. *Stem Cells Int* (2016) 2016:4285215. doi:10.1155/2016/4285215
- Sharma RR, Pollock K, Hubel A, McKenna D. Mesenchymal stem or stromal cells: a review of clinical applications and manufacturing practices. *Transfusion* (2014) 54:1418–37. doi:10.1111/trf.12421
- Luger D, Lipinski MJ, Westman PC, Glover DK, dimastromatteo J, Frias JC, et al. Intravenously-delivered mesenchymal stem cells: systemic anti-inflammatory effects improve left ventricular dysfunction in acute myocardial infarction and ischemic cardiomyopathy. *Circ Res* (2017) 120(10):1598–613. doi:10.1161/CIRCRESAHA.117.310599
- Murphy MB, Moncivais K, Caplan AI. Mesenchymal stem cells: environmentally responsive therapeutics for regenerative medicine. *Exp Mol Med* (2013) 45:e54. doi:10.1038/emmm.2013.94
- Nolta JA. "Next-generation" mesenchymal stem or stromal cells for the *in vivo* delivery of bioactive factors: progressing toward the clinic. *Transfusion* (2016) 56(4):15S–7S. doi:10.1111/trf.13564
- Anderlini P, Champlin RE. Biologic and molecular effects of granulocyte colony-stimulating factor in healthy individuals: recent findings and current challenges. *Blood* (2008) 111:1767–72. doi:10.1182/blood-2007-07-097543
- Kurdi M, Booz GW. G-CSF-based stem cell therapy for the heart-unresolved issues part A: paracrine actions, mobilization, and delivery. *Congest Heart Fail* (2007) 13:221–7. doi:10.1111/j.1527-5299.2007.07111.x
- Adeegbe DO, Nishikawa H. Natural and induced T regulatory cells in cancer. *Front Immunol* (2013) 4:190. doi:10.3389/fimmu.2013.00190
- Lindau D, Gielen P, Kroesen M, Wesseling P, Adema GJ. The immunosuppressive tumour network: myeloid-derived suppressor cells, regulatory T cells and natural killer T cells. *Immunology* (2013) 138:105–15. doi:10.1111/imm.12036
- Soares MB, Silva-Mota KN, Lima RS, Bellintani MC, Pontes-de-Carvalho L, Ribeiro-dos-Santos R. Modulation of chagasic cardiomyopathy by interleukin-4: dissociation between inflammation and tissue parasitism. *Am J Pathol* (2001) 159:703–9. doi:10.1016/S0002-9440(10)61741-5
- Silva DN, De Freitas Souza BS, Azevedo CMH, Vasconcelos JF, Carvalho RH, Soares MBP, et al. Intramyocardial transplantation of cardiac mesenchymal

## AUTHOR CONTRIBUTIONS

DS, JV, CA, CV, BP, VR, GC, PD, SM, and CN performed the experiments. DS, BS, JV, VR, and BP analyzed the data. DS, BS, RR-d-S, and MS conceived the study and wrote the manuscript.

## ACKNOWLEDGMENTS

The authors acknowledge the Brazilian agencies FINEP, CNPq, and FAPESB for research funding.

## SUPPLEMENTARY MATERIAL

The Supplementary Material for this article can be found online at <https://www.frontiersin.org/articles/10.3389/fimmu.2018.01449/full#supplementary-material>.

**FIGURE S1** | Experimental design. **(A)** Establishment of dose and administration regimen. C57BL/6 mice were treated with a single dose of  $10^6$  mesenchymal stem cells (MSCs) or MSC\_G-CSF (i.p) and serial hemograms were performed during 7 days. **(B)** Cell tracking was performed in C57BL/6 mice chronically infected with *T. cruzi* (6 months after infection) 3 and 7 days after administration of  $10^6$  MSCs or MSC\_G-CSF (i.p), for detection of GFP+ cells and human granulocyte-colony stimulating factor gene in the heart. **(C)** C57BL/6 infected with *T. cruzi* was treated 6 months after infection with  $10^6$  MSCs or MSC-GCSF, every 7 days, during 60 days. Saline-treated and naïve mice were used as controls. Mice were euthanized for 30 days after the first administration of cells for evaluation of recruitment of myeloid-derived suppressor cells and regulatory T cells to the heart.

- stem cells reduces myocarditis in a model of chronic Chagas disease cardiomyopathy. *Stem Cell Res Ther* (2014) 5:81. doi:10.1186/scrt470
- Larocca TF, Souza BS, Silva CA, Kaneto CM, Alcantara AC, Azevedo CM, et al. Transplantation of adipose tissue mesenchymal stem cells in experimental chronic chagasic cardiopathy. *Arq Bras Cardiol* (2013) 100(5):460–8. doi:10.5935/abc.20130058
  - Jasmin, Jelicks LA, Tanowitz HB, Peters VM, Mendez-Otero R, Campos de Carvalho AC, et al. Molecular imaging, biodistribution and efficacy of mesenchymal bone marrow cell therapy in a mouse model of Chagas disease. *Microbes Infect* (2014) 16:923–35. doi:10.1016/j.micinf.2014.08.016
  - Vasconcelos JF, Souza BSF, Lins TFS, Garcia LMS, Kaneto CM, Sampaio GP, et al. Administration of granulocyte colony-stimulating factor induces immunomodulation, recruitment of T regulatory cells, reduction of myocarditis and decrease of parasite load in a mouse model of chronic Chagas disease cardiomyopathy. *FASEB J* (2013) 27:4691–702. doi:10.1096/fj.13-229351
  - Gonçalves GVM, Silva DN, Carvalho RH, Souza BSF, da Silva KN, Vasconcelos JF, et al. Generation and characterization of transgenic mouse mesenchymal stem cell lines expressing hIGF-1 or hG-CSF. *Cytotechnology* (2018) 70(2):577–91. doi:10.1007/s10616-017-0131-2
  - Pinto ARAR, Chandran A, Rosenthal NANA, Godwin JWJW. Isolation and analysis of single cells from the mouse heart. *J Immunol Methods* (2013) 393:74–80. doi:10.1016/j.jim.2013.03.012
  - Adeegbe D, Serafini P, Bronte V, Zoso A, Ricordi C, Inverardi L. *In vivo* induction of myeloid suppressor cells and CD4(+)Foxp3(+) T regulatory cells prolongs skin allograft survival in mice. *Cell Transplant* (2011) 20:941–54. doi:10.3727/096368910X540621
  - Dos Santos RR, Rassi S, Feitosa G, Grecco OT, Rassi A, Da Cunha AB, et al. Cell therapy in chagas cardiomyopathy (Chagas arm of the multicenter randomized trial of cell therapy in cardiopathies study): a multicenter randomized trial. *Circulation* (2012) 125:2454–61. doi:10.1161/CIRCULATIONAHA.111.067785
  - Carvalho AB, Goldenberg RCDS, Campos de Carvalho AC. Cell therapies for Chagas disease. *Cytotherapy* (2017) 19:1339–49. doi:10.1016/j.jcyt.2017.07.014
  - Souza BSF, Silva DN, Carvalho RH, Sampaio GLA, Paredes BD, Aragão França L, et al. Association of cardiac galectin-3 expression, myocarditis, and fibrosis

- in chronic Chagas disease cardiomyopathy. *Am J Pathol* (2017) 187:1134–46. doi:10.1016/j.ajpath.2017.01.016
21. Liao W, Pham V, Liu L, Riazifar M, Pone EJ, Zhang SX, et al. Mesenchymal stem cells engineered to express selectin ligands and IL-10 exert enhanced therapeutic efficacy in murine experimental autoimmune encephalomyelitis. *Biomaterials* (2016) 77:87–97. doi:10.1016/j.biomaterials.2015.11.005
  22. Daneshmandi S, Karimi MH, Pourfathollah AA. TGF- $\beta$ 1 transduced mesenchymal stem cells have profound modulatory effects on DCs and T cells. *Iran J Immunol* (2017) 14(1):13–23. doi:10.1016/j.ijiv.2017.01.016
  23. Morris ES, MacDonald KPA, Rowe V, Johnson DH, Banovic T, Clouston AD, et al. Donor treatment with pegylated G-CSF augments the generation of IL-10-producing regulatory T cells and promotes transplantation tolerance. *Blood* (2004) 103:3573–81. doi:10.1182/blood-2003-08-2864
  24. Zhou L, Miao K, Yin B, Li H, Fan J, Zhu Y, et al. The cardioprotective role of myeloid-derived suppressor cells in heart failure. *Circulation* (2018). doi:10.1161/CIRCULATIONAHA.117.030811
  25. Li W, Zhang X, Chen Y, Xie Y, Liu J, Feng Q, et al. G-CSF is a key modulator of MDSC and could be a potential therapeutic target in colitis-associated colorectal cancers. *Protein Cell* (2016) 7:130–40. doi:10.1007/s13238-015-0237-2
  26. Arocena AR, Onofrio LI, Pellegrini AV, Carrera Silva AE, Paroli A, Cano RC, et al. Myeloid-derived suppressor cells are key players in the resolution of inflammation during a model of acute infection. *Eur J Immunol* (2014) 44:184–94. doi:10.1002/eji.201343606
  27. Goñi O, Alcaide P, Fresno M. Immunosuppression during acute *Trypanosoma cruzi* infection: involvement of Ly6G (Gr1+)CD11b+immature myeloid suppressor cells. *Int Immunol* (2002) 14:1125–34. doi:10.1093/intimm/14.11.1125
  28. Kvakana H, Kleinewietfeld M, Qadri F, Park JK, Fischer R, Schwarz I, et al. Regulatory T cells ameliorate angiotensin II-induced cardiac damage. *Circulation* (2009) 119:2904–12. doi:10.1161/CIRCULATIONAHA.108.832782
  29. Yang J-Z, Zhang J-Q, Sun L-X. Mechanisms for T cell tolerance induced with granulocyte colony-stimulating factor. *Mol Immunol* (2016) 70:56–62. doi:10.1016/j.molimm.2015.12.006
  30. Franzke A, Piao W, Lauber J, Gatzlaff P, Könecke C, Hansen W, et al. G-CSF as immune regulator in T cells expressing the G-CSF receptor: implications for transplantation and autoimmune diseases. *Blood* (2003) 102:734–9. doi:10.1182/blood-2002-04-1200
  31. de Araújo FF, Vitelli-Avelar DM, Teixeira-Carvalho A, Antas PRZ, Gomes JAS, Sathler-Avelar R, et al. Regulatory T cells phenotype in different clinical forms of Chagas' disease. *PLoS Negl Trop Dis* (2011) 5(5):e992. doi:10.1371/journal.pntd.0000992
  32. de Araújo FF, Corrêa-Oliveira R, Rocha MOC, Chaves AT, Fiuza JA, Fares RCG, et al. Foxp3+CD25highCD4+regulatory T cells from indeterminate patients with Chagas disease can suppress the effector cells and cytokines and reveal altered correlations with disease severity. *Immunobiology* (2012) 217:768–77. doi:10.1016/j.imbio.2012.04.008
  33. Soares MBP, de Lima RS, Rocha LL, Vasconcelos JF, Rogatto SR, dos Santos RR, et al. Gene expression changes associated with myocarditis and fibrosis in hearts of mice with chronic chagasic cardiomyopathy. *J Infect Dis* (2010) 202:416–26. doi:10.1086/653481
  34. Nogueira LG, Santos RHB, Fiorelli AI, Mairena EC, Benvenuti LA, Bocchi EA, et al. Myocardial gene expression of T-bet, GATA-3, Ror- $\gamma$  t, FoxP3, and hallmark cytokines in chronic Chagas disease cardiomyopathy: an essentially unopposed T-Type response. *Mediators Inflamm* (2014) 2014:914326. doi:10.1155/2014/914326
  35. Rossi MA. The pattern of myocardial fibrosis in chronic Chagas' heart disease. *Int J Cardiol* (1991) 30:335–40. doi:10.1016/0167-5273(91)90012-E
  36. Lattes R, Lasala MB. Chagas disease in the immunosuppressed patient. *Clin Microbiol Infect* (2014) 20:300–9. doi:10.1111/1469-0691.12585
  37. Pereira MES, Santos LMT, Araújo MSS, Brener Z. Recrudescence induced by cyclophosphamide of chronic *Trypanosoma cruzi* infection in mice is influenced by the parasite strain. *Mem Inst Oswaldo Cruz* (1996) 91:71–4. doi:10.1590/S0074-02761996000100011

**Conflict of Interest Statement:** The authors declare that the research was conducted in the absence of any commercial or financial relationships that could be construed as a potential conflict of interest.

The reviewer FA declared a shared affiliation, though no other collaboration, with several of the authors DS, BS, JV, CA, VR, CN, and MS to the handling Editor.

Copyright © 2018 Silva, Souza, Vasconcelos, Azevedo, Valim, Paredes, Rocha, Carvalho, Daltro, Macambira, Nonaka, Ribeiro-dos-Santos and Soares. This is an open-access article distributed under the terms of the Creative Commons Attribution License (CC BY). The use, distribution or reproduction in other forums is permitted, provided the original author(s) and the copyright owner are credited and that the original publication in this journal is cited, in accordance with accepted academic practice. No use, distribution or reproduction is permitted which does not comply with these terms.

## CAPÍTULO II

Neste capítulo, descrevemos os efeitos imunomoduladores e regenerativos da terapia com células-tronco mesenquimais que superexpressam hIGF-1 no modelo experimental de cardiopatia chagásica crônica.



Artigo publicado na revista *Stem cells International*, vol. 2018, julho de 2018.

<https://doi.org/10.1155/2018/9108681>

**IGF-1-overexpressing mesenchymal stem/stromal cells promote immunomodulatory and pro-regenerative effects in chronic experimental Chagas disease**

## Research Article

# IGF-1-Overexpressing Mesenchymal Stem/Stromal Cells Promote Immunomodulatory and Proregenerative Effects in Chronic Experimental Chagas Disease

Daniela N. Silva,<sup>1,2</sup> Bruno S. F. Souza,<sup>1,2,3</sup> Carine M. Azevedo,<sup>1,2</sup> Juliana F. Vasconcelos,<sup>1,2</sup> Paloma G. de Jesus,<sup>1</sup> Malena S. Feitoza,<sup>1</sup> Cassio S. Meira ,<sup>1</sup> Gisele B. Carvalho,<sup>1</sup> Bruno Raphael Cavalcante,<sup>1</sup> Ricardo Ribeiro-dos-Santos,<sup>1,3</sup> and Milena B. P. Soares <sup>1,2,3</sup>

<sup>1</sup>Center for Biotechnology and Cell Therapy, São Rafael Hospital, Salvador, BA, Brazil

<sup>2</sup>Gonçalo Moniz Institute, FIOCRUZ, Salvador, BA, Brazil

<sup>3</sup>National Institute of Science and Technology for Regenerative Medicine, Rio de Janeiro, RJ, Brazil

Correspondence should be addressed to Milena B. P. Soares; [milena@bahia.fiocruz.br](mailto:milena@bahia.fiocruz.br)

Received 20 April 2018; Accepted 3 July 2018; Published 24 July 2018

Academic Editor: Jun Liu

Copyright © 2018 Daniela N. Silva et al. This is an open access article distributed under the Creative Commons Attribution License, which permits unrestricted use, distribution, and reproduction in any medium, provided the original work is properly cited.

Mesenchymal stem/stromal cells (MSCs) have been investigated for the treatment of diseases that affect the cardiovascular system, including Chagas disease. MSCs are able to promote their beneficial actions through the secretion of proregenerative and immunomodulatory factors, including insulin-like growth factor-1 (IGF-1), which has proregenerative actions in the heart and skeletal muscle. Here, we evaluated the therapeutic potential of IGF-1-overexpressing MSCs (MSC\_IGF-1) in a mouse model of chronic Chagas disease. C57BL/6 mice were infected with Colombian strain *Trypanosoma cruzi* and treated with MSCs, MSC\_IGF-1, or vehicle (saline) six months after infection. RT-qPCR analysis confirmed the presence of transplanted cells in both the heart and skeletal muscle tissues. Transplantation of either MSCs or MSC\_IGF-1 reduced the number of inflammatory cells in the heart when compared to saline controls. Moreover, treatment with MSCs or MSC\_IGF-1 significantly reduced TNF- $\alpha$ , but only MSC treatment reduced IFN- $\gamma$  production compared to the saline group. Skeletal muscle sections of both MSC- and MSC\_IGF-1-treated mice showed a reduction in fibrosis compared to saline controls. Importantly, the myofiber area was reduced in *T. cruzi*-infected mice, and this was recovered after treatment with MSC\_IGF-1. Gene expression analysis in the skeletal muscle showed a higher expression of pro- and anti-inflammatory molecules in MSC\_IGF-1-treated mice compared to MSCs alone, which significantly reduced the expression of TNF- $\alpha$  and IL-1 $\beta$ . In conclusion, our results indicate the therapeutic potential of MSC\_IGF-1, with combined immunomodulatory and proregenerative actions to the cardiac and skeletal muscles.

## 1. Introduction

In the field of regenerative medicine, mesenchymal stem/stromal cells (MSCs) are promising tools for the development of novel advanced therapy medicinal products to treat chronic inflammatory diseases [1]. MSCs can be easily obtained from different sources, including the bone marrow, adipose tissue, and umbilical cord tissue, allowing for the development of both autologous and allogeneic therapies [2]. Several clinical trials that have been performed have demonstrated the safety of the clinical application of MSCs [3]. In order to improve the therapeutic effects of MSCs,

genetic modification for the overexpression of specific growth factors is currently being investigated [4, 5].

The release of trophic paracrine factors by MSCs has been associated with many of the proregenerative and immunomodulatory effects observed in the context of MSC-based therapies [2]. One of such growth factors is insulin-like growth factor-1 (IGF-1), which has been shown to exert proregenerative actions in skeletal muscle, promoting muscle cell proliferation and differentiation, histological recovery of muscle fiber type and size, and functional improvements [6, 7]. Moreover, IGF-1 induces myocyte hypertrophy and satellite cell activation and increases protein synthesis

in differentiated myofibers [8]. In heart tissue, IGF-1 was shown to improve engraftment of MSCs, promoting neovascularization and inhibiting cardiomyocyte death [9, 10].

Chagas disease is an infectious disease caused by the intracellular parasite *Trypanosoma cruzi*. Previously confined to the Latin American region, Chagas disease has now spread to other continents due to population migration [11]. Cardiac complications occur in approximately 30% of infected subjects, which may present arrhythmias and heart failure [12]. Tissue analysis reveals the presence of chronic myocarditis, myocytolysis, and an intense interstitial fibrosis, as the result of a combination of persistent parasitism, microvascular inflammation, neurogenic dysfunction, and autoimmune responses [13]. These processes are also observed in the mouse model of Chagas disease caused by a myotropic *Trypanosoma cruzi* strain, which develops a progressive inflammatory response and fibrosis in the heart, along with an intense skeletal myositis, in the chronic phase of infection [14]. Modulation of the exacerbated inflammatory response in combination with the stimulation of endogenous regeneration represents a promising therapeutic approach for Chagas disease.

The ability of MSCs to modulate immune responses and fibrosis has been demonstrated in the context of *T. cruzi* infection in mice [15–18]. We have previously generated and characterized a bone marrow-derived MSC cell line overexpressing IGF-1 [19]. In the present study, we investigated the therapeutic potential of IGF-1-overexpressing MSCs in the experimental model of chronic Chagas disease, by evaluating their immunomodulatory and proregenerative effects in the heart and skeletal muscles.

## 2. Materials and Methods

**2.1. Animals.** Six- to eight-week-old female C57BL/6 mice were used for *T. cruzi* infection. Age-matched naïve mice were kept under the same conditions during the experiments, to serve as uninfected controls. All animals were raised and maintained in the animal facility of the Center for Biotechnology and Cell Therapy, São Rafael Hospital (Salvador, Brazil), and provided with rodent diet and water ad libitum. Animals were handled according to the National Institutes of Health guidelines for animal experimentation. All procedures described had prior approval from the local animal ethics committee under number 012/09 (São Rafael Hospital, Bahia, Brazil).

**2.2. Culture of IGF-1-Overexpressing MSCs.** A genetically modified MSC line with stable overexpression of human IGF-1 (MSC\_IGF-1) was previously generated using bone marrow MSCs obtained from GFP transgenic mice [19]. Briefly, MSCs were transduced with a lentiviral vector for overexpression of hIGF-1, and clones were characterized by polymerase chain reaction (PCR) and enzyme-linked immunosorbent assay (ELISA) to assess transgene expression. The cells were also shown to maintain MSCs' characteristics, including phenotypic markers, trilineage differentiation potential, and reduced inhibition of lymphocyte proliferation. MSC\_IGF-1 was cultured in Dulbecco's Modified Eagle's

Medium (DMEM) supplemented with 10% fetal bovine serum (FBS) and 1% penicillin/streptomycin (all from Thermo Fisher Scientific, Waltham, MA, USA) in a humidity-controlled incubator at 37°C and 5% CO<sub>2</sub>, with complete medium replacement every three days.

**2.3. *T. cruzi* Infection and Cell Therapy.** Mice were infected by intraperitoneal injection with 1000 trypomastigotes of Colombian *T. cruzi* strain, obtained from culture supernatants of infected LLC-MK2 cells. Six months after the infection, mice were randomly assigned into three groups: MSCs ( $n = 10$ ), MSC\_IGF-1 ( $n = 10$ ), or saline ( $n = 8$ ). Age-matched naïve mice were used as normal controls ( $n = 10$ ). Cell transplantation was performed by four intravenous injections of cell suspensions containing either 10<sup>6</sup> MSCs or MSC\_IGF-1, in saline, with an interval of 15 days between each injection. An equal volume of vehicle (100  $\mu$ L) was used in the saline group (Figure 1(a)).

**2.4. Morphometric Analyses.** Mice were euthanized two months after the initiation of the cell therapy protocol, under anesthesia with ketamine and xylazine. Heart and skeletal muscles were removed and fixed in 10% buffered formalin. Tissue sections were analyzed by light microscopy after paraffin embedding, followed by standard hematoxylin and eosin (H&E) staining. Inflammatory cells were counted using the software Image-Pro Plus v.7.0 (Media Cybernetics, Rockville, MD, USA). The number of inflammatory cells was determined by counting 10 fields (400x magnification) per heart or skeletal muscle section. Sirius Red-stained sections were entirely digitalized using a confocal microscope A1+ (Nikon, Tokyo, Japan). The percentage of fibrosis was determined by analysis of whole sections of heart or skeletal muscle, stained with Sirius Red with a semiautomatic morphometric protocol, using Image-Pro Plus v.7.0 (Media Cybernetics, Rockville, Maryland, USA). Two blinded investigators performed the analyses.

**2.5. Immunofluorescence Analyses.** Skeletal muscle sections of 10  $\mu$ m were fixed with 4% paraformaldehyde and incubated overnight at 4°C with skeletal myosin primary antibody diluted 1:50 (Sigma-Aldrich, St. Louis, MO, USA). On the following day, the sections were incubated for 1 h with secondary antibody anti-rabbit IgG Alexa Fluor 488 conjugate at dilution of 1:600 (Thermo Fisher Scientific). Nuclei were stained with 4,6-diamidino-2-phenylindole (VECTASHIELD mounting medium with DAPI H-1200; Vector Laboratories, Burlingame, CA, USA). The presence of fluorescent fibers was determined by observation in the A1+ confocal microscope (Nikon). Quantifications of stained areas were performed in large image captured under 100x magnification, using the Image-Pro Plus v.7.0 software (Media Cybernetics).

**2.6. Cytokine Measurement.** Cytokine concentrations were evaluated in the serum by ELISA, using DuoSet kits for tumor necrosis factor alpha (TNF- $\alpha$ ), interferon gamma (IFN- $\gamma$ ), interleukin 10 (IL-10), and transforming growth factor beta (TGF- $\beta$ ), according to the manufacturer's instructions (R&D Systems, Minneapolis, MN, USA).

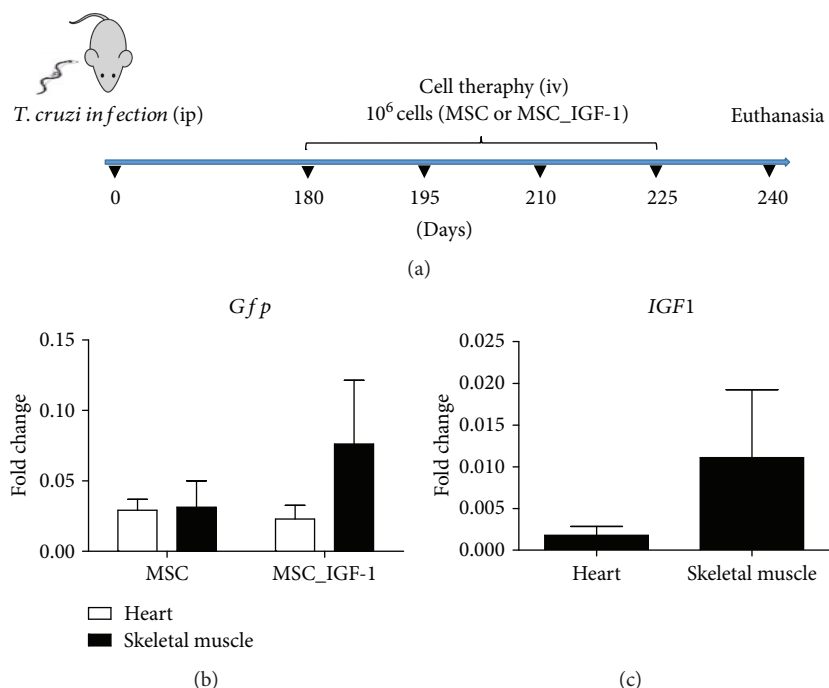


FIGURE 1: Experimental design and cell tracking. C57BL/6 mice were infected with 1000 *T. cruzi* trypomastigotes (Colombian strain) and treated, during the chronic phase, with  $10^6$  MSCs or MSC\_IGF-1, intravenously, every 15 days, during 60 days (a). Saline-treated and naïve mice were used as controls. Heart and skeletal muscle tissues were collected 15 days after the last administration of cells for RT-qPCR analysis of GFP (b) or human IGF-1 gene expression (c). Values represent the mean  $\pm$  SEM of 5–7 animals/group.

**2.7. Real-Time Reverse Transcription Polymerase Chain Reaction (RT-qPCR).** Total RNA was isolated from heart and skeletal muscle samples with a TRIzol reagent (Thermo Fisher Scientific), and concentration was determined by photometric measurement. High-Capacity cDNA Reverse Transcription Kit (Thermo Fisher Scientific) was used to synthesize cDNA of 1  $\mu$ g RNA by following the manufacturer's recommendations. RT-qPCR assays were performed to detect the expression levels of *Tnf* (Mm00443258\_m1), *Ifng* (Mm00801778\_m1), *Nos2* (Mm01309898m1), *Arg1* (Mm00475988\_m1), *Il1b* (Mm00434228\_m1), *Il10* (Mm00439616\_m1), *Tgfb1* (Mm00441724\_m1), *Ptprc* (mm01293577\_m1), and *Cox2* (Mm01307329\_m1). For the detection of GFP and human IGF-1 mRNA, the following primer sequences were used in real-time PCR assays: GFP: 5'-AGCAGAACACCCCATCG-3' and 3'-TCCAGCAGG ACCATGTGATC-5' and hIGF-1 5'CCAAGACCCAGAAG GAAGTACA-3' and 3'-TGCCATGTCACTCTTCACTCC-5'. The RT-qPCR amplification mixtures contained 20  $\mu$ g template cDNA, TaqMan Master Mix (10  $\mu$ L), and probes in a final volume of 20  $\mu$ L (all from Thermo Fisher Scientific). All reactions were run in duplicate on an ABI 7500 Sequence Detection System (Thermo Fisher Scientific) under standard thermal cycling conditions. The mean cycle threshold (Ct) values from duplicate measurements were used to calculate expression of the target gene, with normalization to an internal control, *Gapdh*, using the 2-DCt formula. Experiments with coefficients of variation greater than 5% were excluded. A nontemplate control (NTC) and nonreverse transcription controls (No-RT) were also included.

**2.8. Statistical Analyses.** Statistical comparisons between groups were performed by Student's *t*-test when comparing two groups and ANOVA followed by a Newman-Keuls post hoc test for multiple comparisons, using a GraphPad Prism program (Software Inc., San Diego, CA, USA) version 5.0. Results were considered significant when  $P < 0.05$ .

### 3. Results

**3.1. MSCs and MSC\_IGF-1 Are Detected in the Heart and Skeletal Muscles following Transplantation to Chronic Chagasic Mice.** A treatment regimen composed of repeated intravenous injections of MSCs or MSC\_IGF-1 (Figure 1(a)) was associated with increased mortality (40% for the MSC group and 30% for the MSC\_IGF-1 group) in mice chronically infected with *T. cruzi*, due to pulmonary embolism. Surviving mice ( $n = 6$  for the MSC group and  $n = 7$  for the MSC\_IGF-1 group) were euthanized two months following the initiation of the treatment regimen for histological and gene expression analyses and quantification of cytokines (Figure 1(a)).

First, we evaluated the presence of transplanted cells in the heart and skeletal muscles by detection of the transgene mRNAs by RT-qPCR. GFP was used to detect both MSCs and MSC\_IGF-1, while hIGF-1 was used to detect MSC\_IGF-1. We detected GFP mRNA in the hearts of six out of seven mice from the MSC\_IGF-1 group and five out of six mice in the MSC group (Figure 1(b)). While no expression of hIGF-1 was found in mouse hearts from the MSC group, four out of seven mice in the MSC\_IGF-1 group were



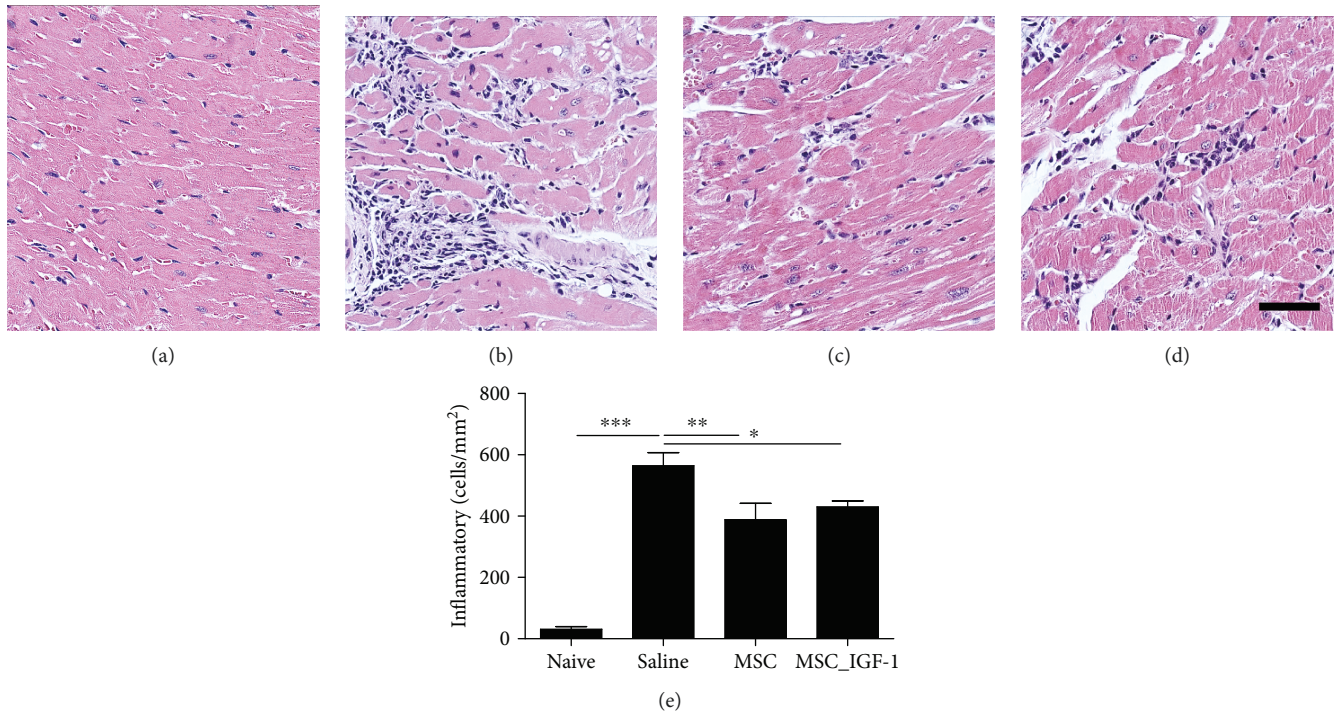


FIGURE 2: Quantification of inflammatory cells infiltrating the heart. Representative images of heart sections from mice euthanized two months after cell therapy with MSCs, MSC\_IGF-1, or untreated controls. Heart sections were stained with H&E, and the number of inflammatory cells was quantified, comparing naïve (a) and infected mice treated with saline (b) MSCs (c) or MSC\_IGF-1 (d). Bars = 50  $\mu$  m. (e) Number of inflammatory cells per mm<sup>2</sup> in H&E-stained sections. Data represent the mean  $\pm$  SEM of 5–7 animals/group. \* $P < 0.05$ , \*\* $P < 0.01$ , and \*\*\* $P < 0.001$ .

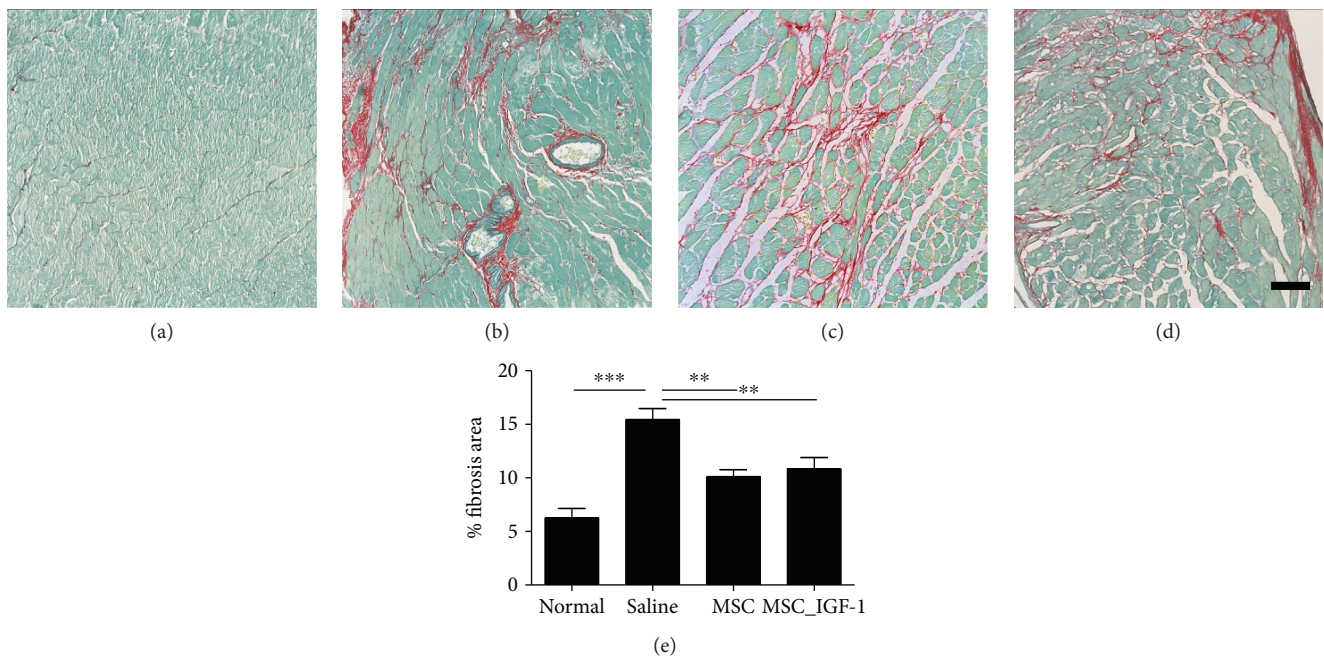


FIGURE 3: Quantification of cardiac fibrosis. Representative images of heart sections stained with Sirius Red obtained from naïve (a) or infected mice treated with saline (b), MSCs (c), or MSC\_IGF-1 (d). Bars = 50  $\mu$ m. (e) Quantification of the percentage of cardiac fibrosis area. Results are expressed as mean  $\pm$  SEM of 5–7 animals/group. \*\* $P < 0.01$  and \*\*\* $P < 0.001$ .

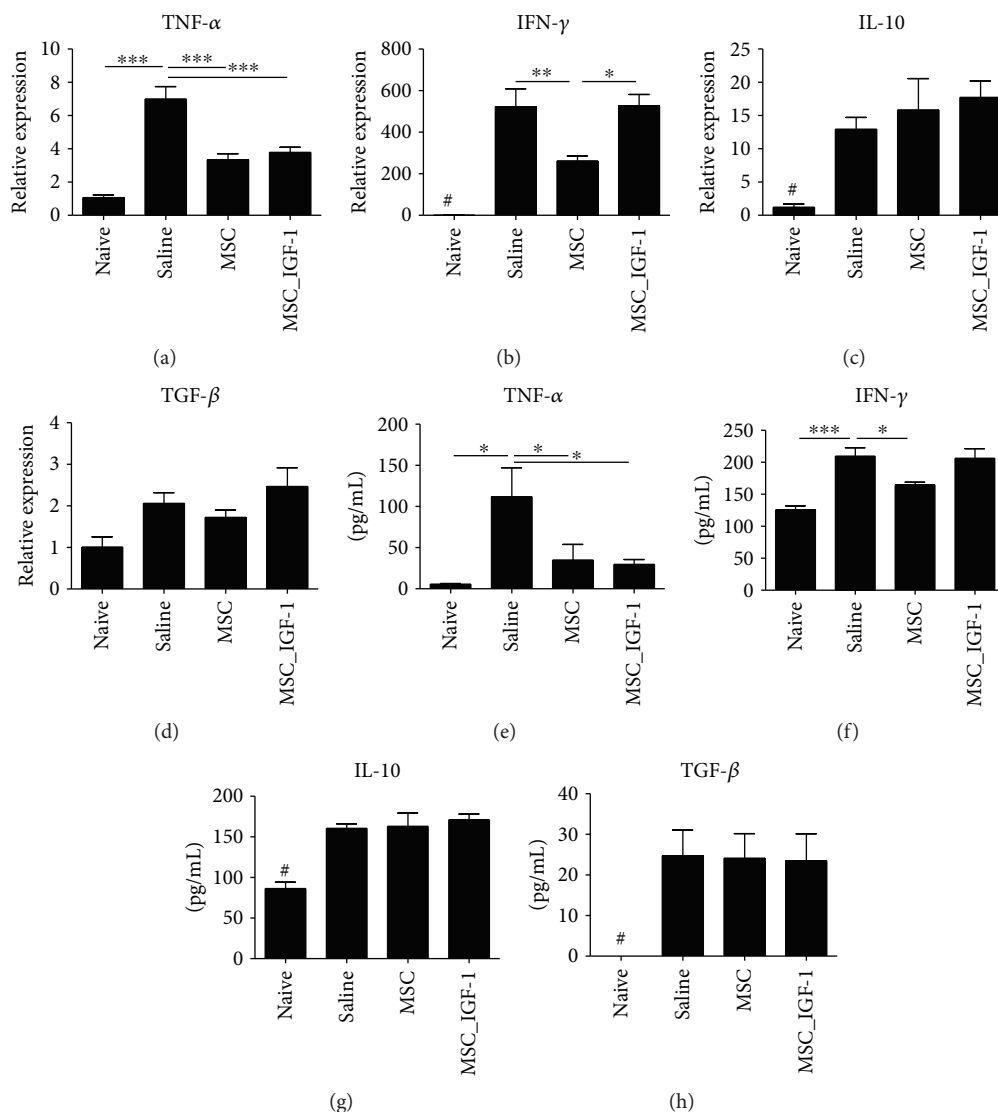


FIGURE 4: Cytokine evaluation in the heart and serum after cell therapy. Samples or infected mice treated with saline, MSCs, or MSC\_IGF-1 were collected two months following the initiation of the cell therapy protocol and analyzed by RT-qPCR in the heart tissue for gene expression (a–d) and by ELISA in the serum for protein quantification (e–h) of TNF- $\alpha$  (a, e), IFN- $\gamma$  (b, f), IL-10 (c, g), and TGF- $\beta$  (d, h). Data represent the mean  $\pm$  SEM of 5–7 mice per group. \* $P < 0.05$ , \*\* $P < 0.01$ , \*\*\* $P < 0.001$ , and # $P < 0.0001$  compared to other groups.

positive for the expression of this mRNA (Figure 1(c)). In the skeletal muscle, all mice treated with MSCs were positive for GFP, while 4 out of 7 mice presented both expressions of GFP and hIGF-1 in mice treated with MSC\_IGF-1 (Figures 1(b) and 1(c)).

**3.2. Cell Therapy with MSCs and MSC\_IGF-1 Modulates Cardiac Inflammation and Fibrosis.** Next, we evaluated the effects of cell therapy by tissue analysis in the hearts of chagasic mice. All mice chronically infected with *T. cruzi* presented intense inflammatory infiltrates in the myocardium, which were mainly composed of mononuclear cells (Figures 2(a)–2(d)). Infiltrating inflammatory cells were quantified, and a significant reduction in the number of cells was measured in both MSC- and MSC\_IGF-1-treated mice, when compared to saline-treated controls (Figure 2(e)). Diffuse areas of cardiac fibrosis, distributed along the atria,

atrioventricular junction, and ventriculi, were observed in all *T. cruzi*-infected mice and not in all naïve controls (Figures 3(a)–3(d)). A reduction in the fibrotic area was also observed in the hearts of mice treated with either MSCs or MSC\_IGF-1, when compared to saline-treated controls (Figure 3(e)).

Additionally, the expression levels of proinflammatory and anti-inflammatory genes were evaluated in heart samples. Treatment with MSCs or MSC\_IGF-1 produced a statistically significant reduction in the expression of TNF- $\alpha$ , while IFN- $\gamma$  gene expression was reduced only in MSC-treated mouse hearts (Figures 4(a) and 4(b)). No significant differences were observed in TGF- $\beta$  or IL-10 gene expression between MSC-, MSC\_IGF-1-, and saline-treated groups (Figures 4(c) and 4(d)).

We also investigated the systemic immunomodulatory effects of cell therapy by quantification of cytokines in the

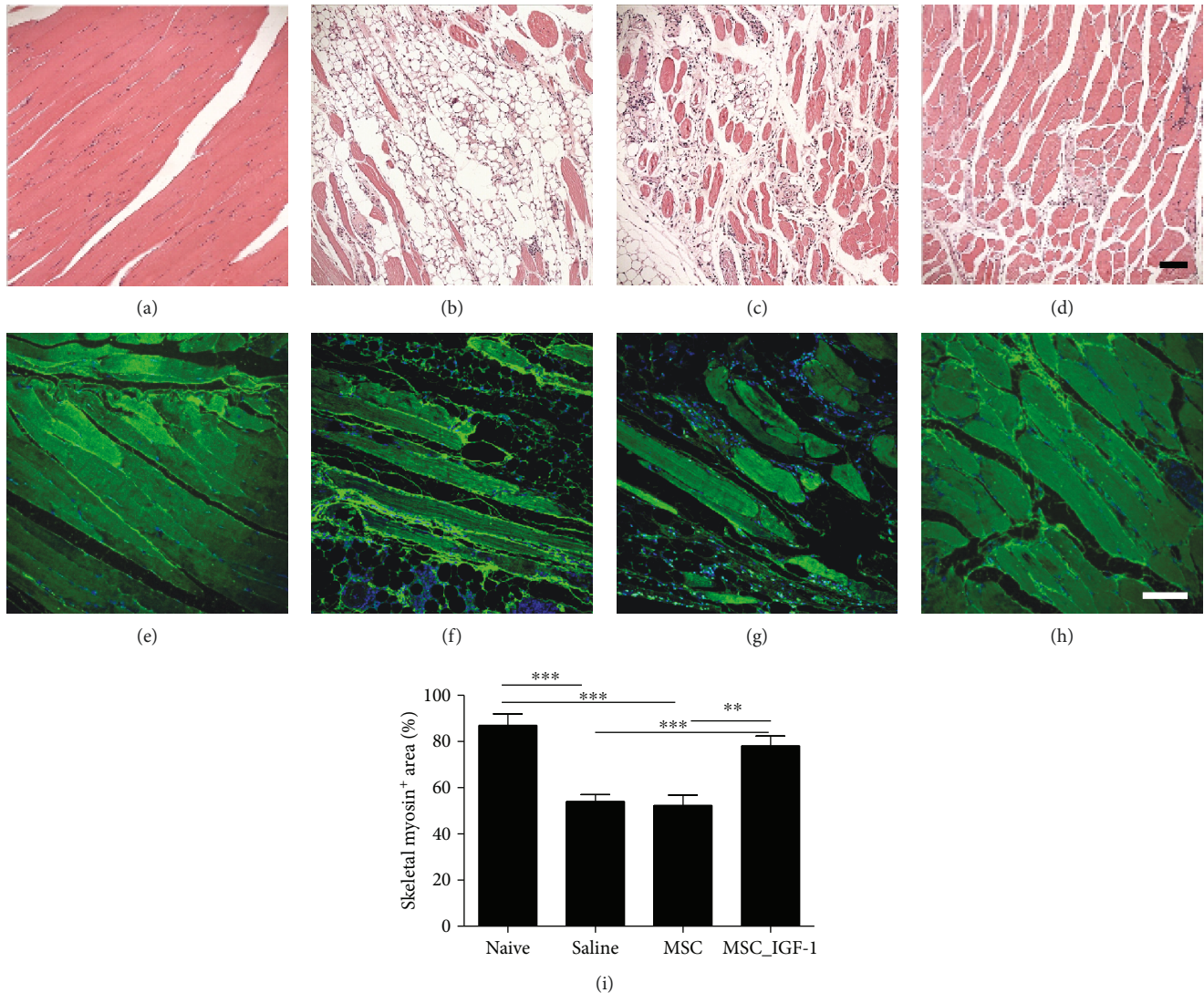


FIGURE 5: Proregenerative effects of therapy with MSC\_IGF-1 in the skeletal muscle. Representative images of skeletal muscle sections stained with H&E, obtained from naïve (a) or infected mice treated with saline (b), MSCs (c), or MSC\_IGF-1 (d), showing destruction of myofibers and substitution for fibrosis and adipose tissue in infected mice, when compared to naïve mice, and recovery in MSC\_IGF-1-treated mice (d). Skeletal myosin staining in skeletal muscle sections from naïve (e) or infected mice (f) treated with saline (g), MSCs (h), or IGF-1 (i), confirming the enhanced presence of myosin<sup>+</sup> myofibers in MSC\_IGF-1-treated mice. Bars = 100  $\mu$ m. (j) Quantification of the skeletal myosin<sup>+</sup> area. \*\* $P < 0.01$  and \*\*\* $P < 0.001$ .

serum. Similar to the findings in the heart tissue, the levels of TNF- $\alpha$  were reduced significantly in the groups treated with either MSCs or MSC\_IGF-1, although IFN- $\gamma$  levels decreased only in the MSC-treated group (Figures 4(e) and 4(f)). No statistically significant differences were observed in TGF- $\beta$  or IL-10 serum levels, when comparing treated mice to saline controls (Figures 4(g) and 4(h)).

**3.3. Proregenerative and Immunomodulatory Actions of MSC\_IGF-1 in the Skeletal Muscle of Mice Chronically Infected with *T. cruzi*.** Skeletal muscle from naïve mice presented a normal microscopic structure, with preserved myocytes, as observed by H&E staining (Figure 5(a)). In contrast, sections from *T. cruzi*-infected mice of saline and MSC groups presented clear signs of skeletal muscle

destruction and substitution for fibrosis and adipose tissue (Figures 5(b) and 5(c)). In MSC\_IGF-1-treated mice, however, we observed a marked preservation of the myofibers (Figure 5(d)). This finding was confirmed by quantification of the area occupied by myofibers, visualized by positive staining for skeletal myosin (Figures 5(e)–5(h)). Naïve mice had a significantly higher myosin<sup>+</sup> area than saline- or MSC-treated mice and presented a similar pattern to MSC\_IGF-1 mice (Figure 5(i)).

Muscle sections of naïve mice presented low interstitial cellularity (Figure 6(a)), while *T. cruzi*-infected mice were infiltrated predominantly by mononuclear cells between myofibers and surrounding blood vessels (Figures 6(b)–6(d)). Significant deposition of fibrosis was also observed in skeletal muscle sections of infected mice, compared to

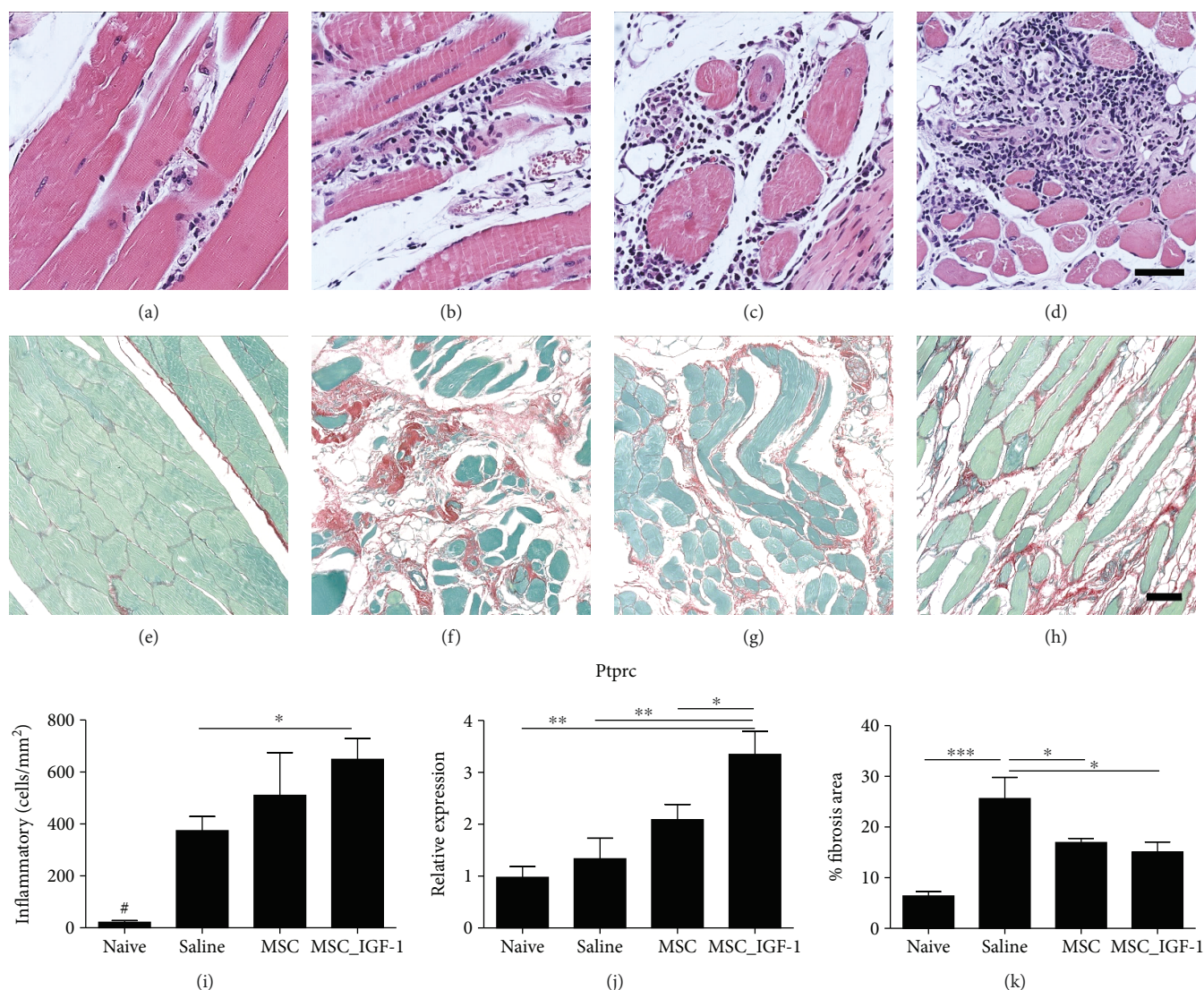


FIGURE 6: Quantification of inflammatory infiltrates and fibrosis area in the skeletal muscle. Representative images of skeletal muscle sections stained by conventional H&E stain for analysis of inflammatory infiltrates in naïve (a) or infected mice submitted to treatment with saline (b), MSCs (c), or MSC\_IGF-1 (d). Representative images of Sirius Red staining for quantification of the fibrosis area in the skeletal muscle of naïve (e) or infected mice submitted to treatment with saline (f), MSCs (g), or MSC\_IGF-1 (h). Bars = 50  $\mu$ m. Quantification of inflammatory cells by morphometry (i) and evaluation of *Ptprc* expression by RT-qPCR (j). (k) Percentage of the fibrosis area quantified by analysis of whole sections stained with Sirius Red-stained skeletal muscle. Data represent the mean  $\pm$  SEM of 5–7 mice per group. \* $P < 0.05$ , \*\* $P < 0.01$ , \*\*\* $P < 0.001$ , and # $P < 0.0001$ .

naïve controls (Figures 6(e)–6(h)). However, morphometric analysis did not show a reduction in the number of infiltrating inflammatory cells in mice treated with either MSCs or MSC\_IGF-1, when compared to saline-treated mice. In fact, we found that mice treated with MSC\_IGF-1 presented a significantly higher number of inflammatory cells (Figure 6(i)). This was corroborated by RT-qPCR analysis for the detection of PTPRC mRNA, demonstrating a significantly higher expression level for CD45, a panleukocyte marker (Figure 6(j)). The quantification of fibrosis by morphometric analysis in Sirius Red-stained sections showed that both treatments with MSCs and MSC\_IGF-1 were able to reduce fibrosis in the skeletal muscle (Figure 6(k)).

Finally, gene expression analysis of the skeletal muscle tissue revealed that treatment with MSCs was able to significantly reduce the expression of proinflammatory cytokines  $TNF-\alpha$  and  $IL-1\beta$  when compared to saline-treated mice. This was not observed for MSC\_IGF-1-treated mice, which showed no significantly different expression levels, when compared to saline-treated mice (Figures 7(a) and 7(b)). In fact, MSC\_IGF-1-treated skeletal muscle had increased expression of *COX2* gene (Figure 7(c)). MSC\_IGF-1 treatment did not significantly alter the expression of *iNOS* and *arginase* genes, markers of M1 and M2 macrophages, respectively (Figures 7(d) and 7(e)). Finally, a significantly higher expression of the *IL-10* gene was seen in the MSC\_IGF-1 group compared to the other groups (Figure 7(f)).

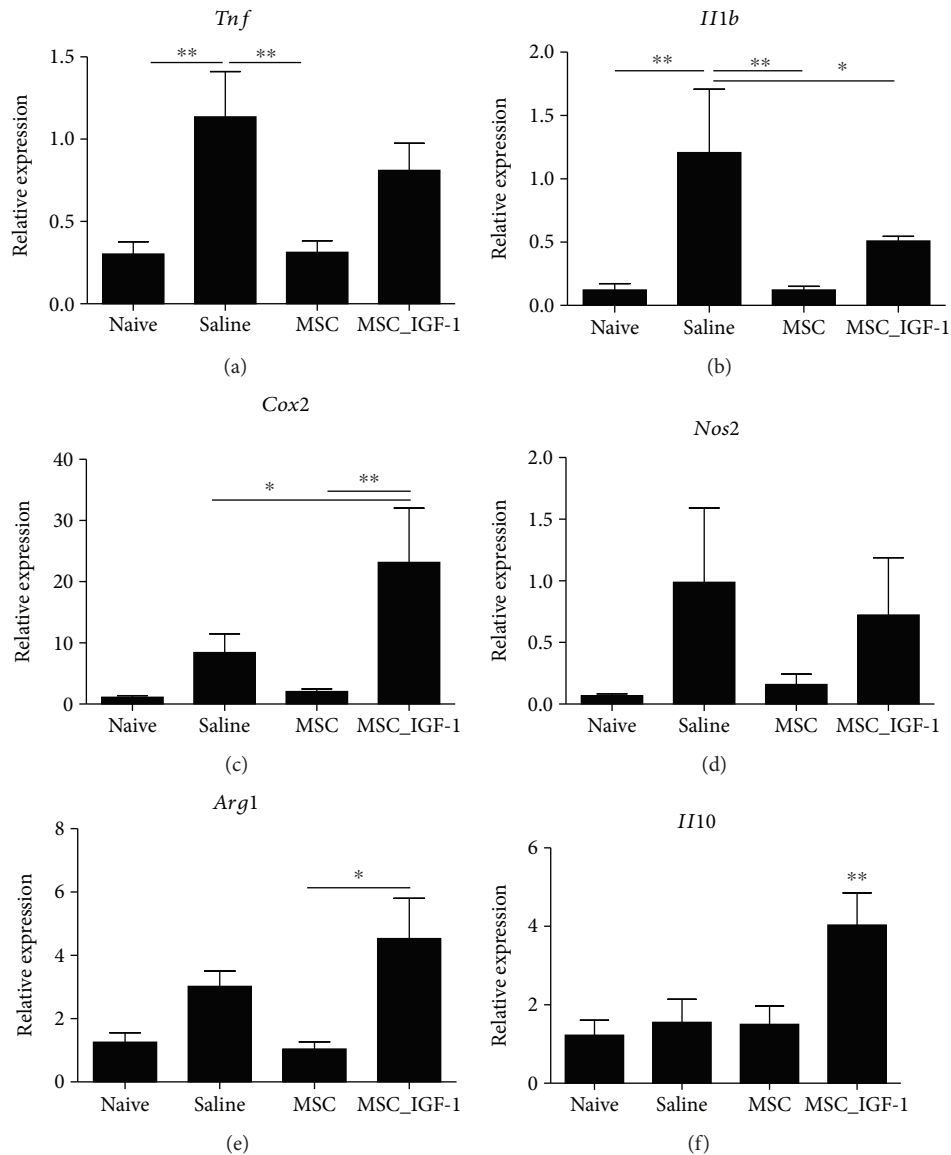


FIGURE 7: Gene expression analysis in the skeletal muscle. Skeletal muscle samples of uninfected or chagasic mice treated with MSCs, MSC\_IGF-1, or saline were removed two months after therapy and analyzed by RT-qPCR for the expression of *Tnf* (a), *Ilb* (b), *Cox2* (c), *Nos2* (d), *Arg1* (e), and *Il10* (f). Data represent the mean  $\pm$  SEM of 5–7 mice per group. \* $P < 0.05$  and \*\* $P < 0.01$ .

#### 4. Discussion

In the present study, we evaluated whether IGF-1 overexpression can increase the immunomodulatory and/or regenerative actions of MSCs in the context of experimental Chagas disease cardiomyopathy. We found that transplantation of MSC\_IGF-1 reduced cardiac inflammation and fibrosis, in a similar magnitude to the effect observed in MSC-treated mice. When skeletal muscle tissue was evaluated, however, a marked regenerative effect was observed in mice transplanted with MSC\_IGF-1 cells.

IGF-1 has been associated with processes involved in both cardiac and skeletal muscle regeneration [7, 8, 20]. These studies, however, have focused on the role of IGF-1 in the regeneration after acute injuries to the skeletal muscle, while its role in a chronic setting, in the presence of

persistent myositis, has not been addressed. We have previously shown that IGF-1 gene expression is increased in the heart and skeletal muscles in the acute phase of infection with *T. cruzi* in mice [21]. Here, we found that MSC\_IGF-1 had a clear effect in the regeneration of the skeletal muscle from mice chronically infected with *T. cruzi*, in which the loss of skeletal myofibers could be the result of direct damage induced by *T. cruzi* infection associated with sarcopenia induced by chronic inflammation and increased local and circulating levels of TNF- $\alpha$  [22]. The fact that circulating TNF- $\alpha$  levels were equally modulated by both MSCs and MSC\_IGF-1 suggests that the recovery of skeletal myofibers by IGF-1-overexpressing cells is not a consequence of immunomodulatory actions but possibly be the result of direct actions mediated by IGF-1 in the skeletal muscle.

The role of IGF-1 in the activation of satellite cell and muscle regeneration is well established [23]. It is also known that inflammation is crucial for muscle repair, and macrophages play an important role in this process by secreting IGF-1 to promote activation and proliferation of Pax7<sup>+</sup> satellite cells [24]. Interestingly, recruitment of bone marrow cells to the skeletal muscle was also previously shown to contribute to myogenesis in a Pax7-/Myod-independent way [25]. Moreover, we have previously demonstrated the direct contribution of bone marrow-derived cells in the regeneration of myofibers during *T. cruzi* infection, in a bone marrow chimera experimental model [21].

The interaction between immune cells and muscle regeneration has been previously explored, and suppression of macrophage activity impairs muscle regeneration, leading to severe fibrosis [26]. Macrophage subtypes are also associated with different stages of the myogenic program, since proinflammatory (M1) macrophages predominate during the proliferative stage of muscle regeneration and anti-inflammatory (M2) macrophages are involved during the differentiation stage [27]. In the present study, therapy with MSC\_IGF-1 was associated with increased numbers of mononuclear cells infiltrating the skeletal muscle, along with high expression of inflammatory mediators, such as TNF- $\alpha$  and IL-1 $\beta$ , along with the anti-inflammatory cytokine IL-10. These results could be explained by direct actions of IGF-1, but it is also possible that immune response directed towards the transgenes—GFP and hIGF-1—could have been elicited, and this was not investigated in the present study.

An interesting finding was the increased expression of COX2 in the skeletal muscle tissue of MSC\_IGF-1-transplanted mice. IGF-1 signaling can induce COX2 expression in different cell types, including keratinocytes [28], mammary glands [29], and various tumor cells [30–32]. COX2 is an enzyme involved in arachidonic acid metabolism, responsible for the production of eicosanoids, including thromboxanes and prostaglandins, which are important inflammatory mediators. Importantly, prostaglandin E2 has been demonstrated to play a crucial role in processes of myoblast proliferation and regeneration, and functional recovery has been demonstrated [33, 34]. We found the expression of hIGF-1 in the muscle tissues of transplanted mice, indicating that this factor may be locally involved in the COX2 upregulation observed in our study and suggesting the participation of PGE2 in the muscle regeneration promoted by MSC\_IGF-1 in chronic chagasic mice.

Several cell types have been investigated in therapies directed towards Chagas disease. Bone marrow mononuclear cells were initially tested in preclinical studies and were associated with a reduction in cardiac inflammation and fibrosis [35], mainly due to their immunomodulatory action [36], but failed to significantly improve the heart function in a randomized clinical trial [37]. MSCs have also been previously studied in experimental models of Chagas disease and were associated with significant improvements in inflammation and fibrosis [16, 18]. One significant limitation of our mouse model of Chagas disease is the lack of left ventricular dysfunction, which does not allow for the investigation of functional cardiac improvements that could be associated

with the therapy. This limits our conclusions to aspects of immunomodulation, fibrosis, and regeneration, which were evaluated at the tissue level. Additional preclinical studies using a different model would be necessary to evaluate the potential of this gene and cell therapy in improving left ventricular function. To date, the results of clinical trials with MSCs in the treatment of heart failure of other etiologies have been modest, at best [38]. However, no clinical studies with MSCs in Chagas disease patients with cardiac dysfunction have been performed so far.

In conclusion, our results indicate that the overexpression of growth factors may be an interesting approach for improving the therapeutic potential of MSCs, since IGF-1 overexpression promoted increased proregenerative actions in association with maintained immunomodulatory and antifibrotic actions, when compared to regular MSCs, in the mouse model of chronic Chagas disease.

### Data Availability

The data used to support the findings of this study are included within the article.

### Conflicts of Interest

The authors declare that there is no conflict of interest regarding the publication of this paper.

### Acknowledgments

The authors acknowledge the Brazilian agencies FINEP, CNPq, and FAPESB for research funding.

### References

- [1] M. B. Murphy, K. Moncivais, and A. I. Caplan, “Mesenchymal stem cells: environmentally responsive therapeutics for regenerative medicine,” *Experimental & Molecular Medicine*, vol. 45, no. 11, article e54, 2013.
- [2] L. D. S. Meirelles, A. M. Fontes, D. T. Covas, and A. I. Caplan, “Mechanisms involved in the therapeutic properties of mesenchymal stem cells,” *Cytokine & Growth Factor Reviews*, vol. 20, no. 5-6, pp. 419–427, 2009.
- [3] R. R. Sharma, K. Pollock, A. Hubel, and D. McKenna, “Mesenchymal stem or stromal cells: a review of clinical applications and manufacturing practices,” *Transfusion*, vol. 54, no. 5, pp. 1418–1437, 2014.
- [4] J. A. Nolte, ““Next-generation” mesenchymal stem or stromal cells for the in vivo delivery of bioactive factors: progressing toward the clinic,” *Transfusion*, vol. 56, no. 4, pp. 15S–17S, 2016.
- [5] S. Kumar, D. Chanda, and S. Ponnazhagan, “Therapeutic potential of genetically modified mesenchymal stem cells,” *Gene Therapy*, vol. 15, no. 10, pp. 711–715, 2008.
- [6] C. Sassoli, D. Nosi, A. Tani et al., “Defining the role of mesenchymal stromal cells on the regulation of matrix metalloproteinases in skeletal muscle cells,” *Experimental Cell Research*, vol. 323, no. 2, pp. 297–313, 2014.
- [7] J. D. Schertzer and G. S. Lynch, “Comparative evaluation of IGF-I gene transfer and IGF-I protein administration for

- enhancing skeletal muscle regeneration after injury,” *Gene Therapy*, vol. 13, no. 23, pp. 1657–1664, 2006.
- [8] E. R. Barton-Davis, D. I. Shoturma, and H. L. Sweeney, “Contribution of satellite cells to IGF-I induced hypertrophy of skeletal muscle,” *Acta Physiologica Scandinavica*, vol. 167, no. 4, pp. 301–305, 1999.
- [9] N. Kanemitsu, K. Tambara, G. U. Premaratne et al., “Insulin-like growth factor-1 enhances the efficacy of myoblast transplantation with its multiple functions in the chronic myocardial infarction rat model,” *The Journal of Heart and Lung Transplantation*, vol. 25, no. 10, pp. 1253–1262, 2006.
- [10] C. Enoki, H. Otani, D. Sato, T. Okada, R. Hattori, and H. Imamura, “Enhanced mesenchymal cell engraftment by IGF-1 improves left ventricular function in rats undergoing myocardial infarction,” *International Journal of Cardiology*, vol. 138, no. 1, pp. 9–18, 2010.
- [11] N. Klein, I. Hurwitz, and R. Durvasula, “Globalization of Chagas disease: a growing concern in nonendemic countries,” *Epidemiology Research International*, vol. 2012, Article ID 136793, 13 pages, 2012.
- [12] C. Bern, “Chagas’ disease,” *The New England Journal of Medicine*, vol. 373, no. 5, pp. 456–466, 2015.
- [13] J. A. Marin-Neto, E. Cunha-Neto, B. C. Maciel, and M. V. Simões, “Pathogenesis of chronic Chagas heart disease,” *Circulation*, vol. 115, no. 9, pp. 1109–1123, 2007.
- [14] M. B. Soares, K. N. Silva-Mota, R. S. Lima, M. C. Bellintani, L. Pontes-de-Carvalho, and R. Ribeiro-dos-Santos, “Modulation of chagasic cardiomyopathy by interleukin-4: dissociation between inflammation and tissue parasitism,” *The American Journal of Pathology*, vol. 159, no. 2, pp. 703–709, 2001.
- [15] D. B. Mello, I. P. Ramos, F. C. P. Mesquita et al., “Adipose tissue-derived mesenchymal stromal cells protect mice infected with *Trypanosoma cruzi* from cardiac damage through modulation of anti-parasite immunity,” *PLoS Neglected Tropical Diseases*, vol. 9, no. 8, article e0003945, 2015.
- [16] D. N. Silva, B. S. De Freitas Souza, C. M. H. Azevedo et al., “Intramyocardial transplantation of cardiac mesenchymal stem cells reduces myocarditis in a model of chronic Chagas disease cardiomyopathy,” *Stem Cell Research & Therapy*, vol. 5, no. 4, p. 81, 2014.
- [17] Jasmin, L. A. Jelicks, H. B. Tanowitz et al., “Molecular imaging, biodistribution and efficacy of mesenchymal bone marrow cell therapy in a mouse model of Chagas disease,” *Microbes and Infection*, vol. 16, no. 11, pp. 923–935, 2014.
- [18] T. F. Larocca, B. S. de Freitas Souza, C. A. Silva et al., “Transplantation of adipose tissue mesenchymal stem cells in experimental chronic chagasic cardiopathy,” *Arquivos Brasileiros de Cardiologia*, vol. 100, no. 5, pp. 460–468, 2013.
- [19] G. V. M. Gonçalves, D. N. Silva, R. H. Carvalho et al., “Generation and characterization of transgenic mouse mesenchymal stem cell lines expressing *hIGF-1* or *hG-CSF*,” *Cytotechnology*, vol. 70, no. 2, pp. 577–591, 2017.
- [20] G. Castellano, F. Affuso, P. Di Conza, and S. Fazio, “The GH/IGF-1 axis and heart failure,” *Current Cardiology Reviews*, vol. 5, no. 3, pp. 203–215, 2009.
- [21] B. S. F. Souza, C. M. Azevedo, R. S. Lima et al., “Bone marrow cells migrate to the heart and skeletal muscle and participate in tissue repair after *Trypanosoma cruzi* infection in mice,” *International Journal of Experimental Pathology*, vol. 95, no. 5, pp. 321–329, 2014.
- [22] S. L. Budui, A. P. Rossi, and M. Zamboni, “The pathogenetic bases of sarcopenia,” *Clinical Cases Mineral and Bone Metabolism*, vol. 12, pp. 22–26, 2015.
- [23] S. Machida and F. W. Booth, “Insulin-like growth factor 1 and muscle growth: implication for satellite cell proliferation,” *The Proceedings of the Nutrition Society*, vol. 63, no. 2, pp. 337–340, 2004.
- [24] J. Tonkin, L. Temmerman, R. D. Sampson et al., “Monocyte/macrophage-derived IGF-1 orchestrates murine skeletal muscle regeneration and modulates autocrine polarization,” *Molecular Therapy*, vol. 23, no. 7, pp. 1189–1200, 2015.
- [25] A. Xynos, P. Corbella, N. Belmonte, R. Zini, R. Manfredini, and G. Ferrari, “Bone marrow-derived hematopoietic cells undergo myogenic differentiation following a Pax-7 independent pathway,” *Stem Cells*, vol. 28, no. 5, pp. 965–973, 2010.
- [26] M. Segawa, F. S. Ichiro, Y. Yamamoto et al., “Suppression of macrophage functions impairs skeletal muscle regeneration with severe fibrosis,” *Experimental Cell Research*, vol. 314, no. 17, pp. 3232–3244, 2008.
- [27] J. G. Tidball and S. A. Villalta, “Regulatory interactions between muscle and the immune system during muscle regeneration,” *American Journal of Physiology Regulatory, Integrative and Comparative Physiology*, vol. 298, no. 5, pp. R1173–R1187, 2010.
- [28] H. J. Kim and T. Y. Kim, “IGF-II-mediated COX-2 gene expression in human keratinocytes through extracellular signal-regulated kinase pathway,” *Journal of Investigative Dermatology*, vol. 123, no. 3, pp. 547–555, 2004.
- [29] J. Tian, I. Lambertz, T. R. Berton et al., “Transgenic insulin-like growth factor-1 stimulates activation of COX-2 signaling in mammary glands,” *Molecular Carcinogenesis*, vol. 51, no. 12, pp. 973–983, 2012.
- [30] O. Stoeltzing, W. Liu, F. Fan et al., “Regulation of cyclooxygenase-2 (COX-2) expression in human pancreatic carcinoma cells by the insulin-like growth factor-I receptor (IGF-IR) system,” *Cancer Letters*, vol. 258, no. 2, pp. 291–300, 2007.
- [31] Z. Cao, L.-Z. Liu, D. A. Dixon, J. Z. Zheng, B. Chandran, and B.-H. Jiang, “Insulin-like growth factor-I induces cyclooxygenase-2 expression via PI3K, MAPK and PKC signaling pathways in human ovarian cancer cells,” *Cellular Signalling*, vol. 19, no. 7, pp. 1542–1553, 2007.
- [32] A. Di Popolo, A. Memoli, A. Apicella et al., “IGF-II/IGF-I receptor pathway up-regulates COX-2 mRNA expression and PGE2 synthesis in Caco-2 human colon carcinoma cells,” *Oncogene*, vol. 19, no. 48, pp. 5517–5524, 2000.
- [33] B. A. Bondesen, S. T. Mills, K. M. Kegley, and G. K. Pavlath, “The COX-2 pathway is essential during early stages of skeletal muscle regeneration,” *American Journal of Physiology Cell Physiology*, vol. 287, no. 2, pp. C475–C483, 2004.
- [34] A. T. V. Ho, A. R. Palla, M. R. Blake et al., “Prostaglandin E2 is essential for efficacious skeletal muscle stem-cell function, augmenting regeneration and strength,” *Proceedings of the National Academy of Sciences of the United States of America*, vol. 114, no. 26, pp. 6675–6684, 2017.
- [35] M. B. P. Soares, R. S. Lima, L. L. Rocha et al., “Transplanted bone marrow cells repair heart tissue and reduce myocarditis in chronic chagasic mice,” *The American Journal of Pathology*, vol. 164, no. 2, pp. 441–447, 2004.
- [36] M. B. P. Soares, R. S. Lima, B. S. F. Souza et al., “Reversion of gene expression alterations in hearts of mice with chronic

chagasic cardiomyopathy after transplantation of bone marrow cells," *Cell Cycle*, vol. 10, no. 9, pp. 1448–1455, 2011.

- [37] R. R. Dos Santos, S. Rassi, G. Feitosa et al., "Cell therapy in chagas cardiomyopathy (Chagas arm of the multicenter randomized trial of cell therapy in cardiopathies study): a multicenter randomized trial," *Circulation*, vol. 125, no. 20, pp. 2454–2461, 2012.
- [38] M. Hao, R. Wang, and W. Wang, "Cell therapies in cardiomyopathy: current status of clinical trials," *Analytical Cellular Pathology*, vol. 2017, Article ID 9404057, 20 pages, 2017.





**Hindawi**

Submit your manuscripts at  
[www.hindawi.com](http://www.hindawi.com)



## 6 DISCUSSÃO

A doença de Chagas é uma das principais doenças negligenciadas no mundo, principalmente, pela falta de investimento no desenvolvimento de novas drogas anti-parasitárias, como também pela falta do desenvolvimento de terapias que visam ao controle da resposta imune e que promovam a regeneração tecidual. Diante desse contexto, nosso grupo vem estudando diferentes estratégias terapêuticas com o objetivo de desenvolver potenciais terapias para o tratamento da CCC, seja através do desenvolvimento de drogas anti-parasitárias, anti-inflamatórias e anti-fibróticas, seja através do desenvolvimento de terapias que visem à substituição celular (Anexos I-IV; SOARES et al., 2004; LAROCCA et al., 2013; SILVA et al., 2014, SOUZA et al., 2014).

Neste trabalho, investigamos o potencial terapêutico de CTMs modificadas geneticamente para a superexpressão dos fatores G-CSF e IGF-1 no tratamento da CCC experimental. De maneira geral, observamos mecanismos múltiplos de potencialização dos efeitos terapêuticos das CTMs pela modificação genética, sumarizados na **figura 4**, que são representados principalmente por ações pró-regenerativas no músculo esquelético e sobre a modulação da resposta imune por meio do recrutamento de populações celulares imunossupressoras e modulação de fatores e citocinas pró- e anti-inflamatórias.

Inicialmente, geramos e caracterizamos as CTMs da medula óssea que superexpressam G-CSF e IGF-1 humanos (ANEXO II). De um modo geral, os dados deste trabalho demonstraram que a modificação genética não altera as principais características das CTMs, tais como seu potencial de diferenciação, o perfil fenotípico e, principalmente, seu potencial imunomodulador.

Em seguida, avaliamos o potencial terapêutico das CTMs modificadas geneticamente no modelo experimental da CCC causada pela infecção crônica pela cepa Colombiana do *T. cruzi*. Neste modelo experimental, há o desenvolvimento de miocardite difusa, com intenso infiltrado inflamatório no coração. A destruição progressiva das fibras cardíacas é fruto da persistência parasitária e intensa resposta inflamatória, que leva ao comprometimento do sistema de condução elétrica do coração, o que caracteriza o nosso modelo experimental como arritmogênico (MACAMBIRA et al., 2009; SOARES; LAIN-PONTES; RIBEIRO-DOS-SANTOS, 2001). Apesar de observarmos alterações morfológicas no tecido cardíaco de camundongos infectados pelo *T. cruzi* semelhante ao que ocorre em humanos, a avaliação

funcional cardíaca realizada neste estudo limitou-se às técnicas de ergometria e eletrocardiografia, pois a avaliação por ecocardiografia não se mostrou sensível para detectar as alterações morfológicas que ocorrem no coração, já que camundongos C57Bl/6 infectados cronicamente pela cepa Colombiana do *T. cruzi* não desenvolvem uma cardiopatia dilatada. Nesse modelo arritmogênico, são detectadas alterações eletrocardiográficas que variam desde bloqueio átrio ventricular de primeiro grau até a dissociação completa do eixo de condução elétrica entre o átrio e o ventrículo (MACAMBIRA et al., 2009). Outras técnicas, como a ressonância magnética, podem ser úteis para a avaliação funcional cardíaca neste modelo experimental, permitindo uma melhor detecção e análise das alterações morfológicas do coração e os efeitos terapêuticos da terapia celular.

Em ambos os trabalhos descritos nesta tese, foi demonstrado que a utilização de CTMs sem modificação genética possui efeito imunomodulador e anti-fibrótico no coração dos animais tratados com CTM, comparado ao grupo controle tratado com salina. Os efeitos terapêuticos relacionados a imunomodulação são demonstrados, principalmente, pela redução da expressão de  $TNF\alpha$  e  $IFN\gamma$  no coração, bem como pela redução do número de células inflamatórias no miocárdio. Adicionalmente, a redução da fibrose foi demonstrada pela morfometria do coração, na qual observou-se menor área de fibrose cardíaca nos grupos tratados com CTM comparado ao grupo controle tratado com veículo. Esses resultados reforçam os efeitos imunomodulador e anti-fibrótico das CTMs demonstrados previamente em outros trabalhos do nosso grupo, nos quais o tratamento com CTMs da medula óssea e de outras fontes, mostrou-se eficaz na redução da miocardite e fibrose no coração (ANEXO I; LAROCCA, 2013; SILVA et al., 2014). Em consonância com esses dados, outros estudos que utilizam o modelo de cardiopatia chagásica dilatada causada pela infecção crônica da cepa Brazil do *T. cruzi*, também descreveram o efeito imunomodulador e anti-fibrótico das CTMs derivadas da medula óssea e tecido adiposo, nos quais evidenciaram redução da miocardite e modulação de citocinas anti-inflamatória IL-10 e das pró-inflamatórias  $TNF\alpha$  e  $IFN\gamma$ , (JASMIN et al., 2014; MELLO et al., 2015).

Embora os efeitos terapêuticos da utilização de CTMs de diferentes fontes terem se mostrado promissores nos estudos realizados por nós e por outros grupos, sua utilização ainda não foi explorada em estudos clínicos da doença de Chagas. Apesar de observarmos um crescente número de estudos que mostram o potencial terapêutico das CTMs na área da medicina regenerativa, algumas limitações desta aplicação têm sido estudadas a fim de resolver problemas, como a baixa retenção celular, enxertia e incapacidade de sobrevivência das células

transplantadas no ambiente de lesão tecidual (PARK et al., 2015). Visando solucionar questões como essas, os estudos estão focando em potencializar os efeitos terapêuticos das CTMs através do direcionamento do seu potencial em secretar fatores com efeitos tróficos. Aqui, nós buscamos potencializar os efeitos das CTMs utilizando a modificação genética como ferramenta para promover a superexpressão do G-CSF e IGF-1 humanos, descritos como fatores com potencial terapêutico na doença de Chagas.

O G-CSF é um fator de crescimento amplamente utilizado na prática clínica com potencial imunomodulatório e regenerativo bem descritos (BENDALL;BRADSTOCK, 2014). No modelo experimental da doença de Chagas, nosso grupo demonstrou que o tratamento com G-CSF recombinante promoveu um efeito benéfico ao coração dos animais chagásicos, no qual foi observado redução da inflamação e fibrose do tecido cardíaco, bem como melhora da função cardíaca (VASCONCELOS et al., 2013). No primeiro capítulo deste trabalho, avaliamos se a combinação dos efeitos terapêuticos do G-CSF com a terapia celular, poderia oferecer um benefício terapêutico adicional ao observado nos estudos com o G-CSF recombinante, já que as CTMs possuem a capacidade de migrar para sítios de lesão e secretar fatores tróficos que poderiam agir sinergicamente aos efeitos terapêuticos do G-CSF secretado localmente.

Inicialmente, observamos que a terapia com CTM-G-CSF promoveu o aumento de leucócitos na circulação periférica e aumentou a capacidade migratória das CTMs para o coração. Em seguida, descrevemos os efeitos terapêuticos das CTM-G-CSF na modulação da resposta imune e da fibrose no coração dos animais cronicamente infectados pelo *T. cruzi*. Nossos resultados demonstraram que as CTM-G-CSF possui efeito imunomodulador superior às CTMs selvagens, promovendo a redução da inflamação e fibrose no coração de forma mais eficaz. Interessantemente, esses efeitos foram associados ao aumento do número de células imunossupressoras no coração, tais como linfócitos T regulatórios Foxp3<sup>+</sup> produtores de IL10 e MDSCs com atividade imunomoduladora. Esses achados corroboram com os resultados obtidos em outros estudos, os quais demonstraram que a terapia com G-CSF aumenta o recrutamento de células T regulatórias que modulam a resposta imune em transplantes alogênicos e no modelo experimental da doença de Chagas (FRANZKE et al., 2003; MORRIS et al., 2004; VASCONCELOS et al., 2013).

A população de células MDSCs tem sido descrita como células supressoras do sistema imunológico, que é expandida em situações de respostas inflamatórias intensas ou condições infecciosas, inclusive na infecção pelo *T. cruzi* (AROCENA et al., 2014). Cuervo e colaboradores demonstraram, durante a infecção pelo *T. cruzi* em camundongos, a presença das duas subpopulações de MDSCs, monocítica e granulocítica no coração (CUERVO et al., 2011).

Nos nossos experimentos, não só detectamos ambas as populações, como também vimos que a população monocítica (M-MDSC) estava aumentada no coração dos animais tratados com CTM-G-CSF.

Sabe-se que a subpopulação monocítica de MDSC é conhecida por expressar iNOS e Arg1, os quais contribuem fortemente para o papel imunomodulador dessas células (GABRILOVICH; NAGARAJ, 2009). Neste estudo, as MDSCs mobilizadas para o coração dos animais tratados com CTM-G-CSF foram caracterizadas por citometria de fluxo, a fim de categorizá-las como monocíticas ou granulocíticas utilizando a combinação dos marcadores CD11b, GR1, LY6C e LY6G. A caracterização das MDSCs é bastante questionada, tendo em vista a grande variedade de marcadores utilizados para sua fenotipagem (BRONTE et al., 2016). Alguns autores discutem a necessidade de validação da caracterização das MDSCs por mais de uma técnica (DORHOI; PLESSIS, 2018). A análise da expressão de iNOS e Arg1 nas M-MDSC mobilizadas para o coração dos animais tratados com CTM-G-CSF poderá confirmar seu perfil fenotípico. Além disso, essa análise contribuiria para o entendimento do tênue balanço entre a expressão de iNOS e Arg1, as quais podem atuar no controle da inflamação e multiplicação do parasito no tecido cardíaco.

Apesar de nossos resultados terem demonstrado que o efeito da terapia com CTM-G-CSF não foi superior aos resultados obtidos utilizando o G-CSF recombinante, pioneiramente, demonstramos que a modificação genética de CTMs potencializa seus efeitos terapêuticos, no contexto da doença de Chagas. Adicionalmente, a utilização de estratégias como essas podem ser úteis para aumentar a mobilização de células imunossupressoras para atuar de forma benéfica no tratamento de pacientes chagásicos crônicos.

No segundo capítulo deste trabalho, investigamos se a superexpressão do hIGF-1 pelas CTMs aumentaria seu potencial imunomodulador e pró-regenerativo no contexto da cardiomiopatia experimental da doença de Chagas. Neste estudo, foi observado que os efeitos relacionados à redução da inflamação e fibrose no coração foram semelhantes entre os grupos submetidos à terapia celular. Porém, as análises histológicas do músculo esquelético revelam que o percentual de área ocupada por miosina esquelética é significativamente maior no grupo tratado com CTMs que superexpressam hIGF-1, comparado às CTMs selvagens e ao grupo controle tratado com salina. Adicionalmente, observou-se o aumento de células inflamatórias no músculo esquelético dos animais tratados com CTM-IGF-1, juntamente com o aumento das citocinas inflamatórias TNF $\alpha$  e IL-1 $\beta$ . Estes dados reforçam a ideia de que o efeito regenerativo observado nos animais tratados com CTM-IGF-1 pode ser explicado pela ação direta do IGF-1 no músculo esquelético, sugerindo que o benefício adicional observado não é consequência das

ações imunomoduladoras desta terapia, mas sim, através de outros mecanismos de ação que ainda não foram avaliados.

Avaliações da regulação da via PI3k/Akt, bem como a proliferação e diferenciação de células satélites, poderão ser úteis na elucidação do efeito regenerativo observado no músculo esquelético pelo hIGF-1 produzido pelas CTMs. Sabidamente, o IGF-1 atua no anabolismo tecidual, aumentando a síntese protéica, promovendo hipertrofia e hiperplasia em vários tipos celulares, incluindo mioblastos do músculo esquelético (PRESTES et al., 2006). A via de sinalização PI3k /Akt é uma das principais vias envolvidas na síntese protéica do músculo esquelético. Um dos principais fatores que levam a ativação da PI3k é a interação entre o IGF-1 com seu receptor (LEGER et al., 2006; LAU; LEUNG, 2012). A avaliação da ativação da PI3k no músculo esquelético dos animais tratados com as CTM-IGF-1 é, portanto, de interesse para demonstrar a ação direta do hIGF-1 produzido pelas CTMs no tecido muscular esquelético.

Outra forma de avaliar se o hIGF-1 produzido pelas CTMs estaria atuando diretamente sobre o músculo esquelético, seria através do estudo das células satélites. O fator de transcrição Pax7 (*Paired box 7*) é restritamente expresso nas células satélites, bem como MyoD1 (*Myogenic differentiation 1*) que são utilizados como marcadores para identificação de células satélites no tecido muscular esquelético (LUO;RENAULT; RANDO et al., 2005). A co-marcação do Pax7 e MyoD são utilizados para caracterizar células satélites em diferenciação. Dando continuidade a esse estudo, estamos avaliando a presença de células satélites duplamente marcadas para Pax7 e MyoD. Análises como essas poderão responder se o efeito regenerativo observado no músculo esquelético dos animais tratados com CTM-IGF-1 é fruto da proliferação e diferenciação de células satélites em células musculares esqueléticas.

O estudo do potencial terapêutico das CTMs em cardiologia tem sido bastante explorado. Já os estudos que utilizam CTM geneticamente modificadas encontram-se em nível experimental, no qual avalia-se principalmente o aumento de sobrevivência e exertia celular e ampliação do potencial terapêutico relacionado a vascularização e regeneração do miocárdio (JADCZIK et al., 2017).

Os resultados dos estudos clínicos revelam que o principal efeito da terapia com CTMs nas doenças cardíacas estão relacionados a estimulação da angiogênese no tecido cardíaco lesado. Um discreto efeito sobre a fibrose e restauração da função contrátil foi observado. Além disso, o potencial de diferenciação nos principais tipos celulares que compõem o coração (cardiomiócitos, células endoteliais e células do músculo liso) é bastante questionado. Apesar dos estudos *in vitro* demonstrarem esse potencial, este é um ponto bastante discutido nos estudos clínicos que revelam que este não é o mecanismo de ação primário das CTMs

(VECELLIO et al., 2012). Neste trabalho, não avaliamos o potencial de diferenciação das células transplantadas em cardiomiócitos, células endoteliais ou células do músculo liso. Porém, estudos futuros podem responder se as CTMs geneticamente modificadas para a expressão de G-CSF e IGF-1 possuem esse potencial ou atuam estimulando a diferenciação de outras células em cardiomiócitos, células endoteliais e células do músculo liso.

Outro ponto bastante discutido acerca da utilização das CTMs em cardiologia é o fato de poucas células alcançarem a área de lesão e permanecerem retidas no tecido cardíaco, mesmo quando injetadas diretamente no tecido ou na circulação cardíaca (KARANTALIS; HARE, 2015). O fato do coração ser um órgão dinâmico, que funciona como uma bomba, dificulta a retenção das células transplantadas, contribuindo para perda de eficiência terapêutica, já que um número de células adequado é necessário para atuar nos processos de regeneração do miocárdio (KIM; SHAPIRO; FLYNN et al., 2015).

Dessa forma, a via de administração representa um dos fatores importantes para obtenção do efeito terapêutico desejado. Já foi demonstrado que aproximadamente 1% das CTMs injetadas na circulação periférica alcançam as áreas de lesão e que a maioria das células injetadas ficam retidas no pulmão, fígado e baço (BARBASH et al., 2003; SCHREPFER, 2007). Além disso, a injeção periférica de células via endovenosa ou intra-arterial, podem desencadear complicações pós-transplante atribuídas à embolia pulmonar e microembolia vascular (FISCHER, 2009; GE et al., 2014).

Os transplantes das CTMs no modelo de doença de Chagas crônico foram realizados pelas vias endovenosa, intraperitoneal e intracardíaca. No estudo que avaliou o potencial terapêutico das CTMs que superexpressam hIGF-1, as células foram injetadas por via endovenosa. Após os transplantes, foi observado cerca de 40% de mortalidade nos grupos dos animais submetidos à terapia celular. Já nos transplantes do mesmo número de células realizados pelas vias intraperitoneal e intracardíaca, realizadas no estudo que avalia o potencial terapêutico das CTMs que superexpressam G-CSF, não foi observado mortalidade em decorrência do transplante celular. Estes dados reforçam o fato de eventos adversos, como embolia pulmonar, estarem relacionados ao transplante de CTMs pela via endovenosa, sendo esta via menos segura do que as vias intraperitoneal e intracardíaca para o transplante de células em animais com a doença de Chagas crônica.

Os transplantes das células utilizando as vias intraperitoneal, intracardíaca e endovenosa mostram-se funcionais na entrega das células nos órgãos de interesse, pois em ambos os estudos, detectamos a presença de células GFP e a expressão dos fatores G-CSF e IGF-1 humanos no coração e músculo esquelético dos animais. O emprego de técnicas mais sensíveis

para realizar o rastreamento das células após o transplante, sejam por imagem ou biologia molecular, é extremamente útil em terapia celular. Neste trabalho, foi utilizada a reação em cadeia da polimerase (PCR) para fazer o rastreio das células transplantadas, já que células GFP não foram observadas no coração ou músculo esquelético dos animais. Em situações como estas, a baixa retenção e sobrevivência das células nos órgãos-alvo podem contribuir para a falta de identificação dessas células por microscopia. Para resolver problemas como estes, alguns trabalhos descrevem a necessidade da utilização de nanopartículas carreadoras e matrizes injetáveis ou semi-sólidas que são biodegradáveis a fim de promover um arcabouço de adesão e suplementação de fatores que favorecem a enxertia e sobrevivência das células transplantadas em maior número e por mais tempo no órgão de interesse (LU et al., 2009; IFKOVITS et al., 2010; SEIF-NARAGHI et al., 2013). Possivelmente, o emprego dessas estratégias nos transplantes das CTM-G-CSF e CTM-IGF-1 possam aumentar mais ainda o efeito terapêutico observado neste estudo.

Embora tenhamos dificuldade na identificação das células transplantadas nos órgãos de interesse, o efeito terapêutico observado em ambos os estudos pode ser atribuído aos efeitos tróficos das CTMs. Shabbir e colaboradores (2009) demonstraram que as CTMs utilizadas no modelo experimental de infarto agudo do miocárdio beneficiou a regeneração do tecido cardíaco através dos efeitos tróficos das CTMs e não necessariamente pela presença dessas células na área de lesão do miocárdio (SHABBIR et al., 2009).

Devido às limitações encontradas com a utilização das CTMs na área da cardiologia, diferentes metodologias estão sendo empregadas a fim de aumentar sua eficácia terapêutica. Estes métodos envolvem (I) a combinação da terapia celular com farmacoterapia (KANG et al., 2012), (II) modificação genética (NOLTA, 2016), (III) co-cultivo com fatores que induzem a diferenciação em tipos celulares específicos ou potencializam seus efeitos tróficos (GUO et al., 2008; HAHN et al., 2008; QAYYUM et al., 2012), e (IV) o encapsulamento ou utilização de matrizes para aumentar a retenção celular (KAI et al., 2014; BLOCKI et al., 2015). Dentre estes métodos, neste trabalho foi utilizada a modificação genética utilizando vetores lentivirais para potencializar os efeitos das CTMs através da secreção ectópica do G-CSF e IGF-1 humanos. Este método apresenta algumas vantagens em relação aos outros descritos para modificação genética de CTMs. A alta eficiência e a transcrição estável do transgene representam seu diferencial com relação aos outros métodos já descritos (PARK et al., 2015). No entanto, deve-se levar em consideração os riscos inerentes a utilização destes vetores na terapia celular. A ocorrência de eventos adversos, tais como citotoxicidade, imunogenicidade e oncogenicidade,



já foi descrita (WALTHER; STEIN, 2000). Sendo assim, a segurança das terapias que utilizam células modificadas geneticamente ainda permanece sob investigação (DEVETZI et al., 2018).

A fim de viabilizar a utilização das CTMs geneticamente modificadas na prática clínica, problemas tais como o potencial tumorigênico podem ser resolvidos através da inserção de genes “suicidas” na construção dos vetores carreadores. A transcrição de genes suicidas tem efeito citotóxico, que impacta na sobrevivência e proliferação celular (KALIMUTHU et al., 2017). O primeiro, e mais comumente utilizado, é o gene suicida do vírus herpes simples 1 timidina quinase (HSV1-TK), que é capaz de promover a conversão do ganciclovir em um metabólito citotóxico, o ganciclovir trifosfato (BONINI et al., 2007). Atualmente, tem sido utilizada a combinação da utilização do HSV1-TK e um sistema de controle de ativação induzido por droga. Sistemas de ativação como o TetO, que é regulado pela presença ou ausência da doxiciclina, são eficazes na regulação da expressão desse gene suicida, que pode ser ativado condicionalmente nos casos de tumorigênese ou proliferação celular exacerbada (BONINI et al., 2007; BARESE, et al., 2012).

Apesar do potencial tumorigênico das células geneticamente modificadas não ter sido avaliado neste estudo, em ambos os trabalhos, não foi observada a formação de tumor após eutanásia dos animais. Sendo assim, as ferramentas de modificação genética utilizadas para modificar as células testadas se mostraram eficazes e seguras no contexto do tratamento da cardiomiopatia chagásica experimental durante o tempo avaliado. Porém, o emprego de técnicas mais seguras para geração de células modificadas geneticamente representa uma etapa importante para o desenvolvimento de produtos celulares com potencial de serem utilizadas futuramente na prática clínica.

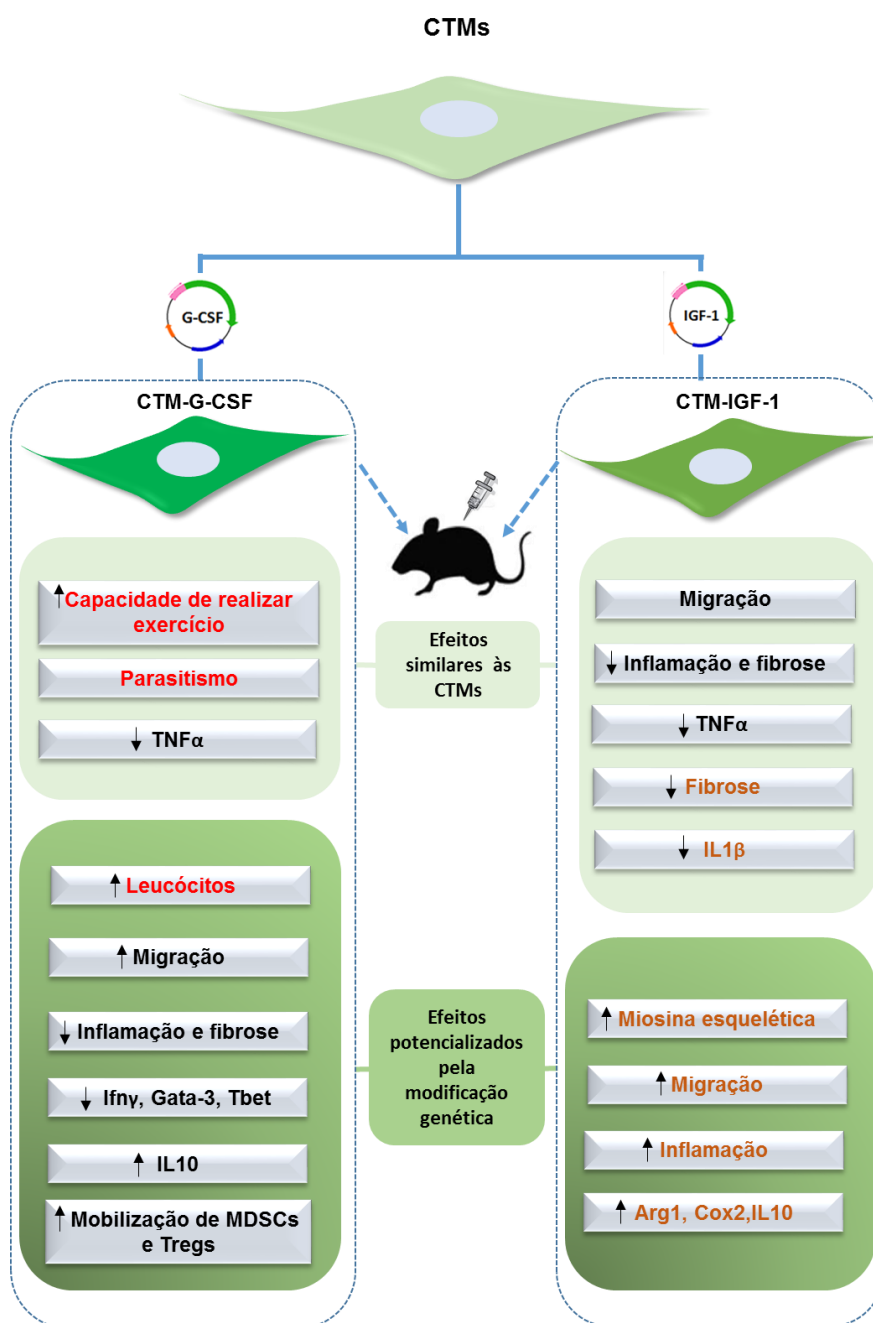


**Figura 4: Representação esquemática dos efeitos terapêuticos das células-tronco mesenquimais modificadas geneticamente na CCC experimental.** Os efeitos em preto representam as ações no coração, enquanto os efeitos em laranja representam as ações no músculo esquelético. Em vermelho, estão representados os efeitos sobre a capacidade de realizar exercício, o parasitismo no baço e número de leucócitos no sangue periférico.

## 7 CONCLUSÃO

Neste estudo foi demonstrado pioneiramente que o tratamento com CTMs da medula óssea que superexpressam hG-CSF ou hIGF-1 potencializou o efeito terapêutico das células-tronco mesenquimais através de ações imunomoduladoras e pró-regenerativas no coração e músculo esquelético de camundongos cronicamente infectados por *T. cruzi*. Desse modo, a terapia celular utilizando células-tronco mesenquimais geneticamente modificadas para superexpressão de fatores com potenciais terapêuticos representa uma estratégia promissora para o desenvolvimento de novas terapias para a cardiomiopatia chagásica crônica. Além disso, nossos resultados indicam um papel benéfico das MDSCs na regulação de respostas imunes patológicas, abrindo novos caminhos para o desenvolvimento de terapias celulares para a doença de Chagas.

**REFERÊNCIAS**

ALBELLA, B. et al. Ex vivo expansion of hematopoietic stem cells. **Methods Molecular Biology**, v.215, p. 363-373, 2003.

ANDERLINI, P.; CHAMPLIN, R.E. Biologic and molecular effects of granulocyte colony-stimulating factor in normal individuals: recent findings and current challenges. **Blood**, 7543, 2007.

AROCENA, A. R. et al. Myeloid-derived suppressor cells are key players in the resolution of inflammation during a model of acute infection. **European Journal of Immunology**, v. 44, n. 1, p. 184–194, 2014.

BAJETTO, A. et al. Glial and neuronal cells express functional chemokine receptor CXCR4 and its natural ligand stromal cell-derived factor 1. **Journal of Neurochemistry**, v. 73, n. 6, p. 2348–2357, 1999.

BARANIAK, P. R.; MCDEVITT, T. C. Stem cell paracrine actions and tissue regeneration. **Regenerative Medicine**, v. 5, n. 1, p. 121-143, 2010.

BARBASH, I. M. et al. Systemic Delivery of Bone Marrow–Derived Mesenchymal Stem Cells to the Infarcted Myocardium. **Feasibility, Cell Migration, and Body Distribution**, v. 108, n. 7, p. 863–868, 2003.

BARESE, C. N. et al. Thymidine kinase suicide gene-mediated ganciclovir ablation of autologous gene-modified rhesus hematopoiesis. **Molecular Therapy**, v. 20, n. 10, p. 1932–1943, 2012.

BARTHOLOMEW, A. et al. Mesenchymal stem cells suppress lymphocyte proliferation in vitro and prolong skin graft survival in vivo. **Experimental Hematology**, v. 30, n. 1, p. 42- 48, 2002.

BASTOS, C. J. C. et al. Clinical outcomes of thirteen patients with acute chagas disease acquired through oral transmission from two urban outbreaks in Northeastern Brazil. **Plos Neglected Tropical Diseases**, v. 4, n. 6, p. 16–17, 2010.

BELTRAMI, A. P. et al. Adult cardiac stem cells are multipotent and support myocardial regeneration. **Cell**, v. 114, p. 763-776, 2003.

BENDALL, L. J.; BRADSTOCK, K. F. G-CSF: From granulopoietic stimulant to bone marrow stem cell mobilizing agent. **Cytokine and Growth Factor Reviews**, 2014.

BENZIGER, C. P.; DO CARMO, G. A. L.; RIBEIRO, A. L. P. Chagas Cardiomyopathy: Clinical Presentation and Management in the Americas. **Cardiology Clinics**, 2017.

BIANCONE, L. et al. Therapeutic potential of mesenchymal stem cell-derived microvesicles. **Nephrology Dialysis Transplantation**, v. 27, n. 8, p. 3037–3042, 2012.

BLOCKI, A. et al. Microcapsules engineered to support mesenchymal stem cell (MSC) survival and proliferation enable long-term retention of MSCs in infarcted myocardium. **Biomaterials**, v. 53, p. 12–24, 2015.

BOCCHI, E. A. et al. Granulocyte-colony stimulating factor or granulocyte-colony stimulating factor associated to stem cell intracoronary infusion effects in non ischemic refractory heart failure. **International Journal of Cardiology**, v. 138, n. 1, p. 94–97, 2010.

BONINI, C. et al. The suicide gene therapy challenge: How to improve a successful gene therapy approach. **Molecular Therapy**, 2007.

BOXALL, S. A. et al. Markers for Characterization of Bone Marrow stem cells. **Stem Cells International**, v. 2012, 2012.

BRENER, Z.; ANDRADE, Z. A.; BARRAL-NETO, M. **Trypanosoma cruzi e a doença de Chagas**. 2 ed. Rio de Janeiro: Guanabara Koogan, 2000. p. 152-174.

BRONTE, V. et al. Recommendations for myeloid-derived suppressor cell nomenclature and characterization standards. **Nature Communications**, v. 7, 2016.

CANTINIEAUX, D. et al. Conditioned medium from bone marrow-derived mesenchymal stem cells improves recovery after spinal cord injury in rats: an original strategy to avoid cell transplantation. **PLoS One**, v. 8, n. 8, p. e69515, 2013.

CAPLAN, A. I. Adult mesenchymal stem cells for tissue engineering versus regenerative medicine. **Journal of Cellular Physiology**, v. 213, p. 341-347, 2007.

CHAPMAN, A. R. The ethics of patenting human embryonic stem cells. **Kennedy Inst Ethics J**, v. 19, p. 261-88, 2009.

CHEN, S. L. et al.. Effect on left ventricular function of intracoronary transplantation of autologous bone marrow mesenchymal stem cell in patients with acute myocardial infarction. **American Journal of Cardiology**, v. 94, n.1, p. 92-95, 2004.

CHENG, Z. et al. Targeted migration of mesenchymal stem cells modified with CXCR4 gene to infarcted myocardium improves cardiac performance. **Molecular Therapy**, v. 16, n. 3, p. 571–579, 2008.

CONTI, E. et al. IGF-1 and atherothrombosis: relevance to pathophysiology and therapy. **Clinical science**, v. 120, n. 9, p. 377–402, 2011.

CUNHA-NETO, E. et al. Immunological and non-immunological effects of cytokines and chemokines in the pathogenesis of chronic Chagas disease cardiomyopathy. **Memórias do Instituto Oswaldo Cruz**, v. 104, p. 252–258, 2009.

DA SILVA MEIRELLES, L. P.C; CHAGASTELLES; N.B. NARDI, Mesenchymal stem cells reside in virtually all post-natal organs and tissues. **J Cell Sci**, v.119, p. 2204-2213, 2006.

DAI W., et al. Allogeneic mesenchymal stem cell transplantation in postinfarcted rat myocardium: Short- and long-term effects. **Circulation**, v. 112, n. 2, p. 214-223, 2005.

DELCAÏRE, A. et al. Exosome Display technology: Applications to the development of new diagnostics and therapeutics. **Blood Cells, Molecules, and Diseases**, v. 35, n. 2, p. 158–168, 2005.

DEVETZI, M. et al. Genetically-modified stem cells in treatment of human diseases: Tissue kallikrein (KLK1)-based targeted therapy (Review). **International Journal of Molecular Medicine**, p. 1177–1186, 2018.

DOMINICI, M.; et al. Minimal criteria for defining multipotent mesenchymal stromal cells. The international Society for Cellular Therapy position statement. **Cytotherapy**, v. 8, p. 315–317, 2006.

DORAN, P. M. Cartilage tissue engineering: What have we learned in practice? **Methods in Molecular Biology**, v. 1340, p. 3–21, 2015.

DORHOI, A.; PLESSIS, N. DU. Monocytic myeloid-derived suppressor cells in chronic infections. **Frontiers in Immunology**, v. 8, p. 1–15, 2018.

DORRONSORO, A. et al. Human mesenchymal stromal cells modulate T-cell responses through TNF- $\alpha$ -mediated activation of NF- $\kappa$ B. **European Journal of Immunology**, v. 44, n. 2, p. 480–488, 2014.

DOS SANTOS, R. R. et al. Cell therapy in chagas cardiomyopathy (Chagas arm of the multicenter randomized trial of cell therapy in cardiopathies study): A multicenter randomized trial. **Circulation**, v. 125, n. 20, p. 2454–2461, 2012.

DUTRA, W. O. et al. Immunoregulatory networks in human Chagas disease. **Parasite immunology**, v. 36, n. 8, p. 377–387, 2014.

EGLITIS, M. A.; MEZEY, E. Hematopoietic cells differentiate into both microglia and macroglia in the brains of adult mice. **Proceedings of the National Academy Science**, v. 94, p. 4080–4085, 1997.

ENOKI, C. et al. Enhanced mesenchymal cell engraftment by IGF-1 improves left ventricular function in rats undergoing myocardial infarction. **International Journal of Cardiology**, v. 138, n. 1, p. 9–18, 2010.

FERRARI, G. et al. Muscle regeneration by bone marrow-derived myogenic progenitors. **Science**, v. 279, p.1528–1530, 1998.

FISCHER, U. M. et al. Pulmonary passage is a major obstacle for intravenous stem cell delivery: the pulmonary first-pass effect. **Stem Cells and Development**, v. 18, n. 5, p. 683–692, 2009.

FRANZKE, A. The role of G-CSF in adaptive immunity. **Cytokine and Growth Factor Reviews**, 2006.

FRIEDENSTEIN, A.J.; CHAILAKHJAN, R.K.; LALYKINA, K.S. The development of fibroblast colonies in monolayer cultures of guinea-pig bone marrow and spleen cells. **Cell Tissue Kinetic**, v. 3, p. 393-403, 1970.

FUJITA, J. et al. Administration of granulocyte colony-stimulating factor after myocardial infarction enhances the recruitment of hematopoietic stem cell-derived myofibroblasts and contributes to cardiac repair. **Stem Cells**, v. 25, p. 2750–2759, 2007.

GABRILOVICH, D. I.; NAGARAJ, S. Myeloid-derived-suppressor cells as regulators of the immune system. **Nature Reviews Immunology**, v. 9, n. 3, p. 162–174, 2009.

GE, J. et al. The Size of Mesenchymal Stem Cells is a Significant Cause of Vascular Obstructions and Stroke. **Stem Cell Reviews and Reports**, v. 10, n. 2, p. 295–303, 2014.

GERVOIS, P. et al. Stem Cell-Based Therapies for Ischemic Stroke: Preclinical Results and the Potential of Imaging-Assisted Evaluation of Donor Cell Fate and Mechanisms of Brain Regeneration. **Medicinal Research Reviews**, 2016.

GLENNIE, S. et al. Bone marrow mesenchymal stem cells induce division arrest anergy of activated T cells. **Blood**, v. 105, n. 7, p. 2821-2827, 2005.

GNECCHI, M. et al. Paracrine mechanisms in adult stem cell signaling and therapy. **Circulation Research**, v. 103, n. 11, p. 1204-1219, 2008.

GOMES, J. A. et al. Evidence that development of severe cardiomyopathy in human Chagas' disease is due to a Th1-specific immune response. **Infection and Immunity**, v. 71, n. 3, p. 1185-1193, 2003.

GOODELL, M. A.; NGUYEN, H.; SHROYER, N. Somatic stem cell heterogeneity: Diversity in the blood, skin and intestinal stem cell compartments. **Nature Reviews Molecular Cell Biology**, v. 16, n. 5, p. 299–309, 2015.

GUO, J. et al. Insulin-like growth factor 1 improves the efficacy of mesenchymal stem cells transplantation in a rat model of myocardial infarction. **Journal Biomedical Science**, v. 15, n. 1, p. 89-97, 2008.

HACEIN-BEY-ABINA, S. et al. Insertional oncogenesis in 4 patients after retrovirus-mediated gene therapy of SCID-X1. **Journal of Clinical Investigation**, v. 118, n. 9, p. 3132–3142, 2008.

HAGMANN, S. et al. Different culture media affect growth characteristics, surface marker distribution and chondrogenic differentiation of human bone marrow-derived mesenchymal stromal cells. **BMC skeletal Disorders**, v. 14, 2013.

HAHN, J. Y. et al. Pre-treatment of mesenchymal stem cells with a combination of growth factors enhances gap junction formation, cytoprotective effect on cardiomyocytes, and therapeutic efficacy for myocardial infarction. **Journal of the American College of Cardiology**, v. 51, n. 9, p. 933–943, 2008.

HARADA, M. et al. G-CSF prevents cardiac remodeling after myocardial infarction by activating the Jak-Stat pathway in cardiomyocytes. **Nature Medicine**, v. 11, n. 3, p. 305–311, 2005.

HARE, J. M. et al. Comparison of allogeneic vs autologous bone marrow–derived mesenchymal stem cells delivered by transendocardial injection in patients with ischemic cardiomyopathy. **JAMA**, v. 308, n. 22, p. 2369, 2012.

HILL, W. D. et al. SDF-1 (CXCL12) Is Upregulated in the ischemic penumbra following stroke: association with bone marrow cell homing to injury. **Journal of Neuropathology and Experimental Neurology**, v. 63, n. 1, p. 84–96, 2004.

HO, A. D.; WAGNER, W.; FRANKE, W. Heterogeneity of mesenchymal stromal cell preparations. **Cytotherapy**, 2008.

HO, A. T. V. et al. Prostaglandin E2 is essential for efficacious skeletal muscle stem-cell function, augmenting regeneration and strength. **Proceedings of the National Academy of Sciences**, p. 201-220, 2017.

HODGKINSON, C. P. et al. Emerging concepts in paracrine mechanisms in regenerative cardiovascular medicine and biology. **Circulation Research**, 2016.

HOFSTETTER, C. P. et al. Marrow stromal cells form guiding strands in the injured spinal cord and promote recovery. **Proceedings of the National Academy of Sciences**, v. 99, n. 4, p. 2199–2204, 2002.

HUANG, B.; TABATA, Y.; GAO, J. Q. Mesenchymal stem cells as therapeutic agents and potential targeted gene delivery vehicle for brain diseases. **Journal of Controlled Release**, v. 162, n. 2, p. 464–473, 2012.

HUANG, X.-P. et al. Differentiation of allogeneic mesenchymal stem cells induces immunogenicity and limits their long-term benefits for myocardial repairclinical perspective. **Circulation**, v. 122, n. 23, p. 2419–2429, 2010.

HUANG, M.-B. et al. Insulin-like growth factor-1 receptor is regulated by microRNA-133 during skeletal myogenesis. **PloS one**, v. 6, n. 12, p. e29173, 2011.

IFKOVITS, J. L. et al. Injectable hydrogel properties influence infarct expansion and extent of postinfarction left ventricular remodeling in an ovine model. **Proceedings of the National Academy of Sciences**, v. 107, n. 25, p. 11507–11512, 2010.

IMBERTI, B. et al. Insulin-like growth factor-1 sustains stem cell mediated renal repair. **Journal of the American Society of Nephrology**, v. 18, n. 11, p. 2921–2928, 2007.

IWANAGA, K., et al. Effects of G-CSF on cardiac remodeling after acute myocardial infarction in swine. **Biochemical Biophysical Research Communications**, v. 325, p. 1353–1359, 2004.

JACKSON, K.A. et al. Stem cells: a minireview. **Journal of Cellular Biochemistry**, v. 38, Supl. p. 1-6, 2002.



JACKSON, K.A.; MI, T.; GOODELL, M.A. Hematopoietic potential of stem cell isolated from murine skeletal muscle. **Proceedings of the National Academy of Sciences**, v. 96, p. 14482-14486, 1999.

JADCZYK, T. et al. Innovative diagnostics and treatment: Nanorobotics and stem cells. **Nanotheranostics**, 2017.

JASMIN et al. Molecular imaging, biodistribution and efficacy of mesenchymal bone marrow cell therapy in a mouse model of Chagas disease. **Microbes and Infection**, v. 16, n. 11, p. 923–935, 2014.

Jl, J. F. et al. Interactions of chemokines and chemokine receptors mediate the migration of mesenchymal stem cells to the impaired site in the brain after hypoglossal nerve injury. **Stem Cells**, v. 22, n. 3, p. 415–427, 2004.

JONES, J. I.; CLEMMONS, D. R. Insulin-like growth factors and their binding proteins: biological actions. **Endocrine Reviews**, v.16, n. 1, p. 3-34, 1995.

JUNIOR, P. A. S. et al. Experimental and clinical treatment of Chagas disease: A review. **American Journal of Tropical Medicine Hygiene**, v. 97, n. 5, p. 1289-1303, 2017.

KADI, F. et al. Satellite cells and myonuclei in young and elderly women and men. **Muscle & Nerve**, v. 29, n. 1, p. 120–127, 2004.

KAI, D. et al. Stem cell-loaded nanofibrous patch promotes the regeneration of infarcted myocardium with functional improvement in rat model. **Acta Biomaterialia**, v. 10, n. 6, p. 2727–2738, 2014.

KALIMUTHU, S. et al. Genetically engineered suicide gene in mesenchymal stem cells using a Tet-On system for anaplastic thyroid cancer. **PLoS ONE**, v. 12, n. 7, p. 1–19, 2017.

KANEMITSU, N. et al. Insulin-like growth factor-1 enhances the efficacy of myoblast transplantation with its multiple functions in the chronic myocardial infarction rat model. **Journal of Heart and Lung Transplantation**, v. 25, n. 10, p. 1253-1262, 2006.

KANG, S. K. et al. Journey of mesenchymal stem cells for homing: Strategies to enhance efficacy and safety of stem cell therapy. **Stem Cells International**, 2012.

KARANTALIS, V.; HARE, J. M. Use of mesenchymal stem cells for therapy of cardiac disease. **Circulation Research**, v. 116, n. 8, p. 1413–1430, 2015.

KARSHIEVA, S. S.; KRASIKOVA, L. S.; BELYAVSKII, A. V. Mesenchymal stem cells as tool for antitumor therapy. **Molecular Biology**, v. 47, n. 1, p. 45–54, 2013.

KAWADA H, et al. Nonhematopoietic mesenchymal stem cells can be mobilized and differentiate into cardiomyocytes after myocardial infarction. **Blood**, v.104, 2004.

KIM, J.; SHAPIRO, L.; FLYNN, A. The clinical application of mesenchymal stem cells and cardiac stem cells as a therapy for cardiovascular disease. **Pharmacology and Therapeutics**, v. 151, p. 8–15, 2015.

KOOIJMAN, R. Regulation of apoptosis by insulin-like growth factor (IGF)-I. **Cytokine & Growth Factor Review**, v. 17, n. 4, p. 305-323, 2006.

KRAMPERA, M. et al. Mesenchymal stem cells for bone, cartilage, tendon and skeletal muscle repair. **Bone**, v. 39, n. 4, p. 678-83, 2006.

KRANSDORF, E. P. et al. Pathology of chronic chagas cardiomyopathy in the United States: A detailed review of 13 cardiectomy cases. **American Journal of Clinical Pathology**, 2016.

KRAUSE, D.S. Plasticity of marrow-derived stem cells. **Gene Therapy**, v. 9, p.754-758, 2002.

LAFLAME, M. A.; MURRY, C. E. Regenerating the heart. **Nature Biotechnology**, v. 23, p. 845-856. 2005.

LAROCCA, T. F. et al. Transplantation of adipose tissue mesenchymal stem cells in experimental chronic chagasic cardiopathy. **Arquivos Brasileiros de Cardiologia**, 2013.

LAU, M. T.; LEUNG, P. C. K. The PI3K/Akt/mTOR signaling pathway mediates insulin-like growth factor 1-induced E-cadherin down-regulation and cell proliferation in ovarian cancer cells. **Cancer Letters**, v. 326, n. 2, p. 191–198, 2012.

LAVIOLA, L.; NATALICCHIO, A.; GIORGINO, F. The IGF-I signaling pathway. **Current Pharmaceutical Desing**, v.1 3, n. 7, p. 663-669, 2007.

LAZENNEC, G. et al. Concise review: adult multipotent stromal cells and cancer: risk or benefit? **Stem cells** , v. 26, n. 6, p. 1387–94, 2008.

LE BLANC, K. et al. Mesenchymal stem cells for treatment of steroid-resistant, severe, acute graft-versus-host disease: a phase II study. **Lancet**, v. 371, n. 9624, p. 1579–1586, 2008.

LE BLANC, K. et al. Mesenchymal stem cells inhibit and stimulate mixed lymphocyte cultures and mitogenic responses independently of the major histocompatibility complex. **Scandinavian Journal of Immunology**, v. 57, n. 1, p. 11–20, 2003.

LE BLANC, K.; MOUGIAKAKOS, D. Multipotent mesenchymal stromal cells and the innate immune system. **Nature Reviews Immunology**, 2012.

LÉGER, B. et al. Akt signalling through GSK-3 $\beta$ , mTOR and Foxo1 is involved in human skeletal muscle hypertrophy and atrophy. **Journal of Physiology**, v. 576, n. 3, p. 923–933, 2006.

LEWIS, P.; HENSEL, M.; EMERMAN, M. Human immunodeficiency virus infection of cells arrested in the cell cycle. **The EMBO journal**, v. 11, n. 8, p. 3053–8, 1992.

LI, B. et al. Monitoring live human mesenchymal stromal cell differentiation and subsequent selection using fluorescent RNA-based probes. **Scientific Reports**, v. 6, 2016.

LI, S.; HUANG, L. Nonviral gene therapy: promises and challenges. **Gene Therapy**, v.7, n.1, p.31-34, 2000.

LI, Y. et al.. Insulin-like growth factor 1 enhances the migratory capacity of mesenchymal stem cells. **Biochemical and Biophysical Research Communications**, v. 356, n. 3, p. 780- 784, 2007.

LIECHTENSTEIN, T.; PEREZ-JANICES, N.; ESCORS, D. Lentiviral vectors for cancer immunotherapy and clinical applications. **Cancers**, 2013.

LIU, N.; PATZAK, A.; ZHANG, J. CXCR4-overexpressing bone marrow-derived mesenchymal stem cells improve repair of acute kidney injury. *American journal of physiology. Renal Physiology*, v. 305, n. 7, p. F1064–73, 2013.

LIU, Z.J.; ZHUGE, Y.; VELAZQUEZ, O. C. Trafficking and differentiation of mesenchymal stem cells. **Journal of Cellular Biochemical**, v. 106, p. 984–991, 2009.

LU, W.-N. et al. Functional improvement of infarcted heart by co-injection of embryonic stem cells with temperature-responsive chitosan hydrogel. **Tissue Engineering Part A**, v. 15, n. 6, p. 1437–1447, 2009.

LUO, D.; RENAULT, V. M.; RANDO, T. A. The regulation of Notch signaling in muscle stem cell activation and postnatal myogenesis. **Cell and Developmental Biology**, 2005.

MACAMBIRA, S. G. et al. Granulocyte colony-stimulating factor treatment in chronic Chagas disease: preservation and improvement of cardiac structure and function. **Faseb journal**, v. 23, n. 11, p. 3843–3850, 2009.

MACDONALD, K. P. A. et al. Modification of T Cell responses by stem cell mobilization requires direct signaling of the T Cell by G-CSF and IL-10. **The Journal of Immunology**, v. 192, n. 7, p. 3180–3189, 2014.

MAJKA, M. et al. Concise review: Mesenchymal stem cells in cardiovascular regeneration: Emerging research directions and clinical applications. **Stem Cells Translational Medicine**, v. 6, p. 1859–1867, 2017.

MALLIARAS, K. et al. Innate heart regeneration: endogenous cellular sources and exogenous therapeutic amplification. **Expert Opinion on Biological Therapy**, 2016.

MANNELLO, F.; TONTI, G.A. Concise review: no breakthroughs for human mesenchymal and embryonic stem cell culture. **Stem Cells**, v. 25, n. 7, p. 1603-1609, 2007.

MARIN-NETO, J. A. et al. Chagas heart disease. In: YUSUF, S. et al. (Eds). **Evidence-based cardiology**. 3rd edn. London: BMJ Books, p. 823-841. 2010.

MARKEL, T. A. et al. VEGF is critical for stem cell-mediated cardioprotection and a crucial paracrine factor for defining the age threshold in adult and neonatal stem cell function. **AJP: Heart and Circulatory Physiology**, v. 295, n. 6, p. 2308–2314, 2008.

MAROFI, F. et al. Mesenchymal stromal/stem cells: A new era in the cell-based targeted gene therapy of cancer. **Frontiers in Immunology**, v. 8, dec. 2017.

MARTÍ-CARVAJAL, A. J.; KWONG, J. S. W. Pharmacological interventions for treating heart failure in patients with Chagas cardiomyopathy. **Cochrane Database of Systematic Reviews**, v. 7, n. 7, 2016.

MARTIN, C.M. et al. Persistent expression of the ATP-binding cassette transporter, Abcg2, identifies cardiac SP cells in the developing and adult heart. **Developmental Biology**, v. 265, p. 262–275, 2003.

MARTINS, A.; HAN, J.; KIM, S. O. The multifaceted effects of granulocyte colony-stimulating factor in immunomodulation and potential roles in intestinal immune homeostasis. **IUBMB Life**, 2010.

MARTINS-MELO, F. R. et al. Prevalence of Chagas disease in Brazil: a systematic review and meta-analysis. **Acta Tropical**, v. 130, p. 167-174, 2014.

MARTIRE, A. et al. Mesenchymal stem cells attenuate inflammatory processes in the heart and lung via inhibition of TNF signaling. **Basic Research in Cardiology**, v. 111, n. 5, p. 54, 2016.

MATSUO, A. L. et al. In vitro and in vivo trypanocidal effects of the cyclopalladated compound 7a, a drug candidate for treatment of Chagas disease. **Antimicrobial Agents and Chemotherapy**, v. 54, n. 8, p. 3318-3325, 2010.

MAYA, J. D. et al. Chagas disease: Present status of pathogenic mechanisms and chemotherapy. **Bióloga Research**, v. 43, p. 323-31, 2010.

MELLO, D. B. et al. Adipose tissue-derived mesenchymal stromal cells protect mice infected with *Trypanosoma Cruzi* from cardiac damage through modulation of anti-parasite immunity. **PLOS Neglected Tropical Diseases**, v. 9, n. 8, 2015.

MELVE, G. K. et al. Immunomodulation induced by stem cell mobilization and harvesting in healthy donors: Increased systemic osteopontin levels after treatment with granulocyte colony-stimulating factor. **International Journal of Molecular Sciences**, v. 17, n. 7, 2016.

MIROTSOU, M. et al. Secreted frizzled related protein 2 (Sfrp2) is the key Akt-mesenchymal stem cell-released paracrine factor mediating myocardial survival and repair. **Proceedings of the National Academy of Sciences**, v. 104, n. 5, p. 1643–1648, 2007.

MONCAYO, À.; SILVEIRA, A. C. Current epidemiological trends for Chagas disease in Latin America and future challenges in epidemiology, surveillance and health policy. **Memórias do Instituto Oswaldo Cruz**, v. 104, n. Suppl. 1, p. 17-30, 2009.

MORRIS, E. S. et al. Donor treatment with pegylated G-CSF augments the generation of IL-10-producing regulatory T cells and promotes transplantation tolerance. **Blood**, v. 103, n. 9, p. 3573–3581, 2004.

MURPHY, L. J.; BELL, G. I.; FRIESEN, H. G. Tissue distribution of insulin-like growth factor I and II messenger ribonucleic acid in the adult rat. **Endocrinology**, v. 120, n. 4, p. 1279–1282, 1987.

MUSARO, A. et al. Localized Igf-1 transgene expression sustains hypertrophy and regeneration in senescent skeletal muscle. **Nature Genetics**, v. 27, n. 2, p. 195–200, 2001.

MUSARO, A. et al. Stem cell-mediated muscle regeneration is enhanced by local isoform of insulin-like growth factor 1. **Proceedings of the National Academy of Sciences**, v. 101, n. 5, p. 1206–1210, 2004.

NAGAYA N., et al. Transplantation of mesenchymal stem cells improves cardiac function in a rat model of dilated cardiomyopathy. **Circulation**, v. 112, p. 1128-35, 2005.

NAKAE, J.; KIDO, Y.; ACCILI, D. Distinct and overlapping functions of insulin and IGF-I receptors. **Endocrine Reviews**, 2001.

NARDI, N. et al. Terapia gênica. **Ciência e Saúde Coletiva**, v. 7, n. 1, p. 109-116, 2002.

NAYAK, S.; HERZOG, R. W. Progress and prospects: Immune responses to viral vectors. **Gene Therapy**, 2010.

NOGUEIRA, L. G. et al. Myocardial gene expression of T-bet, GATA-3, Ror- $\gamma$ t, FoxP3, and hallmark cytokines in chronic Chagas disease cardiomyopathy: an essentially unopposed TH1-type response. **Mediators Inflammation**, v. 2014, 2014.

NOLTA, J. A. “Next-generation” mesenchymal stem or stromal cells for the in vivo delivery of bioactive factors: Progressing toward the clinic. **Transfusion**, v. 56, n. 4, p. 15S–17S, 2016.

OH, H. et al. Cardiac progenitor cells from adult myocardium: homing, differentiation, and fusion after infarction. **Proceedings of the National Academy of Sciences**, v. 100, n.21, p. 12313-12318, 2003.

ORLIC, D. et al. Bone marrow cells regenerate infarcted myocardium. **Nature**, v. 410, n. 6829, p. 701-5, 2001.

ORLIC, D. et al. Mobilized bone marrow cells repair the infarcted heart, improving function and survival. **Proceedings of the National Academy of Sciences**, v. 98, n. 18, p. 10344-10349, 2001.

OTANI, K. et al. Nonviral delivery of siRNA into mesenchymal stem cells by a combination of ultrasound and microbubbles. **Journal of Controlled Release**, v. 133, n. 2, p. 146–153, 2009.

PAPPA, K. I.; ANAGNOU, N. P. Novel sources of fetal stem cells: where do they fit on the developmental continuum? **Regenerative Medicine**, v 4, p. 423-433, 2009.

PAREKKADAN, B. et al. Mesenchymal stem cell-derived molecules reverse fulminant hepatic failure. **PLOS One**, v. 2, n. 9, p. 941, 2007.

PARK, J. S. et al. Engineering mesenchymal stem cells for regenerative medicine and drug delivery. **Methods**, v. 84, p. 3–16, 2015.

PARK, J. S. et al. Non-viral gene delivery of DNA polyplexed with nanoparticles transfected into human mesenchymal stem cells. **Biomaterials**, v. 31, n. 1, p. 124–132, 2010.

PASSIER, R., LAAKE, W.L., MUMMERY, L.C. Stem cell based therapy and lessons from the heart. **Nature**, v. 453, p. 322-329, 2008.

PÉREZ-MOLINA, J. A.; MOLINA, I. Chagas disease. **Lancet**, v. 391, n. 10115, p. 82-94, 2018.

PEROBELLI, S. M. et al. G-CSF–Induced Suppressor IL-10 + neutrophils promote regulatory T Cells that inhibit graft-versus-host disease in a long-lasting and specific way. **The Journal of Immunology**, v. 197, n. 9, p. 3725–3734, 2016.

PETIT, I. et al. G-CSF induces stem cell mobilization by decreasing bone marrow SDF-1 and up-regulating CXCR4. **Nature Immunology**, v. 3, n. 7, p. 687-694, 2002.

PFEFFER, M.A.; BRAUNWALD, E. Ventricular remodeling after myocardial infarction: experimental observations and clinical implications. **Circulation**, v. 81, p.1161-72, 1990.

PONTE, A. L. et al. The in vitro migration capacity of human bone marrow mesenchymal stem cells: comparison of chemokine and growth factor chemotactic activities. **Stem cells**, v. 25, n. 7, p. 1737–1745, 2007.

PRESTES, J. et al. Efeitos do fator de crescimento insulínico-I sobre o músculo esquelético e suas relações com o exercício físico. **Revista Brasileira de Ciência e Movimento**, v. 14, n. 3, p. 97–104, 2006.

PROCKOP, D. J. Repair of tissues by adult stem/progenitor cells (MSCs): Controversies, myths, and changing paradigms. **Molecular Therapy**, 2009.

PSALTIS, P. J. et al. Concise review: mesenchymal stromal cells: potential for cardiovascular repair. **Stem Cells**, v. 26, n. 9, p. 2201-10, 2008.

QAYYUM, A. A. et al. Adipose-derived mesenchymal stromal cells for chronic myocardial ischemia (MyStromalCell Trial): Study design. **Regenerative Medicine**, v. 7, n. 3, p. 421–428, 2012.

RAPER, S. E. et al. Fatal systemic inflammatory response syndrome in a ornithine transcarbamylase deficient patient following adenoviral gene transfer. **Molecular Genetics and Metabolism**, v. 80, n. 1-2, p. 148–158, 2003.

RASSI, A.; RASSI, A.; MARIN-NETO, J. A. Chagas disease. **Lancet**, 2010.

RODRIGUES, M. M.; OLIVEIRA, A. C.; BELLIO, M. The immune response to Trypanosoma cruzi: Role of toll-like receptors and perspectives for vaccine development. **Journal of Parasitology Research**, 2012.

ROWE, R. G. et al. Engineering hematopoietic stem cells: lessons from development. **Cell Stem Cell**, 2016.

SAGE, E. K.; THAKRAR, R. M.; JANES, S. M. Genetically modified mesenchymal stromal cells in cancer therapy. **Cytotherapy**, 2016.

SAKATA, D.; YAO, C.; NARUMIYA, S. Prostaglandin E2, an immunoactivator. **Journal of Pharmacological Sciences**, v. 112, n. 1, p. 1–5, 2010.

SCHMUNIS, JR. et al. Epidemiology of Chagas disease in non-endemic countries: the role of international migration. **Memórias do Instituto Oswaldo Cruz**, v. 102, Suppl. 1, p. 31-40, 2009.

SCHREPFER, S. et al. Stem cell transplantation: the lung barrier. **Transplantation Proceedings**, v. 39, n. 2, p. 573–576, 2007.

SEIF-NARAGHI, S. B. et al. Safety and efficacy of an injectable extracellular matrix hydrogel for treating myocardial infarction. **Science Translational Medicine**, v. 5, n. 173, 2013.

SERRANO, A. L. et al. Interleukin-6 Is an Essential Regulator of Satellite Cell-Mediated Skeletal Muscle Hypertrophy. **Cell Metabolism**, v. 7, n. 1, p. 33–44, 2008.

SHABBIR, A. et al. Heart failure therapy mediated by the trophic activities of bone marrow mesenchymal stem cells: a noninvasive therapeutic regimen. **AJP: Heart and Circulatory Physiology**, v. 296, n. 6, p. H1888–H1897, 2009.

SHI, R. Z.; LI, Q. P. Improving outcome of transplanted mesenchymal stem cells for ischemic heart disease. **Biochemical and Biophysical Research Communications**, v. 376, n. 2, p. 247–250, 2008.

SILVA, D. N. et al. Intramyocardial transplantation of cardiac mesenchymal stem cells reduces myocarditis in a model of chronic Chagas disease cardiomyopathy. **Stem Cell Research and Therapy**, v. 5, n. 4, 2014.

SOARES, M. B. P. et al. Reversion of gene expression alterations in hearts of mice with chronic chagasic cardiomyopathy after transplantation of bone marrow cells. **Cell Cycle**, v. 10, n. 9, p. 1448–1455, 2011.

SOARES, M. B. P. et al. Transplanted bone marrow cells repair heart tissue and reduce myocarditis in chronic chagasic mice. **American Journal of Pathology**, v. 164, n. 2, p. 441–447, 2004.

SOARES, M. B. P.; PONTES-DE-CARVALHO, L.; RIBEIRO-DOS-SANTOS, R. The pathogenesis of Chagas' disease: When autoimmune and parasite-specific immune responses meet. **Anais da Academia Brasileira de Ciências**, v. 73, n. 4, p. 546–559, 2001.

SOMIA, N.; VERMA, I. M. Gene therapy: trials and tribulations. **Nature Review Genetics**, v. 1, n. 2, p. 91-99, 2000.

SOUZA, B. S. D F. et al. Bone marrow cells migrate to the heart and skeletal muscle and participate in tissue repair after *Trypanosoma cruzi* infection in mice. **International Journal of Experimental Pathology**, v. 95, n. 5, p. 321–329, 2014.

STAMM, C. et al.. Autologous bone-marrow stem-cell transplantation for myocardial regeneration. **Lancet**, v. 361, n. 9351, p. 45-46, 2003.

SUGANO, Y., et al. Granulocyte colony-stimulating factor attenuates early ventricular expansion after experimental myocardial infarction. **Cardiovascular Research**, v. 65, p. 446–456, 2005.

TAKAHASHI, K.; YAMANAKA, S. Induction of pluripotent stem cells from mouse embryonic and adult fibroblast cultures by defined factors. **Cell**, v. 126, n. 4, p. 663-76, 2006.

TALMADGE, J. E.; GABRILOVICH, D. I. History of myeloid derived suppressor cells (MDSCs) in the macro- and micro-environment of tumour-bearing hosts. **Nature. Reviews Cancer**, v. 13, n. 10, p. 739–752, 2013.

TARLETON, R. L. et al. The challenges of Chagas disease-grim outlook or glimmer of hope. **PLOS Medicine**, v. 12, p. e332, 2007.

TEIXEIRA, A. R.; NASCIMENTO, R. J. STURM, N. R. Evolution and pathology in Chagas disease: a review. **Memórias do Instituto Oswaldo Cruz**, v. 101, n. 5, p. 463-491, 2006.

THOMSON, J. A. Embryonic stem cell lines derived from human blastocysts. **Science**, v. 282, n. 5391, p. 1145–1147, 1998.

TSE, W. T. et al.. Suppression of allogeneic t-cell proliferation by human marrow stromal cells: implications in transplantation. **Transplantation**, v.75, n. 3, p. 389-97, 2003.

UCHIMURA, E. et al. Method for reverse transfection using gold colloid as a nano-scaffold. **Journal of Bioscience and Bioengineering**, v. 103, n. 1, p. 101–103, 2007.

VASCONCELOS, J. F. et al. Administration of granulocyte colony-stimulating factor induces immunomodulation, recruitment of T regulatory cells, reduction of myocarditis and decrease of parasite load in a mouse model of chronic Chagas disease cardiomyopathy. **FASEB Journal**, v. 27, n. 12, p. 4691–4702, 2013.

VECELLIO, M. et al. In Vitro epigenetic reprogramming of human cardiac mesenchymal stromal cells into functionally competent cardiovascular precursors. **PLoS ONE**, v. 7, n. 12, 2012.

VILAS-BOAS, F. et al. Early results of bone marrow cell transplantation to the myocardium of patients with heart failure due to Chagas disease. **Arquivos Brasileiros de Cardiologia**, v. 87, n. 2, p. 159–166, 2006.

VOGEL, G. Stem cells: new excitements, persistent questions. **Science**, v. 290, p. 1672-1674, 2000.

WAGERS, A.J.; WEISSMAN, L. Plasticity of adult stem cells. **Cell**, v. 116, p. 639-648, 2004.

WAGNER, J. et al. Optimizing mesenchymal stem cell-based therapeutics. **Current Opinion in Biotechnology**, 2009.



WRIGHT, J. D. et al. Tumor-derived G-CSF facilitates neoplastic growth through a granulocytic myeloid-derived suppressor cell-dependent mechanism. **PLoS ONE**, v. 6, n. 11, p. 70–80, 2011.

WALTHER, W.; STEIN, U. Viral vectors for gene transfer: A review of their use in the treatment of human diseases. **Drugs**, 2000.

WATT, F.M.; HOGAN, B.L.M. Out of eden: stem cells and their niches. **Science**, v. 287, p. 1427-1430, 2000.

WHO. Chagas Disease (American Trypanosomiasis). **Infectious Diseases**, v. 2013, n. 4/29/2013, p. 1065–1072, 2017.

WYSE, R. D.; DUNBAR, G. L.; ROSSIGNOL, J. Use of genetically modified mesenchymal stem cells to treat neurodegenerative diseases. **International Journal of Molecular Sciences**, v. 15, n. 2, p. 1719–1745, 2014.

XIAN, C. J.; FOSTER, B. K. Repair of injured articular and growth plate cartilage using mesenchymal stem cells and chondrogenic gene therapy. **Current Stem Cell Research & Therapy**, v. 1, n. 2, p. 213–29, 2006.

YLÄ-HERTTUALA, S. Endgame: Glybera finally recommended for approval as the first gene therapy drug in the European union. **Molecular Therapy**, v. 20, n. 10, p. 1831–1832, 2012.

YOSHIDA, N. Trypanosoma cruzi infection by oral route: how the interplay between parasite and host components modulates infectivity. **Parasitology International**, v. 57, n. 02, p. 105-109, 2008.

YU, X. et al. Overexpression of CXCR4 in mesenchymal stem cells promotes migration, neuroprotection and angiogenesis in a rat model of stroke. **Journal of the Neurological Sciences**, v. 316, n. 1-2, p. 141–149, 2012.

ZAGO, M.A. Células-tronco: origens e propriedades. In: ZAGO, M. A.; COVAS, D. T. (OrgS.) **Células-tronco: a nova fronteira da medicina**. São Paulo: Atheneu, 2006. p. 21-34.

**ANEXOS**

## ANEXO I

SOUZA, B. S. F; SILVA, K. N; **SILVA, D. N**; ROCHA, V. P.C; PAREDES, B. D; AZEVEDO, C.M.C; NONAKA, C. K. V; CARVALHO, G.B; VASCONCELOS, J. F; DOS-SANTOS, R. R; SOARES, M. B. P. Galectin-3 Knockdown Impairs Survival, Migration, and Immunomodulatory Actions of Mesenchymal Stromal Cells in a Mouse Model of Chagas Disease Cardiomyopathy. **Stem cells international**, v. 2017, p. 13, 2017.

## Research Article

# Galectin-3 Knockdown Impairs Survival, Migration, and Immunomodulatory Actions of Mesenchymal Stromal Cells in a Mouse Model of Chagas Disease Cardiomyopathy

Bruno Solano de Freitas Souza,<sup>1,2</sup> Kátia Nunes da Silva,<sup>2</sup> Daniela Nascimento Silva,<sup>2</sup> Vinícius Pinto Costa Rocha,<sup>1</sup> Bruno Diaz Paredes,<sup>2</sup> Carine Machado Azevedo,<sup>1,2</sup> Carolina Kymie Nonaka,<sup>1,2</sup> Gisele Batista Carvalho,<sup>2</sup> Juliana Fraga Vasconcelos,<sup>1,2</sup> Ricardo Ribeiro dos Santos,<sup>2</sup> and Milena Botelho Pereira Soares<sup>1,2</sup>

<sup>1</sup>Gonçalo Moniz Institute, FIOCRUZ, Salvador, BA, Brazil

<sup>2</sup>Center for Biotechnology and Cell Therapy, São Rafael Hospital, Salvador, BA, Brazil

Correspondence should be addressed to Milena Botelho Pereira Soares; [milena@bahia.fiocruz.br](mailto:milena@bahia.fiocruz.br)

Received 10 February 2017; Revised 27 May 2017; Accepted 5 June 2017; Published 10 July 2017

Academic Editor: Luc van der Laan

Copyright © 2017 Bruno Solano de Freitas Souza et al. This is an open access article distributed under the Creative Commons Attribution License, which permits unrestricted use, distribution, and reproduction in any medium, provided the original work is properly cited.

Therapies based on transplantation of mesenchymal stromal cells (MSC) hold promise for the management of inflammatory disorders. In chronic Chagas disease cardiomyopathy (CCC), caused by chronic infection with *Trypanosoma cruzi*, the exacerbated immune response plays a critical pathophysiological role and can be modulated by MSC. Here, we investigated the role of galectin-3 (Gal-3), a beta-galactoside-binding lectin with several actions on immune responses and repair process, on the immunomodulatory potential of MSC. Gal-3 knockdown in MSC did not affect the immunophenotype or differentiation potential. However, Gal-3 knockdown MSC showed decreased proliferation, survival, and migration. Additionally, when injected intraperitoneally into mice with CCC, Gal-3 knockdown MSC showed impaired migration in vivo. Transplantation of control MSC into mice with CCC caused a suppression of cardiac inflammation and fibrosis, reducing expression levels of CD45, TNF $\alpha$ , IL-1 $\beta$ , IL-6, IFN $\gamma$ , and type I collagen. In contrast, Gal-3 knockdown MSC were unable to suppress the immune response or collagen synthesis in the hearts of mice with CCC. Finally, infection with *T. cruzi* demonstrated parasite survival in wild-type but not in Gal-3 knockdown MSC. These findings demonstrate that Gal-3 plays a critical role in MSC survival, proliferation, migration, and therapeutic potential in CCC.

## 1. Introduction

Mesenchymal stromal cells (MSC) are multipotent stem cells with the ability to differentiate into mesoderm-derived cell lineages, such as chondrocytes, osteocytes, and adipocytes [1]. Described by Friedenstein and colleagues in 1970 [2], MSC are plastic-adherent cells presenting fibroblast-like morphology and are characterized by the expression of specific surface markers and demonstration of trilineage differentiation potential. MSC can be easily obtained from different organs and tissues of adult individuals, being present among the most studied cell types in cell therapies [1].

The potential use of MSC to treat inflammatory and autoimmune disorders is based on several described immunomodulatory actions, including inhibition of the activation of T and B lymphocytes, NK cells, and dendritic cells and stimulation of regulatory T cell differentiation [3]. The anti-inflammatory actions of MSC are well studied and found to be mediated by IL-10, TGF- $\beta$ , PGE2, HGF, and IDO (for human cells) or iNOS (for mouse cells). Galectin-3 (Gal-3) has also been suggested as a critical mediator of immunomodulatory actions of human MSC [4, 5].

Galectins are a group of galactoside-binding lectins that regulate various biological processes. Gal-3 is present in the

extracellular and intracellular compartments, being involved in cell adhesion, migration, apoptosis, inflammation, and tissue repair [6]. Expression of Gal-3 in fibroblasts is associated with proliferation and synthesis of extracellular matrix components, contributing to scar formation [7–9]. In endothelial precursor cells, Gal-3 promotes proliferation and angiogenesis [10]. While the role of Gal-3 in immune cells has been extensively studied, the actions affected by Gal-3 expression in MSC are not well established. Being highly expressed in inflammatory and fibrogenic microenvironments in tissues [11], Gal-3 is likely to affect MSC biology and response, naturally or in a cell therapy scenario.

Cell therapy has been investigated as a potential alternative treatment for Chagas disease cardiomyopathy, a relevant cause of chronic heart failure in Latin America which results from *Trypanosoma cruzi* infection [12, 13]. An exacerbated immune response directed against the parasite and to host antigens plays a central role in the pathogenesis of CCC, leading to progressive cardiomyocyte loss, fibrosis, arrhythmia, and loss of ventricular function [13]. Previously, it was demonstrated that transplantation of MSC into mice chronically infected with *T. cruzi* caused a reduction of myocarditis and modulation of fibrosis [14–16]. Additionally, we have shown that Gal-3 expression is increased in the hearts of chronic chagasic mice and in human samples [17, 18]. *T. cruzi* infection induces increased Gal-3 expression in different cell types, which favors parasite adhesion, migration, invasion, and reduces antiparasitic immune responses [19–23]. Here, we investigated the potential involvement of Gal-3 in the ability of MSC to migrate and exert immunomodulatory actions in a mouse model of CCC, also investigating potential actions in parasite-host cell interactions.

## 2. Materials and Methods

**2.1. Animal Procedures.** Six- to eight-week-old female C57BL/6 mice were used in this study. All animals were raised and maintained at the animal facility of the Center for Biotechnology and Cell Therapy, São Rafael Hospital, in rooms with controlled temperature ( $22 \pm 2^\circ\text{C}$ ) and humidity ( $55 \pm 10\%$ ), continuous air flow, and 12 h light/12 h dark cycles (6 am–6 pm) and provided with rodent diet and water ad libitum. Mice were handled according to the NIH guidelines for animal experimentation, and the study received prior approval by the animal ethics committee at São Rafael Hospital.

**2.2. Isolation and Culture of MSC.** Bone marrow cells were obtained from the tibiae and femurs by flushing and were cultured in Dulbecco's modified Eagle's medium (DMEM; ThermoFisher Scientific, Waltham, MA, USA), 10% fetal bovine serum (ThermoFisher Scientific), and 1% penicillin/streptomycin (ThermoFisher Scientific) in a humidified incubator at  $37^\circ\text{C}$  with 5% atmospheric  $\text{CO}_2$ . The medium was changed every 2–3 days and, when the culture reached 90% confluency, the cells were passaged with trypsin-EDTA 0.25% solution (ThermoFisher Scientific).

**2.3. Galectin-3 Knockdown.** Stable Gal-3 knockdown was achieved by MSC or J774 macrophages by transduction with lentiviral vectors carrying a shRNA sequence targeting *Lgals3* gene or scrambled control (*Lgals3\_shRNA1* 5'-GAT TTCAGGAGAGGGGAATGAT-3'; one *Lgals3\_scrbl\_shRNA* 5'-AGGTATGAGTCGAGATTGAGA-3'), as previously described [18]. Culture medium was replaced and the cells were cultured for an additional 48 h, being assessed for GFP reporter gene expression by using an inverted fluorescence microscope (Eclipse Ti-E; Nikon, Tokyo, Japan). The cells were expanded and knockdown efficiency for each shRNA was evaluated by confocal microscopy and qPCR analyses.

**2.4. Flow Cytometry Analysis.** For immunophenotyping, MSC lines were passaged and centrifuged and the pellet was resuspended in PBS. A total of  $5 \times 10^5$  cells was used for labeling with the following antibodies in the concentration 1/50: Sca1PE-Cy7 (BD Biosciences, San Jose, CA, USA), CD45-PerCP (eBioscience, San Diego, CA, USA), CD44-PE (BD Bioscience), CD90-APC (BD Bioscience), CD34-AlexaFluor647 (BD Bioscience), and control isotypes. Cells were incubated in  $100 \mu\text{L}$  of binding buffer (ThermoFisher Scientific) with annexin-V-FITC and 7-AAD (BD Biosciences, San Jose, CA, USA) for 15 minutes in the dark at RT. After the incubation period, cells were washed twice with PBS, and the data acquisition and analysis were performed using a LRSFortessa flow cytometer (BD Biosciences). At least 10,000 events were acquired and analyzed.

**2.5. Trilineage Differentiation Assay.** Adipogenic, osteogenic, and chondrogenic differentiations were performed using commercially available kits, following the manufacturer's instructions (ThermoFisher Scientific). For adipogenic differentiation, cells were cultured in 24-well plates in an adipogenic induction medium, StemPro Adipogenesis Differentiation Kit. Lipid inclusions were detected on differentiation day 14, by fixation in 4% paraformaldehyde and staining with Oil red solution. For osteogenic differentiation, the cells were cultured in a specific osteogenic differentiation medium, StemPro Osteogenesis Differentiation Kit. Half the differentiation medium was changed every two days. Calcium-rich matrix deposition was observed by staining with Alizarin red 2%. For chondrogenic differentiation, cells were cultured for 21 days in chondrogenic differentiation medium, StemPro Chondrogenesis Differentiation Kit. Proteoglycan synthesis was evaluated after staining with Alcian Blue solution. The images were captured with an inverted microscope (Eclipse Ti, Nikon, Tokyo, Japan).

**2.6. Endothelial Cell Differentiation.** Differentiation of MSC to endothelial cells was performed by incubating the cells with EGM-2 medium (Lonza, Basel, Switzerland), as previously described [15]. Endothelial tube formation assay was performed to observe capillary-like 3-D structures by plating the differentiated cells on Matrigel (Corning, Corning, NY, USA). The images were captured using an inverted microscope (Eclipse Ti, Nikon).

**2.7. Proliferation Assay.** For comparative evaluation of the proliferation rate among different MSC lines, the cells were plated in 96-well plates, at a density of  $10^4$  cells/well, in a final volume of 200  $\mu$ L, in triplicate, and cultured in DMEM supplemented with 10% FBS. After 24 h, plates were pulsed with 1  $\mu$ Ci of methyl- $^3$ H thymidine (PerkinElmer) for 18 h, and proliferation was assessed by measurement of  $^3$ H-thymidine uptake by using a Chameleon  $\beta$ -plate counter (Hydrex; Turku, Finland).

**2.8. Cell Migration Analyses.** MSC were plated in wells of a 24-well plate, at a cell density of  $5 \times 10^4$  cells/cm $^2$ . Live cell imaging was performed using the Operetta High Content Imaging System (Perkin Elmer) under controlled temperature (37°C) and atmospheric CO $_2$  (5%). Digital phase-contrast images were acquired at 10x magnification (10x high NA objective) using Operetta's automatic digital phase-contrast algorithm. Image acquisition interval was set to 10 min during 16 h. Images were segmented using the Find Cells building block of the Harmony 3.5.2 software (Perkin Elmer), which provides a dedicated algorithm for segmenting digital phase-contrast images. The segmented cells were subjected to cell tracking using the Track Objects building block. Properties that describe cell migration per time point were calculated, such as displacement. Representative graphs of mean square displacement for each well is shown. For in vitro wound healing assay, MSC were cultured in a 6-well plate until a monolayer was formed. A pipette tip was used to make a scratch along the well, and the area was photographed at time point 0 and after 3 days for gap distance measurements.

**2.9. *T. cruzi* Infection and Cell Transplantation.** Trypomastigotes of the myotropic Colombian *T. cruzi* strain were obtained from culture supernatants of infected LLC-MK2 cells, as previously described [24]. Then, C57BL/6 mice were infected by intraperitoneal injection with 1000 *T. cruzi* trypomastigotes in PBS. Infection was confirmed by following parasitemia at different time points after infection.

Six months after infection, mice were randomly assigned into three groups: control MSC, Gal-3 knockdown MSC, or saline. The administration regimen consisted of one weekly intraperitoneal injection of a suspension of  $10^6$  MSC, or equal volume of saline (100  $\mu$ L). Mice were euthanized by cervical dislocation under anesthesia with ketamine (100 mg/kg) and xylazine (10 mg/kg), on the 7th week after the beginning of the treatment, for analysis.

For in vitro infections, MSC or J774 macrophages were incubated with *T. cruzi* trypomastigotes (MOI = 10) for 24 h. Then, the wells were washed and the medium replaced. Cells were fixed, stained with DAPI for parasite quantification in the Operetta system (PerkinElmer), or submitted for transmission electron microscopy processing and analysis. For ultrastructural analysis, cells were fixed at 4°C for 12 h in a solution of 3% glutaraldehyde (Sigma-Aldrich) in PBS, washed with 0.1 M sodium cacodylate buffer, and postfixed in osmium tetroxide 1% for 30 min. Dehydration was performed by using a graded series of acetone solutions, then the samples were embedded in epoxy

resin Polybed812 (Electron Microscopy Sciences, Hatfield, PA, USA). Ultrathin sections were obtained using EM UC7 ultramicrotome (Leica, Wetzlar, Germany) and contrasted with uranyl acetate and lead citrate. The sections were analyzed using a transmission electron microscope JEM1230 JEOL (Tokyo, Japan) at 80 kV.

**2.10. Real-Time Reverse Transcription Polymerase Chain Reaction (RT-qPCR).** Dissociated cells, heart, and spleen samples were subjected to total RNA extraction using TRIzol reagent (Thermo Scientific). The RNA concentration was determined by spectrophotometry. Next, cDNA was synthesized, starting with 1  $\mu$ g RNA using High Capacity cDNA Reverse Transcription Kit (Thermo Scientific), following the manufacturer's instructions. RT-qPCR assays were performed to detect the expression levels of *Tbet* (Mm\_00450960\_m1), *Tnf* (Mm\_00443258\_m1), *Ifng* (Mm\_00801778\_m1), *Col1a1* (Mm\_0801666\_g1), *Il1b* (Mm\_0043228\_m1), *Il6* (Mm\_00446190\_m1), and *Ptprc* (Mm\_01293577\_m1). The RT-qPCR amplification mixtures contained 20 ng template cDNA, Taqman Master Mix (10  $\mu$ L), and probes in a final volume of 20  $\mu$ L (all from Thermo Scientific). The reactions were run in duplicate on an ABI7500 Sequence Detection System (Thermo Scientific) under standard thermal cycling conditions. The mean Ct (cycle threshold) values from duplicate measurements were used to calculate the expression of the target gene, with normalization to an internal control—*Gapdh* (mm99999915\_g1), using the 2- $\Delta$ Ct formula. Experiments with coefficients of variation greater than 5% were excluded. A nontemplate control and non-reverse transcription controls were also included.

**2.11. Histology and Morphometric Analyses.** Hearts were collected and fixed in 10% buffered formalin. Heart sections were analyzed by light microscopy after paraffin embedding, followed by standard hematoxylin and eosin (H&E), or Sirius red staining. Sirius red-stained sections were entirely digitalized using a confocal microscope A1+ (Nikon). The percentage of fibrosis was determined by analysis of whole sections stained with Sirius red-stained heart sections and semiautomatic morphometric quantification using Image Pro Plus v.7.0. Two blinded investigators performed the analyses.

**2.12. Immunofluorescence Analysis.** Immunostainings for detection of Gal-3 expression were performed in MSC plated on coverslips. The cells were fixed with paraformaldehyde 4% and incubated overnight at 4°C with the primary antibody goat anti-Gal-3, diluted 1:400 (Santa Cruz Biotechnology, Dallas, TX, USA). On the following day, sections were incubated for 1 h with phalloidin conjugated with Alexa Fluor 488 (1:200; ThermoFisher Scientific) mixed with the secondary antibody anti-goat IgG Alexa Fluor 568 (1:1000; ThermoFisher Scientific). Proliferating cells were evaluated by KI67 staining (anti-Ki67 1:1000; ThermoFisher Scientific), followed by anti-rabbit IgG Alexa Fluor 568 (1:1000 ThermoFisher Scientific). Dead cells were stained with PI (BD Biosciences). Nuclei were stained with 4,6-diamidino-2-phenylindole (VECTASHIELD

mounting medium with DAPI H-1200; Vector Laboratories, Cambridgeshire, UK). The presence of fluorescent cells was determined by observation using an A1+ confocal microscope (Nikon).

**2.13. Statistical Analyses.** Continuous variables are presented as means  $\pm$  SEM. Parametric data were analyzed using Student's unpaired *t*-test, for comparisons between two groups, and 1-way ANOVA, followed by Bonferroni post hoc test for multiple-comparison test, using Prism 6.0 (GraphPad Software). Values of  $P < 0.05$  were considered statistically significant.

### 3. Results

Bone marrow-derived MSC lines were generated by transduction with lentiviral vectors containing the shRNA sequence targeting Gal-3 gene or a nontargeting scrambled sequence. The MSC lines were assessed for Gal-3 expression, in order to confirm the knockdown efficiency by confocal microscopy and qPCR analysis (Figures 1(a), 1(b), and 1(c)). Gal-3 was expressed in the cytoplasm and inside the nuclei of wild-type (Figure 1(a)) and control vector-transduced MSC lines. Cells transduced with the vector containing the shRNA sequence for Gal-3 knockdown showed a marked reduction of Gal-3 expression (Figure 1(b)). This finding was confirmed quantitatively at the mRNA level by RT-qPCR analysis (Figure 1(c)).

MSC lines were then characterized in order to ensure the maintenance of the phenotype and biological properties that define MSC. Immunophenotyping by flow cytometry showed a similar pattern of expression of surface markers by the different cell lines, with a positive staining for the MSC markers CD44, CD90, and Sca-1, and low frequency of cells expressing hematopoietic lineage markers CD45 and CD34 (Figure 1(d)). Next, we assessed the multipotential of MSC by a trilineage differentiation assay *in vitro*. Upon induction by specific culture media, Gal-3 knockdown and control MSC lines were able to efficiently undergo osteogenic, chondrogenic, and adipogenic differentiation (Figure 2(a)). Additionally, knockdown of Gal-3 in MSC did not interfere with their ability to form capillary-like structures when cultured in endothelium-inducer medium (Figure 2(b)).

Next, MSCs were analyzed regarding proliferation rate and survival. We found that Gal-3 knockdown MSC present decreased proliferation rate when compared to controls, as measured by  $^3\text{H}$ -thymidine incorporation (Figure 3(a)). Moreover, the number of cells undergoing apoptosis was higher in Gal-3 knockdown MSC, when compared to controls, after incubation with  $10\ \mu\text{M}$   $\text{H}_2\text{O}_2$  (Figure 3(b)).

Galectin 3 is known to affect cell-extracellular matrix protein binding and cell migration processes [25, 26]. To investigate whether Gal-3 knockdown interferes with migration of MSC, we assessed the *in vitro* migratory ability of Gal-3 knockdown MSC and control cell lines *in vitro*. Gal-3 knockdown caused a decreased migration *in vitro* in a wound healing assay when compared to control MSC (Figures 4(a), 4(b), 4(c), 4(d), and 4(e)). Additionally,

by using displacement cell tracking by time-lapse image analysis, we found that Gal-3 knockdown caused a reduction in the mobility of MSC when compared to controls (Figures 4(f), 4(g), and 4(h)).

In order to test if Gal-3 knockdown could impair MSC therapeutic actions in an *in vivo* setting, the cells were administered *i.p.* into mice chronically infected with *T. cruzi*, a model of chronic Chagas disease cardiomyopathy (Figure 5(a)). First, the ability of MSC to migrate to the spleen and heart was evaluated shortly after transplantation, by qPCR analysis of GFP mRNA expression. GFP expression was detected in the spleens as early as 30 min after cell transplantation and increased at the 3 h time point. However, significantly lower levels of GFP mRNA expression were detected in the spleens of mice transplanted with Gal-3 knockdown MSC when compared to control MSC, both 30 min and 3 h after the cell administration. Negligible levels of GFP were detected in the hearts at the same time points (Figure 5(b)).

Next, we investigated the long-term effects of cell transplantation in *T. cruzi*-infected mice. Groups of mice received weekly *i.p.* injections of  $10^6$  MSC—wild-type or Gal-3 knockdown cell line—for five weeks. A vehicle control group was injected with equal volumes of saline solution (Figure 5(a)). Seven weeks after the beginning of the treatment, mice were euthanized for histological and molecular evaluations.

Histological analysis of heart sections revealed the presence of multifocal inflammatory infiltrates predominantly composed by mononuclear cells in *T. cruzi*-infected mice (Figures 5(c), 5(d), 5(e), and 5(f)). The levels of PTPRC—which encodes for CD45, a pan-leukocyte marker—in heart samples were decreased in the hearts of mice treated with wild-type MSC, but not with Gal-3 knockdown MSC (Figure 5(g)). Similarly, treatment with wild-type MSC, but not with Gal-3 knockdown MSC, reduced the expression of genes in the heart which are associated with inflammation, such as IL-1 $\beta$ , IL-6, and TNF $\alpha$  (Figures 5(h), 5(i), and 5(j)). The levels of expression of IFN $\gamma$  and T-bet, associated with Th1 responses, were significantly reduced by treatment with wild-type MSC. However, treatment with Gal-3 knockdown MSC did not reduce IFN $\gamma$  or T-bet expression, when compared to infected controls (Figures 5(k) and 5(l)).

The analysis of Sirius red-stained heart sections of *T. cruzi*-infected mice showed extensive areas of fibrosis (Figures 6(a), 6(b), and 6(c)). While the fibrosis content in the heart was not changed between the groups, collagen synthesis, as measured by collagen type I (*Col1a1*) gene expression, was reduced with wild-type MSC, but not with Gal-3 knockdown MSC (Figures 6(d) and 6(e)).

Since Gal-3 has been previously associated with the process of infection by *T. cruzi* [27], we hypothesized that Gal-3 is required for parasite life cycle also in MSC. In order to test that hypothesis, the MSC lines were submitted to *in vitro T. cruzi* infection. We found that Gal-3 expression is increased 48 and 72 h after *T. cruzi* infection in wild-type MSC (Figure 7(a)). Moreover, both wild-type MSC and Gal-3 knockdown MSC were successfully infected by *T. cruzi*, presenting a similar percentage of infection and number of

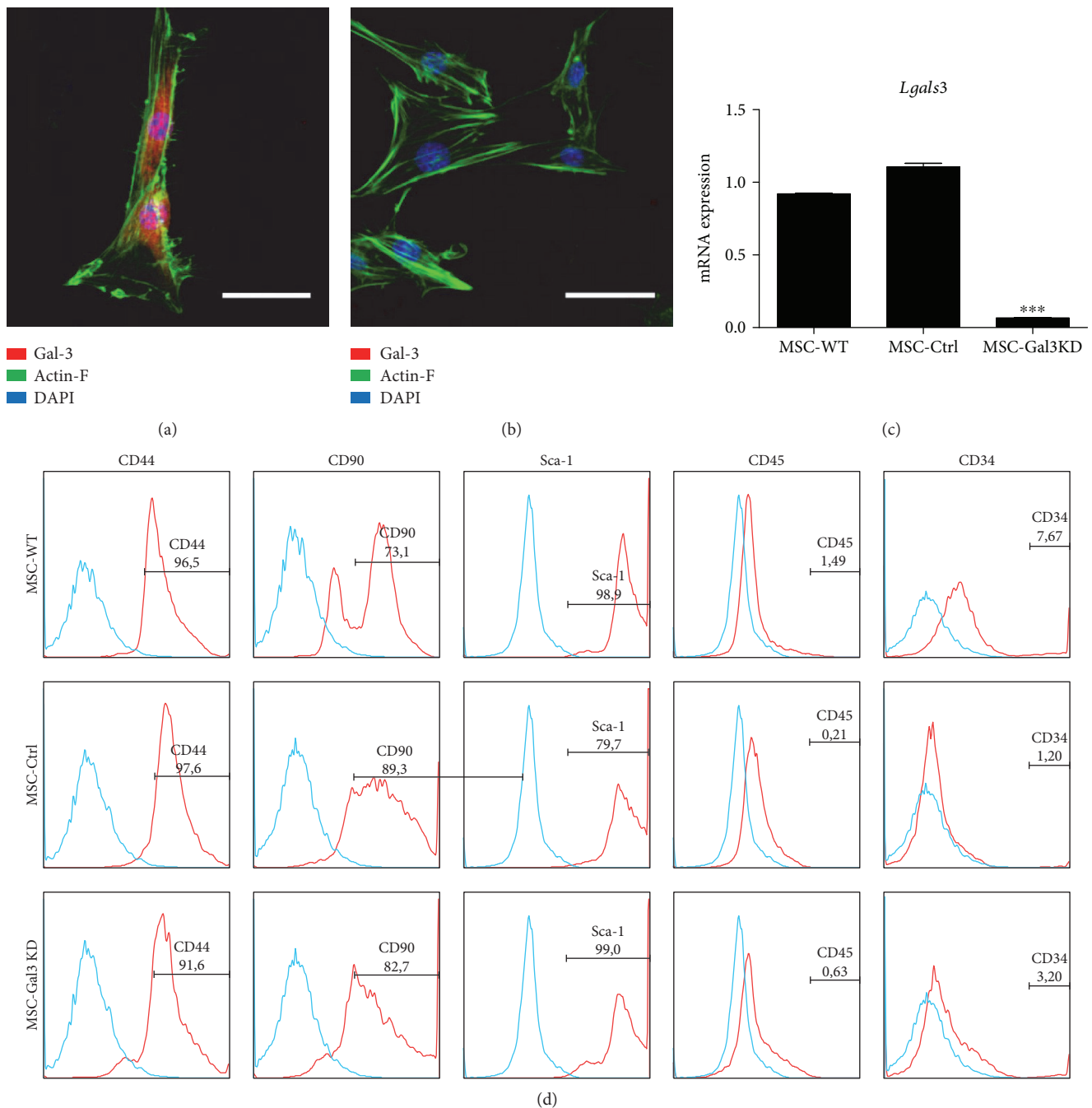


FIGURE 1: Evaluation of Gal-3 knockdown efficiency and characterization of MSC lines. Confocal microscopy images showing Actin-F (green), Gal-3 (red), and nuclei stained with DAPI (blue) in wild-type (a) and Gal-3 knockdown MSC (b). Scale bars = 20  $\mu\text{m}$ . (c) Gene expression analysis of *Lgals3* by qRT-PCR. \*\*\* $P < 0.001$ , compared to the other groups. (d) Histograms demonstrating expression of surface marker characteristics of MSC and low expression of hematopoietic markers, analyzed by flow cytometry.

parasites per cell 24 h after infection. However, at 48 and 72 h after infection, Gal-3 knockdown MSC presented a significantly lower percentage of infection and number of parasites per cell (Figure 7(b)). At the same time points evaluated, no differences were observed regarding the percentage of proliferating (KI67<sup>+</sup>) and dead cells (PI staining), between the infected MSC lines (data not shown). In order to evaluate if this was a cell-type specific effect,

infection was performed also in J774 macrophages. Gal-3 knockdown was also associated with a lower percentage of infection and number of parasites per cell in J774 macrophages (Figures 7(c) and 7(d)).

Ultrastructure analysis by transmission electron microscopy was performed in MSC infected with *T. cruzi*, showing that *T. cruzi* efficiently evade the parasitophorous vacuoles and multiply in the cytosol in wild-type MSC



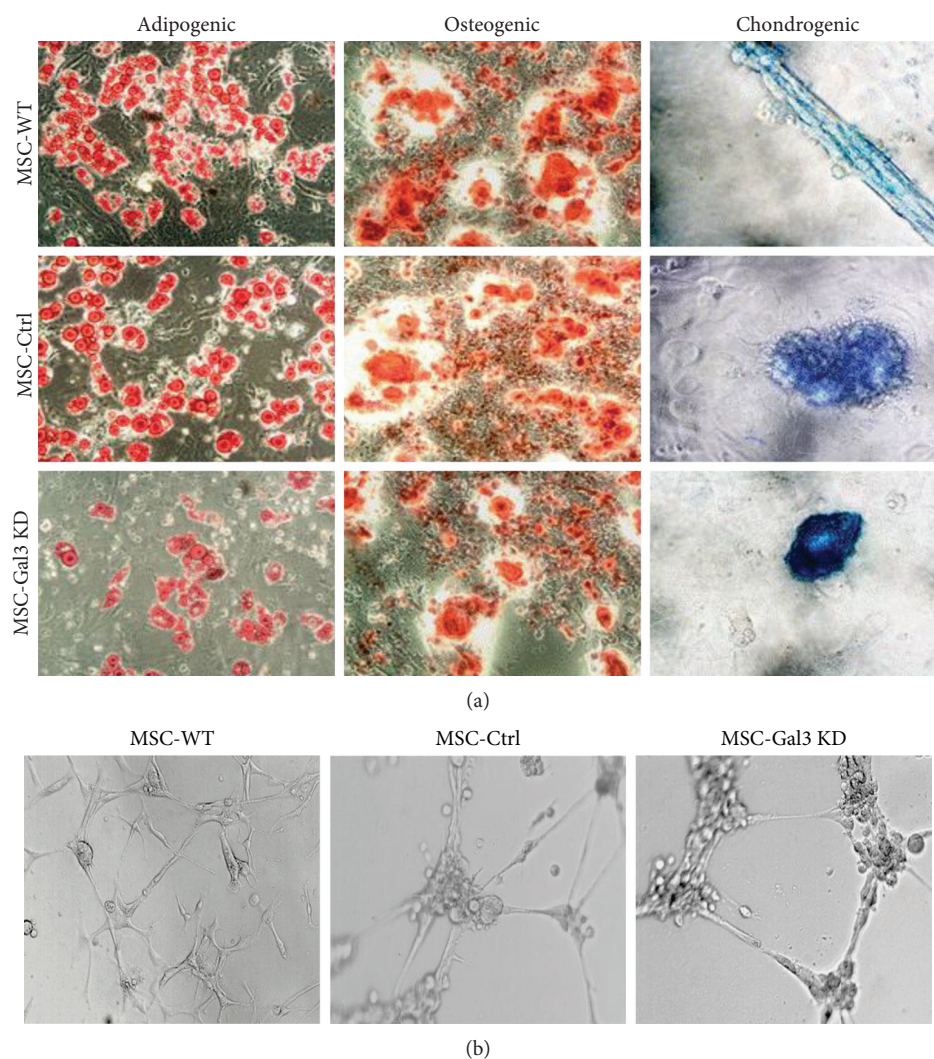


FIGURE 2: Characterization of MSC lines by differentiation assays. (a) Trilineage differentiation assay performed in MSC lines to generate adipocytes, visualized by Oil red staining, osteocytes, visualized by alizarin red staining, and chondrocytes, visualized by Alcian blue staining, respectively. (b) Angiogenic ability demonstrated by endothelial tube formation assay on Matrigel. MSC-WT = wild-type MSC; MSC-Ctrl = MSC transduced with a nontargeting shRNA vector; MSC-Gal3KD = Gal-3 knockdown MSC. Magnification = 200x.

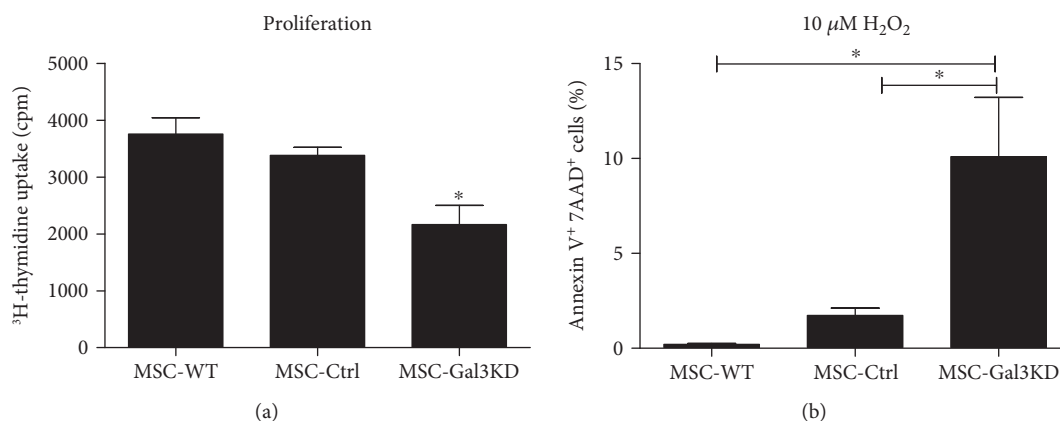


FIGURE 3: Effects of Gal-3 knockdown on cell proliferation and survival. (a) Proliferation rate in different MSC lines, evaluated by <sup>3</sup>H-thymidine incorporation assay. \**P* < 0.05, compared to the other groups. (b) Apoptosis analysis by Annexin V/7-AAD assay, comparing the rate of cells undergoing apoptosis after incubation with 10 μM H<sub>2</sub>O<sub>2</sub>. MSC-WT = wild-type MSC; MSC-Ctrl = MSC transduced with a nontargeting shRNA vector; MSC-Gal3KD = Gal-3 knockdown MSC. \**P* < 0.05.

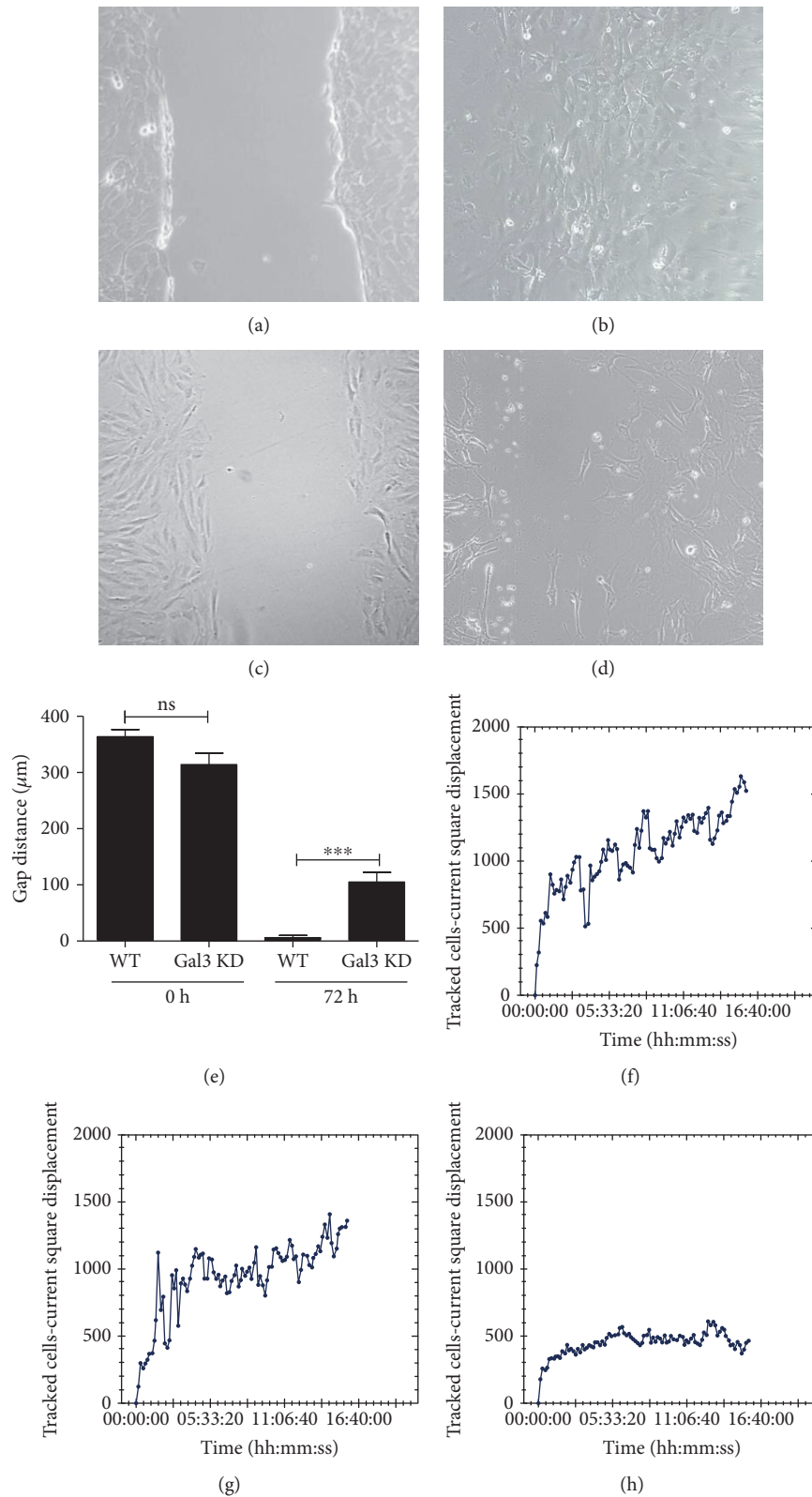
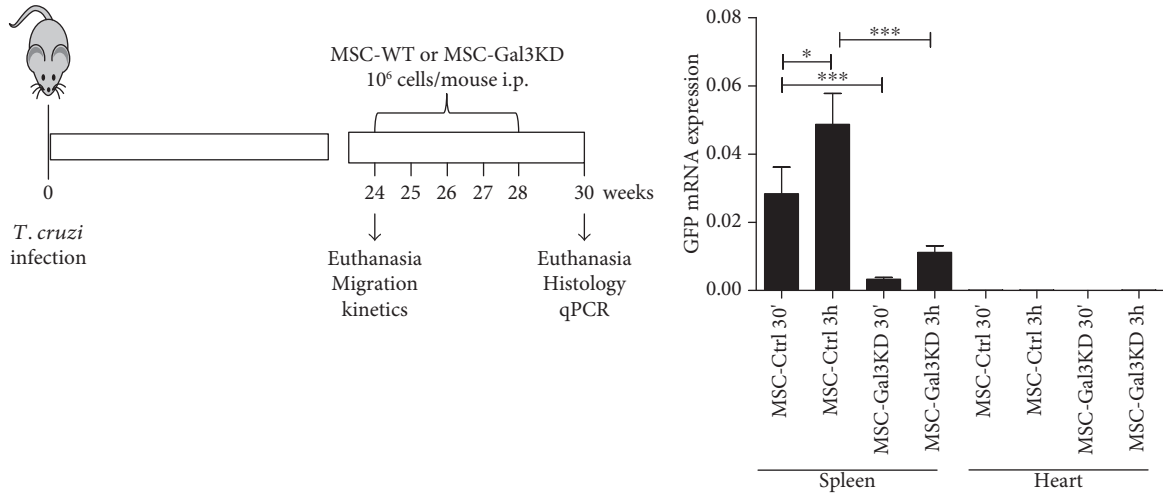
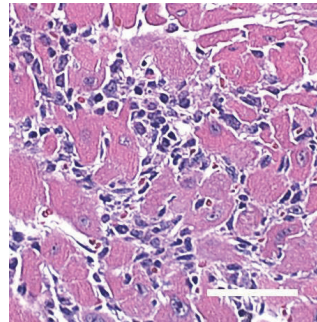
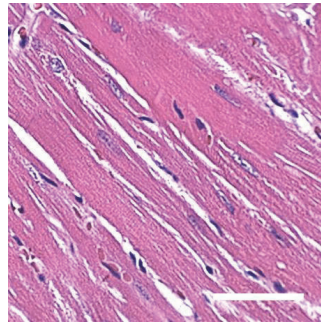


FIGURE 4: Gal-3 knockdown MSC exhibit defective migration and displacement in vitro. Migration was evaluated by the wound healing assay. Phase contrast representative images showing scratch area at day 0 for wild-type MSC (a) and Gal-3 knockdown MSC (c), and at day 3 for wild-type MSC (b) and Gal-3 knockdown MSC (d). (e) Gap distance was evaluated at 72 h and compared to time 0. \*\*\* $P < 0.001$ . (f–h) Mean square displacements were obtained by individually tracked cells at various time points, from the time of the first position, until the end of the overnight incubation of MSC-WT (d), MSC-Ctrl (e), and MSC-Gal3KD (f). MSC-WT = wild-type MSC; MSC-Ctrl = MSC transduced with a nontargeting shRNA vector; MSC-Gal3KD = Gal-3 knockdown MSC.



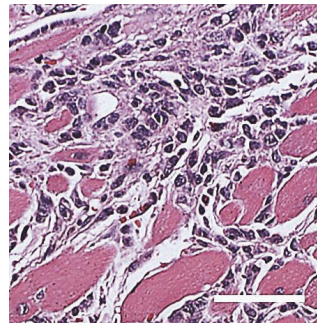
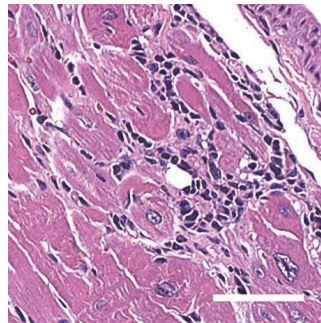
(a)

(b)



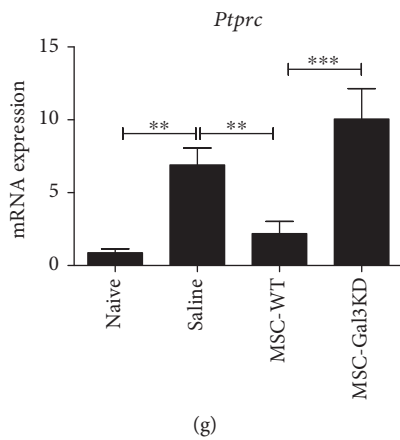
(c)

(d)

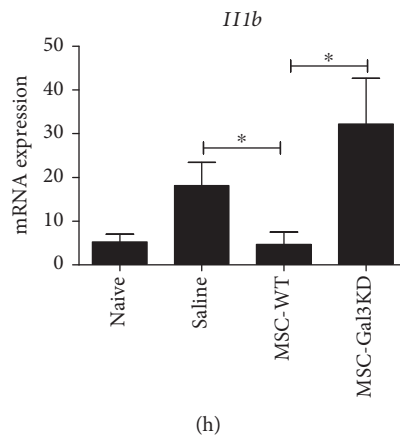


(e)

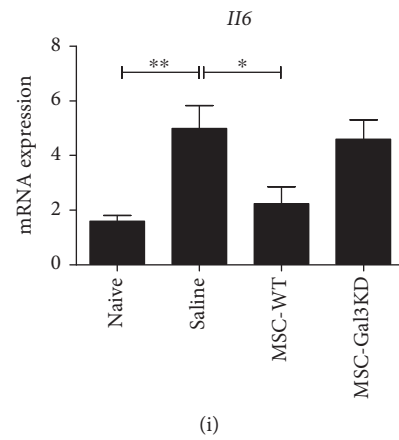
(f)



(g)



(h)



(i)

FIGURE 5: Continued.

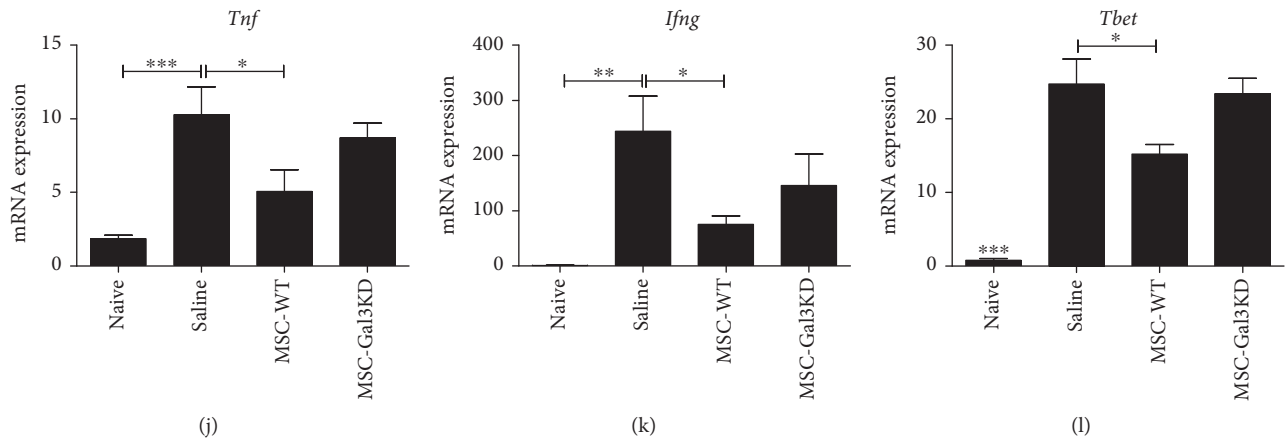


FIGURE 5: Effects of the transplantation of MSC lines in a mouse model of chronic *T. cruzi* infection. (a) Study design. (b) Cell migration and homing to spleens and hearts were evaluated by amplification of GFP mRNA by qRT-PCR. (c–f) Representative images of H&E stained heart sections of naïve mice (c), infected and administered with saline (d), MSC-WT (e), or MSC-Gal3KD (f). Quantification of mRNA expression levels of CD45 coding gene (PTPRC), evaluated qRT-PCR (g). RTqPCR analysis of gene expression in the heart tissue of the cytokines IL1- $\beta$  (h), IL-6 (i), TNF- $\alpha$  (j), IFN- $\gamma$  (k), and Th1-associated transcription factor T-bet (l). \* $P < 0.05$ ; \*\* $P < 0.01$ ; \*\*\* $P < 0.001$ . MSC-WT = wild-type MSC; MSC-Ctrl = MSC transduced with a nontargeting shRNA vector; MSC-Gal3KD = Gal-3 knockdown MSC.

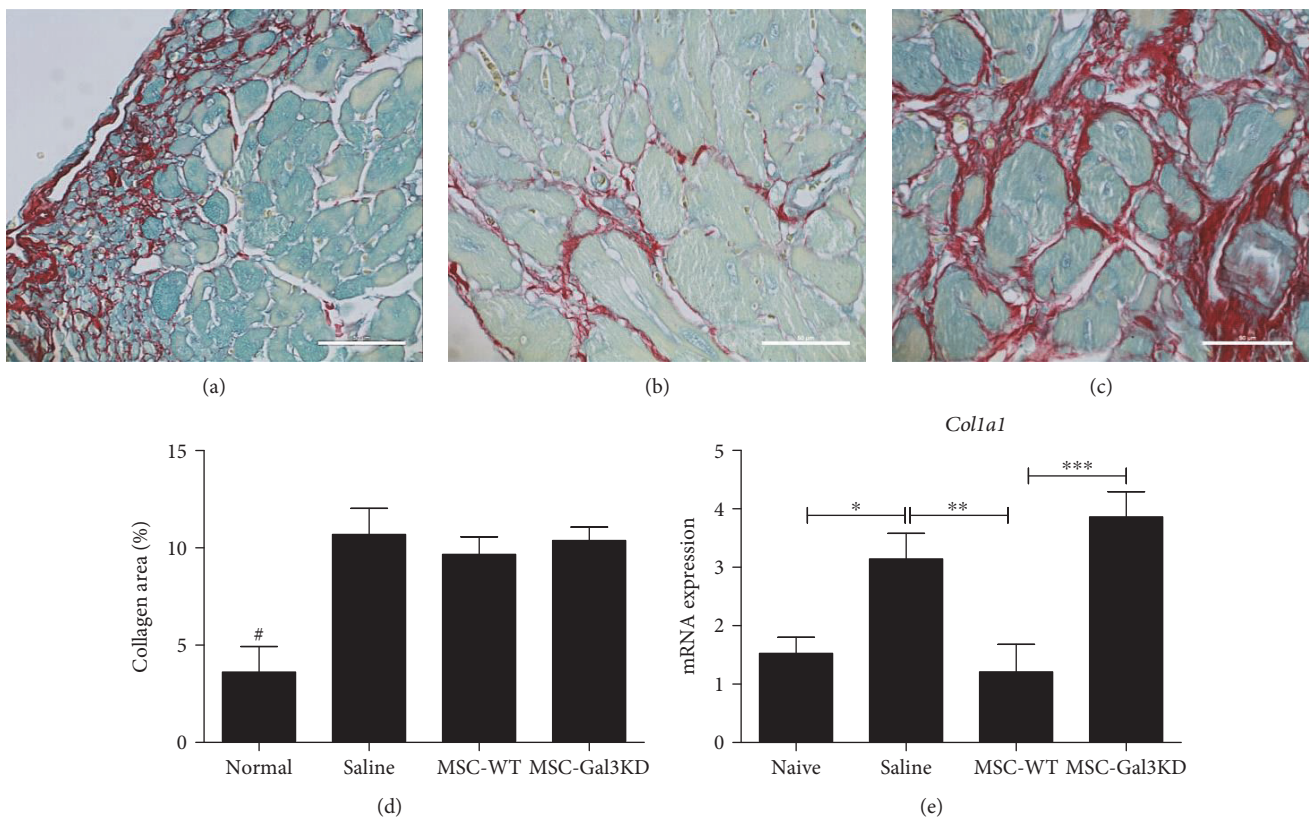


FIGURE 6: Modulation of collagen synthesis in the heart after administration of MSC. Representative images of Sirius red stained heart sections of *T. cruzi* infected mice administered with saline (a), MSC-WT (b), or MSC-Gal3KD (c). (d) Quantification of the collagen-stained area by morphometry. (e) Type I collagen (*Coll1*) gene expression analysis by qRT-PCR in the heart tissue. \* $P < 0.05$ ; \*\* $P < 0.01$ ; \*\*\* $P < 0.001$ ; # $P = 0.01$ , compared to the other groups.

(Figures 8(a), 8(c), and 8(e)). In contrast, *T. cruzi* remained inside the vacuoles in Gal-3 knockdown MSC and were frequently observed destroyed in the following days (Figures 8(b), 8(d), and 8(f)).

#### 4. Discussion

Gal-3 is a multifunctional lectin with diverse, concordant, and occasionally opposing actions, when expressed by

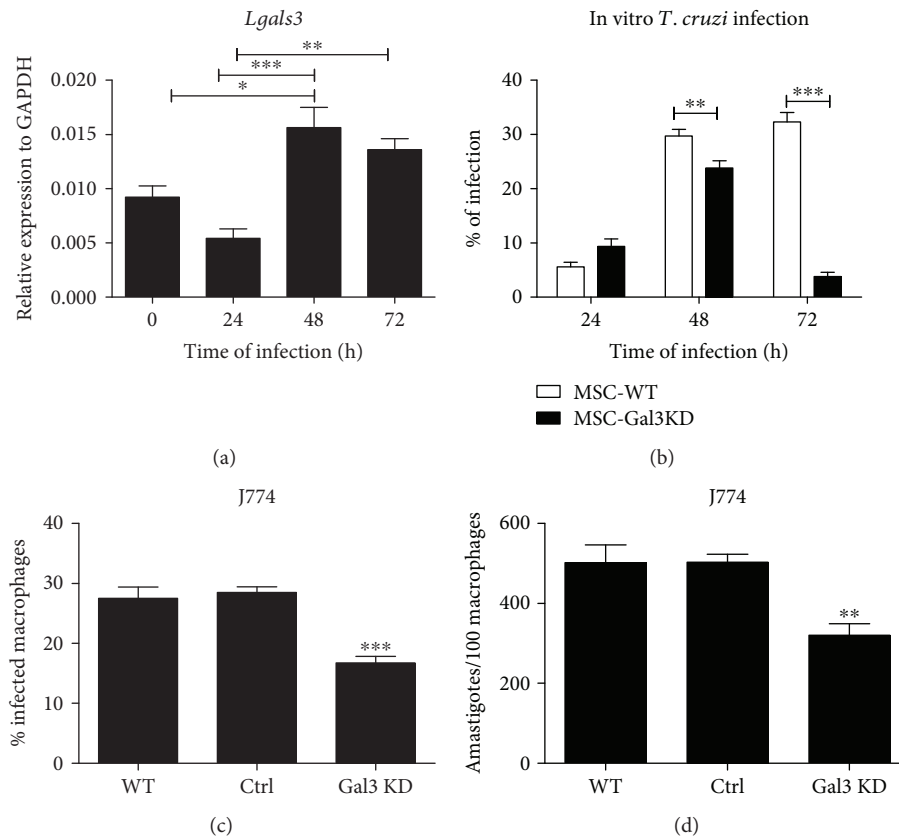


FIGURE 7: Gal-3 knockdown impairs *T. cruzi* infectivity in vitro. (a) Gene expression of Gal-3 is increased 48 h and 72 h after infection of MSC-WT with *T. cruzi*. (b) Percentage of *T. cruzi* infection in MSC-WT and MSC-Gal3KD lines during the first 72 h. (c) Percentage of infection and (d) number of parasites per cell in J774 macrophages nontransduced (WT) or transduced with control vector (Ctrl) or Gal-3 shRNA (Gal3 KD). \* $P < 0.05$ ; \*\* $P < 0.01$ ; \*\*\* $P < 0.001$ .

different cell types and either in extracellular or intracellular compartments [6]. Adhesion, proliferation, and migration are processes that are consistently favored by Gal-3 expression in different cell types, and increased Gal-3 expression play a role in migration and invasion by neoplastic cells [28]. In the present study, we showed that Gal-3 knockdown in MSC was associated with decreased migration and proliferative capacity. These results are in accordance with a recent study using bone marrow-derived MSC obtained from miniature pigs [29]. Here, we showed that Gal-3 plays key roles supporting cell proliferation, migration, and survival, with an impact in therapeutic effects observed after transplantation in a mouse model of chronic Chagas disease cardiomyopathy.

The process of migration and homing of MSC inflammatory sites is still poorly understood and may involve different adhesion molecules, chemokines, and receptors, such as the CXCR4/SDF-1 axis [30]. Gal-3 was recently found to promote migration of MSC through inhibition of RhoA-GTP activity, enhancement of p-AKT (ser473) expression, and regulation of p-Erk1/2 levels [29]. Based on these data and in our findings, it is reasonable to suggest that Gal-3 plays a significant role in MSC migration and homing, which could have several implications in a cell transplantation setting.

In the chronic Chagas disease model, Gal-3 expression by MSC was associated with increased migration from the peritoneal cavity to the spleen. The spleen was also characterized as a reservoir for inflammatory monocytes that emigrate from the subcapsular red pulp and populate inflammatory sites [31]. By reaching the spleen, MSC may be able to exert immunomodulatory actions, with systemic repercussions, as observed previously [32]. Besides regulating lymphocyte populations, MSC also were shown to promote expansion of regulatory populations of monocytes and granulocytes, known as myeloid-derived suppressor cells (MDSC), through HGF secretion [33]. By migrating to heart tissues of *T. cruzi* mice, MDSC were shown to suppress T lymphocytes present in the inflammatory infiltrate [34]. Indeed, i.p.-transplanted MSC showed negligible migration to the heart, but were still able to promote immunomodulation with detectable effects in the heart disease. In mice transplanted with Gal-3 knockdown MSC, however, in which a reduced cell migration to the spleens was observed, inflammation and fibrosis remained at the level of saline controls.

During the chronic phase of Chagas disease cardiomyopathy, different mechanisms are associated with the exacerbated immune response found in the heart, including parasite persistence and autoimmunity [13]. The ability of transplanted MSC to decrease cardiac inflammation in

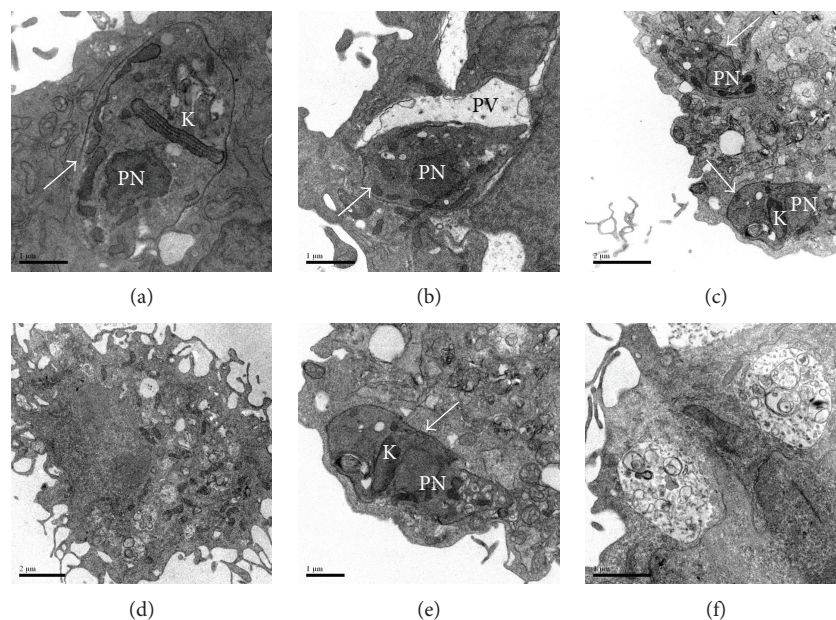


FIGURE 8: Ultrastructural analysis of *T. cruzi* infected MSC. Viable parasites were found in the cytosol of MSC-WT (a) and inside parasitophorous vacuoles of MSC-Gal3KD (b), 24 h after infection. (c and e) Viable parasites are seen in the cytosol of MSC-WT 72 h after infection. (d and f) Absence of viable parasites and presence of large vacuoles containing degraded material in the MSC-Gal3KD 72 h after infection. White arrows = viable parasites; K = kinetoplast; PN = parasite nucleus; PV = parasitophorous vacuole.

experimental *T. cruzi* infected mice was shown before in studies that applied systemic and local delivery routes for cell transplantation [14–16, 35]. Here, we demonstrated that transplanted MSC caused downregulation of inflammatory cytokines directly involved in the disease pathogenesis, such as TNF- $\alpha$  and IFN- $\gamma$  [13]. The immunomodulatory effects observed in the heart tissue were not associated with a high recruitment and homing of MSC to the cardiac tissue, favoring the hypothesis that these cells exert a systemic modulatory action at lymphoid organs such as the spleen, where we did observe migration of MSC. This is corroborated by our finding that Gal-3 knockdown MSC had a significantly lower migration efficiency to the spleen and exerted a lower immunomodulatory action than wild-type MSC.

Regarding parasite persistence, in addition to its presence in the heart, it has been demonstrated that tissues rich in stromal cells, such as the adipose tissue, are reservoirs of *T. cruzi* [13, 36]. A role for MSC as reservoirs for *T. cruzi* in the human disease setting is possible, but has yet to be determined. Here, we show that MSC are efficiently infected by *T. cruzi*, which replicates with time of infection in vitro. Moreover, we found that Gal-3 does not interfere in the invasion process, but it is involved in the further steps of the parasite life cycle. Our data is in accordance with previous work that describes a role for Gal-3 in the step of parasite evasion from the parasitophorous vacuole to the cytosol in macrophages, a critical step for *T. cruzi* life cycle [21].

Gal-3 expression was increased by *T. cruzi* infection in the host cell in the present study, and in previous reports [27]. It has been demonstrated that Gal-3 overexpression induced by infection is important for the parasite cycle, since it can facilitate processes such as adhesion to extracellular matrix, host cell entry, and evasion from parasitophorous

vacuole [20, 37]. However, Gal-3 overexpression induced by *T. cruzi* has been also associated with modulation of different aspects of the antiparasitic immune response, by inhibiting plasma cell differentiation and production of immunoglobulins [22] and promoting the release of immature thymocytes [23]. Whether increased Gal-3 expression by MSC contributes or not to the modulation of immune responses in the acute infection by *T. cruzi* is a question that needs further investigation.

## 5. Conclusion

In conclusion, Gal-3 is involved in the mechanisms of infection by *T. cruzi* and is a mediator of the immunomodulatory actions performed by MSC in a chronic Chagas disease cardiomyopathy model. Gal-3 knockdown decreased MSC survival, migration, and engraftment capabilities, leading to decreased therapeutic effects. Therefore, Gal-3 has the potential to be applied as a predictive biomarker, as part of the quality control on cell preparations to be therapeutically applied, but this merits further investigation.

## Conflicts of Interest

The authors declare that there is no conflict of interest regarding the publication of this paper.

## Acknowledgments

This work was supported by funding from CNPq, FAPESB, and FINEP. The authors would like to thank Dr. Cláudio Pereira Figueira for the technical assistance in the transmission electron microscopy analysis.

## References

- [1] M. Dominici, K. Le Blanc, I. Mueller et al., “Minimal criteria for defining multipotent mesenchymal stromal cells. The International Society for Cellular Therapy position statement,” *Cytotherapy*, vol. 8, no. 4, pp. 315–317, 2006.
- [2] A. J. Friedenstein, R. K. Chailakhjan, and K. S. Lalykina, “The development of fibroblast colonies in monolayer cultures of guinea-pig bone marrow and spleen cells,” *Cell and Tissue Kinetics*, vol. 3, no. 4, pp. 393–403, 1970.
- [3] F. Gao, S. M. Chiu, D. A. Motan et al., “Mesenchymal stem cells and immunomodulation: current status and future prospects,” *Cell Death & Disease*, vol. 7, article e2062, 2016.
- [4] M. Sioud, A. Mobergslie, A. Boudabous, and Y. Fløisand, “Mesenchymal stem cell-mediated T cell suppression occurs through secreted galectins,” *International Journal of Oncology*, vol. 38, no. 2, pp. 385–390, 2011.
- [5] M. Sioud, A. Mobergslie, A. Boudabous, and Y. Fløisand, “Evidence for the involvement of galectin-3 in mesenchymal stem cell suppression of allogeneic T-cell proliferation,” *Scandinavian Journal of Immunology*, vol. 71, no. 4, pp. 267–274, 2010.
- [6] A. Krześlak and A. Lipińska, “Galectin-3 as a multifunctional protein,” *Cellular & Molecular Biology Letters*, vol. 9, no. 2, pp. 305–328, 2004.
- [7] A. C. Mackinnon, M. A. Gibbons, S. L. Farnworth et al., “Regulation of transforming growth factor- $\beta$ 1-driven lung fibrosis by galectin-3,” *American Journal of Respiratory and Critical Care Medicine*, vol. 185, no. 5, pp. 537–546, 2012.
- [8] N. C. Henderson, A. C. Mackinnon, S. L. Farnworth et al., “Galectin-3 regulates myofibroblast activation and hepatic fibrosis,” *Proceedings of the National Academy of Sciences of the United States of America*, vol. 103, no. 13, pp. 5060–5065, 2006.
- [9] M. Kolatsi-Joannou, K. L. Price, P. J. Winyard, and D. A. Long, “Modified citrus pectin reduces galectin-3 expression and disease severity in experimental acute kidney injury,” *PLoS One*, vol. 6, no. 4, article e18683, 2011.
- [10] S. Y. Wan, T. F. Zhang, and Y. Ding, “Galectin-3 enhances proliferation and angiogenesis of endothelial cells differentiated from bone marrow mesenchymal stem cells,” *Transplantation Proceedings*, vol. 43, no. 10, pp. 3933–3938, 2011.
- [11] N. C. Henderson and T. Sethi, “The regulation of inflammation by galectin-3,” *Immunological Reviews*, vol. 230, no. 1, pp. 160–171, 2009.
- [12] M. C. Nunes, W. Dones, C. A. Morillo, J. J. Encina, A. L. Ribeiro, and Council on Chagas Disease of the Interamerican Society of Cardiology, “Chagas disease: an overview of clinical and epidemiological aspects,” *Journal of the American College of Cardiology*, vol. 62, no. 9, pp. 767–776, 2013.
- [13] M. B. Soares, L. Pontes-De-Carvalho, and R. Ribeiro-Dos-Santos, “The pathogenesis of Chagas’ disease: when auto-immune and parasite-specific immune responses meet,” *Anais da Academia Brasileira de Ciências*, vol. 73, no. 4, pp. 547–559, 2001.
- [14] T. F. Larocca, B. S. Souza, C. A. Silva et al., “Transplantation of adipose tissue mesenchymal stem cells in experimental chronic chagasic cardiopathy,” *Arquivos Brasileiros de Cardiologia*, vol. 100, no. 5, pp. 460–468, 2013.
- [15] D. N. Silva, B. S. de Freitas Souza, C. M. Azevedo et al., “Intramyocardial transplantation of cardiac mesenchymal stem cells reduces myocarditis in a model of chronic Chagas disease cardiomyopathy,” *Stem Cell Research & Therapy*, vol. 5, no. 4, p. 81, 2014.
- [16] Jasmin, L. A. Jelicks, H. B. Tanowitz et al., “Molecular imaging, biodistribution and efficacy of mesenchymal bone marrow cell therapy in a mouse model of Chagas disease,” *Microbes and Infection*, vol. 16, no. 11, pp. 923–935, 2014.
- [17] M. B. Soares, R. S. Lima, B. S. Souza et al., “Reversion of gene expression alterations in hearts of mice with chronic chagasic cardiomyopathy after transplantation of bone marrow cells,” *Cell Cycle*, vol. 10, no. 9, pp. 1448–1455, 2011.
- [18] B. S. F. Souza, D. N. Silva, R. H. Carvalho et al., “Association of Cardiac galectin-3 expression, myocarditis, and fibrosis in chronic Chagas disease cardiomyopathy,” *The American Journal of Pathology*, vol. 187, no. 5, pp. 1134–1146, 2017.
- [19] T. N. Moody, J. Ochieng, and F. Villalta, “Novel mechanism that *Trypanosoma cruzi* uses to adhere to the extracellular matrix mediated by human galectin-3,” *FEBS Letters*, vol. 470, no. 3, pp. 305–308, 2000.
- [20] Y. Y. Kleshchenko, T. N. Moody, V. A. Furtak, J. Ochieng, M. F. Lima, and F. Villalta, “Human galectin-3 promotes *Trypanosoma cruzi* adhesion to human coronary artery smooth muscle cells,” *Infection and Immunity*, vol. 72, no. 11, pp. 6717–6721, 2004.
- [21] L. C. Reignault, E. S. Barrias, L. C. Soares Medeiros, W. de Souza, and T. M. de Carvalho, “Structures containing galectin-3 are recruited to the parasitophorous vacuole containing *Trypanosoma cruzi* in mouse peritoneal macrophages,” *Parasitology Research*, vol. 113, no. 6, pp. 2323–2333, 2014.
- [22] E. V. Acosta-Rodríguez, C. L. Montes, C. C. Motrán et al., “Galectin-3 mediates IL-4-induced survival and differentiation of B cells: functional cross-talk and implications during *Trypanosoma cruzi* infection,” *Journal of Immunology*, vol. 172, no. 1, pp. 493–502, 2004.
- [23] E. Silva-Monteiro, L. Reis Lorenzato, O. Kenji Nihei et al., “Altered expression of galectin-3 induces cortical thymocyte depletion and premature exit of immature thymocytes during *Trypanosoma cruzi* infection,” *The American Journal of Pathology*, vol. 170, no. 2, pp. 546–556, 2007.
- [24] M. B. Soares, R. S. de Lima, L. L. Rocha et al., “Gene expression changes associated with myocarditis and fibrosis in hearts of mice with chronic chagasic cardiomyopathy,” *The Journal of Infectious Diseases*, vol. 202, no. 3, pp. 416–426, 2010.
- [25] C. Danella Polli, K. Alves Toledo, L. H. Franco et al., “Monocyte migration driven by galectin-3 occurs through distinct mechanisms involving selective interactions with the extracellular matrix,” *ISRN Inflammation*, vol. 2013, Article ID 259256, 9 pages, 2013.
- [26] X. Gao, V. Balan, G. Tai, and A. Raz, “Galectin-3 induces cell migration via a calcium-sensitive MAPK/ERK1/2 pathway,” *Oncotarget*, vol. 5, no. 8, pp. 2077–2084, 2014.
- [27] T. C. Cardenas, C. A. Johnson, S. Pratap et al., “Regulation of the extracellular matrix interactome by *Trypanosoma cruzi*,” *The Open Parasitology Journal*, vol. 4, pp. 72–76, 2010.
- [28] A. Fortuna-Costa, A. M. Gomes, E. O. Kozłowski, M. P. Stelling, and M. S. Pavão, “Extracellular galectin-3 in tumor progression and metastasis,” *Frontiers in Oncology*, vol. 4, p. 138, 2014.
- [29] Q. Gao, Y. Xia, L. Liu et al., “Galectin-3 enhances migration of miniature pig bone marrow mesenchymal stem cells through inhibition of RhoA-GTP activity,” *Scientific Reports*, vol. 6, article 26577, 2016.


- [30] J. Leibacher and R. Henschler, "Biodistribution, migration and homing of systemically applied mesenchymal stem/stromal cells," *Stem Cell Research & Therapy*, vol. 7, p. 7, 2016.
- [31] F. K. Swirski, M. Nahrendorf, M. Etzrodt et al., "Identification of splenic reservoir monocytes and their deployment to inflammatory sites," *Science*, vol. 325, no. 5940, pp. 612–616, 2009.
- [32] S. A. Acosta, N. Tajiri, J. Hoover, Y. Kaneko, and C. V. Borlongan, "Intravenous bone marrow stem cell grafts preferentially migrate to spleen and abrogate chronic inflammation in stroke," *Stroke*, vol. 46, no. 9, pp. 2616–2627, 2015.
- [33] B. L. Yen, M. L. Yen, P. J. Hsu et al., "Multipotent human mesenchymal stromal cells mediate expansion of myeloid-derived suppressor cells via hepatocyte growth factor/c-met and STAT3," *Stem Cell Reports*, vol. 1, no. 2, pp. 139–151, 2013.
- [34] H. Cuervo, N. A. Guerrero, S. Carbajosa et al., "Myeloid-derived suppressor cells infiltrate the heart in acute *Trypanosoma cruzi* infection," *Journal of Immunology*, vol. 187, no. 5, pp. 2656–2665, 2011.
- [35] D. B. Mello, I. P. Ramos, F. C. Mesquita et al., "Adipose tissue-derived mesenchymal stromal cells protect mice infected with *Trypanosoma cruzi* from cardiac damage through modulation of anti-parasite immunity," *PLoS Neglected Tropical Diseases*, vol. 9, no. 8, article e0003945, 2015.
- [36] A. V. Ferreira, M. Segatto, Z. Menezes et al., "Evidence for *Trypanosoma cruzi* in adipose tissue in human chronic Chagas disease," *Microbes and Infection*, vol. 13, no. 12-13, pp. 1002–1005, 2011.
- [37] F. C. Machado, L. Cruz, A. A. da Silva et al., "Recruitment of galectin-3 during cell invasion and intracellular trafficking of *Trypanosoma cruzi* extracellular amastigotes," *Glycobiology*, vol. 24, no. 2, pp. 179–184, 2014.



## ANEXO II

GONÇALVES, G. V. M; **SILVA, D. N**; CARVALHO, R. H; SOUZA, B. S. F; SILVA, K. N; VASCONCELOS, J. F; PAREDES, B. D; NONAKA, C. K. V; DOS-SANTOS, R. R; SOARES, M. B. P. Generation and characterization of transgenic mouse mesenchymal stem cell lines expressing hIGF-1 or hG-CSF. **Cytotechnology**, v. 70, p. 577-591, 2018.

# Generation and characterization of transgenic mouse mesenchymal stem cell lines expressing *hIGF-1* or *hG-CSF*

Gabrielle V. M. Gonçalves · Daniela N. Silva · Rejane H. Carvalho ·  
Bruno S. F. Souza · Kátia Nunes da Silva · Juliana F. Vasconcelos ·  
Bruno D. Paredes · Carolina K. V. Nonaka · Ricardo Ribeiro-dos-Santos ·  
Milena B. P. Soares 

Received: 21 December 2016 / Accepted: 31 July 2017 / Published online: 2 September 2017  
© Springer Science+Business Media B.V. 2017

**Abstract** Mesenchymal stem cells (MSC) are promising tools in the fields of cell therapy and regenerative medicine. In addition to their differentiation potential, MSC have the ability to secrete bioactive molecules that stimulate tissue regeneration. Thus, the overexpression of cytokines and growth factors may enhance the therapeutic effects of MSC. Here we generated and characterized mouse bone marrow MSC lines overexpressing hG-CSF or hIGF-1. MSC lines overexpressing hG-CSF or hIGF-1 were generated through lentiviral vector mediated gene transfer. The expression of hG-CSF or hIGF-1 genes in the clones produced was quantified by qRT-PCR, and the proteins were detected in the cell supernatants

by ELISA. The cell lines displayed cell surface markers and differentiation potential into adipocytes, osteocytes and chondrocytes similar to the control MSC cell lines, indicating the conservation of their phenotype even after genetic modification. IGF-1 and G-CSF transgenic cells maintained immunosuppressive activity. Finally, we performed a comparative gene expression analysis by qRT-PCR array in the cell lines expressing hIGF-1 and hG-CSF when compared to the control cells. Our results demonstrate that the cell lines generated may be useful tools for cell therapy and are suitable for testing in disease models.

**Keywords** Mesenchymal stem cells · Growth factors · G-CSF · IGF-1

---

G. V. M. Gonçalves · D. N. Silva · R. H. Carvalho ·  
B. S. F. Souza · K. N. da Silva · J. F. Vasconcelos ·  
B. D. Paredes · C. K. V. Nonaka · R. Ribeiro-dos-Santos ·  
M. B. P. Soares  
Center for Biotechnology and Cell Therapy, Hospital São  
Rafael, Salvador, BA 41253-190, Brazil

D. N. Silva · B. S. F. Souza · K. N. da Silva ·  
J. F. Vasconcelos · M. B. P. Soares (✉)  
Gonçalo Moniz Institute, Oswaldo Cruz Foundation  
(FIOCRUZ), Rua Waldemar Falcão, 121, Salvador,  
BA 40296-710, Brazil  
e-mail: milena@bahia.fiocruz.br

B. S. F. Souza · B. D. Paredes · R. Ribeiro-dos-Santos ·  
M. B. P. Soares  
National Institute of Science and Technology for  
Regenerative Medicine, Rio de Janeiro, RJ, Brazil

## Introduction

Mesenchymal stem cells (MSCs) are plastic-adherent stromal cells with a fibroblast-like morphology and the potential to be differentiated into different cell types, both in vitro and in vivo (Friedenstein et al. 1966; Pittenger et al. 1999). MSCs can be easily obtained from different tissues, such as the bone marrow and adipose tissue, being suitable for therapeutic applications, in autologous or allogeneic transplantations. Therapies with MSCs have been extensively studied in animal models and in clinical studies for a variety of

diseases (Wang et al. 2012). In the clinical setting, not only safety and feasibility of MSC-based therapies have been demonstrated, but also different degrees of beneficial effects were reported in different disease scenarios, making MSCs a promising tool for applications in the regenerative medicine field (Kim and Cho 2013).

Most of the therapeutic properties of MSCs have been attributed to the paracrine effects exerted by a plethora of secreted soluble mediators, which modulate biological processes involved in inflammation, fibrosis and angiogenesis (Parekkadan et al. 2007; Caplan and Dennis 2006; Phinney and Prockop 2007). Significant interest has been directed to the immunomodulatory actions of MSCs, which are able to suppress the activation of different immune cells, such as macrophages, dendritic cells and lymphocytes *in vitro* and *in vivo* (Najar et al. 2016; Prockop and Oh 2012; Le Blanc and Mougiakakos 2012).

Among the soluble factors secreted by human MSCs are G-CSF and IGF-1, which are growth factors capable of inducing an array of biological activities, including cell growth, mobilization, proliferation, survival and immunomodulation (Schinköthe et al. 2008; Baraniak and McDevitt 2010).

Previous studies have demonstrated that the secretome and biological properties of MSCs can be affected by the microenvironment to which the cells are exposed (Phinney and Prockop 2007; Wang et al. 2014). Thus, approaches to enhance the therapeutic properties, homing and survival of transplanted MSCs are of great interest in order to improve the efficacy of a cell therapy protocol. In order to achieve this, one possible approach is to enhance growth factor expression and secretion through genetic modification (Wagner et al. 2009). Genetically modified MSCs overexpressing growth factors or presenting increased expression of endogenous proteins can be protected against stress and apoptotic agents thus increasing their survival after transplantation (Wagner et al. 2009). Moreover, through genetic modification, it is possible to sustain the expression of key genes, reducing the influence of detrimental microenvironments.

Considering all the inherent properties of MSCs described above, and the possibility to improve the therapeutic applications already under investigation, the present study aimed at the generation and characterization of MSC lines overexpressing growth factors: IGF-1 or G-CSF. The genetic modification of

MSCs for increased transcription of each factor may contribute directly or indirectly to improve the repair of injured tissues.

## Materials and methods

### Isolation and culture of mouse bone marrow MSCs

Male 4–8 weeks-old EGFP transgenic C57BL/6 mice were used to obtain bone marrow MSCs. Animals were raised and maintained at the animal facility of the Center for Biotechnology and Cell Therapy, Hospital São Rafael (Salvador, Brazil), with access to food and water *ad libitum*. This study was approved by the local ethics committee for animal use at the Hospital São Rafael (CEUA-HSR). Bone marrow cells were obtained from the tibiae and femurs by flushing and were centrifuged at 1500 rpm for 10 min. The pellet was resuspended in 10 ml of Dulbecco's Modified Eagle's Medium (DMEM; Gibco ThermoFisher Scientific, Carlsbad, CA, USA), 10% fetal bovine serum (Gibco ThermoFisher Scientific) and 1% penicillin/streptomycin (Gibco ThermoFisher Scientific) and the cell suspension was cultured in plastic flasks in a humidified incubator at 37 °C with 5% atmospheric CO<sub>2</sub>. After 2 days, the medium was completely changed with fresh media, removing the non-adherent cells. Eight days after isolation, upon reaching 90% confluence, adherent cells were detached by the addition of a trypsin–EDTA (0.25%) solution (Gibco ThermoFisher Scientific). Cultured bone marrow-derived MSCs were maintained in a humidified incubator at 37 °C and atmosphere with 5% CO<sub>2</sub>, under medium replacement every 3 days for expansion and use for generation of different cell lines.

### Lentiviral production

A second-generation lentiviral system was used to produce non-replicative lentiviral particles carrying the genes of interest, *hIGF-1* or *hG-CSF*. The three vectors composing the system were: (1) psPAX2, a packaging plasmid (Addgene, Cambridge, MA, USA, plasmid #12260); (2) pMD2.G, envelope protein expressing plasmid (Addgene plasmid #12259); and (3) pEGIP, expression vector for stable integration of GFP expression cassette with puromycin selection (Addgene plasmid #26777) (Zou et al. 2009). For the

generation of the lentiviral *hIGF-1* or *hG-CSF* expressing vectors, the coding sequences for these genes were amplified by PCR using *pBLAST49-hIGF1A* (Invivogen, San Diego, CA, USA) as template with the following primer sequences: *hIGF1\_BamHI\_F-TAACGGATCCCCGGTCACCATGGGA* AA and *hIGF\_BsrGI\_R-AATCTTGTACAGAGGGTCTTCCTACATCCT*; or *pORF9-hGCSFb* (Invivogen) as template with the oligonucleotides *hG-CSF\_BamHI\_F-TAACGGATCCCTACCTGAGATCACCG* and *hG-CSF\_BsrGI\_R-AATCTTGTACAGATAAATACATGGGATGG*. The amplicons were subcloned into the pEGIP vector in the BamHI/BsrGI GFP flanked region (Fig. 1a). The constructs, called pEGIP\_IGF-1 and pEGIP\_G-CSF, were sequenced with the primers T7-TAATACGACTCACTATAGGG and Overexp\_Seq\_R-ACACCGCCTTATTCCAAG.

Lentiviral particles carrying *hIGF-1* or *hG-CSF* were produced by the transient co-transfection of HEK 293FT cells with PSPAX2, PMD2.G and transfer vector (pEGIP containing, as gene insert, GFP, *GCSF* or *IGF1*) in a proportion of 2:1:3, respectively, by the calcium phosphate method (Tiscornia et al. 2006). Viral titers were estimated by the transduction of HEK293FT cells with dilutions ( $0$ ,  $10^{-1}$ ,  $10^{-2}$  and  $10^{-3}$ ) of a control lentivirus carrying GFP which was generated using the same method, followed by assessment of the percentage of GFP fluorescent HEK293FT cells by flow cytometry 72 h later. The titer was calculated by using a previously described formula:  $\text{titer} = [F \times C^{\circ}/V] \times DF$ , where  $F$  is the frequency of GFP positive cells;  $C^{\circ}$  is the number of cells in the time of infection;  $V$  is the volume of the lentiviral stock used for transduction; and  $DF$  is the dilution factor (White et al. 1999). The titer found for lentivirus carrying GFP gene ( $10^7$  TU/mL) was then

extrapolated for the lentiviral stocks carrying *hG-CSF* and *hIGF-1* genes, and pEGIP control.

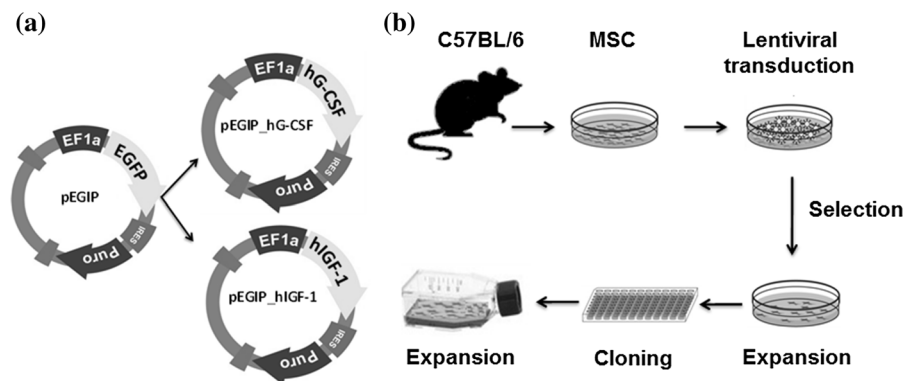
#### Transduction of MSCs

A schematic representation of the process used to generate the transgenic cells is shown in Fig. 1b. The transduction of bone marrow derived MSCs was performed by incubating the cells at passage 8 (80% confluence) for 24 h with the lentiviral stocks at a MOI of 1 of pEGIP, IGF-1 or G-CSF, in the presence of 6  $\mu\text{g/ml}$  polybrene. The efficiency of transduction was 1–10% and was well tolerated by the cells. Culture medium was replaced and cells were cultured for additional 48 h, when 2  $\mu\text{g/ml}$  puromycin (Gibco Thermo Fisher Scientific) was added for selection. Surviving cells were allowed to expand and were then cloned by limiting dilution to generate monoclonal cell lines. The cell lines obtained were expanded for characterization and cryopreserved.

#### Quantitative real-time PCR

Total RNA was extracted from the different MSC cell lines generated in this study using TRIZOL<sup>®</sup> (Thermo Fisher Scientific, Waltham, MA, USA). Quantification of RNA was performed in a spectrophotometer NanoDrop<sup>™</sup> 1000 (Thermo Scientific). The degree of purity concerning the presence of protein contaminants was obtained by calculating the ratio A260 nm: A280 nm, where a ratio between 1.8 and 2.0 is considered a quality indicator. Aliquots of 1  $\mu\text{g}$  of high quality RNA were used for cDNA synthesis using SuperScript III reverse transcriptase after treatment with DNase I, amplification grade according to the manufacturer's protocol. We used primer and probe sets

**Fig. 1** Constructs and experimental design for production of MSC cells transgenic for *hIGF-1* and *hG-CSF*. **a** Design of pEGIP vector and *hIGF-1* and *hG-CSF* constructs. **b** Schematic representation of transgenic MSC lines generation



for the genes of interest (*GCSF*, *IGF1* and *B2m*; Table 1), as well as a customized PCR array assay, all acquired from Thermo Fisher Scientific™. In order to quantify *Nos2* (Mm00440502\_m1), *Ptgs2* (Mm01307329\_m1), *Cxcr4* (Mm01996749\_s1), *Ido1* (Mm00492586\_m1) gene expression, qPCR amplification used Taqman Master Mix and probes (all from ThermoFisher). The detection of *Tnfrsf25* (primerbank ID 6678379a1) gene expression used 5 pmol/μL of primers and SYBR®Green PCR Master Mix. The mean Ct (Cycle threshold) values from triplicate measurements were used to calculate expression of the target gene, normalized with *Gapdh* and *Hprt*. PCR amplification was performed in an ABI7500 Real-Time PCR System (ThermoFisher) under standard thermal cycling conditions. The relative gene expression quantification was calculated using the online app Thermo Fisher Cloud 2.0 and the threshold cycle method of comparative PCR were used to analyse the results (Livak and Schmittgen 2001). Data were analyzed using GraphPad software version 6. The PANTHER (protein annotation through evolutionary relationship) classification system (<http://www.pantherdb.org>) was used to relate the groups according to the gene expression and gene function.

## ELISA

Cell culture supernatants were harvested after 24, 48 or 72 h of culture of the different cell lines and stored at  $-20^{\circ}\text{C}$  until use. The concentrations of hG-CSF and hIGF-1 were quantified using sandwich ELISA kits (R&D Systems, Minneapolis, MN, USA), according to the manufacturer's instructions.

## Flow cytometry analysis

For immunophenotyping, MSC cell lines (P8 after transduction) were trypsinized and resuspended in

0.9% saline solution. The cells ( $5 \times 10^5$ ) were incubated for 30 min with the following antibodies (diluted at 1:100): Sca1-PE-Cy5.5 (Caltag, Buckingham, England), CD45-APC, CD44-PE (BD Biosciences, San Jose, CA, USA), CD29-APC and CD11b-PE (Biolegend, San Diego, CA, USA). Isotype-identical antibodies were used as controls. After incubation, and two PBS washes, the data were acquired and analyzed on the LSRFortessa flow cytometer (BD Biosciences). At least 50,000 events were collected and analyzed.

For cell cycle analysis, cells were harvested from culture flasks by adding Trypsin–EDTA solution (0.25%) (Gibco Thermo Fisher Scientific) and incubating for 5 min at  $37^{\circ}\text{C}$ . Cell suspensions were collected and washed with PBS 1X and centrifuged at  $300 \times g$ . After discarding supernatant, pellets were resuspended in paraformaldehyde (4%) and fixed by 15 min and cells were counted.  $10^6$  cells were collected from samples and were washed with PBS 1X and centrifuged at  $300 \times g$ . Pellets were resuspended in 500 μL PBS 1X and supplemented with RNase A 100 μg/mL (Thermo Scientific), incubated for 20 min at  $37^{\circ}\text{C}$ . Propidium iodide (PI) solution 50 μg/mL (Invitrogen, Carlsbad, CA, USA) was added and incubated for 5 min in room temperature. Cell acquisition was performed in a LSR Fortessa SORP using BD FACS Diva v. 6.5 (BD Biosciences) and data were analyzed using FlowJo VX (Tree Star, Ashland, OR, USA).

## Adipogenic, osteogenic and chondrogenic differentiation

For adipogenic differentiation, cells were cultured in 24-well plates with 13 mm coverslips in complete medium ( $10^4$  cells/well). After reaching 50–60% confluence, the medium was removed and replaced with the adipogenic induction medium StemPro

**Table 1** Oligonucleotide primer sequences

Primers	Sequences 5'–3'	Amplicon (bp)
qPCR-GCSF-F1	CTGGCAGCAGATGGAAGAAGCT	133 pb
qPCR-GCSF-R1	CAGGAAGCTCTGCAGATGGGA	
qPCR-IGF-1_F3	TCTCTTCTACCTGGCGCTGT	134 pb
qPCR-IGF-1_R3	GCTTGTTGAAATAAAAGCCCCTGT	
mmB2M-F	GGTCTTTCTGGTGCTTGTCTCA	115 pb
mmB2M-R	GCAGTTCAGTATGTTTCGGCTTC	

Adipogenesis Differentiation Kit (Gibco Thermo Fisher Scientific). To observe the fatty vacuoles after 14 days in culture, the adipocyte differentiated cells and their controls were fixed in 4% paraformaldehyde and stained with Oil red solution. The images were captured by an AX70 microscope (Olympus, Tokyo, Japan) using ImagePro Plus 7.0 software (Media Cybernetics, Carlsbad, CA, USA). For osteogenic differentiation, the cells were cultured in a specific osteogenic differentiation medium, StemPro Osteogenesis Differentiation Kit (Gibco Thermo Fisher Scientific). Half the differentiation medium was changed every 2 days. Calcium-rich matrix deposition was observed by staining with Alizarin red 2%. For chondrogenic differentiation, cells were cultured for 21 days in standard chondrogenic differentiation medium, StemPro Chondrogenesis Differentiation Kit (Gibco Thermo Fisher Scientific). Proteoglycan synthesis was evaluated after staining with Alcian Blue solution.

#### Lymphocyte proliferation assay

C57BL/6 spleen cell suspensions were prepared in RPMI medium (Gibco Thermo Fisher Scientific) supplemented with 10% fetal bovine serum (Gibco Thermo Fisher Scientific). Mouse splenocytes were cultured in 96-well plates at  $8 \times 10^5$  cells/well, in a final volume of 200  $\mu$ l, in triplicate, in the presence of Dynabeads<sup>®</sup> mouse T-activator CD3/CD28 (bead to cell ratio = 1:1; ThermoFisher Scientific), in the absence or presence of mitomycin-treated MSCs, at different ratios (MSC:splenocytes 1:1, 1:10, 1:100, 1:1000). After 48 h of incubation, plates were pulsed with 1  $\mu$ Ci of methyl-<sup>3</sup>H-thymidine (PerkinElmer, Amersham, Little Chalfont, England) for 18 h. Cell proliferation was assessed by measurement of <sup>3</sup>H-thymidine uptake using a  $\beta$ -plate counter. The inhibition of spleen cell proliferation was determined in relation to controls stimulated by antiCD3/CD28 in absence of MSCs.

#### Wound healing assay

Cell migration was evaluated by an in vitro scratch assay. The cells were passaged, plated on 6-wells plates, and cultured until a confluent monolayer was formed. Then, the scratch was performed by scraping the cell monolayer in a straight line, using a p200 pipet

tip. Medium was exchanged and the cells were incubated overnight. Distance between the edges was evaluated by measuring 100 points for each well in two time points: after performing the scratch and after overnight incubation. The assay was performed in triplicates, and the experiment repeated three times. Results are represented as gap distance variation, established by the subtraction of the mean distance values obtained at timepoint 0 by the values obtained after overnight incubation.

#### Statistical analysis

The results of the experiments were analyzed and continuous variables are presented as mean  $\pm$  SEM. Parametric data were analyzed using Student's *t* test for comparisons between two groups and 1-way ANOVA, followed by Bonferroni post hoc test for multiple-comparison test, using Prism 6.0 (GraphPad Software). *p* values <0.05 were considered statistically significant.

## Results

### Generation of transgenic MSC lines producing hIGF-1 or hG-CSF

Mouse bone marrow-derived MSC lines were transduced with vectors carrying hIGF-1, hG-CSF or GFP control vector (pEGIP), after the culture reached confluency (Fig. 2a). The transduction was well tolerated by the cells, and the puromycin selection step was initiated, leading to complete lethality in non-transduced wells, but survival and appearance of clusters of resistant cells in transduced wells (Figs. 2b–d). The morphology of the transduced and selected cells is shown (Figs. 2e–g). The cell lines generated were assessed by PCR for the expression of the genes of interest. Three clones transgenic for hIGF-1 and two transgenic for hG-CSF were analyzed, confirming the expression of the respective genes (Fig. 3a). As expected, control cell lines—pEGIP transduced and parental MSC lines—did not express the human genes. In order to evaluate the expression levels of the transgenes among the different clones, we performed gene expression analysis by RT-qPCR, which showed that clones IGF-1#1 and G-CSF#2 had the highest gene expression levels

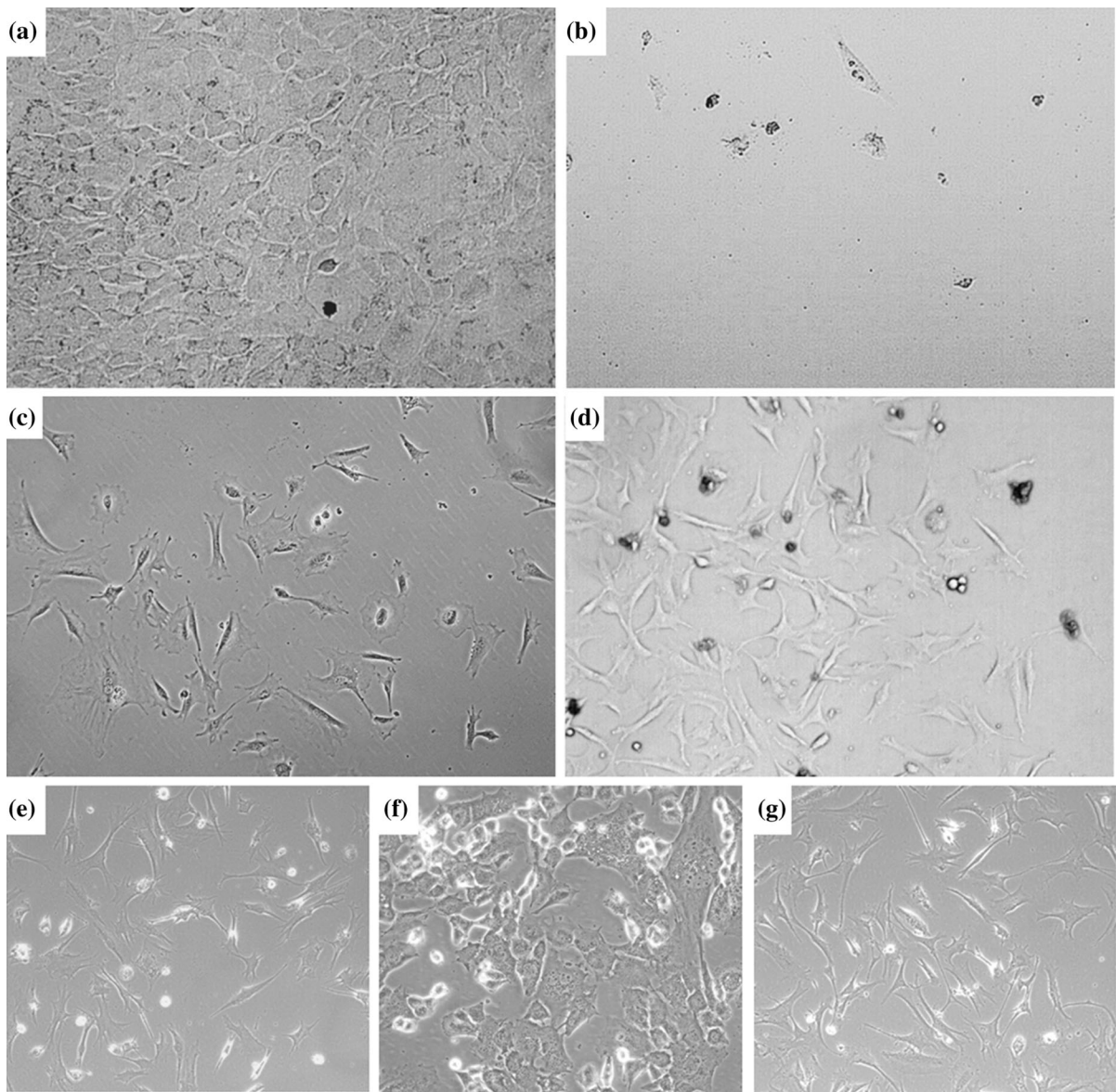


**Fig. 2** Transduction, antibiotic selection and establishment of stable cell cultures. Phase contrast images of the cell culture, showing **a** morphology of MSC before transduction, and after puromycin selection of cells **b** mock-transduced, or transduced

(Fig. 3b). To demonstrate the production of the recombinant proteins, cell culture supernatants were harvested at different time points and assayed by ELISA. Increasing concentrations of hG-CSF were detected in the two G-CSF clones tested (Fig. 3c). Similarly, the three IGF-1 transgenic clones produced hIGF-1. Based on the gene expression analyses, lines IGF-1#1 and G-CSF#2 were selected for further evaluation.

with **c** hIFG-1 and **d** hG-CSF lentiviral vectors, showing clusters of surviving cells. Morphology of expanded cell lines of MSC transduced with **e** hG-CSF, **f** hIGF-1 lentivirus, or **g** control MSC. Magnification = 100× (A, D, E, G) and 200× (B, C, F)

#### Characterization of transgenic MSC lines

Parental and transduced MSC cell lines were submitted to immunophenotype analysis in order to compare the expression levels of cell markers. Similar to the parental MSCs, IGF-1 and G-CSF transgenic MSCs, as well as the pEGIP control, showed high expression of MSC markers, Sca-1, CD29 and CD44, while displaying a low expression of the hematopoietic cell

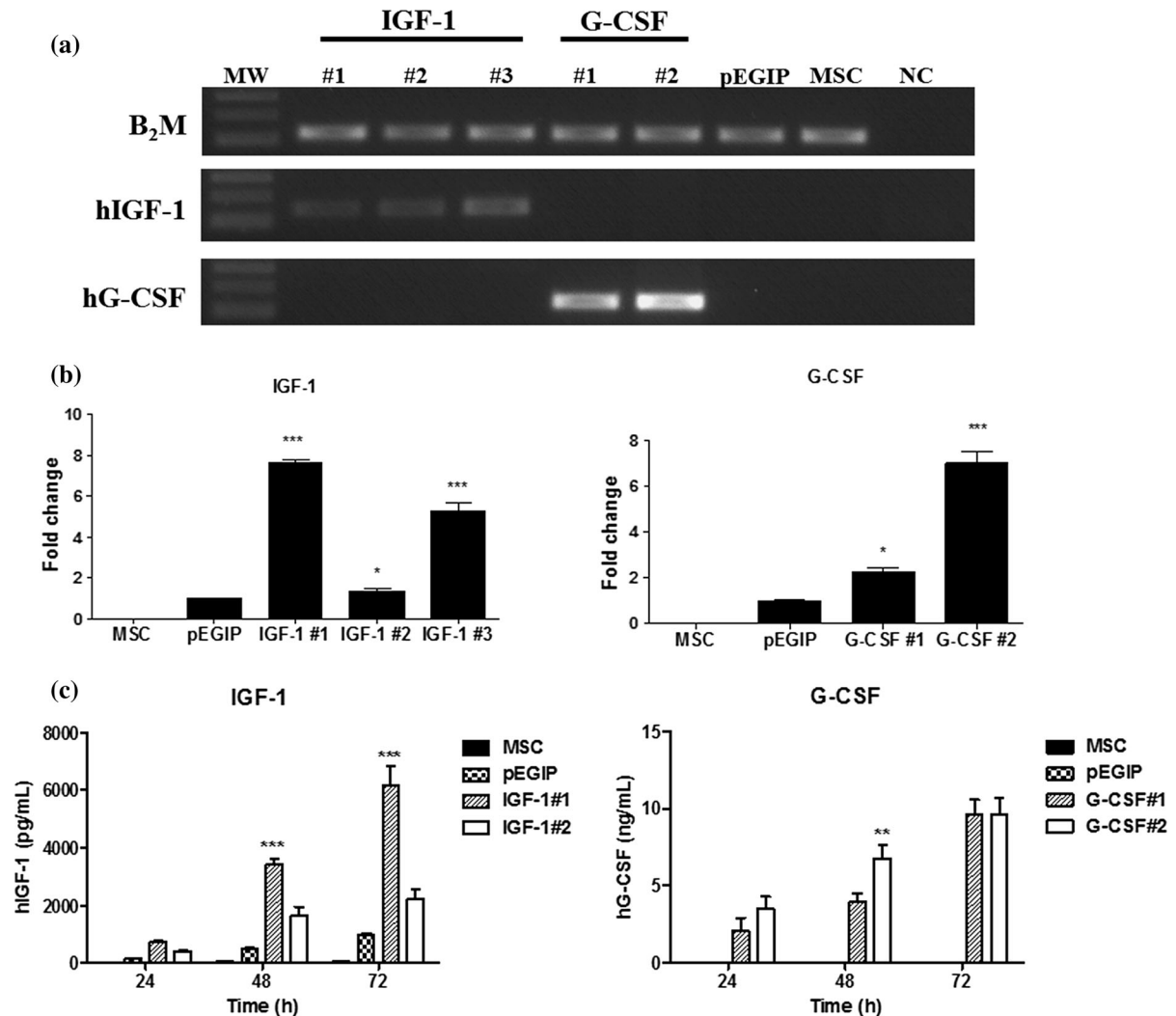


**Fig. 3** Gene and protein expression for hIGF-1 and hG-CSF by transduced MSC cell lines. **a** Amplification of hIGF-1 and hG-CSF transcripts in three IGF-1 clones and two G-CSF clones, respectively. Control pEGIP-transduced and non-transduced MSC did not express the transgenes. NC = negative control. **b** RT-qPCR showing the expression levels of hIGF-1 and hG-CSF genes. **c** Assessment of protein expression in the cell

supernatants of the different MSC lines, 24, 48 and 72 h, by ELISA. Values represent mean  $\pm$  SEM. \*Significantly different from the other groups ( $p < 0.05$ ); \*\*significantly different from G-CSF#1 group ( $p < 0.01$ ); \*\*\*significantly different from the other groups ( $p < 0.001$ ). Two-way ANOVA followed by Bonferroni's test

markers CD45 and CD11b (Table 2). The plasticity of the MSC lines was also investigated, by the induction of adipogenic, osteogenic and chondrogenic differentiation with specific culture media. Transgenic MSCs for hG-CSF and hIGF-1 differentiated into all three lineages, similarly to the parental MSC line (Fig. 4).

When the proliferation rate was evaluated, we found that expression of hIGF-1 transgenic MSC increased proliferation, when compared to the parental MSC line. In contrast, expression of hG-CSF did not

alter cell proliferation (Fig. 5a). Cell cycle analysis by flow cytometry showed that hIGF-1, but not hG-CSF producing MSC lines, had higher percentage of cells in the S and G2/M phase, when compared to the parental MSCs (Fig. 5b).

To investigate whether the transgenic MSCs retained their immunosuppressive capacity, co-cultures of mitogen-stimulated mouse splenocytes and irradiated MSCs were performed. Similar to the parental MSC, the transduced MSC lines hIGF-1, hG-CSF and



**Table 2** Flow cytometry analysis of cell surface markers in MSC lines

Cell marker	MSC	pEGIP	IGF-1	G-CSF
CD44	99.50 ± 0.50	99.50 ± 0.70	89.95 ± 1.67	93.90 ± 6.08
Sca-1	92.20 ± 2.40	98.20 ± 0.98	95.10 ± 6.08	93.15 ± 70.0
CD29	98.20 ± 1.60	99.50 ± 0.50	97.30 ± 3.39	94.5 ± 5.93
CD45	1.50 ± 0.05	0.05 ± 0.07	2.65 ± 3.04	1.05 ± 0.63
CD11b	0.70 ± 0.30	0.75 ± 0.91	1.25 ± 1.76	1.25 ± 0.21

The values represent the mean percentage ± standard deviation of two experiments

pEGIP control caused a concentration-dependent inhibition of lymphocyte proliferation (Fig. 6). The hIGF-1 transduced MSC line, however, had a less potent immunosuppressive capacity than wild-type MSC (Fig. 6). Analysis by RT-qPCR of factors related to immunosuppressive activity, such as COX2 and TSG6, showed no difference between the groups, whereas IDO and iNOS gene expression were undetectable (data not shown).

We next evaluated the expression of CXCR4, a chemokine receptor involved in migration of MSCs, and the migration potential in vitro of the MSC cell lines. As shown in Fig. 7a, hIGF-1, but not hG-CSF transduced MSCs, had increased gene expression of CXCR4 when compared to control MSCs. We performed a wound healing assay in vitro. As shown in Fig. 7b, hIGF-1 and hG-CSF transduced MSCs had similar migration potential when compared to control MSCs.

#### Gene expression analysis

A RT-qPCR array was performed in order to evaluate whether the expression of hIGF-1 and hG-CSF caused alterations on the transcription of genes. Expression of either one of the growth factors caused the upregulation and down regulation of gene transcription when compared to pEGIP control cells (Fig. 8a). The pattern of gene regulation was different when IGF-1 and G-CSF producing cells were compared. However, the main biological categories of the altered genes were similar when the two cell lines were compared: biological regulation, response to stimulus, and apoptotic, cellular, developmental, immune system and metabolism processes (Fig. 8b).

#### Discussion

Genetic modification of MSCs is a strategy currently being investigated as a means to combine gene and cell therapy for regenerative medicine (Porada et al. 2013). A number of techniques have been tested, including several viral vectors, such as adenovirus, lentivirus and retrovirus, as well as other non-viral methods (Reiser et al. 2005). In the present study, we have successfully generated MSC cell lines expressing two growth factors of interest, G-CSF and IGF-1, using lentiviral vectors. The cells obtained were able to produce the growth factors of interest, and maintained the main properties of MSCs, such as immunophenotype, differentiation potential and immunosuppressive activity.

The use of lentiviral vectors, such as the ones used in our work, to achieve high levels of transgene expression without impairing the mesenchymal cell properties was also found to be highly efficient in a previous report (McGinley et al. 2016). Nonetheless, it raises concerns regarding safety associated with the use of viral transduction. This has led to the development of alternative non-viral methods for gene delivery, with higher efficiency and stability (Reiser et al. 2005). Addition of suicide genes in integrating vectors, besides the therapeutic gene, to ensure elimination of cells when desired during the course of a treatment is also being investigated (Nouri et al. 2015). This may be of great relevance when factors capable of increasing cell proliferation are used, in order to control the proliferation of the transgenic MSCs, as well as adjacent cells, when transplanted in vivo. We found here that overexpression of IGF-1 caused an increase in cell proliferation. Although this

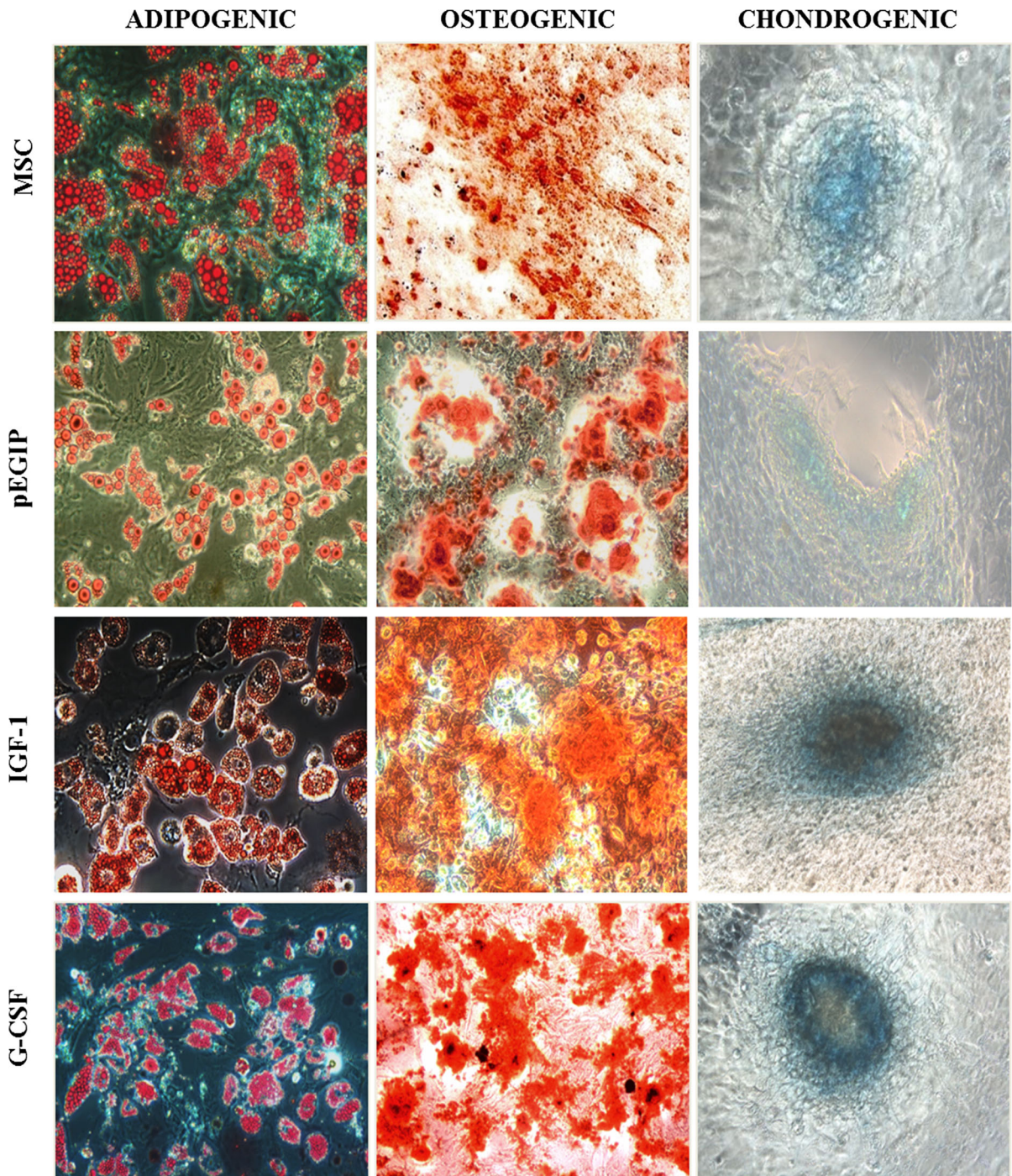


**Fig. 4** Differentiation potential of MSC lines. MSC transgenic for IGF-1 and G-CSF and pEGIP control MSC were incubated for 15 days in the presence of specific media for the induction of adipogenic, osteogenic and chondrogenic differentiation. Cell differentiation was confirmed by positive staining with Oil red

for adipocytes, Alizarin red for osteocytes and Alcian blue for chondrocytes. Adipogenic and osteogenic differentiation magnification: 200 $\times$ . Chondrogenic differentiation magnification: 100 $\times$

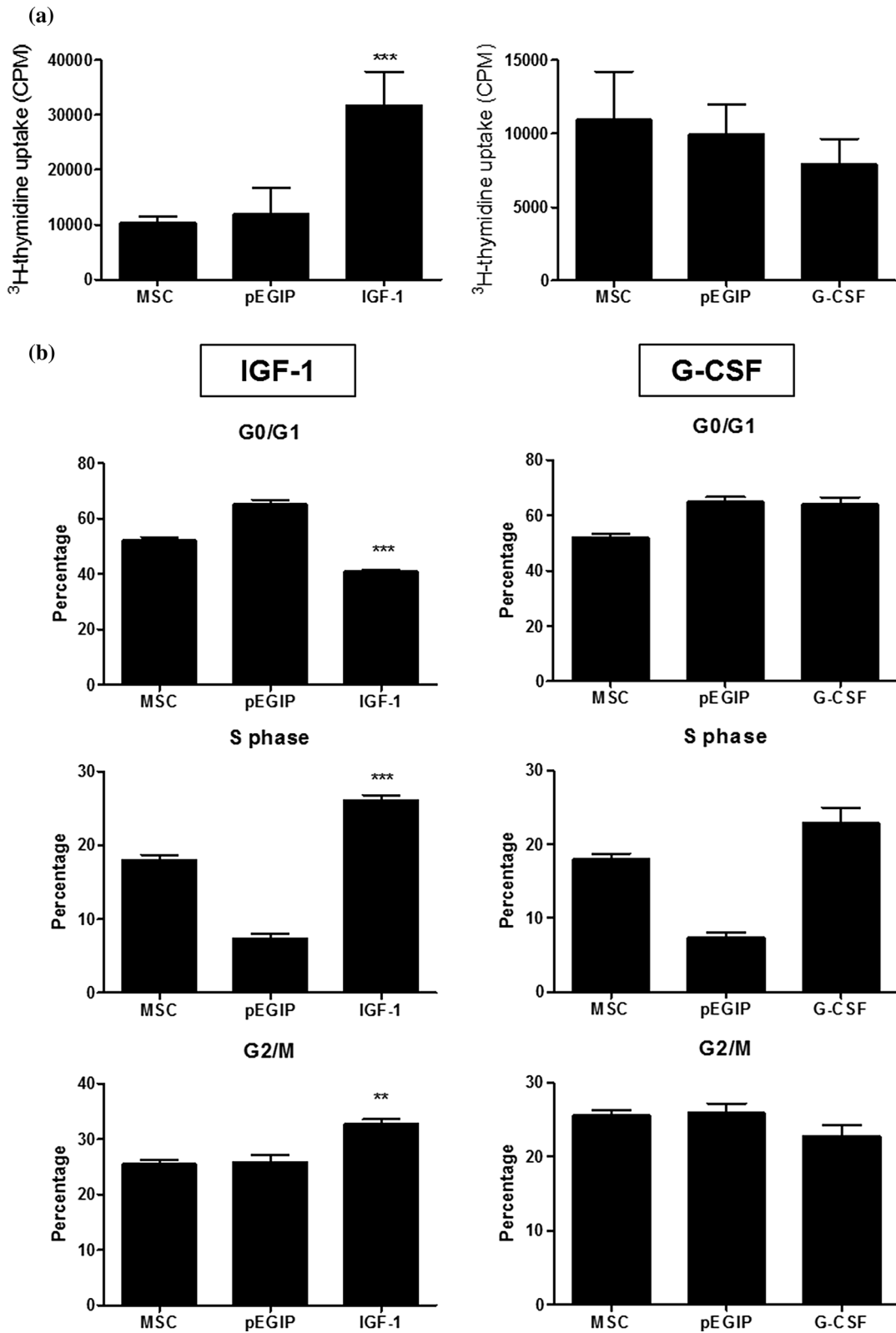


**Fig. 5** Proliferation and cell cycle analysis of MSC lines. **a** Wild type, pEGIP, IFG-1 or G-CSF MSCs were incubated for 2 days in complete culture medium. Assessment of cell proliferation was done by adding  $^3\text{H}$ -thymidine for 18 h followed by quantification of  $^3\text{H}$ -thymidine uptake. Values represent the mean  $\pm$  SEM of triplicate in one representative experiment of two performed. **b** Cell cycle analysis of IFG-1 or G-CSF transgenic MSC lines was done by flow cytometry after PI staining. **\*\*** $p < 0.01$  compared to the other groups. **\*\*\*** $p < 0.001$  compared to the other groups

may be a desirable feature to increase the MSCs when applied into a lesion site, IGF-1 has been associated with cancer development (Yu and Rohan 2000), and therefore any attempt to investigate the therapeutic application of IGF-1 overexpressing MSCs should be performed in a controlled manner in order to assess and ensure safety.

Aiming at improving the use of MSCs in various forms of therapy on the regeneration of damaged

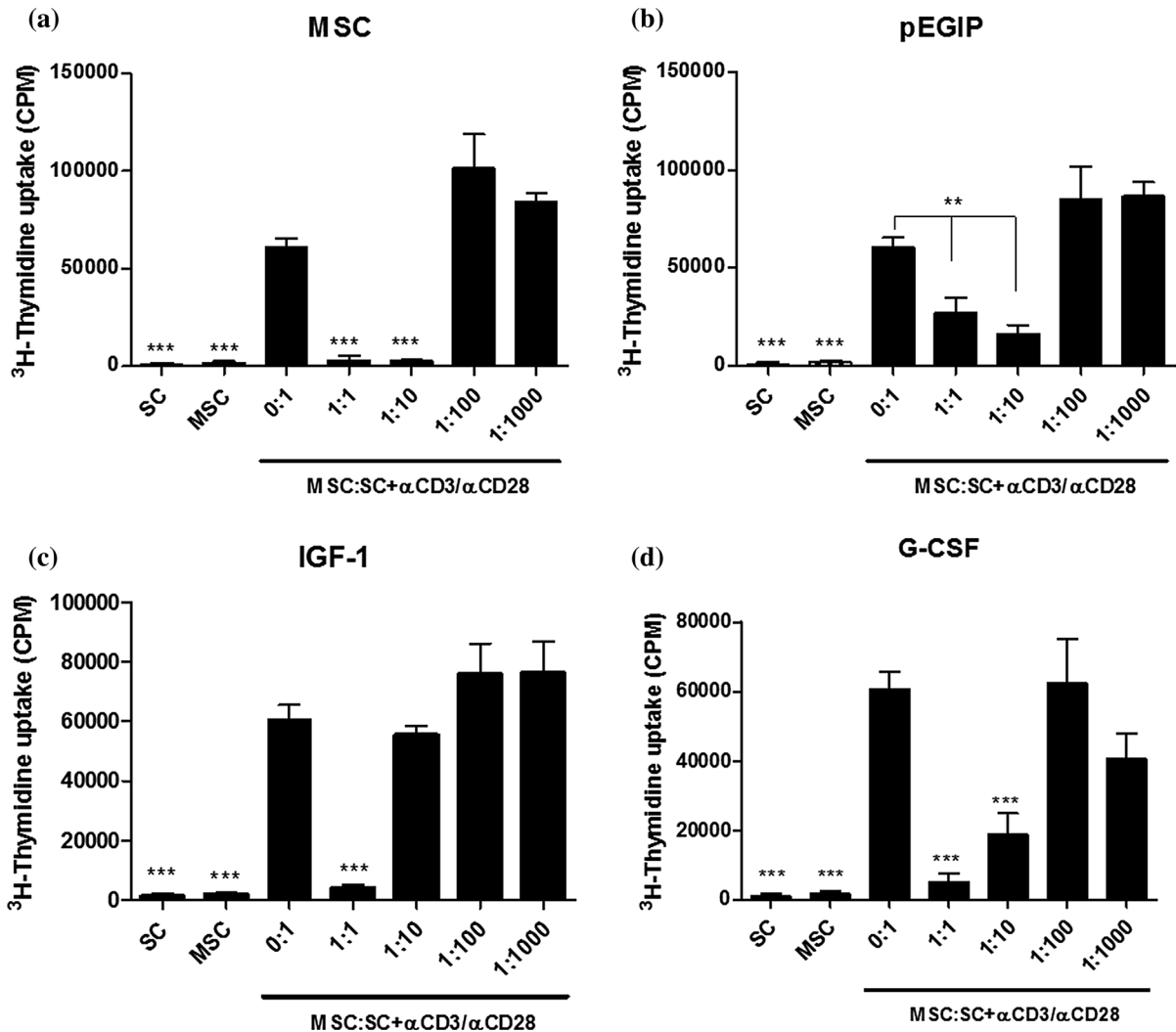


**Fig. 6** In vitro immunomodulatory activity of MSC lines. Mouse splenocytes were cultured without (SC) or with  $\alpha\text{CD3}/\alpha\text{CD28}$ , in the absence (MSC:SC 0:1) or in the presence of irradiated wild-type, pEGIP, IGF-1 or G-CSF MSCs at different ratios (MSC:SC 0:1, 1:1, 1:10, 1:100 and 1:1000). On day 3,  $^3\text{H}$ -thymidine was added for 18 h, followed by quantification of  $^3\text{H}$ -

thymidine uptake for the assessment of spleen cell proliferation. Mouse splenocytes (SC) and mesenchymal stem cells (MSC) cultured without (SC)  $\alpha\text{CD3}/\alpha\text{CD28}$  were used as negative controls. Values represent the mean  $\pm$  SEM of 8 determinations in two experiments performed. **\*\*** $p < 0.01$ ; **\*\*\*** $p < 0.001$  compared to MSC:SC 0.1

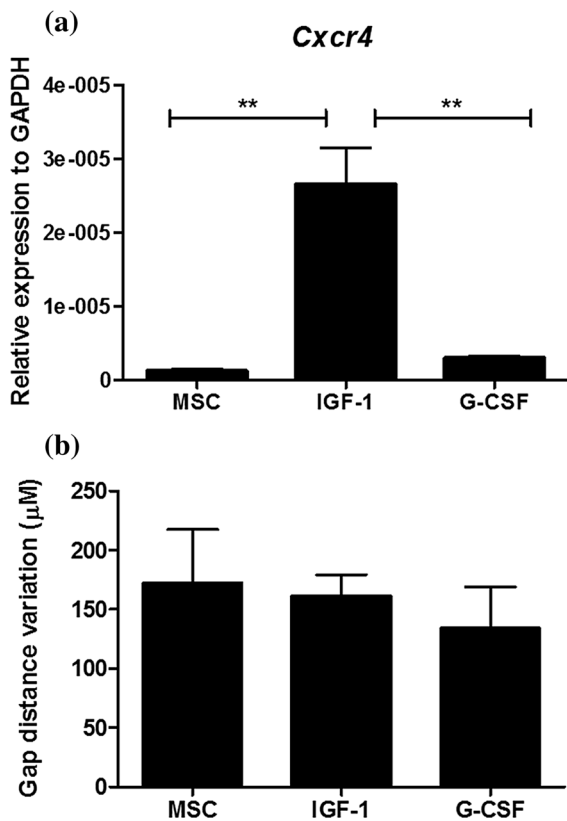


**Fig. 7** *Cxcr4* expression and migration analysis. **a** *Cxcr4* expression profile by qRT-PCR. The mRNA level of each cell line was quantified by qRT-PCR in triplicate for each gene. *Gapdh* and *Hprt* were amplified as internal controls. Data are represented as the mean  $\pm$  SEM (n = 3), two-way ANOVA followed by Bonferroni post-test. \*Statistically significant  $p < 0.05$  compared with control. **b** Wound healing assay showing migration ability of MSC lines

tissues and organs, we generated MSC cell lines expressing G-CSF and IGF-1. Several reports have shown the potential therapeutic use of G-CSF in regenerative medicine, including cardiac (Harada et al. 2005; Ieishi et al. 2007; Macambira et al. 2009), neurological (Huang and Tsai 2014; Guo et al. 2015) and hepatic diseases (Yang et al. 2016). The immunomodulatory potential of G-CSF suggests that transgenic MSC expressing this growth factor may also contribute to the modulation of inflammation at the site of transplantation. IGF-1 was shown to exert beneficial effects on the regeneration of cartilage

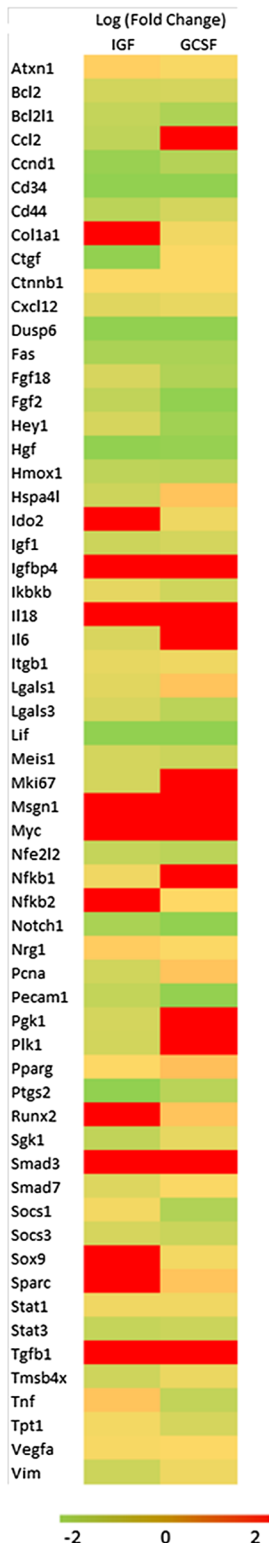
**Fig. 8** Gene expression analysis by RT-qPCR. **a** Heat map representation of relative expression of 60 genes (red, high; green, low), identified by RT-qPCR array analysis in IGF-1 and G-CSF cell lines and pEGIP (control). **b** The pie chart shows the percentage of significantly differentially expressed genes classified according to their involvement in biological process (PANTHER classification system). (Color figure online)

(Schmidt et al. 2006), nervous (Lunn et al. 2015) and skeletal muscle (Song et al. 2013), being a key promoter of cell proliferation. Further studies are needed to address whether the genetically modified cells generated in our study have a better therapeutic efficacy than wild-type cells, and to which diseases they may potentially be applied.

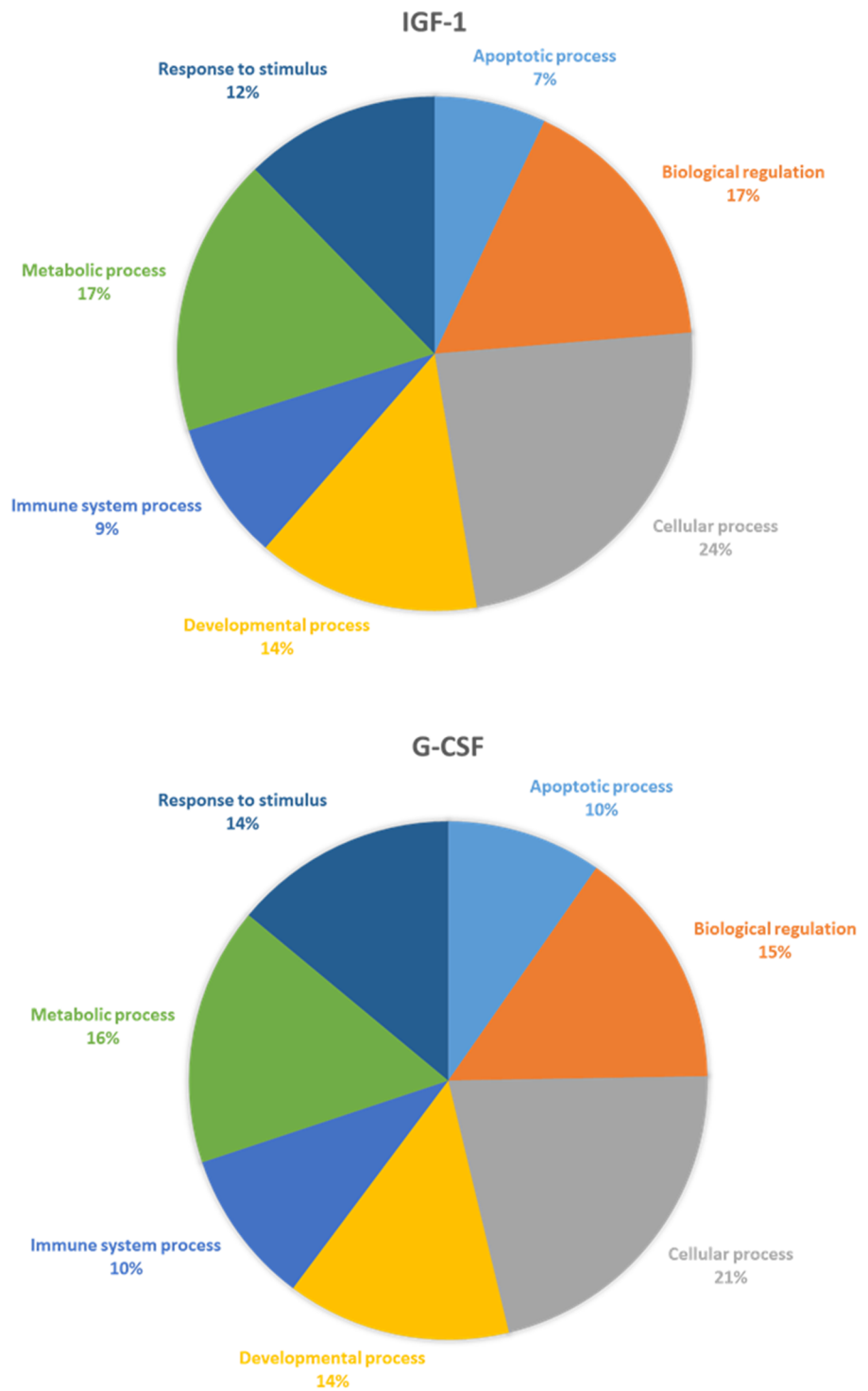
The gene expression analysis performed in our study indicates that increased production of either one of the two growth factors studied here causes alterations on the expression of several genes. MSCs express receptors for G-CSF and IGF-1 (Ponte et al. 2012; Tomasoni et al. 2013), and thus an autocrine action of the transgenic growth factors produced by the engineered MSC may trigger intracellular signaling pathways, leading to gene modulation and possibly alteration of the therapeutic properties of the cells. Since the expression of growth factors alters gene expression profile of MSCs, it is possible that, in addition to the transgene, the secretion of other factors may contribute for any improved beneficial effects of the engineered MSC line.

IGF-1 has been shown to induce the expression of chemokine receptor CXCR4, and its ligand, SDF-1 (Huang et al. 2012; Haider et al. 2008). The role of IGF-1 in promoting the recruitment of stem cells through the CXCR4-SDF-1 axis has been shown in different experimental settings (Huang et al. 2012; Haider et al. 2008; Xinaris et al. 2013; Zhu et al. 2015). Here we showed that IGF-1-overexpressing MSCs have an increased expression of CXCR4. The fact that in the cell migration assay tested there were no differences in cell migration when the IGF-1-MSCs were compared to wild-type MSCs may be due to limitations in the wound scar formation assay used. Further studies are required in order to show whether the IGF-1-transduced cells have an increased migration potential in disease settings.

(a)



(b)



## Conclusion

In conclusion, we generated MSC lines producing high amounts of *hIGF-1* or *hG-CSF*, while maintaining important features of mesenchymal cells. The fact that these cells are positive for GFP will facilitate their tracking in animal models of diseases, and determining if the expression of the growth factor contributes to its increased survival and proliferation *in vivo*, in addition to affecting their therapeutic properties.

**Acknowledgements** This work was supported by The National Council for Scientific and Technological Development (CNPq), The Foundation of Support for Research of the State of Bahia (FAPESB), and Funding Authority for Studies and Projects (FINEP).

## References

- Baraniak PR, McDevitt TC (2010) Stem cell paracrine actions and tissue regeneration. *Regen Med* 5:121–143. doi:[10.2217/rme.09.74](https://doi.org/10.2217/rme.09.74)
- Caplan AI, Dennis JE (2006) Mesenchymal stem cells as trophic mediators. *J Cell Biochem* 98:1076–1084. doi:[10.1002/jcb.20886](https://doi.org/10.1002/jcb.20886)
- Friedenstein AJ, Piatetzky-Shapiro II et al (1966) Osteogenesis in transplants of bone marrow cells. *J Embryol Exp Morphol* 16:381–390
- Guo Y, Liu S et al (2015) G-CSF promotes autophagy and reduces neural tissue damage after spinal cord injury in mice. *Lab Invest* 95:1439–1449. doi:[10.1038/labinvest.2015.120](https://doi.org/10.1038/labinvest.2015.120)
- Haider HKH, Jiang S et al (2008) IGF-1-overexpressing mesenchymal stem cells accelerate bone marrow stem cell mobilization via paracrine activation of SDF-1 $\alpha$ /CXCR4 signaling to promote myocardial repair. *Circ Res* 103:1300–1308
- Harada M, Qin Y et al (2005) G-CSF prevents cardiac remodeling after myocardial infarction by activating the Jak-Stat pathway in cardiomyocytes. *Nat Med* 11:305–311. doi:[10.1038/nm1199](https://doi.org/10.1038/nm1199)
- Huang SP, Tsai RK (2014) Efficacy of granulocyte-colony stimulating factor treatment in a rat model of anterior ischemic optic neuropathy. *Neural Regen Res* 9:1502–1505. doi:[10.4103/1673-5374.139472](https://doi.org/10.4103/1673-5374.139472)
- Huang YL, Qiu RF et al (2012) Effects of insulin-like growth factor-1 on the properties of mesenchymal stem cells *in vitro*. *J Zhejiang Univ Sci B* 13:20–28
- Ieishi K, Nomura M et al (2007) The effect of G-CSF in a myocardial ischemia reperfusion model rat. *J Med Invest* 54:177–183
- Kim N, Cho SG (2013) Clinical applications of mesenchymal stem cells. *Korean J Intern Med* 28:387–402. doi:[10.3904/kjim.2013.28.4.387](https://doi.org/10.3904/kjim.2013.28.4.387)
- Le Blanc K, Mougiakakos D (2012) Multipotent mesenchymal stromal cells and the innate immune system. *Nat Rev Immunol* 12:383–396. doi:[10.1038/nri3209](https://doi.org/10.1038/nri3209)
- Livak KJ, Schmittgen TD (2001) Analysis of relative gene expression data using real-time quantitative PCR and the 2 $(-\Delta\Delta C(T))$  method. *Methods* 25:402–408. doi:[10.1006/meth.2001.1262](https://doi.org/10.1006/meth.2001.1262)
- Lunn JS, Sakowski SA et al (2015) Autocrine production of IGF-I increases stem cell-mediated neuroprotection. *Stem Cells* 33:1480–1489. doi:[10.1002/stem.1933](https://doi.org/10.1002/stem.1933)
- Macambira SG, Vasconcelos JF et al (2009) Granulocyte colony-stimulating factor treatment in chronic Chagas disease: preservation and improvement of cardiac structure and function. *FASEB J* 23:3843–3850. doi:[10.1096/fj.09-137869](https://doi.org/10.1096/fj.09-137869)
- McGinley LM, Sims E et al (2016) Human cortical neural stem cells expressing insulin-like growth factor-I: a novel cellular therapy for Alzheimer's disease. *Stem Cells Transl Med* 5:379–391. doi:[10.5966/sctm.2015-0103](https://doi.org/10.5966/sctm.2015-0103)
- Najar M, Raicevic G et al (2016) The immunomodulatory potential of mesenchymal stromal cells: a story of a regulatory network. *J Immunother* 39:45–59. doi:[10.1097/CJI.000000000000108](https://doi.org/10.1097/CJI.000000000000108)
- Nouri FS, Wang X et al (2015) Genetically engineered therapeutic mesenchymal stem cells for the evaluation of the anticancer efficacy of enzyme/prodrug systems. *J Control Release* 200:179–187. doi:[10.1016/j.jconrel.2015.01.003](https://doi.org/10.1016/j.jconrel.2015.01.003)
- Parekkadan B, van Poll D et al (2007) Mesenchymal stem cell-derived molecules reverse fulminant hepatic failure. *PLoS ONE* 2:e941. doi:[10.1371/journal.pone.0000941](https://doi.org/10.1371/journal.pone.0000941)
- Phinney DG, Prockop DJ (2007) Concise review: mesenchymal stem/multipotent stromal cells: the state of transdifferentiation and modes of tissue repair—current views. *Stem Cells* 25:2896–2902. doi:[10.1634/stemcells.2007-0637](https://doi.org/10.1634/stemcells.2007-0637)
- Pittenger MF, Mackay AM et al (1999) Multilineage potential of adult human mesenchymal stem cells. *Science* 284:143–147
- Ponte AL, Ribeiro-Fleury T et al (2012) Granulocyte-colony-stimulating factor stimulation of bone marrow mesenchymal stromal cells promotes CD34+ cell migration via a matrix metalloproteinase-2-dependent mechanism. *Stem Cells Dev* 21:3162–3172. doi:[10.1089/scd.2012.0048](https://doi.org/10.1089/scd.2012.0048)
- Porada CD, Stem C et al (2013) Gene therapy: the promise of a permanent cure. *N C Med J* 74:526–529
- Prockop DJ, Oh JY (2012) Mesenchymal stem/stromal cells (MSCs): role as guardians of inflammation. *Mol Ther* 20:14–20. doi:[10.1038/mt.2011.211](https://doi.org/10.1038/mt.2011.211)
- Reiser J, Zhang XY et al (2005) Potential of mesenchymal stem cells in gene therapy approaches for inherited and acquired diseases. *Expert Opin Biol Ther* 5:1571–1584. doi:[10.1517/14712598.5.12.1571](https://doi.org/10.1517/14712598.5.12.1571)
- Schinköthe T, Bloch W et al (2008) *In vitro* secreting profile of human mesenchymal stem cells. *Stem Cells Dev* 17:199–206. doi:[10.1089/scd.2007.0175](https://doi.org/10.1089/scd.2007.0175)
- Schmidt MB, Chen EH et al (2006) A review of the effects of insulin-like growth factor and platelet derived growth factor on *in vivo* cartilage healing and repair. *Osteoarthritis Cartil* 14:403–412. doi:[10.1016/j.joca.2005.10.011](https://doi.org/10.1016/j.joca.2005.10.011)
- Song YH, Song JL et al (2013) The therapeutic potential of IGF-I in skeletal muscle repair. *Trends Endocrinol Metab* 24:310–319. doi:[10.1016/j.tem.2013.03.004](https://doi.org/10.1016/j.tem.2013.03.004)
- Tiscornia G, Singer O et al (2006) Production and purification of lentiviral vectors. *Nat Protoc* 1:241–245. doi:[10.1038/nprot.2006.37](https://doi.org/10.1038/nprot.2006.37)

- Tomasoni S, Longaretti L et al (2013) Transfer of growth factor receptor mRNA via exosomes unravels the regenerative effect of mesenchymal stem cells. *Stem Cells Dev* 22:772–780. doi:[10.1089/scd.2012.0266](https://doi.org/10.1089/scd.2012.0266)
- Wagner J, Kean T et al (2009) Optimizing mesenchymal stem cell-based therapeutics. *Curr Opin Biotechnol* 20:531–536. doi:[10.1016/j.copbio.2009.08.009](https://doi.org/10.1016/j.copbio.2009.08.009)
- Wang S, Qu X et al (2012) Clinical applications of mesenchymal stem cells. *J Hematol Oncol* 5:19. doi:[10.1186/1756-8722-5-19](https://doi.org/10.1186/1756-8722-5-19)
- Wang Y, Chen X et al (2014) Plasticity of mesenchymal stem cells in immunomodulation: pathological and therapeutic implications. *Nat Immunol* 15:1009–1016. doi:[10.1038/ni.3002](https://doi.org/10.1038/ni.3002)
- White SM, Renda M et al (1999) Lentivirus vectors using human and simian immunodeficiency virus elements. *J Virol* 73:2832–2840
- Xiniris C, Morigi M et al (2013) A novel strategy to enhance mesenchymal stem cell migration capacity and promote tissue repair in an injury specific fashion. *Cell Transplant* 22:423–436
- Yang Q, Yang Y et al (2016) Effects of granulocyte colony-stimulating factor on patients with liver failure: a meta-analysis. *J Clin Transl Hepatol* 4:90–96. doi:[10.14218/JCTH.2016.00012](https://doi.org/10.14218/JCTH.2016.00012)
- Yu H, Rohan T (2000) Role of the insulin-like growth factor family in cancer development and progression. *J Natl Cancer Inst* 92:1472–1489
- Zhu M, Feng Y et al (2015) Human cerebrospinal fluid regulates proliferation and migration of stem cells through insulin-like growth factor-1. *Stem Cells Dev* 24:160–171
- Zou J, Maeder ML et al (2009) Gene targeting of a disease-related gene in human induced pluripotent stem and embryonic stem cells. *Cell Stem Cell* 5:97–110. doi:[10.1016/j.stem.2009.05.023](https://doi.org/10.1016/j.stem.2009.05.023)



### ANEXO III

SOUZA, B. S. F; **SILVA, D. N**; CARVALHO, R. H; SAMPAIO, G. L. A; PAREDES, B. D; FRANÇA, L. A; AZEVEDO, C. M; VASCONCELOS, J. F; MEIRA, C. S; NETO, P. C; MACAMBIRA, S. G; SILVA, K. N; ALLABHDADI, K. J; TAVORA, F; NETO, J. D. S; RIBEIRO-DOS-SANTOS, R; SOARES, M. B. P. Association of cardiac galectin-3 expression, myocarditis, and fibrosis in chronic Chagas disease cardiomyopathy. **The American Journal of Pathology**, v. 187, p. 1134-1146, 2017.



IMMUNOPATHOLOGY AND INFECTIOUS DISEASES

# Association of Cardiac Galectin-3 Expression, Myocarditis, and Fibrosis in Chronic Chagas Disease Cardiomyopathy



Bruno Solano de Freitas Souza,<sup>\*†</sup> Daniela Nascimento Silva,<sup>†</sup> Rejane Hughes Carvalho,<sup>†</sup> Gabriela Louise de Almeida Sampaio,<sup>†</sup> Bruno Diaz Paredes,<sup>†</sup> Luciana Aragão França,<sup>†</sup> Carine Machado Azevedo,<sup>\*†</sup> Juliana Fraga Vasconcelos,<sup>\*†</sup> Cassio Santana Meira,<sup>\*†</sup> Paulo Chenaud Neto,<sup>†</sup> Simone Garcia Macambira,<sup>\*†‡</sup> Kátia Nunes da Silva,<sup>†</sup> Kyan James Allahdadi,<sup>†</sup> Fabio Tavora,<sup>§</sup> João David de Souza Neto,<sup>§</sup> Ricardo Ribeiro dos Santos,<sup>†</sup> and Milena Botelho Pereira Soares<sup>\*†</sup>

From the Gonçalo Moniz Research Center, \* Oswaldo Cruz Foundation (FIOCRUZ), Salvador; the Center for Biotechnology and Cell Therapy,<sup>†</sup> São Rafael Hospital, Salvador; the Health Sciences Institute,<sup>‡</sup> Federal University of Bahia, Salvador; and Messejana Heart and Lung Hospital,<sup>§</sup> Fortaleza, Brazil

Accepted for publication  
January 19, 2017.

Address correspondence to  
Milena Botelho Pereira Soares,  
Ph.D., Centro de Pesquisas  
Gonçalo Moniz, Fundação  
Oswaldo Cruz, Rua Waldemar  
Falcão, 121, Candeal, Salvador,  
Bahia, Brazil CEP: 40296-  
710. E-mail: [milena@bahia.  
fiocruz.br](mailto:milena@bahia.fiocruz.br).

Chronic Chagas disease cardiomyopathy, caused by *Trypanosoma cruzi* infection, is a major cause of heart failure in Latin America. Galectin-3 (Gal-3) has been linked to cardiac remodeling and poor prognosis in heart failure of different etiologies. Herein, we investigated the involvement of Gal-3 in the disease pathogenesis and its role as a target for disease intervention. Gal-3 expression in mouse hearts was evaluated during *T. cruzi* infection by confocal microscopy and flow cytometry analysis, showing a high expression in macrophages, T cells, and fibroblasts. *In vitro* studies using Gal-3 knockdown in cardiac fibroblasts demonstrated that Gal-3 regulates cell survival, proliferation, and type I collagen synthesis. *In vivo* blockade of Gal-3 with N-acetyl-D-lactosamine in *T. cruzi*-infected mice led to a significant reduction of cardiac fibrosis and inflammation in the heart. Moreover, a modulation in the expression of proinflammatory genes in the heart was observed. Finally, histological analysis in human heart samples obtained from subjects with Chagas disease who underwent heart transplantation showed the expression of Gal-3 in areas of inflammation, similar to the mouse model. Our results indicate that Gal-3 plays a role in the pathogenesis of experimental chronic Chagas disease, favoring inflammation and fibrogenesis. Moreover, by demonstrating Gal-3 expression in human hearts, our finding reinforces that this protein could be a novel target for drug development for Chagas cardiomyopathy. (*Am J Pathol* 2017, 187: 1134–1146; <http://dx.doi.org/10.1016/j.ajpath.2017.01.016>)

Chronic Chagas disease cardiomyopathy (CCC), caused by *Trypanosoma cruzi* infection, is an important cause of morbidity and mortality in endemic countries. It is estimated that approximately 7 million people are infected worldwide, with high prevalence in Latin America and growing incidence in developed countries because of globalization.<sup>1,2</sup> It is estimated that the cardiac form of the disease occurs in approximately 20% to 30% of infected subjects.<sup>2</sup> Antiparasitic drugs are effective during acute infection, but fail to improve established CCC.<sup>3,4</sup> Besides standard heart failure treatment, patients with advanced CCC rely on heart transplantation, which is limited because of organ availability and complications relative to parasite reactivation after immunosuppression therapy.<sup>5</sup>

During CCC, cardiomyocytes are lost as a result of damage caused by immune responses directed to the parasites that persist in the heart, as well as to autoreactive cells directed to heart antigens.<sup>6,7</sup> Although the mechanisms of pathogenesis are not completely understood, several studies indicate the involvement of type 1 helper T-cell lymphocytes associated with high production of interferon- $\gamma$  (IFN- $\gamma$ ), resembling a delayed hypersensitivity reaction.<sup>6</sup> An association between progression to severe chronic forms and a high production of IFN- $\gamma$  was observed in

Supported by National Council for Scientific and Technological Development and Bahia Research Foundation.

Disclosures: None declared.

patients with Chagas disease.<sup>8</sup> Macrophages, a major cell population found in the inflammatory sites, can be activated by IFN- $\gamma$  and tumor necrosis factor- $\alpha$ , two inflammatory cytokines overexpressed in the hearts of mice chronically infected with *T. cruzi*. Furthermore, several genes related to the inflammatory response are up-regulated in heart tissue during the chronic phase of *T. cruzi* infection.<sup>9</sup>

Previous studies suggested that activated macrophages secrete galectin-3 (Gal-3), a molecule involved in the pathogenesis of cardiac dysfunction.<sup>10</sup> Gal-3 is a soluble  $\beta$ -galactoside binding lectin involved in a variety of cellular processes, including proliferation, migration, and apoptosis.<sup>11</sup> The importance of this protein in the regulation of cardiac fibrosis and remodeling has been highlighted by the demonstration of its contribution to the development and progression of heart failure in different experimental settings.<sup>12–14</sup> Serum Gal-3 concentrations are also increased in patients with acute decompensated heart failure. On the basis of these findings, the value of Gal-3 as a prognostic biomarker in patients with chronic heart failure has been investigated.<sup>15</sup>

Previously, we performed transcriptomic analysis in the cardiac tissue of mice chronically infected with *T. cruzi*, and found that *Lgals3*, the gene encoding for Gal-3, is among the most overexpressed genes.<sup>16</sup> By immunofluorescence analysis, we showed that Gal-3 is mainly expressed in inflammatory cells in the hearts of *T. cruzi*-infected mice. We hypothesized that Gal-3 plays a role in the pathogenesis of CCC, contributing to the progression of inflammation and fibrosis. In the present study, we evaluated the expression of Gal-3 during *T. cruzi* infection in mice. Gal-3 expression was also investigated in human heart samples, to validate the expression of this protein in the human disease setting. Finally, we conducted *in vitro* and *in vivo* studies involving genetic and pharmacological blockades of Gal-3 to investigate its potential role in disease pathogenesis and its usefulness as a target for therapeutic development.

## Materials and Methods

### Animal Procedures

Six- to eight-week-old female C57BL/6 mice were used for *T. cruzi* infection and as normal controls. Galectin-3 C57BL/6 mice were used in cell adhesion experiments. All animals were raised and maintained at the animal facility of the Center for Biotechnology and Cell Therapy, Hospital São Rafael, in rooms with controlled temperature (22°C  $\pm$  2°C) and humidity (55%  $\pm$  10%), and continuous air flow. Animals were housed in a 12-hour light/12-hour dark cycle (6AM to 6PM) and provided with standard rodent diet and water ad libitum. Animals were handled according to the NIH guidelines for animal experimentation.<sup>17</sup> All procedures described had prior approval from the local institutional animal ethics committee at Hospital São Rafael (01/13).

### *Trypanosoma cruzi* Infection

Trypomastigotes of the myotropic Colombian *T. cruzi* strain were obtained from culture supernatants of infected LLC-MK2 cells, as previously described.<sup>9</sup> Infection of C57BL/6 mice was performed by i.p. injection of 1000 *T. cruzi* trypomastigotes in saline, and was confirmed through evaluation of parasitemia at different time points after infection.

### Pharmacological Blockade of Gal-3 with N-Lac

C57BL/6 female mice ( $n = 11$ ) chronically infected with *T. cruzi* [6 months postinfection (m.p.i.)] were treated with N-acetyl-D-lactosamine (N-Lac) (Sigma-Aldrich, St. Louis, MO), 5 mg/kg per day, i.p. injections 3 $\times$  per week, for 60 days. Chronically infected mice injected with saline ( $n = 10$ ) and same age naïve mice ( $n = 8$ ) served as controls. Functional analyses were performed, as described below. Mice were euthanized, by cervical dislocation under anesthesia with 5% ketamine (König, São Paulo, Brazil) and 2% xylazine (König Lab), the week after the final N-Lac injection. Heart samples were collected for real-time quantitative PCR and histological analysis. In another experiment, sucrose (Sigma-Aldrich) was administered in the same regimen as N-Lac to C57BL/6 mice, after 6 months of infection with *T. cruzi*. Heart samples were collected for histological analysis.

### Functional Analysis

Electrocardiography was performed using the Bio Amp PowerLab System (PowerLab 2/20; ADInstruments, Sydney, Australia), recording the bipolar lead I. All animals were anesthetized by i.p. injection of 10 mg/kg xylazine and 100 mg/kg ketamine to obtain the records. All data were acquired for computer analysis using Chart 5 for Windows (ADInstruments). The electrocardiographic analysis included heart rate, PR interval, P wave duration, QT interval, QTc, and arrhythmias. The QTc was calculated as the ratio of QT interval by square roots of RR interval.

A motor-driven treadmill chamber for one animal (LE 8700; Panlab, Barcelona, Spain) was used to exercise the animals. The speed of the treadmill and the intensity of the shock (mA) were controlled by a potentiometer (LE 8700 treadmill control; Panlab). After an adaptation period in the treadmill chamber, the mice exercised at five different velocities (7.2, 14.4, 21.6, 28.8, and 36.0 m/minute), with increasing velocity after 5 minutes of exercise at a given speed. Velocity was increased until the animal could no longer sustain a given speed and remained >5 seconds on an electrified stainless-steel grid. Total running distance was recorded.

### Morphometric Analysis

Two months after the therapy, mice were euthanized as mentioned before and hearts were collected and fixed in 10% buffered formalin. Heart sections were analyzed by

light microscopy after paraffin embedding, followed by standard hematoxylin and eosin staining. Inflammatory cells infiltrating heart tissue were counted using a digital morphometric evaluation system. Images were digitized using the slide scanner ScanScope (Leica, Wetzlar, Germany). Morphometric analyses were performed using Image Pro Plus software version 7.0 (Media Cybernetics, Rockville, MD). The inflammatory cells were counted in 10 fields ( $\times 400$  magnification) per heart sample. The percentage of fibrosis was determined using Sirius red–stained heart sections and the Image Pro Plus version 7.0. Two blinded investigators performed the analyses (J.F.V. and C.M.A.).

### Immunofluorescence Analysis

Frozen (10  $\mu\text{m}$  thick) or formalin-fixed, paraffin-embedded (3  $\mu\text{m}$  thick) heart sections were obtained. Paraffin-embedded tissues were deparaffinized and submitted to a heat-induced antigen retrieval step by incubation in citrate buffer (pH = 6.0). Then, sections were incubated overnight at 4°C with the following primary antibodies: anti-Gal-3, diluted 1:400 (Santa Cruz Biotechnology, Dallas, TX) and anti-CD11b, diluted 1:400 (BD Biosciences, San Jose, CA). Next, the sections were incubated for 1 hour with secondary antibodies anti-goat IgG Alexa Fluor 488-conjugated and anti-rat IgG Alexa Fluor 594-conjugated (1:400; ThermoFisher Scientific, Waltham, MA). Immunostaining for *in vitro* experiments was performed in cardiac fibroblasts or bone marrow–derived macrophages plated on coverslips. The cells were fixed with paraformaldehyde 4% and incubated with the primary antibodies: goat anti-Gal-3, diluted 1:400 (Santa Cruz Biotechnology), or rabbit anti-collagen type I, diluted 1:50 (Novotec, Lyon, France). On the following day, sections were incubated for 1 hour with phalloidin conjugated with Alexa Fluor 633 or 488 conjugated, diluted 1:50, mixed with the secondary antibodies anti-goat IgG Alexa Fluor 488-conjugated (1:400) or anti-rabbit IgG Alexa Fluor 568-conjugated (1:200; all from ThermoFisher Scientific), respectively. Nuclei were stained with DAPI (VectaShield mounting medium with DAPI H-1200; Vector Laboratories, Burlingame, CA). The presence of fluorescent cells was determined by observation on a FluoView 1000 confocal microscope (Olympus, Tokyo, Japan) and A1+ confocal microscope (Nikon, Tokyo, Japan). Quantifications of Gal-3<sup>+</sup> cells were performed in 10 random fields captured under  $\times 400$  magnification, using the Image Pro Plus software version 7.0.

### Flow Cytometry Analysis

Control and *T. cruzi*–infected mice were euthanized, hearts were collected, perfused with phosphate-buffered saline (PBS) to remove blood cells, and processed by enzymatic digestion using 0.1% collagenase IV (Sigma-Aldrich) and 10  $\mu\text{g}/\text{mL}$  DNase (Roche, Basel, Switzerland), for 40 minutes, at 37°C. To evaluate the subpopulations of digested cardiac tissue

samples, cell suspensions were allowed to pass through a 70- $\mu\text{m}$  cell strainer (BD Biosciences) and counted. Aliquots of  $10^6$  cells were used for each test tube and 1  $\mu\text{L}$  of Fc blocking reagent (BD Biosciences) was added. The fluorochrome-conjugated antibody panels used for each subpopulation were: i) T lymphocytes: CD45-APC-Cy7, CD3-APC, CD4-PE-Cy5, CD8-PE (BD Biosciences); ii) macrophages: CD45-APC-Cy7, CD11b-APC (eBiosciences, San Diego, CA); iii) fibroblast/fibrocyte: CD45-APC-Cy7, vimentin-APC (Cell Signaling, Danvers, MA). Each antibody was diluted as suggested on the product data sheet. Samples were incubated for 20 minutes at room temperature in the dark. For intracellular staining of Gal-3, samples were washed once in PBS and CytoFix/CytoPerm kit (BD Biosciences) were used as directed on data sheet protocol. Anti-Gal-3-PE (R&D Systems, Minneapolis, MN) antibody was added to macrophages and fibroblast/fibrocyte sample tubes, whereas nonconjugated anti-Gal-3 (Santa Cruz Biotechnology) was added on T lymphocyte sample tube and its detection was performed by addition of anti-mouse IgG-Alexa Fluor 488 (ThermoFisher Scientific). Each incubation step was performed during 30 minutes at room temperature in the dark. Samples were washed twice and resuspended in PBS and added with Hoechst 33258 to exclude cell debris from analysis. Apoptosis was evaluated by annexin V-PI assay. Cells were harvested from culture flasks by adding TrypLE solution (ThermoFisher Scientific) and incubating for 5 minutes at 37°C. Cell suspensions were collected and washed with PBS by centrifugation at  $300 \times g$ . After discarding supernatant, pellets were resuspended in binding buffer (ThermoFisher Scientific) and cells were counted. Apoptosis assays were performed using annexin-V-APC and PI (BD Biosciences) according to the manufacturer's recommendations. Sample acquisition was performed using a BD LSRFortessa SORP cytometer (BD Biosciences) using BD FACS Diva software version 6.2 (BD Biosciences). Ten thousand events were acquired per sample, and the data were analyzed using FlowJo software version 7.5 (FlowJo Enterprise, Ashland, OR).

### Real-Time RT-PCR

Total RNA was isolated from heart samples with TRIzol reagent (ThermoFisher Scientific) and the concentration was determined by spectrophotometry. High Capacity cDNA Reverse Transcription Kit (ThermoFisher Scientific) was used to synthesize cDNA of 1  $\mu\text{g}$  RNA following manufacturer's recommendations. Real-time RT-PCR assays were performed to detect the expression levels of *Tbet* (Mm\_00450960\_m1), *Gata3* (Mm\_00484683\_m1), *Tnf* (Mm\_00443258\_m1), *Ifng* (Mm\_00801778\_m1), *Il10* (Mm\_00439616\_m1), *Foxp3* (Mm\_00475162\_m1), *Lgals3* (Mm\_00802901\_m1), and *MMP9* (Mm\_00444299\_m1). Other primer sequences used in real-time PCR analyses: *Coll1*: 5'-GTCCCTCGACTCCTACATCTTCTGA-3' (forward) and 5'-AAACCCGAGGTATGCTTGATCTGTA' (reverse); *Ccnd1*: 5'-TCCGCAAGCATGCACAGA-3'

(forward) and 5'-GGTGGGTTGGAAATGAACTTCA-3' (reverse); *Cav1*: 5'-GGCACTCATCTGGGGCATTTA-3' (forward) and 5'-CTCTTGATGCACGGTACAACC-3' (reverse). The real-time RT-PCR amplification mixtures contained a 20 ng template cDNA, TaqMan Master Mix (10  $\mu$ L) and probes, constituting a final volume of 20  $\mu$ L (all from ThermoFisher Scientific). All reactions were run in duplicate on an ABI7500 Sequence Detection System (ThermoFisher Scientific) under standard thermal cycling conditions. The mean Ct values from duplicate measurements were used to calculate expression of the target gene, while normalized to an internal control (*Gapdh*) using the 2<sup>-</sup>DCt formula. Experiments with CVs >5% were excluded. A nontemplate control and nonreverse transcription controls were also included.

### Design of shRNAs and Production of Lentiviral Vectors

To stably knock down *Lgals3* expression, we designed shRNA against different regions of the *Lgals3* coding sequence, and a scramble shRNA as control. Target sequences were designed using the online tool siRNA Wizard software version 3.1 (Invivogen, San Diego, CA). All suggested sequences were blasted against the mouse RNA reference sequence database, and the three with the lowest degree of homology to other sequences were selected: *Lgals3*\_shRNA1 5'-GATTTTCAGGAGAGGGAATGAT-3'; *Lgals3*\_shRNA2 5'-GGTCAACGATGCTCACCTACT-3'; *Lgals3*\_shRNA3 5'-CATGCTGATCACAATCATGG-3'; and one *Lgals3*\_scrbl\_shRNA 5'-AGGTATGAGTCGA-GATTGAGA-3'. Sense and antisense single strands, containing the target sequence, a loop sequence (TCAAGAG), and restriction enzyme sites for MluI at the sense sequence and ClaI at the antisense sequence, were synthesized separately. The annealing of both strands to form double-stranded shRNAs was performed by incubating 2.5  $\mu$ mol/L from the sense and antisense strand of each shRNA in 10 mmol/L Tris-HCl (pH 7.5), 0.1 mol/L NaCl, and 1 mmol/L EDTA at 95°C for 5 minutes and then allowing the reaction to cool down to room temperature for at least 2 hours. The double-stranded shRNAs were then phosphorylated using T4 PNK (New England Biolabs, Ipswich, MA) following manufacturer protocol. The shRNAs were cloned into the pLVTHM lentiviral vector (Addgene plasmid 12247), specifically designed for gene knockdown with shRNAs,<sup>18</sup> after the vector was linearized by digestion with MluI and ClaI (New England Biolabs) according to the manufacturer instructions. Each of the produced shRNA constructs were confirmed by sequencing using ABI 3500 platform (ThermoFisher Scientific).

For lentiviral vector production, HEK293 FT cells were cotransfected with each of the shRNA constructs, plus psPAX2 (Addgene plasmid 12260) and pMD2.G (Addgene plasmid 12247) for production of the lentivirus particles, in a proportion of 3:2:1. Viral supernatants were harvested 48 and 72 hours later, pooled, centrifuged to remove cell debris, filtered through 0.45- $\mu$ m filters (Millipore, Billerica, MA), and concentrated by ultracentrifugation. Cardiac

fibroblasts were transduced with the lentivirus by overnight incubation in medium containing lentiviral particles and 6  $\mu$ g/mL polybrene. Knockdown efficiency for each shRNA was evaluated by real-time quantitative PCR using TaqMan probes for *Lgals3* (mm00802901\_m1), *Gapdh* (mm99999915\_g1), *Actb* (mm00607939\_s1), and *Hprt* (mm00496968\_m1) and TaqMan Universal PCR master mix (ThermoFisher Scientific), according to the manufacturer's instructions. Assay was performed in triplicate, and the empty vector was used as control. Ct for *Lgals3* was normalized taking into account the geometric mean of the Ct for *Gapdh*, *Actb*, and *Hprt* ( $\Delta$ Ct). The relative expression was then calculated by the normalized Ct between each *Lgals3* shRNA construct and the empty vector ( $\Delta\Delta$ Ct).

### In Vitro Studies with Cardiac Fibroblasts and Bone Marrow-Derived Macrophages

Cardiac fibroblasts were isolated from hearts of adult C57BL/6 mice, euthanized as described above. Hearts were minced into pieces of 1 mm and incubated with 0.1% collagenase type A (Sigma-Aldrich) at 37°C for 30 minutes, under constant stirring. The cell suspension was passed through a 70- $\mu$ m cell strainer (BD Biosciences), and plastic-adherent cells were selected by 1 hour incubation in gelatin-coated flasks (Sigma-Aldrich). Nonadherent cells from supernatant were removed and adherent cells were cultured with Dulbecco's modified Eagle's medium supplemented with 10% fetal bovine serum and 1% penicillin and streptomycin (all from ThermoFisher Scientific), in a humidified incubator at 37°C with 5% CO<sub>2</sub>. Culture medium was changed every 3 days, and cells were trypsinized (trypsin-EDTA 0.05%; ThermoFisher Scientific) when 80% confluence was reached. Cell cycle studies were performed with CFSE Cell Proliferation Kit (ThermoFisher Scientific), according to the manufacturer's instructions. Proliferation of cardiac fibroblasts was assessed by the measurement of <sup>3</sup>H-thymidine uptake. Cells were plated in 96-well plates, at a density of 10<sup>4</sup> cells/well, in a final volume of 200  $\mu$ L, in triplicate, and cultured in the absence or presence of 30  $\mu$ g/mL rmGal-3 (R&D Systems), with or without 1% modified citrus pectin (ecoNugenics, Santa Rosa, CA). After 24 hours, plates were pulsed with 1  $\mu$ Ci of methyl-<sup>3</sup>H thymidine (PerkinElmer, Waltham, MA) for 18 hours, and proliferation was assessed by measurement of <sup>3</sup>H-thymidine uptake by using a Chameleon  $\beta$ -plate counter (Hydrex, Turku, Finland). Proliferation capacity of Gal-3 knockdown and control cell lines was compared by <sup>3</sup>H-thymidine incorporation, using the same procedures.

To obtain macrophages, bone marrow cells were harvested from femurs of C57BL/6 mice by flushing with cold RPMI 1640 medium. Bone marrow cells were induced to differentiate into macrophages by culture in RPMI 1640 supplemented with 10% fetal bovine serum (ThermoFisher Scientific), 50 U/mL of penicillin, 50  $\mu$ g/mL of streptomycin, 2.0 g/L of sodium bicarbonate, 25 mmol/L HEPES, 2 mmol/L

glutamine, and 30% supernatant obtained from X63-GM-CSF<sup>19</sup> cell line culture, at 37°C and 5% CO<sub>2</sub>. Cells were cultured for 7 days, with half medium changes every 3 days. Differentiated macrophages were plated onto 24-well plates and incubated in medium alone or with 1 µg/mL lipopolysaccharide (Sigma-Aldrich) with or without 50 ng/mL IFN-γ (R&D Systems). After 24 hours, macrophages were detached using a cell scraper and analyzed for Gal-3 expression by flow cytometry, as described above.

## Human Samples

The procedures involving human samples received prior approval by the local Ethics committee at Hospital São Rafael (approval number 51025115.3.0000.0048). Samples were obtained at Messejana Hospital in Fortaleza, Ceará, a medical center specialized for heart transplantation in Brazil. Fragments of explanted hearts from three patients with Chagas disease, confirmed by serological assay, were obtained from left ventricle and septum. Samples were processed in paraffin and stained with hematoxylin and eosin and Sirius Red, or used for immunostaining for detection of Gal-3, as described above.

## Lymphoproliferation Assay

Splenocyte suspensions, obtained from C57Bl/6 mice, were prepared in Dulbecco's modified Eagle's medium supplemented with 10% fetal bovine serum and 50 µg/mL of

gentamicin. Splenocytes were cultured in 96-well plates at  $1 \times 10^6$  cells/well, in triplicate, and lymphocyte proliferation was stimulated or not with concanavalin A (2 µg/mL; Sigma-Aldrich) or Dynabeads mouse T-activator CD3/CD28 (ThermoFisher Scientific), according to the manufacturer's instructions. Cell proliferation was induced in the absence or presence of various concentrations of N-Lac (10, 1, and 0.1 µmol/L). After 48 hours of incubation, 1 µCi of <sup>3</sup>H-thymidine was added to each well, and the plate was incubated for 18 hours. Plates were frozen at -70°C, then thawed and transferred to UniFilter-96 GF/B PEI coated plates (PerkinElmer) with the assistance of a cell harvester. After drying, 50 mL of scintillation cocktail was added in each well, sealed and plate read at liquid scintillation microplate counter. Dexamethasone (Sigma-Aldrich; 10 µmol/L) was used as positive control. Three independent experiments were performed.

## En Face Leukocyte Adhesion Assay

The aorta from the thoracic region and spleens were removed from wild-type and galectin-3 knockout C57Bl/6 mice. Fragments of approximately 1 mm<sup>2</sup> were placed with the intimal side up in 96-well plates previously coated with Matrigel (Corning Inc., Corning, NY) for 30 minutes at 37°C. Endothelium was activated by incubation with 500 ng/mL lipopolysaccharide (Sigma), whereas the splenocyte suspension with 2 µg/mL concanavalin A (Sigma)

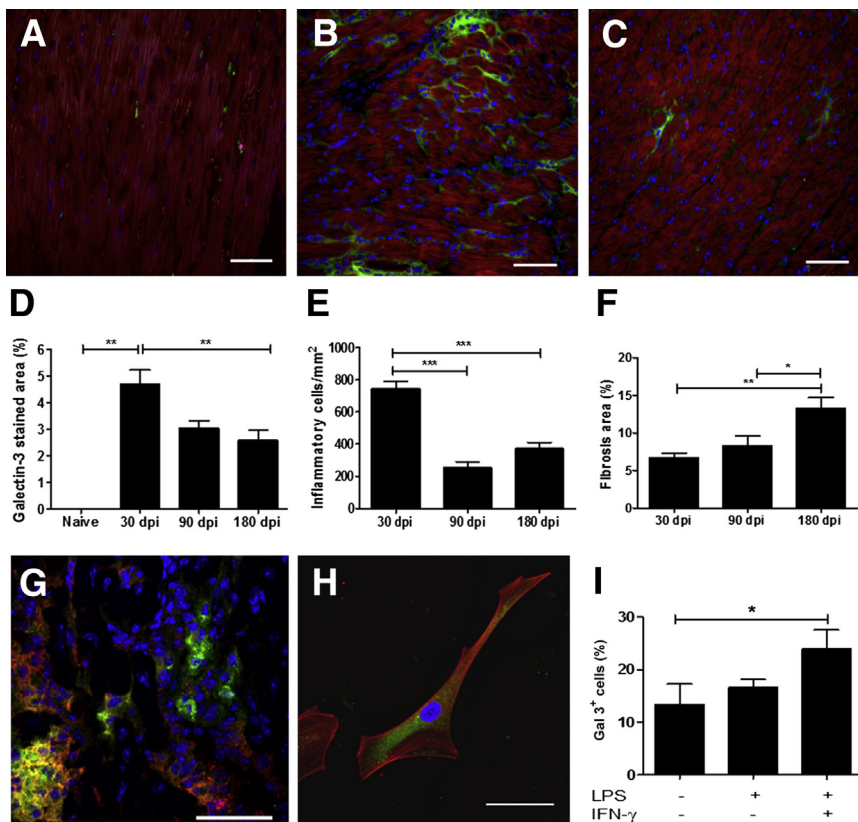


**Figure 1** Gal-3 is overexpressed in mouse hearts after *Trypanosoma cruzi* infection. Confocal microscopy analysis demonstrated the presence of Gal-3<sup>+</sup> cells (green), mainly in areas of inflammatory infiltrates, in naïve (A), at 1 (B) and 6 (C) months postinfection (m.p.i.). Cardiac muscle was stained for actin-F (red), and nuclei were stained with DAPI (blue). D: The cardiac expression of Gal-3 peaked at 1 m.p.i., but remained elevated during the chronic phase of infection, when compared to naïve mice. E: A similar pattern is observed for the number of inflammatory cells infiltrating the heart. F: However, the percentage of fibrosis increased with time. G: Most cells expressing Gal-3 (green) coexpressed the monocyte/macrophage marker CD11b (red). H: Cardiac fibroblasts isolated by enzymatic digestion of heart tissue also express Gal-3 (green). Actin-F is seen in red, and nucleus in blue. I: Bone marrow-derived macrophages stimulated *in vitro* with proinflammatory (M1) inducers interferon-γ (IFN-γ) and lipopolysaccharide (LPS) increase the expression of Gal-3. Data are expressed as means ± SEM. \**P* < 0.05, \*\**P* < 0.01, and \*\*\**P* < 0.001. Scale bars = 50 µm. dpi, days postinfection.

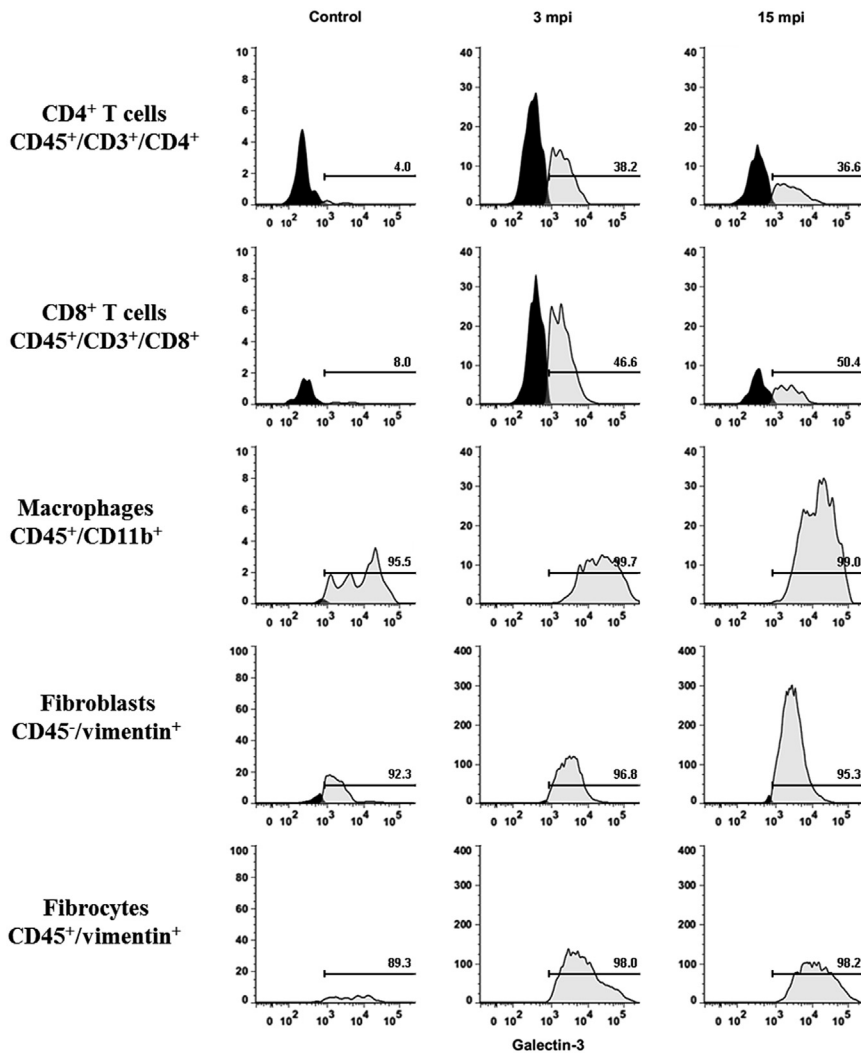


**Figure 2** Gal-3 is increased in different cell types involved in inflammation and tissue repair. Histograms showing flow cytometry analysis from digested heart tissue, obtained from naïve and infected mice, at 3 and 15 months postinfection (m.p.i.). Gal-3<sup>+</sup> T CD4<sup>+</sup> and CD8<sup>+</sup> lymphocytes expressing Gal-3 are increased at 3 and 15 m.p.i. when compared to naïve controls. Most macrophages (CD45<sup>+</sup>/CD11b<sup>+</sup>), fibroblasts (CD45<sup>-</sup>/vimentin<sup>+</sup>), and bone marrow-derived fibrocytes (CD45<sup>+</sup>/vimentin<sup>+</sup>) express Gal-3 (>90%) in all groups, but the mean fluorescence intensity increases with time of infection.

and 500 ng/mL lipopolysaccharide, during a period of 6 hours.

Activated splenocytes were incubated with 1  $\mu\text{mol/L}$  Celltracker Fluorescent Probes (Life Technologies) in serum-free RPMI 1640 medium (Gibco) for 30 minutes and washed three times, before adhesion to the endothelium. Splenocytes ( $5 \times 10^5$ /well) were plated and incubated with the aortic endothelium fragments for 30 minutes at 37°C in the presence or absence of 10  $\mu\text{mol/L}$  N-Lac (Sigma-Aldrich). Plates were then carefully washed three times with warm Hanks' balanced salt solution to remove the nonadherent cells. Three replicates were used for each treatment. Different random areas per well were acquired using a digital camera from an inverted fluorescence microscope. Fluorescent cells were quantified using ImagePro.

#### Inhibition of Cell Migration Assay

C57BL/6 mice, 8 to 12 weeks old, were submitted to euthanasia by cervical dislocation under anesthesia. Spleens

were collected, minced, cells were resuspended in PBS and passed through a 70- $\mu\text{m}$  cell strainer. The cells were resuspended and maintained in RPMI 1640 medium (ThermoFisher Scientific), without serum, supplemented with 2 mmol/L L-glutamine (ThermoFisher Scientific), 0.1% RPMI 1640 vitamin solution (Sigma Aldrich), 1 mmol/L sodium pyruvate, 10 mmol/L HEPES, 50  $\mu\text{mol/L}$  2-mercaptoethanol, and penicillin/streptomycin solution (all from ThermoFisher Scientific). Splenocytes were incubated in starvation during 24 hours at 37°C and 5% CO<sub>2</sub>, in the presence or absence of 10  $\mu\text{mol/L}$  N-Lac. Migration assay was performed using the QCM Chemotaxis Cell Migration Assay, 24-well 3- $\mu\text{m}$  pore (Millipore), according to the manufacturer's instructions. Briefly, splenocytes were counted and  $10^7$  cells in 250  $\mu\text{L}$  were placed in the upper chamber, in serum-free medium, in the presence or absence of N-Lac. RPMI 1640 medium supplemented with 10% fetal bovine serum (ThermoFisher Scientific) with or without 10  $\mu\text{mol/L}$  N-Lac was placed in the bottom chamber. Cells present in the bottom chamber were counted after overnight incubation.

## Statistical Analysis

All continuous variables are presented as means  $\pm$  SEM. Continuous variables were tested for normal distribution using Kolmogorov-Smirnov test. Parametric data were analyzed using unpaired *t* tests, for comparisons between two groups, and one-way analysis of variance, followed by Bonferroni post hoc test for multiple-comparison test, using Prism 6.0 (GraphPad, La Jolla, CA). *P* < 0.05 was considered statistically significant.

## Results

### Gal-3 Expression Is Increased during Experimental *T. cruzi* Infection

We first analyzed the expression of Gal-3 in mouse heart sections obtained at different time points of infection. *Trypanosoma cruzi* infection led to increased expression of Gal-3<sup>+</sup> cells in the myocardium compared to naïve controls, as shown by confocal microscopy (Figure 1, A–C). Quantification of Gal-3 expression showed a significant increase in all time points analyzed, in comparison with uninfected controls (Figure 1D). The number of Gal-3<sup>+</sup> cells was higher at the peak of parasitemia (1 m.p.i.), when an intense acute inflammatory response is found in the heart (Figure 1E). The numbers of Gal-3<sup>+</sup> cells during the chronic phase were sustained, whereas the percentage of fibrosis increased with time (Figure 1F). The population of Gal-3<sup>+</sup> cells in the heart included macrophages (CD11b<sup>+</sup> cells) (Figure 1G) and cardiac fibroblasts (Figure 1H). To investigate the role of proinflammatory signals in the expression of Gal-3 by macrophages, we performed *in vitro* studies to analyze the expression of Gal-3 in activated macrophages. Bone marrow–derived macrophages activated with IFN- $\gamma$  and Toll-like receptor 4 ligand lipopolysaccharide had an increased expression of Gal-3, as demonstrated by flow cytometry analysis (Figure 1I).

To better characterize the cell populations expressing Gal-3, we performed flow cytometry analysis of cells isolated from hearts of *T. cruzi*–infected mice (Figure 2). Both CD4<sup>+</sup> and CD8<sup>+</sup> T cells had increased Gal-3 expression at 3 and 15 m.p.i. when compared to uninfected controls. In addition, macrophages, characterized as CD45<sup>+</sup>/CD11b<sup>+</sup>, composed the cell populations expressing the higher mean fluorescence intensity of Gal-3 (Figure 2). Gal-3 was expressed at low levels in fibroblasts (vimentin<sup>+</sup>/CD45<sup>−</sup>) in control hearts, and was increased by 52.5% at 3 m.p.i. Gal-3 expression intensity in fibroblasts at 15 m.p.i. returned to levels similar to those found in controls. However, a significant increase in Gal-3 expression was detected in a population of vimentin<sup>+</sup>/CD45<sup>+</sup> cells, characterized as bone marrow–derived fibrocytes, at 3 and 15 m.p.i., when compared to controls (Figure 2).

### Expression of Gal-3 in the Hearts of Subjects with CCC

To evaluate if the presence of Gal-3<sup>+</sup> cells in the myocardium of infected mice could be translatable to the human

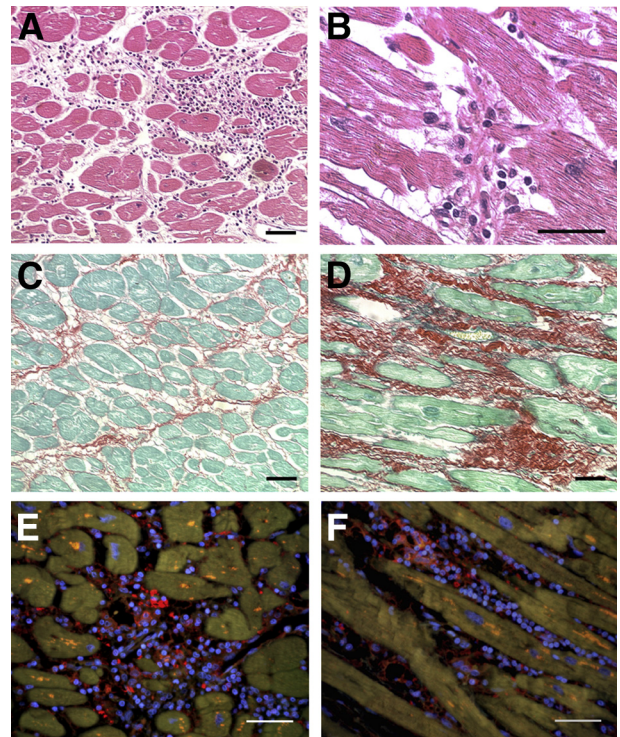


**Figure 3** Gal-3 expression in heart samples from subjects with end-stage Chagas cardiomyopathy. Representative images obtained from explanted heart sections of two subjects with end-stage Chagas cardiomyopathy who underwent heart transplantation. Heart sections were stained with hematoxylin and eosin, showing inflammatory infiltrates composed of mononuclear cells surrounding myofibers (A) and in areas of myocytolysis (B). Heart sections stained with Sirius red showing areas of mild (C) and extensive (D) cardiac fibrosis. E and F: Confocal microscopy analysis from two different subjects, showing Gal-3<sup>+</sup> cells (red) in areas of inflammatory infiltrates. Nuclei are stained with DAPI (blue). Scale bars = 50  $\mu$ m (A–C, E, and F); 25  $\mu$ m (D).

disease, we performed analysis in human heart samples obtained from explants of subjects with chronic Chagas disease cardiomyopathy who underwent heart transplantation. Heart sections were prepared and stained with hematoxylin and eosin for histological analysis, demonstrating the presence of foci of myocarditis, with an inflammatory infiltrate composed mainly of mononuclear cells, leading to the destruction of myofibers (Figure 3, A and B). In addition, an extensive area of diffuse fibrotic scar was found in Sirius red–stained sections (Figure 3, C and D). The expression of Gal-3 in human heart samples was evaluated by analysis using confocal microscopy. We observed the presence of cells, within the inflammatory foci and surrounding the myofibers, expressing variable levels of Gal-3 (Figure 3, E and F).

### Gal-3 Is a Major Regulator of Fibroblast Function

On the basis of the findings of increased Gal-3 expression in fibroblasts during the development of CCC, we performed *in vitro* studies aiming at investigating the role of Gal-3 on different aspects of the biology of these cells. Cardiac



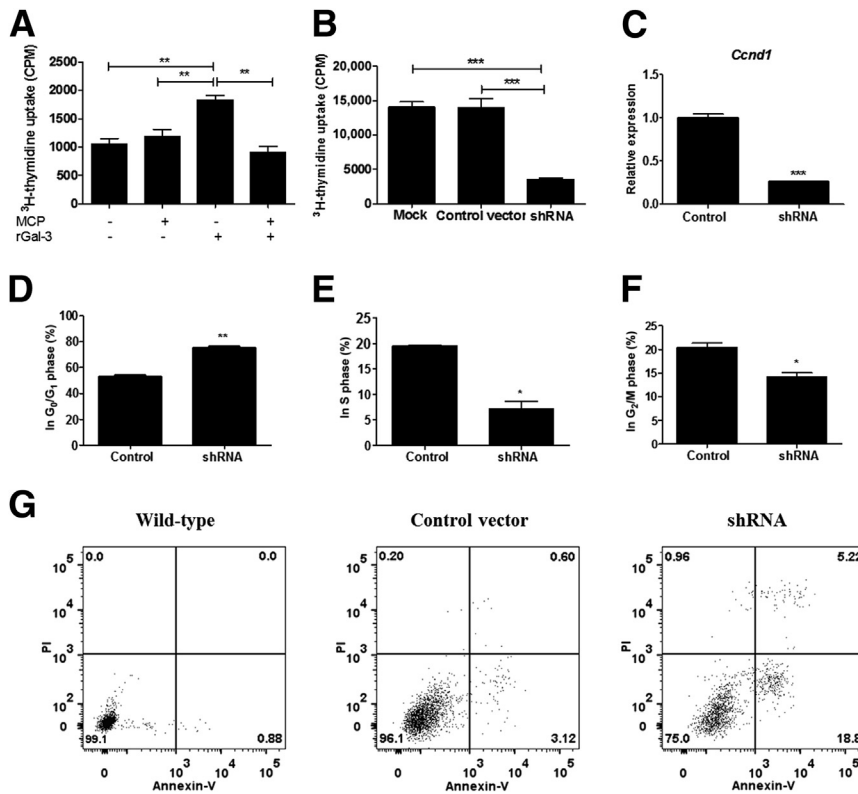


**Figure 4** Gal-3 is crucial for cardiac fibroblast proliferation and survival. Recombinant Gal-3 was added to the cardiac fibroblast culture medium and cell proliferation was measured by  $^3\text{H}$ -thymidine incorporation assay. **A:** Extracellular Gal-3 induced cardiac fibroblast proliferation, which is abolished by addition of modified citrus pectin, a Gal-3 binding partner. **B:** Gal-3 knockdown in cardiac fibroblasts markedly reduces cell proliferation, as evaluated by  $^3\text{H}$ -thymidine incorporation assay. **C:** A reduction in gene expression of cyclin D1 is found by real-time quantitative PCR analysis. Cell cycle analysis was performed by flow cytometry with carboxyfluorescein succinimidyl ester assay, demonstrating that Gal-3 knockdown in cardiac fibroblasts is associated with cell cycle arrest in  $\text{G}_0/\text{G}_1$  phases (**D**) and reduced number of cells in the  $\text{S}$  (**E**) and  $\text{G}_2/\text{M}$  (**F**) phases. **G:** Gal-3 knockdown is associated with increased frequency of apoptosis, as evaluated by annexin V assay. Data are expressed as means  $\pm$  SEM. \* $P < 0.05$ , \*\* $P < 0.01$ , and \*\*\* $P < 0.001$ . CPM, counts per minute; PI, propidium iodide.

fibroblasts isolated from mouse hearts were incubated with mouse recombinant Gal-3 to evaluate their proliferative rate. We found that exogenous recombinant Gal-3, at a micromolar concentration, increased the proliferation of cardiac fibroblasts, whereas addition of modified citrus pectin, a binding partner of Gal-3, blocked the effect of Gal-3 (Figure 4A).

Considering that this effect was observed at high concentrations of exogenous Gal-3, and given the high expression of intracellular Gal-3 in cardiac fibroblasts in experimental CCC, we evaluated the role of endogenous Gal-3 in cardiac fibroblasts. We generated lentiviral vectors encoding shRNA targeting the *Lgals3*, together with green fluorescence protein expression as a reporter gene. Then, cardiac fibroblasts were transduced by lentiviral infection, resulting in the knockdown of Gal-3. The efficiencies of lentiviral infection and knockdown were confirmed by green fluorescence protein reporter gene expression and by quantification of Gal-3 gene and protein expressions by real-time quantitative PCR and immunofluorescence analysis, respectively (>90%) (Supplemental Figure S1, A–E). More important, Gal-3 knockdown in cardiac fibroblasts led to a down-regulation of type I collagen expression (Supplemental Figure S1, F–H).

Gal-3 knockdown was associated with a significant reduction in the proliferative rate of cardiac fibroblasts (Figure 4B). This finding was accompanied by a reduction of cyclin D1 gene expression (Figure 4C). Analysis of caveolin-1 gene expression did not show alterations when

control or Gal-3 knockdown cells were compared (data not shown). Flow cytometry analysis showed cell cycle arrest in Gal-3 knockdown when compared to control cells (increased percentage of  $\text{G}_0/\text{G}_1$  and decreased  $\text{S}$  and  $\text{G}_2/\text{M}$  phases) (Figure 4, D–F).

To determine whether Gal-3 knockdown also affects cell survival, we evaluated the frequency of apoptosis in the culture of cardiac fibroblasts, by annexin V/PI staining and flow cytometry analysis. A higher percentage of apoptotic cells was detected in cultures of cardiac fibroblasts with Gal-3 knockdown when compared to controls (Figure 4G).

#### Treatment with the Gal-3 Blocking Agent N-Lac Reduces Inflammation and Fibrosis in Experimental CCC

To study the role of Gal-3 on the pathogenesis of CCC, we performed a pharmacological blockade of Gal-3 using N-Lac (Figure 5A), during the chronic phase of the infection, when cardiac fibrosis is significantly increased (6 and 8 m.p.i.). We performed functional evaluations (electrocardiographic analysis and treadmill test) before treatment (6 m.p.i.) and after the treatment with N-Lac (8 m.p.i.). *Trypanosoma cruzi* infection caused the development of arrhythmias and cardiac conduction disturbances, such as atrioventricular block, ventricular tachycardia, and ventricular bigeminy. Treatment with N-Lac did not alter the frequencies or the severity of arrhythmias when compared to those found in saline-treated controls (Table 1). Regarding

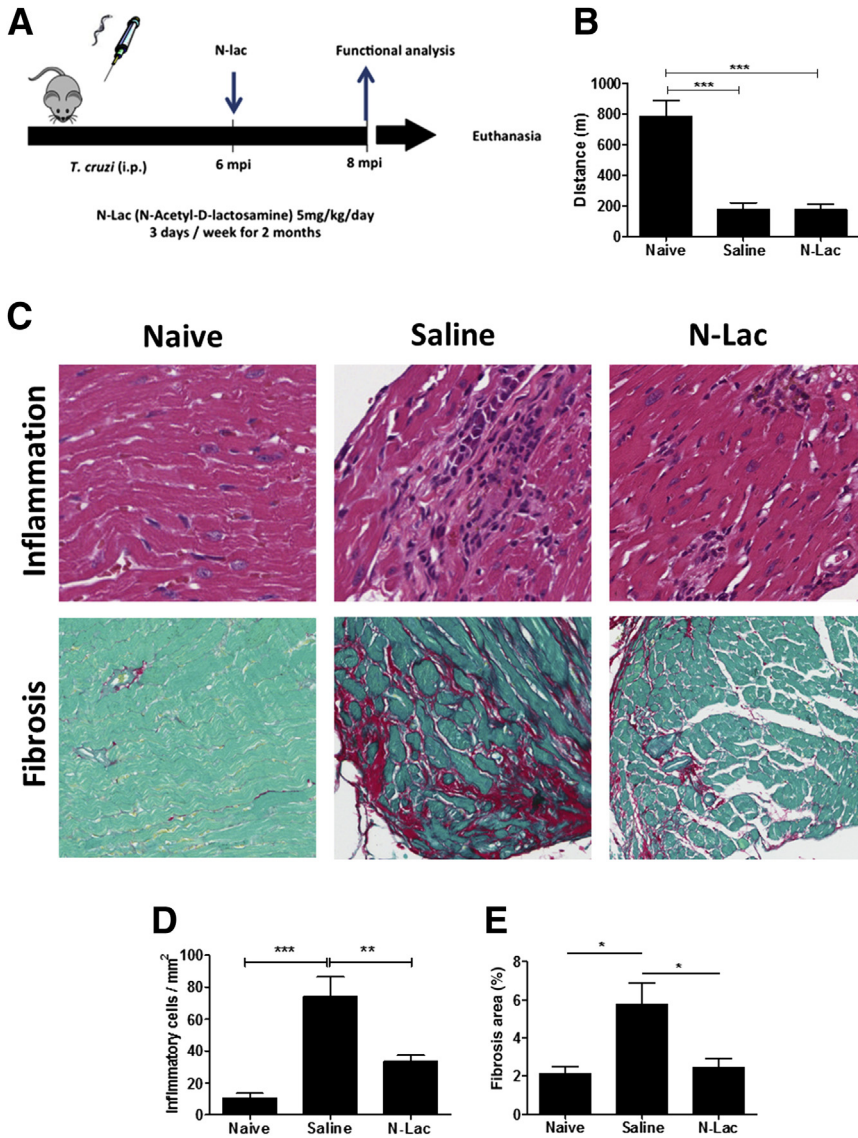


**Figure 5** *In vivo* pharmacological blockade of Gal-3 during the chronic phase of experimental *Trypanosoma cruzi* infection reduces inflammation and fibrosis. **A:** Experimental design. **B:** A lack of functional recovery was observed by analysis of performance in treadmill test 2 months after the beginning of treatment with N-Lac. **C:** A significant reduction in the intensity of cardiac inflammation and fibrosis is observed in heart sections of mice treated with N-Lac stained with hematoxylin and eosin (**top row**) and Sirius red (**bottom row**). Quantifications of the number of inflammatory cells infiltrating the heart (**D**), cardiac fibrosis area (**E**), showing histological improvement in N-Lac treated mice. Data are expressed as means  $\pm$  SEM. \* $P < 0.05$ , \*\* $P < 0.01$ , and \*\*\* $P < 0.001$ . Original magnification,  $\times 200$  (**C**). m.p.i., months postinfection.

the exercise capacity, *T. cruzi*-infected mice had an impaired performance when compared to uninfected controls 6 months after infection (data not shown). N-Lac treatment did not cause any improvement in exercise capacity, because mice treated with this Gal-3 blocker had similar performance in treadmill test to saline-treated mice and a reduced capacity when compared to uninfected controls (**Figure 5B**).

Histological analysis demonstrated the presence of inflammatory infiltrate in the hearts of mice infected with *T. cruzi*, mainly composed of mononuclear cells. The number of inflammatory cells infiltrating the heart, however, was significantly reduced in N-Lac-treated mice, compared to saline-treated controls (**Figure 5, C and D**). In addition, the percentage of heart fibrosis was significantly reduced after N-Lac treatment when compared to saline-treated mice (**Figure 5, C and E**). In addition, a control experiment was performed in which *T. cruzi*-infected mice were treated in

the same regimen with sucrose. Morphometric analysis in the hearts of sucrose-treated mice did not show reduction of inflammatory cells and the fibrotic area in sucrose-treated mice when compared to those treated with saline (**Supplemental Figure S2**).

To investigate whether N-Lac caused modulation of inflammatory mediators, we performed gene expression analysis in the heart tissue (**Figure 6**). N-Lac-treated mice had reduced gene expression of the inflammatory cytokines tumor necrosis factor- $\alpha$  and IFN- $\gamma$  when compared to saline-treated mice. The regulatory cytokine IL-10 was increased in *T. cruzi*-infected mice when compared to uninfected controls, both in saline as well as in N-Lac-treated mice. Moreover, the gene expression of transcription factors T-bet, GATA-3, and FoxP3, associated with T-cell subtypes type 1 helper T cell, type 2 helper T cell, and T regulatory cell, respectively, was increased by *T. cruzi* infection and reduced in mice treated with N-Lac. The gene

**Table 1** ECG Analysis in Uninfected and *Trypanosoma cruzi*-Infected Mice

ECG findings	Uninfected (n = 7)	Pretreatment (n = 19)	Saline (n = 9)	N-Lac (n = 10)
No alterations	7/7	1/19		
Atrial overload		1/19	1/9	
IACD			2/9	
JR		1/19	1/9	
AVB first degree		6/19	3/9	2/10
AVB third degree		5/19	2/9	3/10
SVT		2/19	1/9	1/10
Ventricular bigeminy				3/10
Isorhythmic AVD		2/19	1/9	1/10
AVD			1/9	
IVCD		1/19	1/9	

AVB, atrioventricular block; AVD, atrioventricular dissociation; ECG, electrocardiography; IACD, intra-atrial conduction delay; IVCD, intraventricular conduction delay; JR, junctional rhythm; N-Lac, N-acetyl-D-lactosamine; SVT, supraventricular tachycardia.

expression of chemokine ligand 8 (modified citrus pectin 2) and the chemokine receptor CCR5, which are increased by *T. cruzi* infection, was also reduced after N-Lac treatment. More important, treatment with N-Lac reduced the gene expression of Gal-3 in the hearts of *T. cruzi*-infected mice (Figure 6).

To better investigate the mechanisms by which N-Lac caused reduction of inflammation, we performed lymphoproliferation and migration assays. Mouse splenocytes were stimulated *in vitro* with concanavalin A or anti-CD3/CD28.

Addition of N-Lac at the highest concentration tested (10  $\mu\text{mol/L}$ ) caused a small reduction of lymphoproliferation stimulated by both polyclonal activators (Figure 7, A and B). In contrast, the positive control dexamethasone inhibited the proliferation induced by both stimuli. Last, we tested the effects of N-Lac in adhesion of leukocytes to the endothelium and in cell migration. The adhesion of leukocytes to aorta endothelium in an *en face* assay was significantly blocked by N-Lac using cells and endothelium from wild-type mice, but not from galectin-3 knockout mice (Figure 7C). In fact, cell adhesion of galectin-3 knockout mice was similar to that of pharmacological blockade with N-Lac in wild-type cells (Figure 7C). In addition, the presence of N-Lac significantly inhibited leukocyte migration in a transwell system (Figure 7D).

## Discussion

Gal-3 is a multifunctional lectin that can be found in various cells and tissues, and is detected in the nucleus, cytoplasm, as well as in the extracellular compartment.<sup>11</sup> Notably, Gal-3 may have different, concordant, or opposite actions depending on the cell type and whether it is present in the extracellular or intracellular compartments.<sup>11</sup> Previous studies from our group and others have shown a correlation between inflammation and fibrosis in the heart and Gal-3 expression.<sup>16,32,34</sup> Moreover, host expression of Gal-3 is required for *T. cruzi* adhesion and invasion in human cells.<sup>20</sup> In the present study, we demonstrated the expression of Gal-3 in different cell populations and its role in the promotion

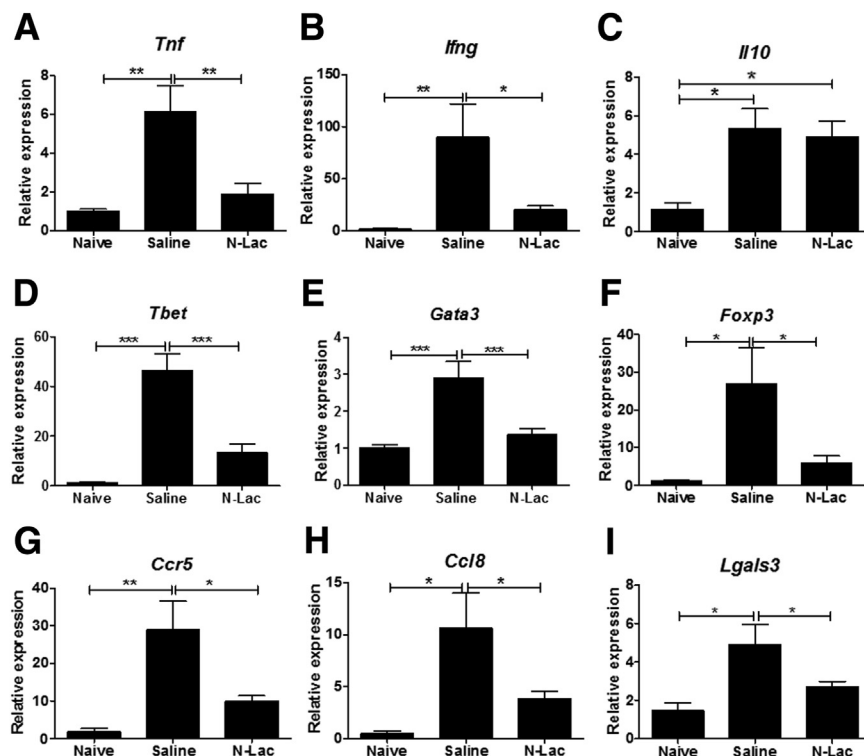


**Figure 6** Modulation of gene expression in chagasic heart after N-Lac treatment. real-time RT-PCR analysis of gene expression in the heart tissue demonstrates that N-Lac treatment is associated with a reduction of inflammatory cytokines tumor necrosis factor (TNF)- $\alpha$  (A) and interferon (IFN)- $\gamma$  (B), and does not alter the expression of IL-10 (C), when compared to saline-treated mice. T-lymphocyte subtype-specific transcription factors associated with type 1 helper T cell (T-bet; D), type 2 helper T cell (GATA-3; E), and T regulatory cell (FOXP3; F) are reduced in N-Lac-treated mice. The expression of genes associated with leukocyte migration and chemotaxis CCR5 (G), chemokine ligand 8 (H), and Gal-3 (I) is also reduced after N-Lac treatment. Data are expressed as means  $\pm$  SEM. \* $P < 0.05$ , \*\* $P < 0.01$ , and \*\*\* $P < 0.001$ .

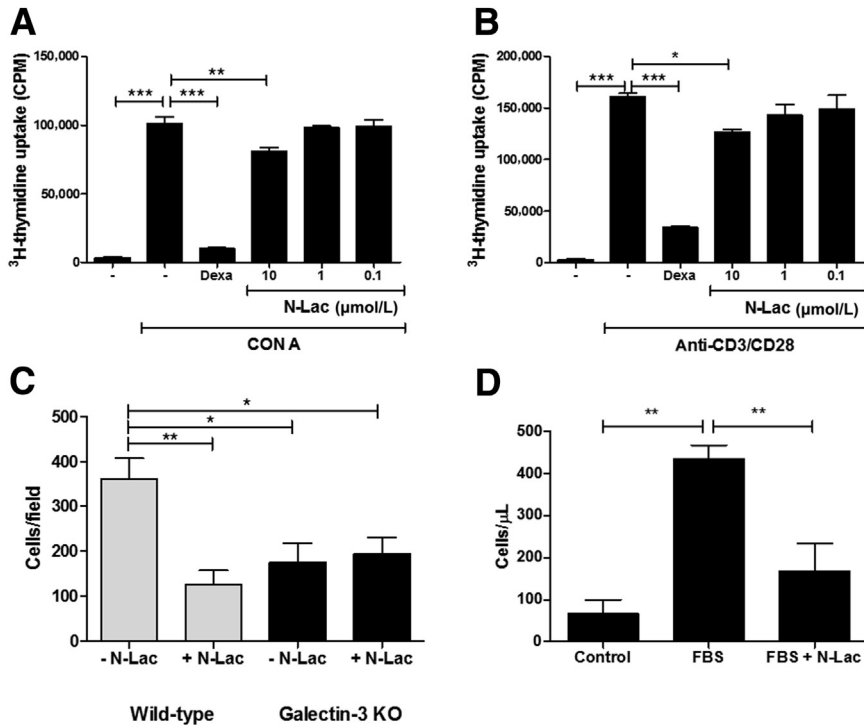


**Figure 7** Effects of N-Lac on splenocyte proliferation and migration *in vitro*. Mouse splenocytes obtained from naïve C57Bl/6 mice were stimulated with concanavalin A (Con A; **A**) or anti-CD3/CD28 (**B**) in the absence or presence of N-Lac or dexamethasone (Dexa; 10  $\mu\text{mol/L}$ ). Lymphoproliferation was assessed by <sup>3</sup>H-thymidine uptake. **C:** *En face* adhesion assay was performed using aorta fragments and splenocytes from wild-type or Gal-3 knockout mice, in the absence or presence of N-Lac. Data show the frequency of adherent cells 30 minutes after incubation. **D:** Mouse splenocytes were submitted to starvation and placed in the upper compartment of a transwell system in the presence or absence of 10  $\mu\text{mol/L}$  N-Lac. Medium with or without fetal bovine serum (FBS) was placed in the lower chamber as a chemoattractant. Cell concentration in the lower chamber after overnight incubation. Data are expressed as means  $\pm$  SEM (**A–D**). \* $P < 0.05$ , \*\* $P < 0.01$ , and \*\*\* $P < 0.001$ . CPM, counts per minute.

of heart inflammation and fibrosis in *T. cruzi*-infected mice. This was achieved by the following: i) immunostaining in chronic Chagas disease human and mouse heart samples showing the presence of Gal-3<sup>+</sup> cells, including macrophages, T cells, fibroblasts, and fibrocytes; ii) blockade of Gal-3 expression in cardiac fibroblasts, showing its role on proliferation and collagen production; and iii) pharmacological blockade *in vivo* in the experimental model, showing significant reduction of inflammation, fibrosis, and production of key inflammatory mediators in the heart.

Previous studies have highlighted a role for Gal-3 in the cardiac remodeling process in different experimental settings, including experimental models of hypertrophic cardiomyopathy and myocardial infarction.<sup>12–14</sup> These reports have focused on Gal-3 effects in cardiac fibroblasts, contributing to cell survival, proliferation, and extracellular matrix synthesis. In CCC, however, a massive infiltration of immune cells is observed in the heart, which leads to persistent immune-mediated myocyte damage, ultimately triggering a progressive fibrogenic response.<sup>6–9</sup>

In the present study, we demonstrated the dynamic expression of Gal-3 in different periods during *T. cruzi* experimental infection and correlated with the findings of human heart analysis, in sections obtained from hearts of subjects with end-stage heart failure due to CCC. Gal-3 expression was observed in a similar pattern in human and mouse heart samples, mainly in areas of inflammatory infiltrates. Gal-3 has been previously described in immune cells and to participate in different aspects of innate and adaptive immune responses.<sup>21–26</sup> In the experimental model, we showed expression of Gal-3 in macrophages and

T cells, two main cell types present in the inflammatory foci in Chagas disease hearts. Moreover, we demonstrated that inflammatory stimuli increase the expression of Gal-3 in macrophages *in vitro*. Because IFN- $\gamma$  and tumor necrosis factor- $\alpha$  are produced in mouse hearts chronically infected with *T. cruzi*, their action may account for the increased Gal-3 expression in macrophages. The described roles for Gal-3 in T-cell biology include the promotion of cell survival, proliferation, T-cell receptor signaling, and migration.<sup>27</sup> In our study, we observed reduction of cell adhesion to endothelium and migration, but not of lymphocyte proliferation, by the Gal-3 inhibitor N-Lac, suggesting that the reduction of inflammation in the hearts of infected mice after N-Lac treatment is mainly because of reduction of cell migration.

In our study, we found that *T. cruzi* infection also increased the expression of Gal-3 in cardiac fibroblasts and, even more intensely, in a population of bone marrow-derived fibrocytes. Although cardiac fibroblasts have been classically described as the most important cell type involved in cardiac fibrosis, different studies have shown that bone marrow-derived fibrocytes play relevant roles in fibrogenesis and remodeling.<sup>28–30</sup> Our data provided from *in vitro* assays in cardiac fibroblasts demonstrated the role of exogenous and endogenous Gal-3 in cell survival, proliferation, and type I collagen synthesis, which is supported by the current literature.<sup>12–14</sup> The fact that extracellular Gal-3 increased cell proliferation only in high concentration and the marked reduction of proliferation in Gal-3 knockdown cells indicate that intracellular Gal-3 has a critical role in cell proliferation regulation. Interestingly, Gal-3 has been

previously shown to enhance cyclin D1 promoter activity,<sup>31</sup> correlating with the cell cycle arrest and decreased expression of cyclin D1 gene in Gal-3 knockdown fibroblasts found in our study. The fact that caveolin-1 gene expression was not increased in Gal-3 knockdown cells reinforces a direct action of Gal-3 in the regulation of cyclin D1 gene transcription.

We have previously shown that *Lgals3* gene expression is up-regulated in the hearts of mice during chronic *T. cruzi* infection.<sup>9,16</sup> The correlation between intensity of myocarditis and presence of collagen type I, Gal-3, and  $\alpha$ -smooth muscle actin—positive cells was also seen in a mouse model of *T. cruzi* infection.<sup>32</sup> Gal-3 was implicated in the process of *T. cruzi* invasion.<sup>33</sup> Altogether, these data suggest that Gal-3 is involved in different aspects of the pathogenesis of CCC, from *T. cruzi* infection to immune response, inflammation, and tissue repair. Interestingly, a reduction of Gal-3 expression in the heart was observed accompanying decreased fibrosis and myocarditis after granulocyte colony-stimulating factor treatment or cell therapy in chronically infected mice.<sup>16,34</sup> In the present study, we showed that the Gal-3 pharmacological blockade with N-Lac significantly modulated the immune response in the hearts from CCC mice, reducing migration of immune cells to the myocardium and decreasing the expression of inflammatory type 1 helper T-cell cytokines and markers of type 2 helper T-cell and T regulatory cell lymphocyte subtypes, to the level of naïve control mice. Notably, the anti-inflammatory cytokine IL-10 was increased when compared to naïve mice. This finding, together with the observed reduced levels of *IFNG* and *TNFA* gene expression, demonstrates a potent anti-inflammatory effect of N-Lac. Moreover, N-Lac treatment was associated with a significant reduction of myocardial fibrosis, which is in accordance with a previous report in a different experimental model.<sup>14</sup> Despite the reduction of inflammation and fibrosis, our results did not correlate with any improvement in functional parameters after N-Lac treatment. This finding does not exclude the possibility of long-term beneficial effects of Gal-3 blockade, nor that N-Lac treatment, at an earlier stage of the infection, which may prevent the deterioration of cardiac function.

The strong binding affinity between galectin-3 and N-acetyl-D-lactosamine has been previously reported.<sup>35</sup> Moreover, in previous studies, similar dose and administration regimen of N-acetyl-D-lactosamine were used to block galectin-3 in mouse models of viral myocarditis<sup>36</sup> and hypertensive cardiac remodeling.<sup>14</sup> The reduction of inflammation and fibrosis observed after N-Lac treatment were not observed in mice treated with sucrose in the same dose and regimen. Moreover, pharmacological (by N-Lac) and genetic (gene knockout) blockade of Gal-3 had similar effects in cell adhesion to endothelium, and indicate that N-Lac does not interfere with selectin binding.

In a translational perspective, Gal-3 could be used in the clinical setting as either a novel biomarker or a therapeutic target. Although the identification of novel noninvasive

biomarkers that adequately predict cardiac fibrosis would be highly desired, in a recent report we showed that plasma Gal-3 levels do not correlate with the intensity of fibrosis, as measured by magnetic resonance imaging, in a recently published transversal study in subjects with CCC.<sup>37</sup> Nonetheless, these data do not exclude the possibility of Gal-3 being useful as a biomarker for prognosis determination, which is currently under investigation in chronic heart failure caused by other etiologies.<sup>38</sup> Thus, the conduction of a longitudinal study in Chagas disease subjects would be required to validate the use of plasma Gal-3 as prognosis biomarker.

In conclusion, herein, we demonstrated that Gal-3 plays an important role in the pathogenesis of experimental chronic Chagas disease, acting in different cell compartments and promoting cardiac inflammation and fibrosis. The finding of Gal-3 expression in human heart samples, in a similar pattern as observed in the mouse model, reinforces its potential as a novel target for drug and therapy development for CCC.

## Acknowledgments

We thank Pamela Daltro for technical assistance in the cardiac functional analysis, Didier Trono for pLVTHM lentiviral vector, Dr. Luiz R. Goulart for providing galectin-3 knockout mice, and Drs. Igor Correia de Almeida and Washington Luis Conrado dos Santos for helpful discussions.

## Supplemental Data

Supplemental material for this article can be found at <http://dx.doi.org/10.1016/j.ajpath.2017.01.016>.

## References


- Andrade DV, Gollob KJ, Dutra WO: Acute Chagas disease: new global challenges for an old neglected disease. *PLoS Negl Trop Dis* 2014, 8:e3010
- WHO: Chagas disease in Latin America: an epidemiological update based on 2010 estimates. *Wkly Epidemiol Rec* 2015, 90:33–44
- Bern C, Montgomery SP, Herwaldt BL, Rassi A Jr, Marin-Neto JA, Dantas RO, Maguire JH, Acquatella H, Morillo C, Kirchhoff LV, Gilman RH, Reyes PA, Salvatella R, Moore AC: Evaluation and treatment of Chagas disease in the United States: a systematic review. *JAMA* 2007, 298:2171–2181
- Morillo CA, Marin-Neto JA, Avezum A; BENEFIT Investigators: Randomized trial of Benznidazole for chronic Chagas' cardiomyopathy. *N Engl J Med* 2015, 373:1295–1306
- Burgos JM, Diez M, Vigliano C, Bisio M, Risso M, Duffy T, Cura C, Bruses B, Favaloro L, Leguizamón MS, Lucero RH, Laguens R, Levin MJ, Favaloro R, Schijman AG: Molecular identification of *Trypanosoma cruzi* discrete typing units in end-stage chronic Chagas heart disease and reactivation after heart transplantation. *Clin Infect Dis* 2010, 51:485–495
- Soares MB, Pontes-De-Carvalho L, Ribeiro-Dos-Santos R: The pathogenesis of Chagas' disease: when autoimmune and parasite-specific immune responses meet. *An Acad Bras Cienc* 2001, 73:547–559

7. Bonney KM, Engman DM: Autoimmune pathogenesis of Chagas heart disease: looking back, looking ahead. *Am J Pathol* 2015, 185:1537–1547
8. Gomes JA, Bahia-Oliveira LM, Rocha MO, Martins-Filho OA, Gazzinelli G, Correa-Oliveira R: Evidence that development of severe cardiomyopathy in human Chagas' disease is due to a Th1-specific immune response. *Infect Immun* 2003, 71:1185–1193
9. Soares MB, de Lima RS, Rocha LL, Vasconcelos JF, Rogatto SR, dos Santos RR, Iacobas S, Goldenberg RC, Iacobas DA, Tanowitz HB, de Carvalho AC, Spray DC: Gene expression changes associated with myocarditis and fibrosis in hearts of mice with chronic chagasic cardiomyopathy. *J Infect Dis* 2010, 202:416–426
10. de Boer RA, Voors AA, Muntendam P, van Gilst WH, van Veldhuisen DJ: Galectin-3: a novel mediator of heart failure development and progression. *Eur J Heart Fail* 2009, 11:811–817
11. Krześlak A, Lipińska A: Galectin-3 as a multifunctional protein. *Cell Mol Biol Lett* 2004, 9:305–328
12. Sharma U, Pokharel S, van Brakel TJ, van Berlo JH, Cleutjens JP, Schroen B, André S, Crijns HJ, Gabius HJ, Maessen J, Pinto YM: Galectin-3 marks activated macrophages in failure-prone hypertrophied hearts and contributes to cardiac dysfunction. *Circulation* 2004, 110:3121–3128
13. González GE, Cassaglia P, Noli Truant S, Fernández MM, Wilensky L, Volberg V, Malchiodi EL, Morales C, Gelpi RJ: Galectin-3 is essential for early wound healing and ventricular remodeling after myocardial infarction in mice. *Int J Cardiol* 2014, 176:1423–1425
14. Yu L, Ruyfrok WP, Meissner M, Bos EM, van Goor H, Sanjabi B, van der Harst P, Pitt B, Goldstein II, Koerts JA, van Veldhuisen DJ, Bank RA, van Gilst WH, Silljé HH, de Boer RA: Genetic and pharmacological inhibition of galectin-3 prevents cardiac remodeling by interfering with myocardial fibrogenesis. *Circ Heart Fail* 2013, 6:107–117
15. Chen A, Hou W, Zhang Y, Chen Y, He B: Prognostic value of serum galectin-3 in patients with heart failure: a meta-analysis. *Int J Cardiol* 2015, 182:168–170
16. Soares MBP, Lima RS, Souza BSF, Vasconcelos JF, Rocha LL, dos Santos RR, Iacobas S, Goldenberg RC, Lisanti MP, Iacobas DA, Tanowitz HB, Spray DC, Campos-de-Carvalho AC: Reversion of gene expression alterations in hearts of mice with chronic chagasic cardiomyopathy after transplantation of bone marrow cells. *Cell Cycle* 2011, 10:1448–1455
17. Committee for the Update of the Guide for the Care and Use of Laboratory Animals; National Research Council: *Guide for the Care and Use of Laboratory Animals: Eighth Edition*. Washington, DC, National Academies Press, 2011
18. Wiznerowicz M, Trono D: Conditional suppression of cellular genes: lentivirus vector-mediated drug-inducible RNA interference. *J Virol* 2003, 77:8957–8961
19. Karasuyama H, Melchers F: Establishment of mouse cell lines which constitutively secrete large quantities of interleukins 2, 3, 4, or 5 using modified cDNA expression vectors. *Eur J Immunol* 1988, 18:97–104
20. Kleshchenko YY, Moody TN, Furtak VA, Ochieng J, Lima MF, Villalta F: Human galectin-3 promotes *Trypanosoma cruzi* adhesion to human coronary artery smooth muscle cells. *Infect Immun* 2004, 72:6717–6721
21. Henderson NC, Sethi T: The regulation of inflammation by galectin-3. *Immunol Rev* 2009, 230:160–171
22. Hsu DK, Yang RY, Pan Z, Yu L, Salomon DR, Fung-Leung WP, Liu FT: Targeted disruption of the galectin-3 gene results in attenuated peritoneal inflammatory responses. *Am J Pathol* 2000, 156:1073–1083
23. Jeon SB, Yoon HJ, Chang CY, Koh HS, Jeon SH, Park EJ: Galectin-3 exerts cytokine-like regulatory actions through the JAK-STAT pathway. *J Immunol* 2010, 185:7037–7046
24. MacKinnon AC, Farnworth SL, Hodkinson PS, Henderson NC, Atkinson KM, Leffler H, Nilsson UJ, Haslett C, Forbes SJ, Sethi T: Regulation of alternative macrophage activation by galectin-3. *J Immunol* 2008, 180:2650–2658
25. Yang RY, Hsu DK, Liu FT: Expression of galectin-3 modulates t-cell growth and apoptosis. *Proc Natl Acad Sci U S A* 1996, 93:6737–6742
26. Chen SS, Sun LW, Brickner H, Sun PQ: Downregulating galectin-3 inhibits proinflammatory cytokine production by human monocyte-derived dendritic cells via RNA interference. *Cell Immunol* 2015, 294:44–53
27. Tribulatti MV, Figini MG, Carabelli J, Cattaneo V, Campetella O: Redundant and antagonistic functions of galectin-1, -3, and -8 in the elicitation of t cell responses. *J Immunol* 2012, 188:2991–2999
28. Chu PY, Mariani J, Finch S, McMullen JR, Sadoshima J, Marshall T, Kaye DM: Bone marrow-derived cells contribute to fibrosis in the chronically failing heart. *Am J Pathol* 2010, 176:1735–1742
29. van Amerongen MJ, Bou-Gharios G, Popa E, van Ark J, Petersen AH, van Dam GM, van Luyn MJ, Harmsen MC: Bone marrow-derived myofibroblasts contribute functionally to scar formation after myocardial infarction. *J Pathol* 2008, 214:377–386
30. Haudek SB, Cheng J, Du J, Wang Y, Hermosillo-Rodriguez J, Trial J, Taffet GE, Entman ML: Monocytic fibroblast precursors mediate fibrosis in angiotensin-II-induced cardiac hypertrophy. *J Mol Cell Cardiol* 2010, 49:499–507
31. Lin HM, Pestell RG, Raz A, Kim HR: Galectin-3 enhances cyclin d(1) promoter activity through sp1 and a camp-responsive element in human breast epithelial cells. *Oncogene* 2002, 21:8001–8010
32. Ferrer MF, Pascuale CA, Gomez RM, Leguizamón MS: DTU I isolates of *Trypanosoma cruzi* induce upregulation of galectin-3 in murine myocarditis and fibrosis. *Parasitology* 2014, 141:849–858
33. Machado FC, Cruz L, da Silva AA, Cruz MC, Mortara RA, Roque-Barreira MC, da Silva CV: Recruitment of galectin-3 during cell invasion and intracellular trafficking of *Trypanosoma cruzi* extracellular amastigotes. *Glycobiology* 2014, 24:179–184
34. Vasconcelos JF, Souza BS, Lins TF, Garcia LM, Kaneto CM, Sampaio GP, de Alcântara AC, Meira CS, Macambira SG, Ribeiro-dos-Santos R, Soares MB: Administration of granulocyte colony-stimulating factor induces immunomodulation, recruitment of T regulatory cells, reduction of myocarditis and decrease of parasite load in a mouse model of chronic Chagas disease cardiomyopathy. *FASEB J* 2013, 27:4691–4702
35. von Mach T, Carlsson MC, Straube T, Nilsson U, Leffler H, Jacob R: Ligand binding and complex formation of galectin-3 is modulated by pH variations. *Biochem J* 2014, 457:107–115
36. Jaquenod De Giusti C, Ure AE, Rivadeneyra L, Schattner M, Gomez RM: Macrophages and galectin 3 play critical roles in CVB3-induced murine acute myocarditis and chronic fibrosis. *J Mol Cell Cardiol* 2015, 85:58–70
37. Noya-Rabelo MM, Larocca TF, Macêdo CT, Torreão JA, Souza BS, Vasconcelos JF, Souza LE, Silva AM, Ribeiro Dos Santos R, Correia LC, Soares MB: Evaluation of Galectin-3 as a novel biomarker for Chagas cardiomyopathy. *Cardiology* 2017, 136:33–39
38. Peacock WF: How galectin-3 changes acute heart failure decision making in the emergency department. *Clin Chem Lab Med* 2014, 52:1409–1412

## ANEXO IV

VASCONCELOS, J.F; MEIRA, C.S; **SILVA, D.N**; NONAKA, C.K.V; DALTRO, P.S; MACAMBIRA, S. G; DOMIZI, P.D; BORGES, V.M; DOS-SANTOS, R.R; SOUZA, B.S; SOARES, M.B.P. Therapeutic effects of sphingosine kinase inhibitor N,N-dimethylsphingosine (DMS) in experimental chronic Chagas disease cardiomyopathy. **Scientific reports**, v. 7, 2017.

# SCIENTIFIC REPORTS



OPEN

## Therapeutic effects of sphingosine kinase inhibitor N,N-dimethylsphingosine (DMS) in experimental chronic Chagas disease cardiomyopathy

Juliana Fraga Vasconcelos<sup>1,2,3</sup>, Cássio Santana Meira<sup>1,2</sup>, Daniela Nascimento Silva<sup>2</sup>, Carolina Kymie Vasques Nonaka<sup>2</sup>, Pâmela Santana Daltró<sup>2</sup>, Simone Garcia Macambira<sup>2,4</sup>, Pablo Daniel Domizi<sup>5</sup>, Valéria Matos Borges<sup>1</sup>, Ricardo Ribeiro-dos-Santos<sup>2</sup>, Bruno Solano de Freitas Souza<sup>1,2</sup> & Milena Botelho Pereira Soares<sup>1,2</sup>

Chagas disease cardiomyopathy is a parasite-driven inflammatory disease to which there are no effective treatments. Here we evaluated the therapeutic potential of N,N-dimethylsphingosine(DMS), which blocks the production of sphingosine-1-phosphate(S1P), a mediator of cellular events during inflammatory responses, in a model of chronic Chagas disease cardiomyopathy. DMS-treated, *Trypanosoma cruzi*-infected mice had a marked reduction of cardiac inflammation, fibrosis and galectin-3 expression when compared to controls. Serum concentrations of galectin-3, IFN $\gamma$  and TNF $\alpha$ , as well as cardiac gene expression of inflammatory mediators were reduced after DMS treatment. The gene expression of M1 marker, iNOS, was decreased, while the M2 marker, arginase1, was increased. DMS-treated mice showed an improvement in exercise capacity. Moreover, DMS caused a reduction in parasite load *in vivo*. DMS inhibited the activation of lymphocytes, and reduced cytokines and NO production in activated macrophage cultures *in vitro*, while increasing IL-1 $\beta$  production. Analysis by qRT-PCR array showed that DMS treatment modulated inflammasome activation induced by *T. cruzi* on macrophages. Altogether, our results demonstrate that DMS, through anti-parasitic and immunomodulatory actions, can be beneficial in the treatment of chronic phase of *T. cruzi* infection and suggest that S1P-activated processes as possible therapeutic targets for the treatment of Chagas disease cardiomyopathy.

The pathological manifestations of chronic Chagas disease, caused by *Trypanosoma cruzi* infection, both in the cardiac and in the digestive form, are associated with the occurrence of an inflammatory reaction<sup>1</sup>. Chronic Chagas disease cardiomyopathy (CCC) involves cardiac myocytes undergoing necrosis and cytolysis via various mechanisms, and areas of myocellular hypertrophy and mononuclear cell infiltration occur<sup>2-4</sup>. In response to the myocardial damage, fibrotic areas occur and may contribute to the disruption of the cardiac conduction system and appearance of dysrhythmias, as well as to myocardial thinning and cardiac hypertrophy<sup>5</sup>. Given the lack of an effective specific therapy, CCC is treated similarly to all other heart failure syndromes using therapies to mitigate symptoms<sup>6</sup>. Therefore, the development of new alternative treatments for CCC is needed.

<sup>1</sup>Instituto Gonçalo Moniz, Fundação Oswaldo Cruz, FIOCRUZ, Salvador, BA, 40296-710, Brazil. <sup>2</sup>Centro de Biotecnologia e Terapia Celular, Hospital São Rafael, Salvador, BA, 41253-190, Brazil. <sup>3</sup>Escola de Ciências da saúde, Universidade Salvador, Salvador, BA, 41720-200, Brazil. <sup>4</sup>Departamento de Bioquímica e Biofísica, Instituto de Ciências da Saúde, Universidade Federal da Bahia, Salvador, BA, 40110-100, Brazil. <sup>5</sup>Centro de Ciências da Saúde, Instituto de Biofísica Carlos Chagas Filho, Universidade Federal do Rio de Janeiro, Rio de Janeiro, RJ, 21944-970, Brazil. Juliana Fraga Vasconcelos and Cássio Santana Meira contributed equally to this work. Correspondence and requests for materials should be addressed to M.B.P.S. (email: [milena@bahia.fiocruz.br](mailto:milena@bahia.fiocruz.br))



Sphingolipid metabolites are emerging as important lipid signaling molecules in both health and disease<sup>7</sup>. Among them, sphingosine-1-phosphate (S1P), produced by phosphorylation of sphingosine (Sph) by sphingosine kinases (SphK1 and SphK2) in response to various stimuli, plays important roles in several cellular processes, including cell growth and cell trafficking<sup>8,9</sup>. The balance of Sph and S1P determines the progress of many diseases and there is evidence that sphingolipid metabolism and the expression of S1P receptors (S1PR1-5) are altered in inflammatory processes<sup>10</sup>. S1P drives the differentiation of different immune cell types, inducing changes in their functional phenotypes and regulating production of pro-inflammatory cytokines and eicosanoids. In particular, S1P has emerged as a central regulator of lymphocyte egress<sup>11,12</sup>.

Due to the persistent inflammation found in CCC, which is a hallmark of the disease, and the critical role of S1P-activated pathways on the regulation of inflammation, we hypothesized that N,N-dimethylsphingosine (DMS), a pan SphK inhibitor, has a beneficial effect in chronic Chagas disease. Thus, in the present study we investigated the effects of DMS in a murine model of chronic Chagas disease cardiomyopathy, as well as its mechanisms of action on *in vitro* assays.

## Results

**Treatment with DMS reduces heart inflammation and fibrosis in *T. cruzi*-infected mice.** Groups of mice chronically infected with *T. cruzi* were treated with DMS or vehicle (saline) (Fig. 1A). Inflammation and fibrosis were evaluated in heart sections two months after the first dose. A diffuse inflammatory response, mainly composed of mononuclear cells, was found in saline-treated infected controls (Fig. 1B). Administration of DMS caused a marked reduction in the number of inflammatory cells, which was statistically significant when compared to vehicle-treated mice (Fig. 1B,C). Gene expression of CD45, a pan-leukocyte marker, which was increased in *T. cruzi* infected mice treated with saline, was also significantly reduced after DMS treatment (Fig. 1D). Similarly, heart sections from DMS-treated mice had a reduced percentage of fibrosis when compared with vehicle-treated mice (Fig. 1B,E).

**Galectin-3 reduction in the heart and sera of chagasic mice after DMS treatment.** We have previously shown the overexpression of galectin-3 in the hearts of chronic chagasic mice<sup>13</sup>. To evaluate the effects of DMS on the expression of this important mediator of inflammation and fibrosis, we performed confocal microscopy analysis in the heart tissue. Vehicle-treated, *T. cruzi*-infected mice had a high expression of galectin-3, while a reduction of galectin-3 expression was seen after DMS treatment (Fig. 1B). Morphometrical analyses revealed a statistically significant difference between the groups (Fig. 1F). Moreover, DMS treatment also caused a significant reduction in the concentration of galectin-3 in the serum of *T. cruzi*-infected mice (Fig. 2C), as well as in the expression of galectin-3 gene in the hearts (Fig. 3A).

**DMS administration modulates the production of inflammatory mediators in *T. cruzi*-infected mice.** CCC has been associated with an increase of IFN $\gamma$  and TNF $\alpha$  production in mice, as well as in humans<sup>14,15</sup>. We observed, both in the sera as well as in the heart, an up regulation in the expression of these two proinflammatory cytokines in the saline-treated chagasic mice, compared to uninfected mice (Figs 2 and 3). The administration of DMS promoted a significant reduction in the concentrations of both cytokines in the sera (Fig. 2A,B), as well as in the expression of their genes in the heart tissue (Fig. 3B,C). We also investigated the production of regulatory cytokines IL-10 and TGF $\beta$ , which are increased in *T. cruzi*-infected mice. TGF $\beta$  concentrations in the sera were similar in both vehicle and DMS-treated infected groups, and increased compared to naive mice (Fig. 2D). The expression of IL-10 gene in the hearts, also increased by *T. cruzi* infection, was reduced after DMS treatment compared to saline group (Fig. 3D). Since macrophages are one of the main cell populations composing the heart inflammatory infiltrate in Chagas disease<sup>15</sup>, we investigated the expression of genes associated with macrophage activation. IL-1 $\beta$  expression in the heart was found to be increased by *T. cruzi* infection and significantly reduced by DMS treatment (Fig. 3F). The expression of iNOS, a marker of M1 activation increased in the hearts of *T. cruzi*-infected mice, was reduced after DMS treatment (Fig. 3G). When M2 activation markers were analyzed, we observed an up regulation of Arg1 gene expression after DMS, while CHI3 was down-regulated in the hearts of DMS-treated mice, when compared to saline-treated controls (Fig. 3H,I).

**DMS improves exercise capacity, reduces parasitism but does not ameliorate cardiac electric disturbances.** The exercise capacity of the experimental groups was evaluated before and after treatment. *T. cruzi*-infected mice ran less time and smaller distance when compared to naive controls (Fig. 4A,B). DMS-treated mice, however, showed a better performance in the treadmill test when compared to saline-treated controls. The majority of *T. cruzi*-infected mice presented severe cardiac conduction disturbances in the EKG records, such as AV blockage, intraventricular conduction disturbances and abnormal cardiac rhythm, six months after infection. At the end of treatment, no improvements were observed in DMS-treated mice, and all *T. cruzi*-infected mice aggravated the conduction disturbances during the observed time (Table 1). To investigate whether the anti-inflammatory response induced by DMS treatment affected the immune response against the parasite, we analyzed the residual *T. cruzi* infection by qRT-PCR in the spleens of infected mice. As shown in Fig. 4C, a significant reduction of parasite load was observed in DMS-treated mice compared to saline-treated controls.

**Modulation of lymphocyte and macrophage functions *in vitro* by DMS.** The inflammatory infiltrate in the hearts of *T. cruzi*-infected mice is mainly composed by T lymphocytes and macrophages<sup>15</sup>. Thus, we tested the effects of DMS *in vitro* in these two cell populations. To investigate whether DMS can directly modulate the activation of lymphocytes, we assessed the proliferation of splenocytes stimulated by concanavalin A (Con A) or anti-CD3 plus anti-CD28. A concentration-dependent inhibition of lymphoproliferation was seen when DMS was added to the cultures (See Supplementary Fig. S1A and B). Additionally, the production of IL-2 and IFN $\gamma$  upon Con A stimulation was significantly reduced by DMS (See Supplementary Fig. S1C and D). Dexamethasone,

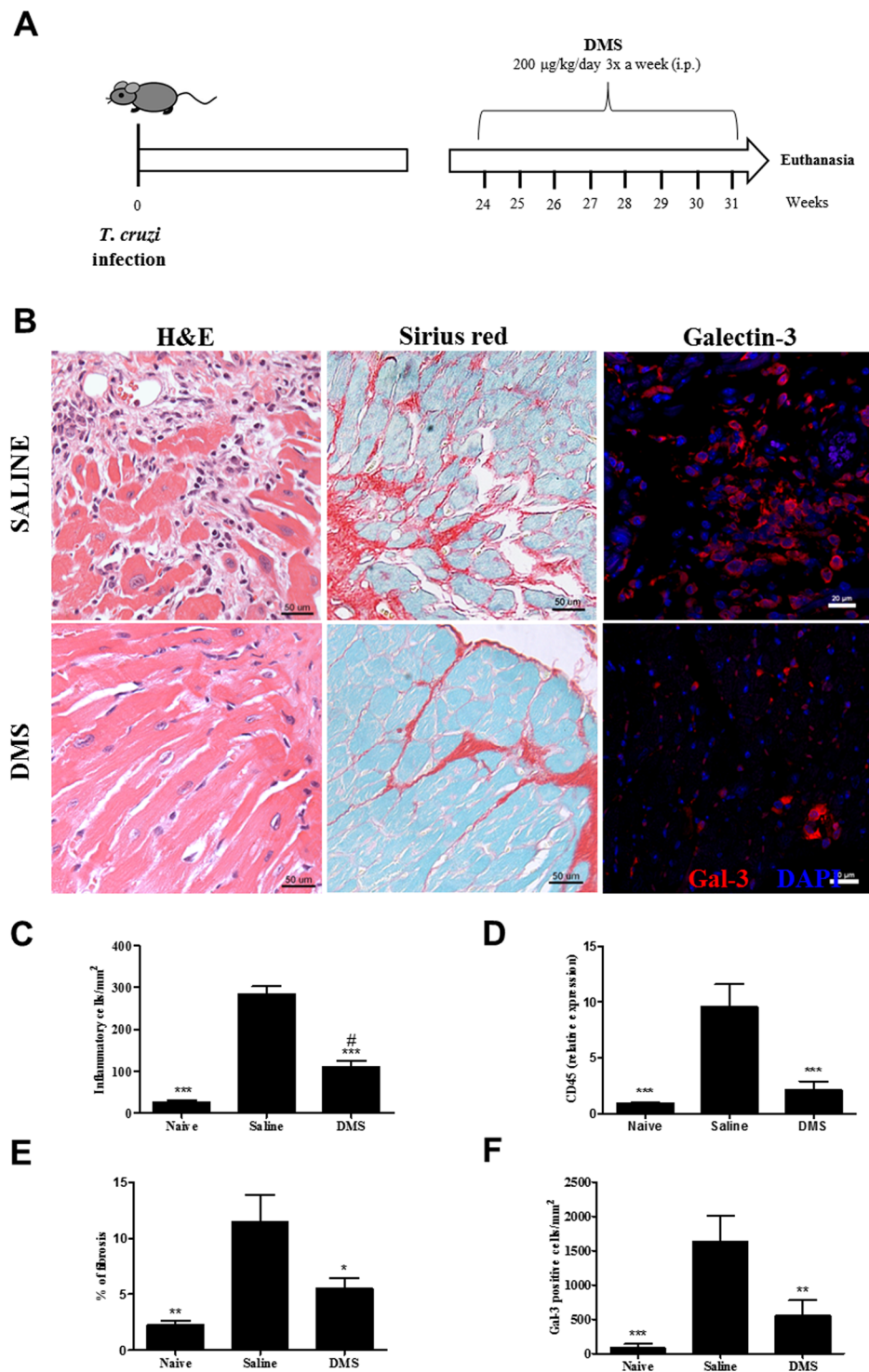


**Figure 1.** Reduction of inflammation, fibrosis and galectin-3 was found in the hearts of DMS-treated mice. (A) Experimental design of *in vivo* treatment. C57BL/6 mice infected with trypomastigotes (Colombian strain) were treated during the chronic phase of infection (6 months post-infection) with DMS (200 µg/Kg/day; 3x week; i.p.). (B) Microphotographs of heart sections stained with hematoxylin and eosin or sirius red or anti-galectin-3 (1:50; red) and DAPI (blue). (C) Inflammatory cells were quantified in heart sections of naive mice, saline-treated chagasic mice, or DMS-treated chagasic mice and integrated by area. (D) The expression of CD45 was evaluated by real-time qRT-PCR using cDNA samples prepared from mRNA extracted from hearts of experimental groups. (E) Fibrotic area is represented by percentage of collagen deposition in heart sections. (F) Quantifications of galectin-3<sup>+</sup> cells in heart sections were performed in ten random fields captured under 400x magnification, using the Image Pro Plus v.7.0 software. Bars represent means ± SEM of 10 mice/group. \*\*\**P* < 0.001; \*\**P* < 0.01; \**P* < 0.05 compared to saline group; #*P* < 0.05 compared to naive group.

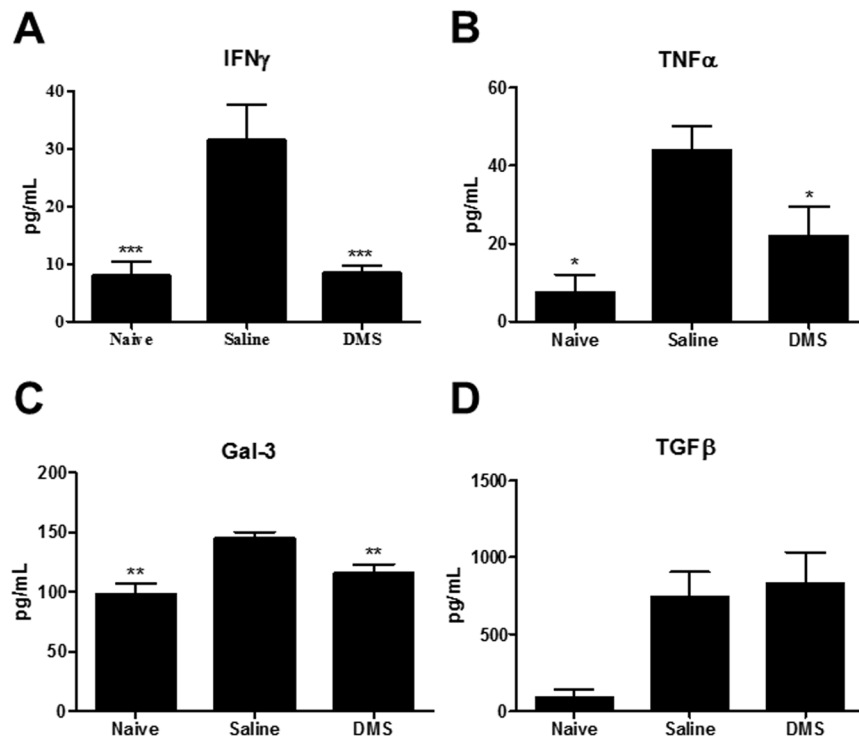


**Figure 2.** Modulation of systemic cytokine production in chronic chagasic mice treated with DMS. Concentrations of IFN $\gamma$  (A), TNF $\alpha$  (B), Gal-3 (C) and TGF $\beta$  (D) in the sera from naive and chagasic mice treated with saline or DMS. Values represent means  $\pm$  SEM of 10 mice/group. \*\*\* $P < 0.001$ ; \*\* $P < 0.01$ ; \* $P < 0.05$  compared to saline group.

a known immunosuppressive agent, reduced proliferation and cytokine production (See Supplementary Fig. S1). Moreover, the addition of DMS to macrophage cultures activated by LPS plus IFN $\gamma$  caused an increase in IL-1 $\beta$  production (See Supplementary Fig. S2A). In contrast, the production of other inflammatory mediators, such as TNF $\alpha$ , IL-6, IL-10 and nitric oxide was reduced in a concentration-dependent manner (See Supplementary Fig. S2B–E). NF- $\kappa$ B activation participates in the regulation of several pro-inflammatory genes, including TNF $\alpha$ . To investigate whether DMS acted through the modulation of NF- $\kappa$ B activation, we performed an assay using RAW cells transduced with a reporter gene under the control of a promoter regulated by NF- $\kappa$ B. As shown in Supplementary Fig. S2F, DMS at 10 and 5  $\mu$ M caused about 20% reduction of luciferase activity induced by activation with LPS and IFN $\gamma$ . To understand if DMS effects in macrophages has off-targets effects by the inhibition of PKC and MAPK, we tested the action of DMS in the presence of specific inhibitors of ERK-1/2 (PD98059) and MAPK (BIS). The inhibition of IL-6 and iNOS production by DMS was not affected by the inhibitors (See Supplementary Fig. S2G and H).

**Antiparasitic effects of DMS *in vitro*.** To investigate the mechanisms by which DMS caused the reduction on parasite load *in vivo*, we evaluated the antiparasitic activity of DMS *in vitro*. To determine whether DMS acts directly on the parasite, we analyzed the effects of DMS on *T. cruzi* trypomastigote cultures (Table 2). Addition of DMS at various concentrations in axenic cultures of *T. cruzi* trypomastigotes allowed the determination of the EC<sub>50</sub> value at 1.98  $\mu$ M, while benznidazole presented an EC<sub>50</sub> of 12.53. Regarding the cytotoxicity of DMS, we determined the CC<sub>50</sub> in mouse macrophage cultures at 9.02  $\mu$ M. Next, we investigated the mechanisms of cell death in trypomastigotes forms of *T. cruzi* induced by DMS, by flow cytometry analysis. Incubation with DMS induced apoptosis of trypomastigotes in a concentration-dependent manner, as shown by the increase in annexin positive cells (see Supplementary Fig. S3). Furthermore, we evaluated the morphology and ultrastructure of trypomastigotes incubated with DMS. Compared with untreated trypomastigotes, parasites exposed to DMS for 24 h exhibited the formation of numerous and atypical vacuoles within the cytoplasm, a large loss of density degeneration of mitochondria and intense vacuolization (Fig. 5A–E). Interestingly, we also observed the presence of myelin-like figures within the cytoplasm (Fig. 5F), which is suggestive of parasite starvation or autophagy induced by DMS. The antiparasitic effects of DMS on the intracellular form of the parasite were also investigated. Macrophages infected *in vitro* by *T. cruzi* had a concentration-dependent reduction in the number of amastigotes and in percentage of infection (Fig. 6A,B). DMS at 5  $\mu$ M presented a similar effect when compared to benznidazole, a standard anti-*T. cruzi* chemotherapy agent (Fig. 6A,B). *T. cruzi*-infected macrophage cultures had an increased production of nitric oxide (Fig. 6C). Addition of DMS caused a concentration-dependent increase of nitric oxide by infected macrophages (Fig. 6C). The transcription of inducible nitric oxide synthase (iNOS) gene, however, was not altered by DMS treatment (Fig. 6D). We also evaluated the production of reactive oxygen species (ROS) in *T. cruzi*-infected macrophage cultures. DMS induced a concentration-dependent increase of ROS

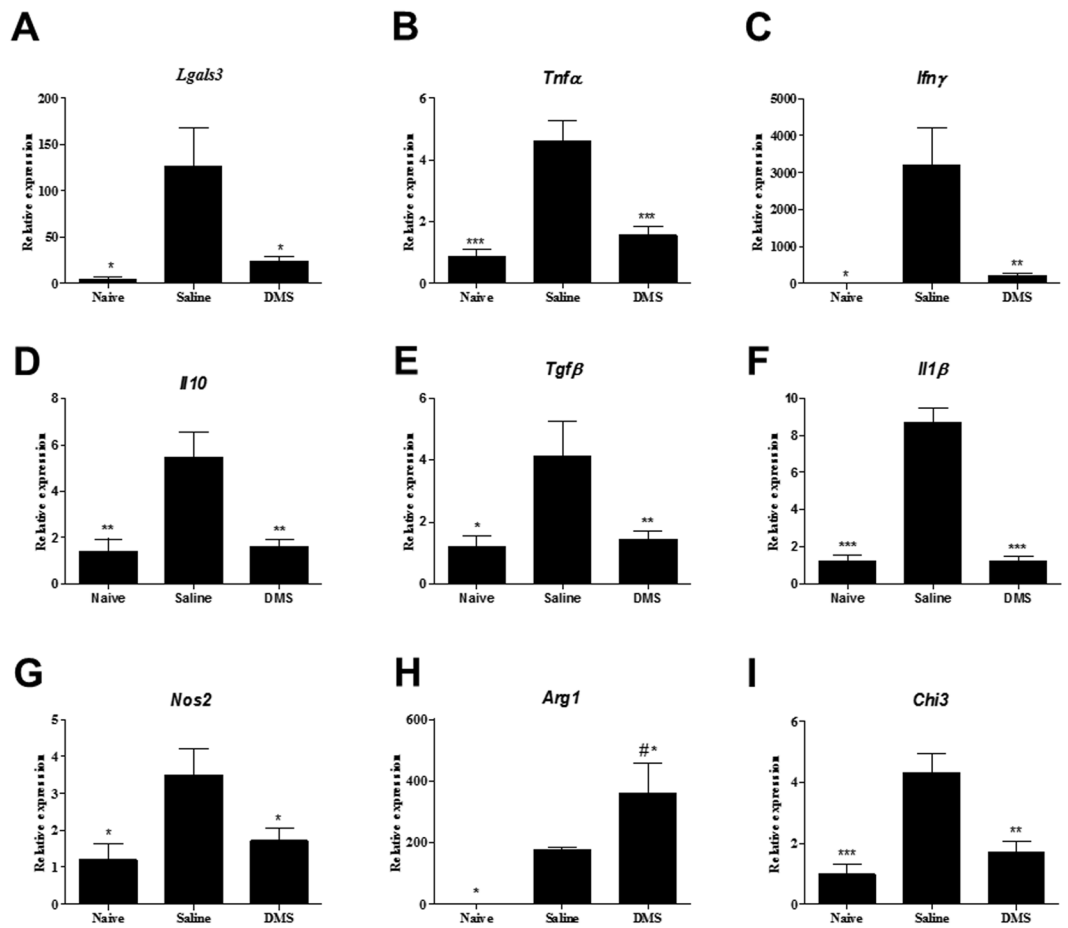


**Figure 3.** Gene expression in the hearts of infected mice after DMS treatment. Analysis of gene expression was performed by real-time qRT-PCR using cDNA samples prepared from mRNA extracted from hearts of naive and chronic Chagasic mice treated with saline or DMS. (A) Gal-3, (B) TNF $\alpha$ , (C) IFN $\gamma$ , (D) IL-10, (E) TGF $\beta$ , (F) IL-1 $\beta$ , (G) NOS2, (H) ARG1 and (I) CHI3 gene expression. Bars represent means  $\pm$  SEM of 10 mice/group. \*\*\* $P < 0.001$ ; \*\* $P < 0.01$ ; \* $P < 0.05$  compared to saline group; # $P < 0.05$  compared to naive group.

(Fig. 6E), as well as the transcription factor NFE2I2, which regulates the expression of key protective enzymes against ROS (Fig. 6F). Additionally, the gene expression of catalase and superoxide dismutase 1, two enzymes involved in ROS degradation, was increased by DMS treatment (Fig. 6G,H).

**Activation of inflammasome pathways in *T. cruzi*-infected macrophages.** *T. cruzi*-infected macrophages incubated with DMS increased IL-1 $\beta$  production, in a concentration-dependent manner (Fig. 6I), suggesting involvement of an inflammasome pathway activation. To confirm that DMS induced inflammasome activation in *T. cruzi*-infected macrophages, we performed a caspase 1 activity assay. Addition of DMS (5  $\mu$ M) to *T. cruzi*-infected macrophages significantly increased the activation of caspase 1, whereas infection by *T. cruzi* alone induced a slight increase of caspase 1 activity (Fig. 6J). The effects of DMS on caspase 1 activation were abrogated by the addition of the caspase 1 inhibitor YVAD (Fig. 6J). To evaluate the regulation of inflammasome pathways by DMS, we performed a qRT-PCR array for inflammasome, including genes involved in innate immunity and NOD-like receptor (NLR) signaling. Macrophages infected with *T. cruzi* for 24 h were incubated with DMS (5  $\mu$ M) during 1 and 24 h and total RNA was extracted for gene expression analysis, compared to uninfected macrophage cultures (see Supplementary Tables 1–7). *T. cruzi* infection alone activated the transcription of genes related to inflammasome pathways, including *Nlrp3*, as well as several genes coding for chemokines and cytokines. Additionally, several genes related to signaling transduction pathways, including Mapk and NF- $\kappa$ B pathway were upregulated (Fig. 7A). Analysis using the reactome pathway database highlighted the main pathways activated by *T. cruzi* infection, which include immune system related genes, NF- $\kappa$ B and TLR pathways (Fig. 8A). The transcription of 17 genes were regulated by *T. cruzi* infection at the two time points evaluated. When changes in *T. cruzi*-infected macrophages at the two time points were compared, we found the expression of 15 genes altered only at 1 h time point (25 h of infection), whereas 2 genes were found altered only at 24 h time point (48 h of infection) (Fig. 7A). DMS treatment alone (24 h) did not induce any gene transcription change (see Supplementary Table S1). When *T. cruzi*-infected macrophages treated or not with DMS were compared, however, we found that DMS treatment suppressed the *T. cruzi* upregulated expression of *Mapk13* (Fig. 7C), *Il6*, *Il33*, *Nfkbib* and *Nlrp1a* (Fig. 7D). Additionally, DMS treatment increased the activation of *Nlr5* and *Nlr1* genes,

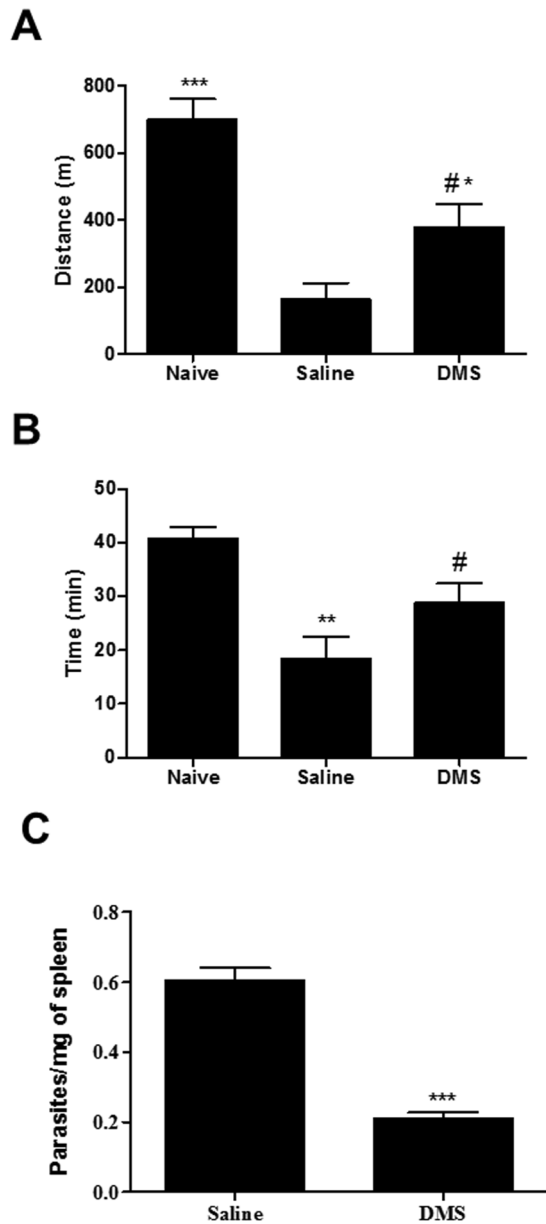


**Figure 4.** Effects of DMS treatment in cardiac function and parasite load. After an adaptation period in the treadmill chamber, naive and saline-treated or DMS-treated chronic Chagasic mice exercised at 5 different velocities (7.2, 14.4, 21.6, 28.8 and 36.0 m/min), with increasing velocity after 5 min of exercise at a given speed. (A) Distance run and (B) Time of exercise on a motorized treadmill. (C) Spleen fragments obtained from normal and *T. cruzi*-infected mice treated with saline or DMS were used for DNA extraction and qRT-PCR analysis for quantification of parasite load (primer 1 5'-GTTTCACACACTGGACACCAA-3' and primer 2 5'-TCGAAAACGATCAGCCGAST-3'). The standard curve of DNA ranged from  $4.7 \times 10^{-1}$  to  $4.7 \times 10^6$ ). Bars represent means  $\pm$  SEM of 8–10 mice/group. \*\*\* $P < 0.001$ ; \*\* $P < 0.01$ ; \* $P < 0.05$  compared to saline group; # $P < 0.05$  compared to naive group.

and had an increasing trend of expression of *Nlrp4*, *Nlrp5*, *Nlrp6*, *Nlrp9* genes when compared to *T. cruzi*-infected cells (Fig. 7B). Analysis using the reactome pathway database showed that, in addition to the pathways induced by *T. cruzi* infection, DMS treatment favoured the activation of RIG and NOD signaling pathways (Fig. 8B).

## Discussion

Persistent inflammation is one of the hallmarks of chronic Chagas disease cardiomyopathy, and leads to a progressive destruction of the myocardium and heart dysfunction<sup>5,6</sup>. Therefore, the development of therapeutic strategies aiming at modulation of inflammation without affecting parasite control is of great interest. Here we show, using a mouse model of chronic Chagas cardiomyopathy which reproduces the pathological findings observed in human hearts, a potent effect of DMS, causing reduction of heart inflammation and fibrosis, modulation of

	NSR		1 <sup>st</sup> AVB		IACD		JR		IVCD		VB		TAVB	
	Pre	Post	Pre	Post	Pre	Post	Pre	Post	Pre	Post	Pre	Post	Pre	Post
CTRL (n = 05)	05	05	—	—	—	—	—	—	—	—	—	—	—	—
INF + Saline (n = 11)	—	—	07	02	—	01	01	—	03	—	01	—	03	06
INF + DMS (n = 11)	03	—	02	01	—	01	02	02	03	—	03	02	02	04

**Table 1.** Number of animals per arrhythmias before treatment (Pre) and at the end of treatment (Post) in naive (CTRL), chronic infected and vehicle-treated (INF + Saline) and chronic infected, DMS-treated (INF + DMS) groups. In infected groups, some animals developed more than one type of arrhythmias. NSR = Normal sinus rhythm, 1<sup>st</sup> AVB = 1<sup>st</sup> degree atrio-ventricular block, IACD = Intra-atrial conduction disturbance, JR = Junctional rhythm, IVCD = Intra-ventricular conduction disturbance, VB = Ventricular bigeminism, TAVB = Total atrio-ventricular dissociation.

Compound	CC <sub>50</sub> MO (μM) <sup>a</sup>	EC <sub>50</sub> Try. (μM) <sup>b</sup>	SI
DMS	9.02 (±0.12)	1.98 (±0.47)	4.5
BDZ	>50	12.53 (±0.55)	>4
GV	0.48 (±0.05)	—	—

**Table 2.** Host cell cytotoxicity and trypanocidal activity of DMS on trypomastigotes forms of *T. cruzi* (Colombian strain). <sup>a</sup>Cell viability of mouse macrophages determined 72 h after treatment. <sup>b</sup>Trypanocidal activity determined 24 h after incubation with compounds. <sup>b</sup>Values represent the mean ± SEM of triplicate. Three independent experiments were performed. EC<sub>50</sub> = effective concentration at 50%. CC<sub>50</sub> = cytotoxic concentration at 50%. BDZ = benznidazole. GV = Gentian violet.

pro-inflammatory mediators and improvement of exercise capacity. Importantly, the residual parasite load found in mice chronically infected with *T. cruzi* was reduced by DMS treatment.

In our study, a marked reduction of inflammation was seen after DMS treatment, as shown by two different analyses, morphometry and qRT-PCR for quantification of CD45 expression. Moreover, the production of IFN $\gamma$  and TNF $\alpha$ , two cytokines known to promote the chronic Chagas myocarditis, were significantly reduced in the heart, as well as in the serum, showing a local and a systemic effect of DMS. The fact that DMS modulates the activation of lymphocytes and macrophages *in vitro* reinforces that, in addition to a reduction of cell migration, a direct effect of the drug on immune cells may cause the potent immunomodulatory effect of DMS observed *in vivo* in our model. In line with this idea, it was recently shown that FTY720, a recently approved drug that inhibits the S1P pathway, also modulates the activation of human T lymphocytes and leads to a reduction of IFN $\gamma$  production<sup>16</sup>.

All of the three major S1P receptor (1–3) subtypes are also expressed in cardiac fibroblasts and participate in cardiac remodeling by the activation of signaling pathways through S1P. Moreover, both FTY720 and DMS have been shown to reduce fibrosis<sup>17–19</sup>. The expression of SphK1 is an important factor regulating the proliferation of cardiac fibroblasts<sup>20</sup>. SphK1-transgenic mice which overproduces endogenous S1P showed 100% occurrence of cardiac fibrosis, involved with activation of the S1P3-Rho family small G protein signaling pathway and increased ROS production<sup>21</sup>. Additionally, DMS-treated mice had a reduced expression of TGF $\beta$  and galectin-3, two pro-fibrogenic factors that stimulate the proliferation and production of extracellular matrix proteins by cardiac fibroblasts<sup>22,23</sup>. Here we observed a reduction on fibrotic area in the heart of DMS-treated mice, corroborating the importance of S1P signaling for heart fibrosis.

An important finding was the antiparasitic effect of DMS, leading to a reduction of parasite load *in vivo*, despite causing a reduction on the production of pro-inflammatory factors, such as IFN $\gamma$  and TNF $\alpha$ , known to play important roles in resistance to *T. cruzi* infection<sup>24,25</sup>. We showed here that DMS has not only a direct effect on the parasite, causing several cellular alterations and death of trypomastigote forms, but also an indirect effect, by inducing the increase of NO and ROS production in infected macrophages *in vitro*. These results are in accordance with a previous report showing S1P down regulating iNOS expression in macrophages through the inhibition of NF- $\kappa$ B, AP-1 and/or STAT-1 activation<sup>26</sup>. This suggests that the inhibition of S1P production by DMS treatment may lead to an increased NO production, also contributing to the *in vivo* antiparasitic mechanisms of DMS.

Chagas disease cardiomyopathy may result from multiple pathological mechanisms, including immune responses against the parasite, as well as self-reactive responses against cardiac antigens<sup>27</sup>. The reduction of parasitism by benznidazole, a drug used to treat Chagas disease, reduces cardiac alterations during the chronic phase of infection<sup>28</sup>. Additionally, the reinforcement of immunological tolerance to myocardial antigens also caused reduction of inflammation in a mouse model of *T. cruzi* infection<sup>29</sup>. Thus, the fact that DMS affects both inflammatory cells as well as the parasite suggests that these effects may contribute to the modulation of inflammation seen after DMS treatment.

SphK is a highly conserved enzyme in eukaryotes, and while there are two isoforms in mammals, only one is found in trypanosomatids. Depletion of *Trypanosoma brucei* SphK causes attenuation of cell division, microtubule elongation at the posterior tip, and altered organelle positioning. SphK inhibitors, such as DMS and safingol,

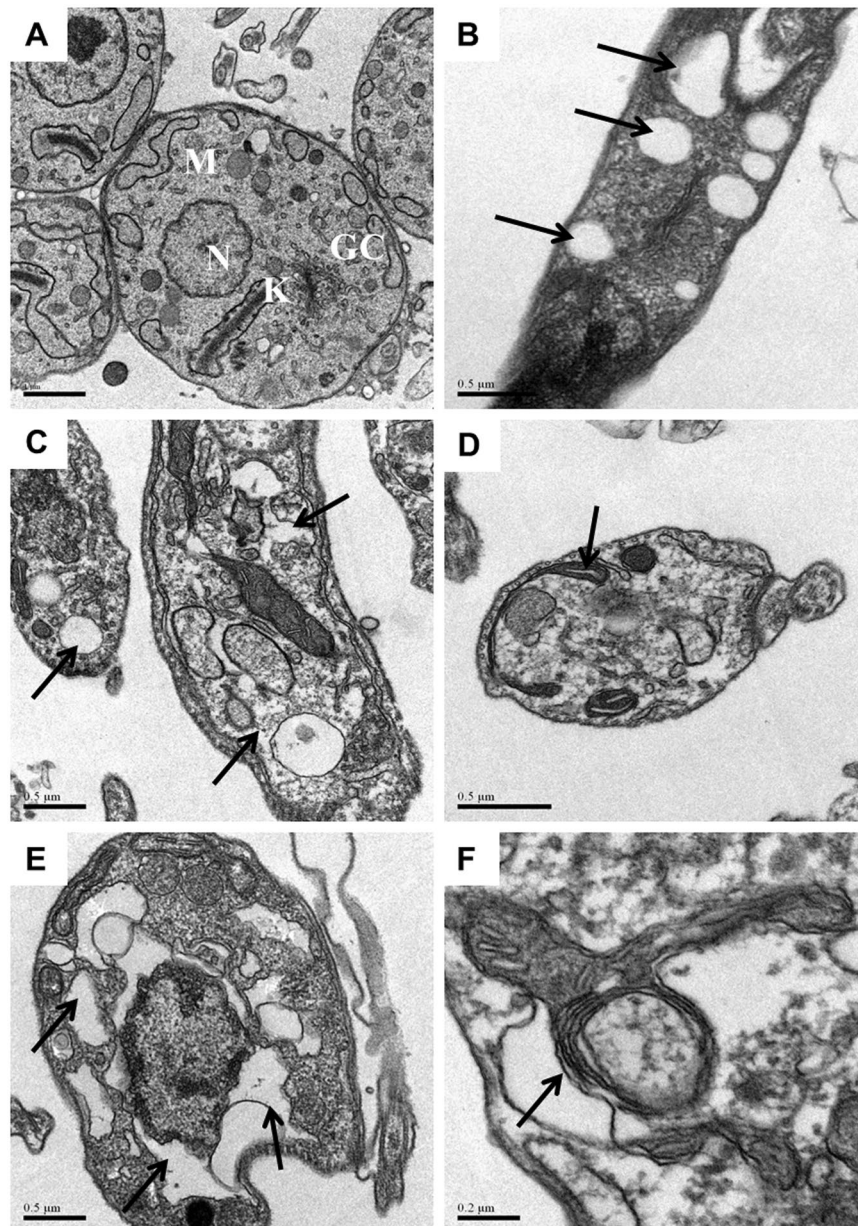


**Figure 5.** Transmission electron micrographs of trypomastigotes treated or not with DMS for 24 h. (A) Untreated trypomastigotes presenting a typical morphology of the nucleus (N), kinetoplast (K), mitochondria (M) and Golgi complex (GC). (B,C) Trypomastigotes treated with DMS (1  $\mu\text{M}$ ) causes the formation of numerous and atypical vacuoles within the cytoplasm accompanied by a large loss of density. (D,E) Trypomastigotes treated with DMS (2  $\mu\text{M}$ ) shows degeneration of mitochondria and intense vacuolization. (F) Trypomastigotes treated with DMS (4  $\mu\text{M}$ ) shows myelin-figures. Black arrows indicate alterations cited. Scale bars: A = 1  $\mu\text{m}$ ; B–E = 0.5  $\mu\text{m}$ ; F = 0.2  $\mu\text{m}$ .

are toxic to *T. brucei*, both of them having a 10-fold therapeutic index versus human cells, suggesting their potential use against *T. brucei* infection<sup>30</sup>. Here we demonstrated that DMS also induces morphological alterations and death in *T. cruzi*, suggesting that TcSphK may be a candidate target for drug development against *T. cruzi*. The reduced parasite load on infected macrophages may be also an important mechanism to reduce the dissemination of parasites, since it is likely that *T. cruzi*-infected macrophages circulate *in vivo*<sup>31</sup>.

A previous study has shown that Sph and its analogues DMS and FTY720 act as a danger-associated molecular patterns (DAMPs), inducing mature IL-1 $\beta$  secretion and promoting inflammasome activation<sup>32</sup>. Both Sph analogues are capable of inducing IL-1 $\beta$  production, and our data reinforces the ability of DMS to activate the inflammasome pathway. *T. cruzi* infection has also been shown to induce inflammasome activation in mice, being a resistance factor to infection by regulating the production of nitric oxide and ROS<sup>33–35</sup>. Here we found that DMS induced inflammasome activation in *T. cruzi*-infected macrophages, as shown by increased caspase-1 activation and IL-1 $\beta$  production. Moreover, DMS increased the production of ROS and NO, which may be

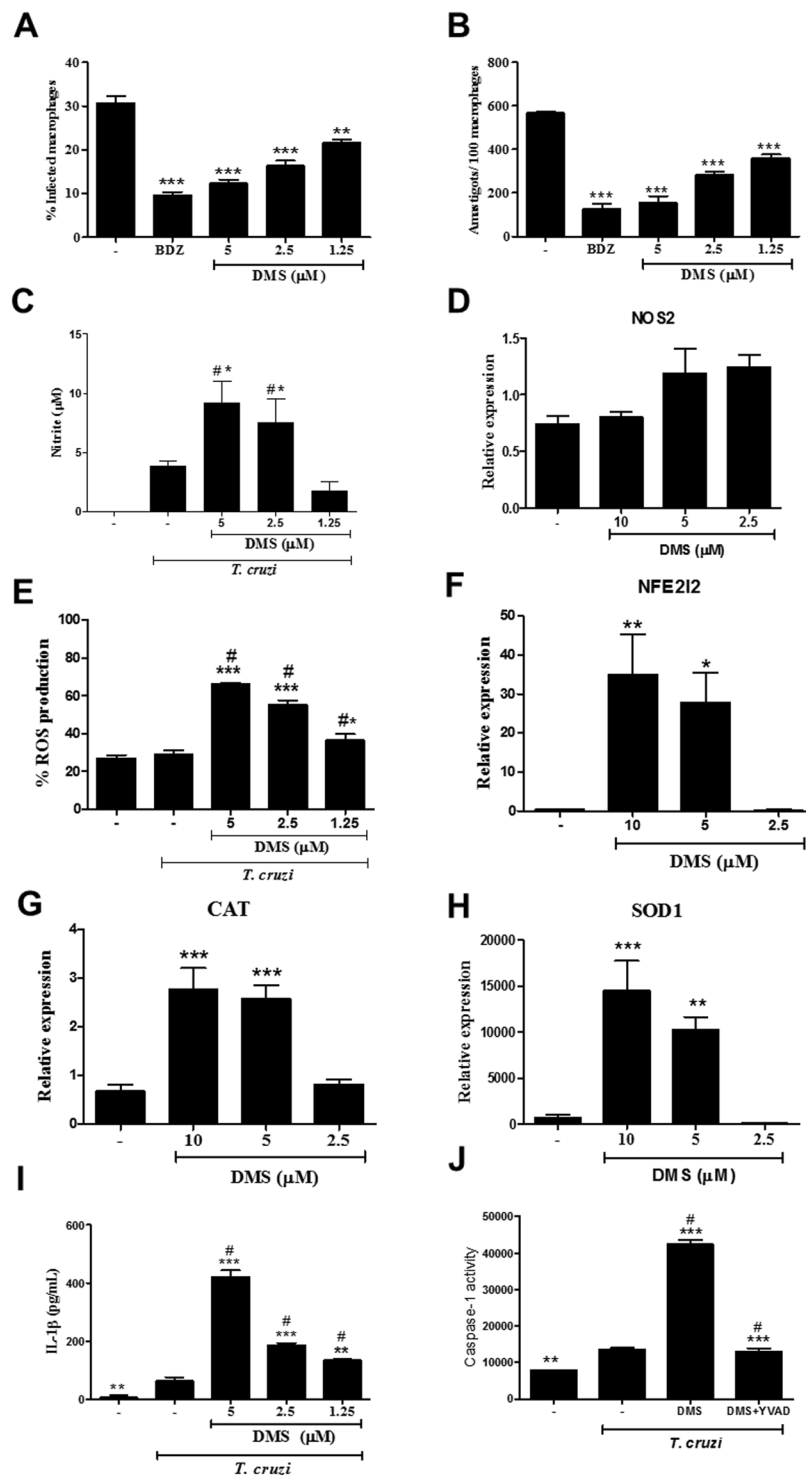


**Figure 6.** DMS inhibits amastigote proliferation in *T. cruzi*-infected macrophages, increases NO and ROS and activates caspase 1. The percentage of infected macrophages (A) and the relative number of amastigotes per 100 macrophages (B) were determined by counting hematoxylin and eosin-stained cultures after 72 hours of treatment. (C) Nitric oxide was determined by Griess method after 72 hours of treatment. (D) Relative expression of NOS2 gene in infected macrophages treated or not with DMS. (E) Reactive oxygen species was quantified by stained with 2',7'-dichlorofluorescein diacetate after 30 minutes of treatment. (F–H) Relative expression of NFE2I2, CAT and SOD1 genes in infected macrophages treated or not with DMS. (I) IL-1 $\beta$  production quantified by ELISA. (J) Caspase-1 activity measured using caspase-Glo 1 inflammasome assay in cultures incubated with complete medium alone, with DMS (5  $\mu$ M) or with DMS and YVAD (a caspase-1 inhibitor) in triplicate for 2 h. Values represent means  $\pm$  SEM of 4 determinations. \*\*\* $P$  < 0.001; \*\* $P$  < 0.01; \* $P$  < 0.05 compared to infected and untreated group; # $P$  < 0.05 compared to uninfected and untreated group.



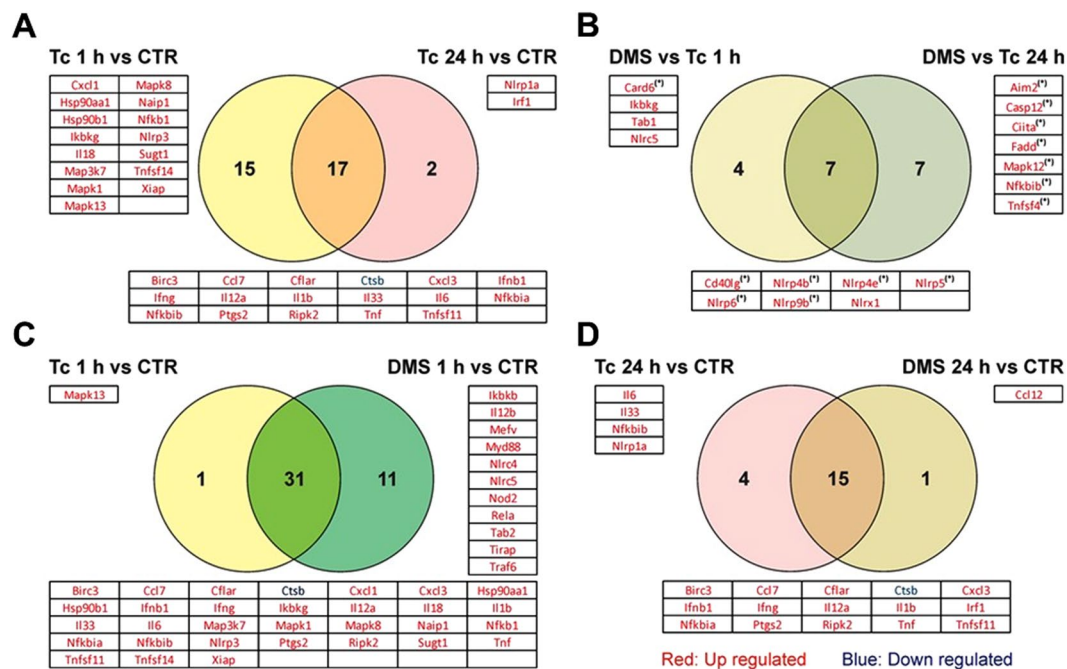


**Figure 7.** Venn diagrams representing differentially expressed genes (DEG) through *T. cruzi* infection with or without DMS treatment. (A) Comparison between DEG after 25 h (Tc 1 h condition) or 48 h (Tc 24 h condition) after *T. cruzi* infection with respect to uninfected macrophages (CTR condition). (B) Analysis of common DEG by DMS treatment for 1 h (DMS 1 h) and 24 h (DMS 24 h) when compared to infected macrophages. (C) Comparison between DEG by *T. cruzi* infection with or without 1 h DMS treatment with respect to uninfected macrophages. (D) Comparison between DEG during 48 h infection with or without 24 h DMS treatment with respect to uninfected macrophages. (\*) indicates genes with  $|FC| \geq 2$  but p-values  $> 0.05$ .

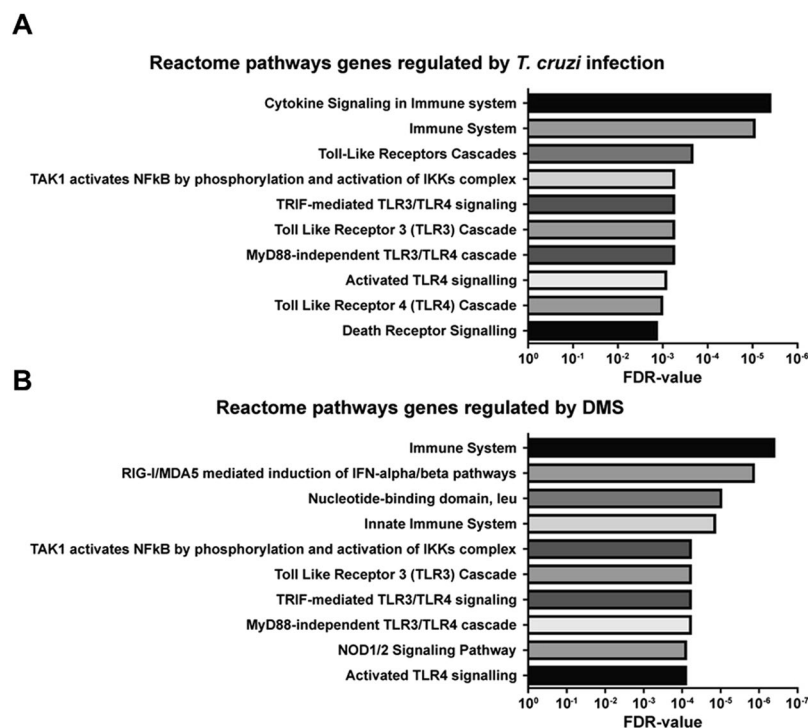


**Figure 8.** Reactome pathway analysis of DEG by *T. cruzi* infection or DMS treatment. (A) Graph representing the 10 most significant pathways in which common DEG by *T. cruzi* at 25 h (Tc 1 h condition) and 48 h (Tc 24 h condition) after infection are involved. (B) Graph representing the 10 most significant pathways in which genes induced by DMS treatment are involved.

contributing to parasite clearance by infected macrophages. Interestingly, the increase on production of nitric oxide was not accompanied by an upregulation of iNOS gene transcription, suggesting that post-transcriptional and post-translational mechanisms are responsible for DMS-induced NO production<sup>36</sup>. The transcription of genes activated in response to ROS production, however, were increased in DMS-treated macrophages, such as NFE2L1, SOD-1 and catalase 1.

In addition to its effects on Sphk, DMS was shown to inhibit the activity of protein kinase C and mitogen-activated protein kinase (MAPK)<sup>37,38</sup>. Although we did not see interference of PKC and MAPK inhibitors on the effects of DMS in macrophage cultures, further studies are required to demonstrate whether the beneficial effects of DMS *in vivo* are solely dependent on Sphk inhibition. The fact that DMS may have off-target effects, however, may not be detrimental, since FTY720 and other approved drugs are known to have off-target effects<sup>39</sup>.

Despite the increased production of IL-1 $\beta$  by DMS-treated macrophages, a reduction of TNF $\alpha$  and IL-6, two proinflammatory cytokines, was found. This may be due to a modulation of NF- $\kappa$ B activation by DMS, as observed in our study and in previous reports<sup>40,41</sup>. The analysis by PCR array performed in our study indicates that DMS induces the expression of inflammasome genes known to repress NF- $\kappa$ B activation, such as *Nlr5* and *Nlr1*<sup>42,43</sup>, which suggests that inhibition of *T. cruzi*-induced NF- $\kappa$ B may be linked to the activation of these inflammasome mediators. Both Sph and its analogue FTY720 have already been described as regulators of the NLRP3-inflammasome and IL-1 $\beta$  release from macrophages<sup>32</sup>. Although NLRP3-inflammasome activation plays a significant role in the activation of IL-1 $\beta$ /ROS and NF- $\kappa$ B signaling of cytokine gene expression for *T. cruzi* control in human and mouse macrophages, it was observed that NLRP3-mediated IL-1 $\beta$ /NF- $\kappa$ B activation is dispensable since it is compensated by ROS-mediated control of *T. cruzi* replication and survival in macrophages<sup>35</sup>. Therefore, our results suggest that, in addition to the NLRP3 inflammasome previously described<sup>32</sup>, DMS activates other inflammasome pathways.

In conclusion, our results demonstrate a potent effect of DMS *in vitro* and *in vivo* by its antiparasitic and immunomodulatory effects and suggest that inflammasome activation is a promising strategy for the development of anti-Chagas disease treatment. Further studies are required to demonstrate the usefulness of inhibitors of S1P pathway, which are being already used in the clinical setting, as potential candidates for the treatment of Chagas disease cardiomyopathy.

## Methods

**Animals.** Four weeks-old male C57BL/6 mice were used in all experiments. They were raised, maintained in the animal facility of the Center for Biotechnology and Cell Therapy, Hospital São Rafael (Salvador, Bahia, Brazil), and provided with rodent diet and water *ad libitum*. All experiments were carried out in accordance with the recommendations of Ethical Issues Guidelines, and were approved by the local ethics committee for animal use under number 001/15 (FIOCRUZ, Bahia, Brazil).

**Trypanosoma cruzi infection and DMS treatment.** Trypomastigotes of the myotropic Colombian *T. cruzi* strain were obtained from culture supernatants of infected LLC-MK2 cells. Infection was performed by intraperitoneal (i.p.) injection of 1000 *T. cruzi* trypomastigotes in saline and parasitemia was monitored during infection. Groups of chronically infected mice were treated i.p. with N,N-dimethylsphingosine (DMS; 200  $\mu$ g/kg; Cayman Chemical, Ann Arbor, MI) based on a previous report by Lai and col. (2008)<sup>44</sup>, 3 $\times$ /week during two months (Fig. 1A). Control infected mice received vehicle (saline solution) in the same regimen. Groups of mice were euthanized one week after therapy, under anesthesia with 5% ketamine (Vetanarcol<sup>®</sup>; Konig, Avellaneda, Argentina) and 2% xylazine (Sedomin<sup>®</sup>; Konig).

**Exercise capacity and electrocardiography analysis.** A motor-driven treadmill chamber for one animal (LE 8700; Panlab, Barcelona, Spain) was used to exercise the animals. The speed of the treadmill and the intensity of the shock (mA) were controlled by a potentiometer (LE 8700 treadmill control; Panlab). Total running distance and time of exercise were recorded.

Electrocardiography was performed using the Bio Amp PowerLab System (PowerLab 2/20; ADInstruments, Castle Hill, NSW, Australia), recording the bipolar lead I. All data were acquired for computer analysis using Chart 5 for Windows (PowerLab). The EKG analysis included heart rate, PR interval, P wave duration, QT interval, QTc, and arrhythmias. The QTc was calculated as the ratio of QT interval by square roots of RR interval (Bazett's formula)<sup>45</sup>.

**Morphometric analysis.** The hearts of all mice were removed and half of each heart was fixed in buffered 10% formalin. Sections of paraffin-embedded tissue were stained by the standard hematoxylin-eosin and Sirius red staining methods for evaluation of inflammation and fibrosis, respectively, by optical microscopy. Images were digitized using a color digital video camera (CoolSnap, Montreal, Canada) adapted to a BX41 microscope (Olympus, Tokyo, Japan). Morphometric analyses were performed using the software Image Pro Plus v.7.0 (Media Cybernetics, San Diego, CA), as described before<sup>46</sup>.

**Confocal immunofluorescence analyses.** Sections of formalin-fixed paraffin embedded hearts were used for detection of galectin-3 expression by immunofluorescence as described before<sup>46</sup>. Sections were incubated overnight with anti-galectin-3, diluted 1:50 (Santa Cruz Biotechnology, Santa Cruz, CA) followed by incubation, for 1 h, with Alexa fluor 633 (1:200) (Molecular Probes, Carlsbad, CA) Nuclei were stained with 4,6-diamidino-2-phenylindole (Vector Laboratories, Burlingame, CA). The presence of fluorescent cells was determined by observation on a FluoView 1000 confocal microscope (Olympus).

**Quantification of parasite load.** For DNA extraction, spleen fragments were submitted to DNA extraction using the NucleoSpin Tissue Kit (Machenerey-Nagel, Düren, Germany), as recommended by the manufacturer. Primers were designed based on the literature<sup>47</sup>, and the quantification of parasite load was performed as described previously<sup>46</sup>. To calculate the number of parasites per milligram of tissue, each plate contained an 8-log standard curve of DNA extracted from trypomastigotes of the Colombian *T. cruzi* strain in duplicate. Data were analyzed using 7500 software 2.0.1 (Applied Biosystems).

**Macrophage infection *in vitro*.** Peritoneal exudate macrophages obtained from C57BL/6 mice, four days after thioglycollate injection, were seeded at a cell density of  $2 \times 10^5$  cells/mL in a 24 well-plate with rounded coverslips on the bottom in RPMI-1640 medium (Sigma-Aldrich, St. Louis, MD) supplemented with 10% fetal bovine serum (FBS; Gibco Laboratories, Gaithersburg, MD) and 50  $\mu$ g/mL of gentamycin (Novafarma, Anápolis, GO, Brazil) and incubated for 24 h. Cells were then infected with trypomastigotes (1:10) for 2 h. Free trypomastigotes were removed by successive washes using saline solution. Cultures were incubated for 24 h to allow full internalization and differentiation of trypomastigotes into amastigotes. Cultures were then incubated in complete medium alone or with test inhibitors for 72 h. Cells were fixed, then stained with hematoxylin and eosin, and submitted to manual counting using an optical microscope (Olympus).

**Real time reverse transcription polymerase chain reaction (qRT-PCR).** RNA was extracted of the heart samples and macrophage cultures using TRIzol (Invitrogen, Molecular Probes, Eugene, OR). cDNA was synthesized using High Capacity cDNA Reverse Transcription Kit (Applied Biosystems). The qPCR was prepared with TaqMan<sup>®</sup> Universal PCR Master Mix (Applied Biosystems). qRT-PCR assays were performed to detect the expression levels of *Ptprc*, *Lgals3*, *Tnf*, *Ifn $\gamma$* , *Il10*, *Tgf $\beta$* , *Nos2*, *Chi3l3*, *Il1 $\beta$* , *Arg1*, *Nfe2l2*, *Cat* and *Sod1*. All reactions were run in triplicate on an ABI 7500 Real Time PCR System (Applied Biosystems) under standard thermal cycling conditions. A non-template control (NTC) and non-reverse transcription controls (No-RT) were also included. The samples were normalized with 18S and *Hprt*. The threshold cycle ( $2^{-\Delta\Delta Ct}$ ) method of comparative PCR was used to analyse the results<sup>48</sup>.

**PCR array.** Peritoneal exudate macrophages ( $2 \times 10^6$  cells/mL) were incubated in 24 well-plates with supplemented RPMI for 24 h. After washing with saline solution to discard non-adherent cells, infection was performed with trypomastigotes (1:10), for 24 h. Free trypomastigotes were removed by successive washes. Cultures were then incubated with complete medium alone or with DMS (5  $\mu$ M) in triplicate for 24 h. RNA was extracted using the Rneasy Plus Mini Kit (Qiagen, Valencia, CA). Quantification of RNA and degree of purity were performed in a spectrophotometer (NanoDrop<sup>™</sup> 1000, Thermo Fisher Scientific, Wilmington, DE). Sample integrity was observed using a 1% agarose gel. cDNA synthesis was performed using the RT2 First Strand kit (Qiagen). For target gene expression analysis, we used RT2 Profiler PCR Arrays Mouse Inflammasome (Qiagen), the SYBR<sup>®</sup>Green system and 96-well plates. The 7500 Real Time PCR was used (Applied Biosystems). All experiments were performed in DNase/RNase free conditions. The analysis was performed by Threshold Cycle Method<sup>48</sup>, obtained by calculating  $2^{-\Delta\Delta Ct}$ . The QIAGEN's qPCR analysis web portal date, available on <http://pcrdataanalysis.sabiosciences.com/pcr/arrayanalysis.php> was used to assist in the analysis, and analysis of differentially expressed genes and pathways prediction were done through free online bioinformatic sites BioVenn ([www.cmbi.ru.nl/cdd/biovenn](http://www.cmbi.ru.nl/cdd/biovenn)) and Enrichr ([amp.pharm.mssm.edu/Enrichr](http://amp.pharm.mssm.edu/Enrichr)).

**Lymphoproliferation assay.** Spleen cell suspensions from naive C57BL/6 mice were prepared in DMEM medium (Life Technologies, GIBCO-BRL, Gaithersburg, MD) supplemented with 10% FBS and 50  $\mu$ g/mL of gentamycin. Splenocytes were cultured in 96-well plates at  $1 \times 10^6$  cells per well, in a final volume of 200  $\mu$ L, in triplicate, in the presence of 2  $\mu$ g/mL concanavalin A (Con A; Sigma-Aldrich) only or with anti-CD3 and anti-CD28 (Thermo Fisher Scientific), in the absence or presence of DMS at different concentrations (2.5, 1.25 or 0.62  $\mu$ M). After 48 h, plates were pulsed with 1  $\mu$ Ci of methyl-<sup>3</sup>H-thymidine (Perkin Elmer, Waltham, MA) for 18 h. The plates were harvested and the <sup>3</sup>H-thymidine uptake was determined using a  $\beta$ -plate counter (Multilabel Reader, Finland). Dexamethasone (Sigma-Aldrich) was used as positive control.

**ELISA assays and determination of nitric oxide production.** Serum samples from the *in vivo* study were used for galectin-3, TNF $\alpha$  and IFN $\gamma$  and TGF $\beta$  determination. Quantification of cytokines was performed by ELISA, using specific antibody kits (R&D Systems, Minneapolis, MN), according to manufacturer's instructions. To estimate the amount of nitric oxide (NO) produced, macrophage culture supernatants were used for nitrite determination by the Griess reaction, as previously described<sup>49</sup>.

**Reactive oxygen species (ROS) production assay.** Thioglycollate-elicited peritoneal exudate macrophages ( $1 \times 10^6$ ) were obtained and infected with *T. cruzi*. Cultures were then incubated with complete medium alone or with DMS for 30 min. After incubation, macrophages were removed from each well using 0.01% trypsin and labeled with 10  $\mu$ M of 2',7'-dichlorofluorescein diacetate (Sigma-Aldrich) for 30 minutes at 37 °C. Cells were then washed and analyzed using a cell analyzer (LSRFortessa; BD Biosciences, San Jose, CA) with FlowJo software (Tree Star, Ashland, OR).

**Caspase 1 activity assay.** Thioglycollate-elicited peritoneal exudate macrophages ( $1 \times 10^6$ ) were obtained and infected with *T. cruzi* as described above. Cultures were then incubated with reagents for 2 h and after that, caspase-1 activity was measured using caspase-Glo<sup>®</sup> 1 inflammasome assay (Promega, Madison, WI), according to the manufacturer's instructions. The luminescence of each sample was measured in a Glomax 20/20 luminometer (Promega).

**Transmission electron microscopy analysis.** *T. cruzi* trypomastigotes ( $5 \times 10^7$ ) were treated with DMS (1, 2 or 4  $\mu\text{M}$ ) and incubated for 24 h at 37°C. After incubation, parasites were fixed for 1 h at room temperature with 2% formaldehyde and 2.5% glutaraldehyde (Electron Microscopy Sciences, Hatfield, PA) in sodium cacodylate buffer (0.1 M, pH 7.2) for 1 h at room temperature. After fixation, parasites were processed for transmission electron microscopy as previously described<sup>50</sup>. Images were obtained in a JEOL TEM-1230 transmission electron microscope.

**Statistical analyses.** All continuous variables are presented as means  $\pm$  SEM. Data were analyzed using 1-way ANOVA, followed by Newman-Keuls multiple-comparison test with Prism 5.0 (GraphPad Software, San Diego, CA). All differences were considered significant at values of  $P < 0.05$ .

## References

1. Dutra, W. O. *et al.* Cellular and genetic mechanisms involved in the generation of protective and pathogenic immune responses in human Chagas disease. *Mem. Inst. Oswaldo Cruz* **104**(Suppl. 1), 208–218 (2009).
2. Andrade, Z. A. Immunopathology of Chagas disease. *Mem Inst Oswaldo Cruz* **94**(Suppl 1), 71e80 (1999).
3. Fuenmayor, C. *et al.* Acute Chagas' disease: immunohistochemical characteristics of T cell infiltrate and its relationship with *T. cruzi* parasitic antigens. *Acta Cardiol* **60**(1), 33–37 (2005).
4. Bonney, K. M. & Engman, D. M. Autoimmune pathogenesis of Chagas heart disease: looking back, looking ahead. *Am J Pathol* **185**(6), 1537–1547 (2015).
5. Tanowitz, H. B. *et al.* Chagas' disease. *Clin Microbiol Rev* **5**(4), 400–419 (1992).
6. Rassi, A. Jr., Rassi, A. & Marin-Neto, J. A. Chagas disease. *Lancet* **375**(9723), 1388–1402 (2010).
7. Arana, L., Gangoiti, P., Ouro, A., Trueba, M. & Gómez-Muñoz, A. Ceramide and ceramide 1-phosphate in health and disease. *Lipids Health Dis* **9**, 15 (2010).
8. Yanagida, K. & Hla, T. Vascular and immunobiology of the circulatory sphingosine 1-phosphate gradient. *Annu Rev Physiol* **79**, 67–91 (2017).
9. Arish, M. *et al.* sphingosine-1-phosphate signaling: unraveling its role as a drug target against infectious diseases. *Drug Discov Today* **21**(1), 133–142 (2016).
10. Maceyka, M. & Spiegel, S. Sphingolipid metabolites in inflammatory disease. *Nature* **510**(7503), 58–67 (2014).
11. Rivera, J., Proia, R. L. & Olivera, A. The alliance of sphingosine-1-phosphate and its receptors in immunity. *Nat Rev Immunol* **8**(10), 753–763 (2008).
12. Cyster, J. G. & Schwab, S. R. Sphingosine-1-phosphate and lymphocyte egress from lymphoid organs. *Annu Rev Immunol* **30**, 69–94 (2012).
13. Soares, M. B. *et al.* Reversion of gene expression alterations in hearts of mice with chronic chagasic cardiomyopathy after transplantation of bone marrow cells. *Cell Cycle* **10**(9), 1448–1455 (2011).
14. Gomes, J. A. *et al.* Evidence that development of severe cardiomyopathy in human Chagas' disease is due to a Th1-specific immune response. *Infect Immun* **71**(3), 1185–1193 (2003).
15. Soares, M. B. *et al.* Gene expression changes associated with myocarditis and fibrosis in hearts of mice with chronic chagasic cardiomyopathy. *J Infect Dis* **202**(3), 416–426 (2010).
16. Mazzola, M. A. *et al.* Identification of a novel mechanism of action of fingolimod (FTY720) on human effector T cell function through TCF-1 upregulation. *J Neuroinflammation* **12**, 245 (2015).
17. Takuwa, Y., Ikeda, H., Okamoto, Y., Takuwa, N. & Yoshioka, K. Sphingosine-1-phosphate as a mediator involved in development of fibrotic diseases. *Biochim Biophys Acta* **1831**(1), 185–192 (2013).
18. Shiohira, S. *et al.* Sphingosine-1-phosphate acts as a key molecule in the direct mediation of renal fibrosis. *Physiol Rep* **1**(7), e00172 (2013).
19. Landeen, L. K., Aroonsakool, N., Haga, J. H., Hu, B. S. & Giles, W. R. Sphingosine-1-phosphate receptor expression in cardiac fibroblasts is modulated by *in vitro* culture conditions. *Am J Physiol Heart Circ Physiol* **292**(6), H2698–2711 (2007).
20. Kacimi, R., Vessey, D. A., Honbo, N. & Karliner, J. S. Adult cardiac fibroblasts null for sphingosine kinase-1 exhibit growth dysregulation and an enhanced proinflammatory response. *J Mol Cell Cardiol* **43**(1), 85–91 (2007).
21. Takuwa, N. *et al.* S1P3-mediated cardiac fibrosis in sphingosine kinase 1 transgenic mice involves reactive oxygen species. *Cardiovasc Res* **85**(3), 484–493 (2010).
22. Araújo-Jorge, T. C. *et al.* Pivotal role for TGF- $\beta$  in infectious heart disease: the case of *Trypanosoma cruzi* infection and its consequent chagasic cardiomyopathy. *Cytok Growth Factors Rev* **19**(5–6), 405–413 (2008).
23. Azibani, F., Fazal, L., Chatziantoniou, C., Samuel, J. L. & Delcayre, C. Hypertension-induced fibrosis: a balance story. *Ann Cardiol Angeiol* **61**(3), 150–155 (2012).
24. Machado, F. S. *et al.* *Trypanosoma cruzi*-infected cardiomyocytes produce chemokines and cytokines that trigger potent nitric oxide-dependent trypanocidal activity. *Circulation* **102**(24), 3003–3008 (2000).
25. Boscardin, S. B. *et al.* Chagas' disease: an update on immune mechanisms and therapeutic strategies. *J Cell Mol Med* **14**(6B), 1373–1384 (2010).
26. Hughes, J. E. *et al.* Sphingosine-1-phosphate induces an antiinflammatory phenotype in macrophages. *Circ Res* **102**(8), 950–958 (2008).
27. Soares, M. B., Pontes-De-Carvalho, L. & Ribeiro-Dos-Santos, R. The pathogenesis of Chagas' disease: when autoimmune and parasite-specific immune responses meet. *An Acad Bras Cienc* **73**(4), 547–559 (2001).
28. Garcia, S. *et al.* Treatment with benznidazole during the chronic phase of experimental Chagas' disease decreases cardiac alterations. *Antimicrob Agents Chemother* **49**(4), 1521–1528 (2005).
29. Pontes-de-Carvalho, L. *et al.* Experimental chronic Chagas' disease myocarditis is an autoimmune disease preventable by induction of immunological tolerance to myocardial antigens. *J Autoimmun* **18**(2), 131–138 (2002).
30. Pasternack, D. A., Sharma, A. I., Olson, C. L., Epting, C. L. & Engman, D. M. Sphingosine kinase regulates microtubule dynamics and organelle positioning necessary for proper G1/S cell cycle transition in *Trypanosoma brucei*. *MBio* **6**(5), e01291–1315 (2015).
31. Lewis, M. D., Francisco, A. F., Taylor, M. C. & Kelly, J. M. A new experimental model for assessing drug efficacy against *Trypanosoma cruzi* infection based on highly sensitive *in vivo* imaging. *J Biomol Screen* **20**(1), 36–43 (2015).
32. Luheshi, N. M., Giles, J. A., Lopez-Castejon, G. & Brough, D. Sphingosine regulates the NLRP3-inflammasome and IL-1 $\beta$  release from macrophages. *Eur J Immunol* **42**(3), 716–725 (2012).
33. Silva, G. K. *et al.* Apoptosis-associated speck-like protein containing a caspase recruitment domain inflammasomes mediate IL-1 $\beta$  response and host resistance to *Trypanosoma cruzi* infection. *J Immunol* **191**(6), 3373–3383 (2013).
34. Gonçalves, V. M. *et al.* NLRP3 controls *Trypanosoma cruzi* infection through a caspase-1-dependent IL-1R-independent NO production. *PLoS Negl Trop Dis* **7**(10), e2469 (2013).
35. Dey, N. *et al.* Caspase-1/ASC inflammasome-mediated activation of IL-1 $\beta$ -ROS-NF $\kappa$ B pathway for control of *Trypanosoma cruzi* replication and survival is dispensable in NLRP3-/- macrophages. *PLoS One* **9**(11), e111539 (2014).
36. Pautz, A. *et al.* Regulation of the expression of inducible nitric oxide synthase. *Nitric Oxide* **23**(2), 75–93 (2010).

37. Sakakura, C. *et al.* Selectivity of sphingosine-induced apoptosis. Lack of activity of DL-erythro-dihydrosphingosine. *Biochem Biophys Res Commun* **246**(3), 827–830 (1998).
38. Kim, J. W. *et al.* Synthesis and evaluation of sphingoid analogs as inhibitors of sphingosine kinases. *Bioorg Med Chem* **13**(10), 3475–3485 (2005).
39. Patmanathan, S. N., Yap, L. F., Murray, P. G. & Paterson, I. C. The antineoplastic properties of FTY720: evidence for the repurposing of fingolimod. *J Cell Mol Med* **19**(10), 2329–2340 (2015).
40. Billich, A. *et al.* Basal and induced sphingosine kinase 1 activity in A549 carcinoma cells: function in cell survival and IL-1beta and TNF-alpha induced production of inflammatory mediators. *Cell Signal* **17**(10), 1203–1217 (2005).
41. Zhang, Z. *et al.* SPHK1 inhibitor suppresses cell proliferation and invasion associated with the inhibition of NF- $\kappa$ B pathway in hepatocellular carcinoma. *Tumour Biol* **36**(3), 1503–1509 (2015).
42. Cui, J. *et al.* NLRX5 negatively regulates the NF-kappaB and type I interferon signaling pathways. *Cell* **141**(3), 483–496 (2010).
43. Xia, X. *et al.* NLRX1 negatively regulates TLR-induced NF- $\kappa$ B signaling by targeting TRAF6 and IKK. *Immunity* **34**(6), 843–853 (2011).
44. Lai, W. Q. *et al.* The role of sphingosine kinase in a murine model of allergic asthma. *J Immunol* **15** **180**(6), 4323–4329 (2008).
45. Berul, C. I., Aronovitz, M. J., Wang, P. J. & Mendelsohn, M. E. *In vivo* cardiac electrophysiology studies in the mouse. *Circulation* **94**(10), 2641–2648 (1996).
46. Vasconcelos, J. F. *et al.* Administration of granulocyte colony-stimulating factor induces immunomodulation, recruitment of T regulatory cells, reduction of myocarditis and decrease of parasite load in a mouse model of chronic Chagas disease cardiomyopathy. *FASEB J* **27**(12), 4691–4702 (2013).
47. Schijman, A. G. *et al.* International study to evaluate PCR methods for detection of *Trypanosoma cruzi* DNA in blood samples from Chagas disease patients. *Plos Negl Trop Dis* **5**(1), e931 (2011).
48. Schmittgen, T. D. & Livak, K. J. Analyzing real-time PCR data by the comparative C(T) method. *Nat Protoc* **3**(6), 1101–1108 (2008).
49. Green, L. C., Wagner, D. A., Glogowski, K., Skipper, P. L. & Wishnok, J. S. Analysis of nitrate, nitrite and [15N] nitrate in biological fluids. *Anal Biochem* **126**(1), 131–138 (1982).
50. Meira, C. S. *et al.* Physalins B and F, seco-steroids isolated from *Physalis angulata* L., strongly inhibit proliferation, ultrastructure and infectivity of *Trypanosoma cruzi*. *Parasitology* **140**(14), 1811–1821 (2013).

## Acknowledgements

This study was supported by funds from the National Council for Scientific and Technological Development (CNPq) and Bahia Research Foundation (FAPESB). The authors thank Adriano Costa de Alcântara for technical assistance in qPCR analysis for parasite load quantification.

## Author Contributions

J.F.V. and C.S.M. performed *in vivo* and *in vitro* experiments, P.S.D. and S.G.M. performed functional analysis, J.F.V. and B.S.F.S. performed morphometric analysis, C.K.V.N., V.M.B. and P.D.D. performed inflammasome analysis, D.N.S. performed genic expression analysis, C.S.M. performed transmission electron microscopy analysis and flow cytometry analysis. M.B.P.S. and J.F.V. wrote the manuscript, and designed figures. All authors contributed to experimental design and conceived experiments. R.R.S. and M.B.P.S. provided overall guidance, funding and assisted in manuscript completion.

## Additional Information

**Supplementary information** accompanies this paper at doi:[10.1038/s41598-017-06275-z](https://doi.org/10.1038/s41598-017-06275-z)

**Competing Interests:** The authors declare that they have no competing interests.

**Publisher's note:** Springer Nature remains neutral with regard to jurisdictional claims in published maps and institutional affiliations.



**Open Access** This article is licensed under a Creative Commons Attribution 4.0 International License, which permits use, sharing, adaptation, distribution and reproduction in any medium or format, as long as you give appropriate credit to the original author(s) and the source, provide a link to the Creative Commons license, and indicate if changes were made. The images or other third party material in this article are included in the article's Creative Commons license, unless indicated otherwise in a credit line to the material. If material is not included in the article's Creative Commons license and your intended use is not permitted by statutory regulation or exceeds the permitted use, you will need to obtain permission directly from the copyright holder. To view a copy of this license, visit <http://creativecommons.org/licenses/by/4.0/>.

© The Author(s) 2017